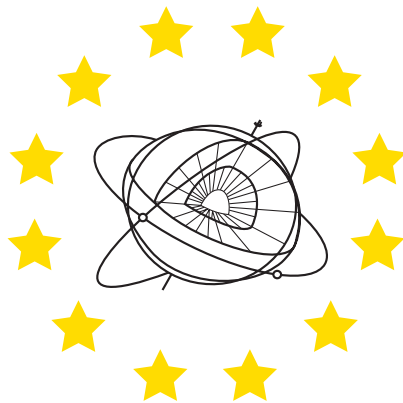


MINISTÈRE DE LA CULTURE, DE L'ENSEIGNEMENT
SUPERIEUR ET DE LA RECHERCHE

Cahiers
du Centre Européen
de Géodynamique
et de Séismologie

Volume 28



Proceedings of the Workshop:

Seismicity patterns in the Euro-Med region

November 17-19, 2008
Hotel Parc Belle-Vue
Luxembourg
(Grand-Duchy of Luxembourg)

Edited by Adrien Oth

Luxembourg 2009

Proceedings of the Workshop:

Seismicity patterns in the Euro-Med region

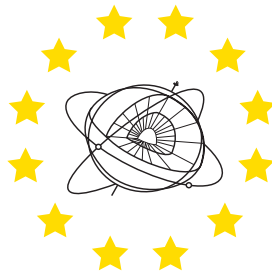
November 17-19, 2008

Hotel Parc Belle-Vue
Luxembourg
Grand-Duchy of Luxembourg

Organized by
The European Center for Geodynamics and Seismology (ECGS)

Supported by

European Center for Geodynamics and Seismology (ECGS)
Fonds National de la Recherche de Luxembourg (FNR)
Musée National d'Histoire Naturelle (MNHN)
The Council of Europe (EUR-OPA)
Ministère de la Culture, de l'Enseignement Supérieur et de la Recherche
International Association of Seismology and Physics of the Earth's Interior (IASPEI)



Scientific Committee & Invited Speakers:

R. Bossu (EMSC/CSEM, France)
Th. Camelbeeck (ROB, Belgium)
L. Chiaraluce (INGV, Italy)
T. Fischer (Univ. Prague, Czech Rep.)
G. Grünthal (GFZ Potsdam, Germany)
A. Hubert-Ferrari (ROB, Belgium)
G. Papadopoulos (NOA, Greece)
S. Pucci (INGV, Italy)
F. Wenzel (Univ. Karlsruhe, Germany)
H. Wust-Bloch (Univ. Tel Aviv, Israel)
A. Ziv (Univ. Ben Gurion, Israel)

Local Organizing Committee:

A. Oth (ECGS, Luxembourg)
C. Galassi (ECGS, Luxembourg)
G. Celli (ECGS/MNHN, Luxembourg)
E. Buttini (ECGS/MNHN, Luxembourg)
M. Bonatz (ECGS, Luxembourg)

Edited by:

Adrien Oth
Luxembourg - 2009

PUBLISHED WITH THE SUPPORT OF

**MINISTÈRE DE LA CULTURE,
DE L'ENSEIGNEMENT SUPÉRIEUR ET DE LA RECHERCHE**

&

FONDS NATIONAL DE LA RECHERCHE



ISBN N° 9 782919 89702-5

Centre Européen de Géodynamique et de Séismologie

Musée National d'Histoire Naturelle
Section Astrophysique et Géophysique, Luxembourg

To Johnny Flick



We dedicate this volume of the *Cahiers du Centre Européen de Géodynamique et de Séismologie* to **Johnny Flick**, who passed away on April 10 2008.

The development of earth science research and the institutions devoted to this branch of science in the Grand-Duchy of Luxembourg are primarily the result of the initiative and devotion of two extraordinary personalities: Johnny Flick, Geodesist at the City of Luxembourg, and Paul Melchior, astronomer at the Royal Observatory of Belgium in Brussels.

In 1963, during the pioneer era of the interdisciplinary earth tides research, they started the observation of gravimetric earth tides in the casemates of the City of Luxembourg. A growing number of international scientific contacts arose from these works and, several years later, led to the idea of organizing meetings for interdisciplinary interested (at that time young) researchers on a regular basis. One should mention that at that time, only twenty years following World War II, the number of scientific conferences and therewith the possibility for direct and personal communication between scientists was severely limited. There was no financial support whatsoever available for realizing their idea, and the initiators were fully aware of the fact that this lack of funding possibilities could only be compensated through their optimism, idealism and personal commitment. Furthermore, due to the high level of anthropogenic noise, the casemates of the City of Luxembourg turned out to be a rather unsuitable location for high-resolution gravimetric measurements. As a consequence, it was necessary to look for an alternative measurement site, should the envisaged luxembourgish conferences have a link with local gravimetric observations and research.

Johnny Flick's searching for a new measurement site with a long-term scientific perspective finally led him to the gypsum mine of Walferdange, which was far enough from the City of Luxembourg in terms of microseismic noise considerations, yet still closeby and easily accessible. Johnny Flick succeeded to obtain the support of the mining operator and the municipality of Walferdange in order to realize the project of an underground geodynamic observatory and the necessary development of

a part of the extensive system of galleries could begin. In the early years, this was mostly achieved on a do-it-yourself basis, and Johnny Flick contributed greatly to these efforts, devoting (as other involved scientists too) his spare time to this project, besides his main profession. Still “somewhat” problematic were the occasional blasts associated with the continuing mining activities – but also this problem was solved in a “pragmatic” way. Following the later termination of mining activities, the final step towards the “Underground Laboratory of Walferdange” (ULW) was completed with extensive public funds. Since then the ULW is open to all interested researchers for geodynamic measurements and instrumental testing and investigations.

Further details on the ULW and its history can also be found in the following book: J. Flick und N. Stomp, *Sciences de la Terre au Luxembourg – Réminiscences*, Musée Nationale d’Histoire Naturelle et Centre Européen de Géodynamique et de Séismologie, Luxembourg 2002, (ISBN 2-919877-00-8).

The now continuously performed scientific work in the gypsum mine of Walferdange proved to be indeed highly useful for the realisation of the above-mentioned idea to organize regular scientific meetings in Luxembourg. Johnny Flick finally succeeded to obtain the necessary support from the government as well as the City of Luxembourg and the municipality of Walferdange, and the first *Journées Luxembourgeoises de Géodynamique* took place in 1971. The venue for the conference was for a long time the former military casern of Walferdange, since it was possible to host the scientists in a reasonably priced way considering the still very limited funds available. The ambiance was rather Spartan and the conference programs were of extraordinary scientific value. The substance and vitality of the *Journées Luxembourgeoises de Géodynamique* are also proven by the fact that now, in 2009, the 95th edition of this conference series is being held!

The main ambition of the Journées was (and is today) to endorse, besides some chosen focus topics, the interdisciplinary aspects of geosciences, and especially encourage young scientists to discover these. It was to a very large extent thanks to the influence and the personality of Johnny Flick that the Journées were marked by an atmosphere of friendship and lightness, which can be described with the term *Spirit of Luxembourg*. The presentations held at the Journées are documented in the respective *Comptes-Rendus*.

Over the years, it turned out to be a sensible idea to also hold, in addition to the Journées, *workshops* exclusively dedicated to special and current topics in earth sciences. The proceedings of these workshops are published in the monograph series *Cahiers du Centre Européen de Géodynamique et de Séismologie* and so far, 27 of these “blue books” have been published.

In the early years, the mentioned scientific activities were fully based on an informal cooperation between dedicated european scientists, who, at the same time, were close friends, with a tight link to the Royal Observatory of Belgium in Brussels. The extending range of activities and contacts with further international scientific institutions made it however necessary to introduce a more formal definition of the status. After surmounting several intermediate steps, the *Centre Européen de Géodynamique et de Séismologie* (European Center for Geodynamics and Seismology – ECGS) was founded as a part of the network of specialized research centers of the

To Johnny Flick

Council of Europe. ECGS is a foundation following luxembourgish law and tightly linked to the Musée National d'Histoire Naturelle (National Museum of Natural History).

All these achievements would not have been possible without the indefatigable work and dedication of Johnny Flick, and the full extent of his accomplishments can by far not be fully reproduced in this summary. As a logical consequence, he was appointed as the first president of the *Centre Européen de Géodynamique et de Séismologie*.

Johnny Flick was an exceptional and versatile personality and has received a variety of awards and honors in his lifetime. It remains to us to say Thank You to Johnny Flick for the last time and to keep the remembrance of Johnny Flick and his lifework alive.

Manfred Bonatz and Adrien Oth
October 2009

Preface

This volume of the “Cahiers du Centre Européen de Géodynamique et de Séismologie” is dedicated to the proceedings of the workshop “Seismicity Patterns in the Euro-Med region”, which was held at the Hotel Parc Belle-Vue in Luxembourg City, from November 17 2008 to November 19 2008.

Europe and the Mediterranean are confronted with a high variability of seismicity patterns. The Mediterranean includes crustal and intermediate-depth seismicity related to the complex African-Eurasian plate interaction. Other areas of lower seismicity are characterized by diffuse and intermittent activity. Some of the seismicity is related to major faults (North Anatolian fault, Dead Sea fault) or subduction zones (Greece, Calabria, Vrancea), some is rather diffuse. The workshop also provided an excellent opportunity to illustrate and discuss the variability of seismicity patterns on the example of the bulletin of the European-Mediterranean Seismological Centre (EMSC), which is now complete for 10 years.

In light of these issues, the main objective of the workshop was to develop an overview on the variability of European seismicity patterns, both spatially and temporally, and its tectonic framework, but also to explore its potential for future earthquake forecasting. Given the fact that a better understanding of this variability of European seismicity patterns is a key step towards improved seismic hazard assessment in Europe, a session dedicated to seismic hazard analysis was also included in the program.

47 participants from 14 countries (Algeria, Belgium, Bulgaria, Czech Republic, France, Germany, Greece, Italy, Israel, Japan, Luxembourg, Macedonia, Morocco and Romania) attended the workshop. The final program included 29 oral presentations (11 of these were invited speakers) and 10 posters, subdivided into 5 sessions:

- Historical and instrumental earthquake catalogues as a critical research infrastructure for Euro-Med seismicity.
- Large earthquakes in subduction zones, seismic hazard analysis.
- The Northern Anatolian and Dead Sea fault systems.
- Seismicity of Central Europe with particular emphasis on the Rhinegraben.
- Statistical analysis of earthquake occurrence, seismicity modeling and implications for forecasting.

It was also possible to us to provide financial support to six participants from Northern Africa (Morocco and Algeria) to attend the meeting, a fact that helped to establish a more thorough communication between scientists from Europe and Northern African countries. An intense discussion ranging from the need to integrate data from Northern Africa into a harmonized (in terms of magnitudes) earthquake catalogue of the Euro-Med region to questions related to earthquake early warning took place among the participants. Of particular interest was also the presentation of a project for active fault mapping in the Near East, presented by Hillel Wust-Bloch from Tel Aviv University, which is maybe the first of its kind to involve an intense scientific collaboration between Israeli, Palestinian and Jordanian scientists.

Preface

We would like to thank all the participants for attending the workshop and turning it into a big success with their presentations. Furthermore, we are very grateful for all the papers received for this proceedings volume, which cover a wide range of seismological problems and make this volume a valuable contribution toward a better understanding of Euro-Med seismicity. We gratefully acknowledge the reviewing efforts of the scientific committee and invited speakers as well as the external reviewers B. Sperner, O. Heidbach and N. d'Oreye for their careful and constructive reviews, which ensure the high scientific quality of these proceedings.

Finally, the workshop organizers would like to thank the Ministère de la Culture, de l'Enseignement Supérieur et de la Recherche, the Fonds National de la Recherche (FNR) and the Council of Europe for providing the financial support without which it would not have been possible to organize this fruitful workshop. The International Association for Seismology and Physics of the Earth's Interior (IASPEI) helped in disseminating the existence of the workshop and the FNR also financially supported the publication of this Volume of the Cahiers. Many thanks also go to C. Galassi and G. Celli for their invaluable support during the organization of the workshop.

Adrien Oth
European Center for Geodynamics and Seismology (ECGS), October 2009

27th ECGS workshop
Seismicity Patterns in the Euro-Med region

Program

MONDAY NOVEMBER 17 2008

10:00 – 11:30 Registration

11:30 – 12:00 Opening session

12:00 – 13:30 Lunch

Historical and instrumental earthquake catalogues as a critical research infrastructure for Euro-Med seismicity

Chair: Papadopoulos, G. A. and Grünthal, G.

13:30 – 14:10 Godey, S., Bossu, R. and Mazet-Roux, G. **(invited)**

Ten years of seismicity in the Euro-Mediterranean region : Panorama of the EMSC bulletin 1998-2007

14:10 – 14:50 Grünthal, G., Schelle, H., Wahlström, R. and Hakimhashemi, A. **(invited)**

Large and small scale seismicity patterns in the Euro-Med region

14:50 – 15:10 Harbi, A., Peresan, A. and Panza, G.F.

Seismicity of Eastern Algeria : ECEA2005 the revised and extended earthquake catalogue

15:10 – 15:30 Sebai, A. and Harbi, A.

Two destructive earthquakes in 1722 South-West of the Capital Algiers (Algeria)

15:30 – 16:00 Coffee break and Poster session

Large earthquakes in subduction zones, seismic hazard analysis

Chair: Wenzel, F. and Oth, A.

16:00 – 16:40 Papadopoulos, G. A. **(invited)**

The seismic history of Crete from 2000 BC to AD 2008 : Earthquakes and tsunamis in the central segment of the Hellenic arc and trench

Program

- 16:40 – 17:00 Brüstle, A., Meier, T. and Friederich, W.
Investigations of historical seismograms of the 1956 Amorgos-Santorini earthquake ($M_S=7.4$)
- 17:00 – 17:40 Sokolov, V. and Wenzel, F. **(invited)**
A preliminary ground-motion prediction model for Baden-Württemberg, Germany
- 17:40 – 18:00 Grünthal, G., Bosse, C. and Stromeyer, D.
New generation of probabilistic seismic hazard assessment of Germany
- 18:00 – 18:20 Miksat, J., Sokolov, V., Wen, K.-L., Wenzel, F. and Chen, Ch.-T.
Analysis of the Taipei basin response using numerical modeling and empirical data

TUESDAY NOVEMBER 18 2008

The North Anatolian and Dead Sea fault systems

Chair: Hubert-Ferrari, A. and Pucci, S.

- 08:00 – 08:40 Hubert-Ferrari, A., Fraser, J., Böes, X., Avsar, U., Vanneste, K. and Altunel, E. **(invited)**
Seismic patterns of the Anatolian fault system (Turkey)
- 08:40 – 09:20 Wust-Bloch, H., Ziv, A., Inbal, A., Al-Zoubi, A., Al-Dabbeek, J. and Ben-Avraham, Z. **(invited)**
Seismicity patterns within the Dead Sea triangle: microseismic and nanoseismic monitoring perspectives
- 09:20 – 09:40 Sandberg, S., Baris, S., Grosser, H., Özer, M.F., Woith, H., Irmak, S.T. and Günther, E.
Seismicity and tectonics of Armutlu Peninsula, Turkey
- 09:40 – 10:00 Garcia-Moreno, D., Hubert-Ferrari, A., Moernaut, J., Fraser, J., Van Daele, M., De Batist, M. and Damci, E.
Structure and evolution of a main segment boundary along the East Anatolian fault, Turkey
- 10:00 – 10:30 Coffee Break and Poster session
- 10:30 – 11:10 Pucci, S., Pantosti, D. and De Martini, P.M. **(invited)**
The Düzce segment of the North Anatolian Fault Zone (Turkey): Understanding its seismogenic behavior through earthquake geology, tectonic geomorphology and paleoseismology

Program

- 11:10 – 11:30 Köhler, N., Wenzel, F. and Böse, M.
Seismicity in the Marmara region (Turkey) and its relation to seismic early warning
- 11:30 – 11:50 Oth, A., Gottschämmer, E., Böse, M. and Wenzel, F.
Optimizing seismic networks for earthquake early warning – the case of Istanbul (Turkey)
- 12:00 – 13:30 Lunch

Seismicity of Central Europe with particular emphasis on the Rhinegraben

Chair: Camelbeeck, Th. and Wenzel, F.

- 13:30 – 14:10 Camelbeeck, Th., Vanneste, K. and Alexandre, P. **(invited)**
The seismic activity in Northwest Europe
- 14:10 – 14:30 Barth, A., Delvaux, D. and Wenzel, F.
Tectonic stress field in rift systems – a comparison of Rhinegraben, Baikal Rift and East African Rift
- 14:30 – 14:50 Lecocq, Th., Van Camp, M., Vanneste, K. and Camelbeeck, Th.
The seismic sequency since July 2008 in central Belgium
- 15:00 – 16:00 Poster session
- 16:00 – 17:30 City Tour
- 17:30 – 19:00 Guided tour to the National Museum of Natural History
- 19:00 Conference dinner at the National Museum of Natural History

WEDNESDAY NOVEMBER 19 2008

Statistical analysis of earthquake occurrence, seismicity modeling and implications for forecasting

Chair: Ziv, A. and Wust-Bloch, H.

- 08:00 – 08:40 Fischer, T., Hainzl, S. and Horálek, J. **(invited)**
Seismicity patterns of earthquake swarms in the West-Bohemia/Vogtland as a tool to the search for their triggering mechanisms
- 08:40 – 09:20 Chiaraluce, L., Chiarabba, C., Collettini, C., Piccinini, D. and Cocco, M. **(invited)**
Anatomy and seismic release of a major normal fault system located along the Northern Apennines of Italy

Program

- 09:20 – 09:40 Vallianatos, F.
Fundamental properties of fracture and seismicity in a non extensive statistical framework
- 09:40 – 10:00 Gospodinov, D. Karakostas, V., Papadimitriou, E. and Ranguelov, B.
Relaxation temporal patterns after eight strong earthquakes in Greece studied through the RETAS model approach
- 10:00 – 10:30 Coffee Break and Poster session
- 10:30 – 11:10 Ziv, A. **(invited)**
The physics of delayed remote aftershocks
- 11:10 – 11:30 Hafez, A.G., Khan, T.A. and Kohda, T.
Clear P-wave arrival of weak events and automatic onset determination using wavelet filter banks
- 11:30 – 11:50 Bouhadad, Y.
Seismic hazard in Eastern Algeria based on the seismic potential of active faults
- 12:00 – 13:30 Lunch
- 13:30 – 13:50 Ouyed, M. and Boughacha, M.S.
Seismicity analysis of Algeria and adjacent regions through 1972-2007
- 13:50 – 14:10 Boughacha, M.S. and Ouyed, M.
Static stress transfer mapping in Northern Algeria and adjacent regions through 1980-2007
- 14:10 – 14:30 Akhouayri, E.-S. and Agliz, D.
Seismic instrumentation development at Agadir City
- 14:30 – 15:30 Discussion and closing session
- 16:00 – 17:00 Visit of the Underground Laboratory at Walferdange

POSTERS

- 01 Daskalaki, E. and Papadopoulos, G.A. *Rupture zones of large earthquakes and seismic potential in the Hellenic arc and trench*
- 02 Kolligri, M. *Seismological aspects and seismotectonics of the Mw 6.4 Kato Achaia (W. Greece) earthquake of 8 June 2008*
- 03 Popa, M., Radulian, M., Mandrescu, N. and Paulescu, D. *Seismicity patterns in Vrancea region as revealed by revised historical and instrumental catalogues*
- 04 Bala, A., Radulian, M., Grecu, B. and Popescu, E. *Source effect vs. site effect of Vrancea earthquakes recorded in Bucharest City, Romania*
- 05 Raileanu, V., Dinu, C., Bala, A., Ardeleanu, L. and Popescu, E. *Crustal seismicity and associated fault fields in Romania*
- 06 Apostol, B.-F. and Balan, S.F. *Statistical distribution of earthquakes and urban seismology in Romania*
- 07 Rogozea, M., Popa, M., Zaharia, B. and Radulian, M. *Vrancea (Romania) seismic cycle modelling on the basis of characteristic space-time-size earthquake distributions*
- 08 Akhouayri, E.-S., Iaasri, H.A., Agliz, D. and Atmani, A. *Agadir's central seismic acquisition management*
- 09 Mihailov, V. and Dojcinovski, D. *Application of the Markov's process in modeling seismic occurrences – a study case*
- 10 Mihailov, V. and Dojcinovski, D. *Seismic monitoring of structures – a tool for seismic hazard reduction*

List of Participants

AKHOUAYRI ES-SAID
UNIVERSITY IBN ZOHR
FACULTY OF SCIENCES
BOITE POSTALE 8106
AGADIR
MOROCCO
akhouayri@msn.com

APOSTOL BOGDAN FELIX
NATIONAL INSTITUTE OF RESEARCH AND
DEVELOPMENT FOR EARTH PHYSICS
12 CALUGARENI STR.
MAGURELE-BUCHAREST / ILFOV
ROMANIA
apostol@infp.infp.ro

BALA ANDREI
NATIONAL INSTITUTE OF RESEARCH AND
DEVELOPMENT FOR EARTH PHYSICS
12 CALUGARENI STR
MAGURELE-BUCHAREST / ILFOV
ROMANIA
bala@infp.ro

BALAN STEFAN FLORIN
NATIONAL INSTITUTE OF RESEARCH AND
DEVELOPMENT FOR EARTH PHYSICS
12 CALUGARENI STR.
MAGURELE-BUCHAREST / ILFOV
ROMANIA
sbalan@infp.infp.ro

BARTH ANDREAS
GEOPHYSICAL INSTITUTE
UNIVERSITY OF KARLSRUHE
HERTZSTRASSE 16
D-76187 KARLSRUHE
GERMANY
andreas.Barth@gpi.uni-karlsruhe.de

BECHET GEORGES
MNHN - MUSEE NATIONAL D'HISTOIRE
NATURELLE
25, RUE MUENSTER
L-2160 LUXEMBOURG
GRAND-DUCHY OF LUXEMBOURG
Georges.bechet@mnhn.lu

BONATZ MANFRED
GeoOBSERVATORIUM ODENDORF
UNIVERSITY BONN
WILKENSTRASSE 49
D-53913 ODENDORF
GERMANY
geo.bonatz@t-online.de

BOUGHACHA M.S.
HOUARI BOUMEDIENE UNIVERSITY OF
SCIENCE AND TECHNOLOGY
DEPARTMENT OF GEOPHYSICS
P.O. BOX 32
EL-ALIA / BAB-EZZOUAR /ALGIERS
16111 ALGERIA
m_sboughacha@yahoo.com

BOUHADAD YOUCEF
NATIONAL CENTER OF APPLIED RESEARCH
IN EARTHQUAKE ENGINEERING (CGS)
1, RUE KADDOUR RAHIM, H-DEY
ALGER
16040 ALGERIA
PHONE : +273 21 49 55 49
FAX : +273 21 49 55 36
ybouhadad@cgs-dz.org

BRÜESTLE ANDREA
RUHR-UNIVERSITY BOCHUM
INSTITUTE OF GEOLOGY, MINERALOGY AND
GEOPHYSICS
GEB. NA 3/171
P.O. BOX 102148
D-44721 BOCHUM
GERMANY
bruestle@geophysik.ruhr-uni-bochum.de

BUTTINI ERIC
ECGS / MNHN
EUROPEAN CENTER FOR GEODYNAMICS AND
SEISMOLOGY
19, RUE JOSY WELTER
L-7256 WALFERDANGE
GRAND-DUCHY OF LUXEMBOURG
ebuttini@ecgs.lu

CAMELBEECK THIERRY
ROYAL OBSERVATORY OF BELGIUM
RINGLAAN 3
B-1180 BRUSSELS
BELGIUM
Thierry.Camelbeeck@oma.be

CELLI GILLES
ECGS / MNHN
EUROPEAN CENTER FOR GEODYNAMICS AND
SEISMOLOGY
19, RUE JOSY WELTER
L-7256 WALFERDANGE
GRAND-DUCHY OF LUXEMBOURG
gilles.cellli@ecgs.lu

CHIARALUCE LAURO
ISTITUTO NAZIONALE DI GEOFISICA E
VULCANOLOGIA
CENTRO NAZIONALE TERREMOTI
VIA DI VIGNA MURATA 605
I-00143 ROMA
ITALY
chiaraluce@ingv.it

List of Participants

DASKALAKI ELENI
NATIONAL OBSERVATORY OF ATHENS
INSTITUTE OF GEODYNAMICS
P.O. BOX 20048
GR-11810 THISSIO , ATHENS
GREECE
edaskal@gein.noa.gr

DONNER STEFANIE
GFZ - GERMAN RESEARCH CENTRE FOR
GEOSCIENCES
TELEGRAFENBERG 456
D-14473 POTSDAM
GERMANY
sberg@gfz-potsdam.de

DRAB LAUREEN
CENTRE NATIONAL DE LA RECHERCHE
LABORATOIRE DE GEOLOGIE
3 ALLEE D'OZONVILLE
F-91200 ATHIS MONS
FRANCE
PHONE : 0033 6 03 39 98 59
drab@geologie.ens.fr

FISCHER TOMAS
CHARLES UNIVERSITY IN PRAGUE
FACULTY OF SCIENCE
ABLERTOVS 6
PRAHA 2
CZECH REPUBLIC
fischer@natur.cuni.cz

GARCIA MORENO DAVID
ROYAL OBSERVATORY OF BELGIUM
RINGLAAN 3
B-1180 BRUSSELS
BELGIUM
D.Garcia.Moreno@oma.be

GOSPODINOV DRAGOMIR
GEOPHYSICAL INSTITUTE
BULGARIAN ACADEMY OF SCIENCES
CENTRALNA POSTA PK 258
4000 PLOVDIV
BULGARIA
drago@geophys.bas.bg

HAFEZ EL NASSER ALI
KYUSHU UNIVERSITY
DEPARTMENT OF COMPUTER SCIENCE AND
COMMUNICATION ENGINEERING
744 MOTOOKA
NISHI-KU
FUKUOKA-SHI
JAPAN
aligamal@kairo.csce.kyushu-u.ac.jp

DOJCINOVSKI DRAGI
INSTITUTE OF EARTHQUAKE ENGINEERING
AND ENGINEERING SEISMOLOGY
UNIVERSITY ST. CYRIL AND METHODIUS
P.O. BOX 101
SKOPJE
1000 REPUBLIC OF MACEDONIA
dragi@pluto.iziis.ukim.edu.mk

D'OREYE NICOLAS
MNHN - MUSEE NATIONAL D'HISTOIRE
NATURELLE
25, RUE MUENSTER
L-2160 LUXEMBOURG
GRAND-DUCHY OF LUXEMBOURG
ndo@ecgs.lu

FEIDER MICHEL
Président du Conseil d'Administration de l'ECGS
ADMINISTRATION DES SERVICES DE SECOURS
1, RUE ROBERT STUMPER
L-2557 LUXEMBOURG
GRAND-DUCHY OF LUXEMBOURG
Michel.feider@secours.etat.lu

GALASSI CORINE
ECGS
EUROPEAN CENTER FOR GEODYNAMICS AND
SEISMOLOGY
19, RUE JOSY WELTER
L-7256 WALFERDANGE
GRAND-DUCHY OF LUXEMBOURG
corine.galassi@ecgs.lu

GODEY STEPHANIE
EMSC - EUROPEAN MEDITERRANEAN
SEISMOLOGICAL CENTRE
COMMISSARIAT A L'ENERGIE ATOMIQUE
CENTRE DAM
ILE DE FRANCE - BRUYERES LE CHATEL
F-91297 ARPAJON
FRANCE
godey@emsc-csem.org

GRUENTHAL GOTTFRIED
GFZ - GERMAN RESEARCH CENTRE FOR
GEOSCIENCES
TELEGRAFENBERG 456
D-14473 POTSDAM
GERMANY
ggrue@gfz-potsdam.de

HARBI ASSIA
CRAAG - CENTRE DE RECHERCHE EN
ASTRONOMIE, ASTROPHYSIQUE ET
GEOPHYSIQUE
ROUTE DE L'OBSERVATOIRE
B.P. 63 - BOUZAREAH
16340 ALGIERS
ALGERIA
harbi.assia@gmail.com

List of Participants

HUBERT-FERRARI AURELIA
ROYAL OBSERVATORY OF BELGIUM
RINGLAAN 3
B-1180 BRUSSELS
BELGIUM
Aurelia.Ferrari@oma.be

KOEHLER NINA
GEOPHYSICAL INSTITUTE
UNIVERSITY OF KARLSRUHE
HERTZSTRASSE 16
D-76187 KARLSRUHE
GERMANY
Nina.Koehler@gpi.uni-karlsruhe.de

LECOQ THOMAS
ROYAL OBSERVATORY OF BELGIUM
RINGLAAN 3
B-1180 BRUSSELS
BELGIUM
thomas.lecocq@oma.be

MIKSAT JOACHIM
GEOPHYSICAL INSTITUTE
UNIVERSITY OF KARLSRUHE
HERTZSTRASSE 16
D-76187 KARLSRUHE
GERMANY
joachim-miksat@gpi.uni-karlsruhe.de

OUYED MERZOUK
HOUARI BOUMEDIENE UNIVERSITY OF
SCIENCE AND TECHNOLOGY
DEPARTMENT OF GEOPHYSICS
P.O. BOX 32
16111 EL-ALIA / BAB-EZZOUAR /ALGIERS
ALGERIA
mouyed@caramail.com

POPA MIHAELA
NATIONAL INSTITUTE OF RESEARCH AND
DEVELOPMENT FOR EARTH PHYSICS
12 CALUGARENI STR.
MAGURELE-BUCHAREST / ILFOV
ROMANIA
mihaela@infp.ro

RADULIAN MIRCEA
NATIONAL INSTITUTE OF RESEARCH AND
DEVELOPMENT FOR EARTH PHYSICS
12 CALUGARENI STR.
MAGURELE-BUCHAREST / ILFOV
ROMANIA
mircea@infp.ro

KHAN MUHAMMAD TAHIR ABBAS
RITSUMEIKAN ASIA PACIFIC UNIVERSITY
1-1 JUMONJIBARU
BEPPU-SHI
874-8577 OITA
JAPAN
tahir@apu.ac.jp

KOLLIGRI MARIA
NATIONAL OBSERVATORY OF ATHENS
INSTITUTE OF GEODYNAMICS
P.O. BOX 20048
GR-11810 THISSIO , ATHENS
GREECE
mkolligri@yahoo.com

MIHAILOV VLADIMIR
INSTITUTE OF EARTHQUAKE ENGINEERING
AND ENGINEERING SEISMOLOGY
UNIVERSITY ST. CYRIL AND METHODIUS
P.O. BOX 101
1000 SKOPJE
REPUBLIC OF MACEDONIA
mihailov@pluto.iziis.ukim.edu.mk

OTH ADRIEN
ECGS
EUROPEAN CENTER FOR GEODYNAMICS AND
SEISMOLOGY
19, RUE JOSY WELTER
L-7256 WALFERDANGE
GRAND-DUCHY OF LUXEMBOURG
adrien.oth@ecgs.lu

PAPADOPOULOS GERASSIMOS
NATIONAL OBSERVATORY OF ATHENS
INSTITUTE OF GEODYNAMICS
P.O. BOX 20048
GR-11810 THISSIO , ATHENS
GREECE
papadop@gein.noa.gr

PUCCI STEFANO
ISTITUTO NAZIONALE DI GEOFISICA E
VULCANOLOGIA
ACTIVE TECTONICS
VIA DI VIGNA MURATA 605
I-00143 ROMA
ITALIA
pucci@ingv.it

RAILEANU VICTOR
NATIONAL INSTITUTE OF RESEARCH AND
DEVELOPMENT FOR EARTH PHYSICS
12 CALUGARENI STR.
MAGURELE-BUCHAREST / ILFOV
ROMANIA
raivic@infp.infp.ro / rai@yahoo.com

List of Participants

SCHARES NICO
VILLE DE LUXEMBOURG
DIRECTION - SERVICES DU GEOMETRE
1-3, RUE DU LABORATOIRE
L-1911 LUXEMBOURG
GRAND-DUCHY OF LUXEMBOURG
nschares@vdl.lu

WENZEL FRIEDEMANN
GEOPHYSICAL INSTITUTE
UNIVERSITY OF KARLSRUHE
HERTZSTRASSE 16
D-76187 KARLSRUHE
GERMANY
Friedemann.wenzel@gpi.uka.de

WUST-BLOCH HILLEL
TEL AVIV UNIVERSITY
GEOPHYSICS & PLANETARY SCIENCE
P.O. BOX 39040
69978 TEL AVIV
ISRAEL
hillel@seismo.tau.ac.il

ZIV ALON
BEN GURION UNIVERSITY OF THE NEGEV
DEPT. OF GEOLOGICAL AND ENVIRONMENTAL
SCIENCES
P.O. BOX 653
84105 BEER-SHEVA
ISRAEL
zival@bgu.ac.il

Ten years of seismicity in the Euro-Mediterranean region: Panorama of the EMSC bulletin 1998-2007

Stéphanie Godey (1), Gilles Mazet-Roux (1), Rémy Bossu (1), Sophie Merrer (1) and Jocelyn Guilbert (2)

- 1) European Mediterranean Seismological Centre, CEA-DAM Ile de France, Bruyères-le-Châtel, 91297 Arpajon, France
- 2) LDG, DASE, CEA-DAM Ile de France, Bruyères-le-Châtel, 91297 Arpajon, France

Abstract

The Euro-Mediterranean Seismological Center (EMSC) is in charge since 1998 of collecting seismological parametric data recorded by local institutes of the Euro-Mediterranean region in order to improve data availability for the seismological community and to rapidly produce a comprehensive bulletin for the region. The goals are to reproduce the seismicity as imaged by the local agencies when events occur within their network and to improve event location in borders regions and off-shore.

The Euro-Med Bulletin now contains ten years of seismicity from January 1998 to December 2007. Event locations have been obtained by merging parametric data collected from 77 seismological agencies. Thanks to the many contributions, the Euro-Med Bulletin displays a high coverage of the region with the collection of data recorded by 2,465 stations. In total, 102,000 events are included for the period 1998-2007. We present here the performances of the Euro-Med Bulletin and their evolution over the years.

Willing to continuously improve its performances, the EMSC is working on further discarding non tectonic events from the current Euro-Med bulletin which could be achieved by setting up additional collection of event type information (from rockburst to mine activity) with the help of the local networks. Additionally, the currently available bulletin will be enriched with low magnitude events and will be recomputed using the global velocity model ak135 as recommended by IASPEI.

Introduction

The European Mediterranean Seismological Center (EMSC), created in 1975, is an international NGO hosted since 1992 by the LDG (Laboratoire de Détection et de Géophysique, CEA France). Its members are seismological institutes and observatories of the Euro-Med region that spans from Iceland in the North West to Yemen in the South East. Its main scientific activities are Real Time Earthquake Information services and the production of the Euro-Med Bulletin (Godey et al., 2006) accessible on the web (www.emsc-csem.org).

The Bulletin activities rely on the collection of manually revised parametric data provided by the seismological networks of the Euro-Med region. After merging the data, the Euro-Med Bulletin is reviewed then published through the internet and provided to the ISC.

The main objectives of the Euro-Med bulletin are to:

- Collect and archive bulletin data from the Euro-Med region.
- Improve data availability for the seismological community through the EMSC database collected since 1998 (including contributors and EMSC bulletins).
- Produce a regular bulletin rapidly after earthquake occurrence in the Euro-Med region with a magnitude threshold of 3.0.
- Reproduce the seismicity when occurring inside the local networks region and improve events location in border regions and off-shore.
- Compute magnitude when station amplitude/period information are provided.

Data Collection and Bulletin Production

The data collected by the EMSC are manually revised parametric information. These information can be either bulletins data which include earthquake source parameters (origin time, epicentre, depth, event type and magnitudes) with the associated arrivals or groups of arrivals for which no location is available. The groups and isolated arrivals are useful as they can be associated to a hypocenter reported by other networks and help constraining the hypocenter location. For all data types, the detailed arrivals information include station code, phase identification, arrival time and amplitude/period information when available. All station codes must be registered at the International Seismological Station Registry, maintained by the ISC and the NEIC. The EMSC has become an important relay from the local institutes helping in the registration of more than 700 stations participating for the first time to international data exchange.

The EMSC encourages data contributors to provide rapidly (weekly or mnthly) their data to ensure their full use in the EMB production. The recommended procedure to provide data to the EMSC is ascii format by email.

The production of the EMB relies on the association of the data collected from several networks and the computation of event hypocenters using the related readings (Godey et al., 2006). The software to perform the association and event location was developed by our host, the LDG and was incorporated in the Euro-Med Bulletin production in the framework of the EPSI project (Earthquake Parameters and Standardised Information for a European-Mediterranean Bulletin). The epicenter location method is based on an improved version of the Geiger algorithm (Geiger, 1910). A triangulation method is applied for local events and a classical Husebye method is performed for teleseismic events. The current location procedure uses both local and global velocity models. The crustal velocity models are provided by the contributing networks or were defined for border regions within the EPSI project. The global velocity models are based on the Jeffreys-Bullen tables for P and S phases (Jeffreys and Bullen, 1940) and Iaspei91 for the other phases (Storchak *et al.*, 2003). For each event, an automatic location is computed using phases from different networks before entering a manual review (for approximately 80% of the events).

Data Contributions and Evolution Over Ten Years

Since 1998, the EMSC has received data from 77 different data contributors from 56 countries (Appendix A). All of the institutes did not provide data continuously, some of them were temporary networks and others have merged under a unique institute. Therefore the maximum number of unique contributors is 71, reached in 2007. The evolution over ten years (Fig. 1) shows a drastic increase in the data collection, particularly in the last years. The large increase observed since 2003 reflects the combined effort of the EMSC and the network operators to establish reliable data exchange procedure. Several networks have started to make their data available to the international community by providing for the first time their data to the EMSC. Among those new contributors, we can name Tunisia, Libya, Egypt, Uzbekistan, Dubai, Latvia, Belarus and Lithuania. Those new contributions made the Euro-Med Bulletin the most complete collection of data for the region.

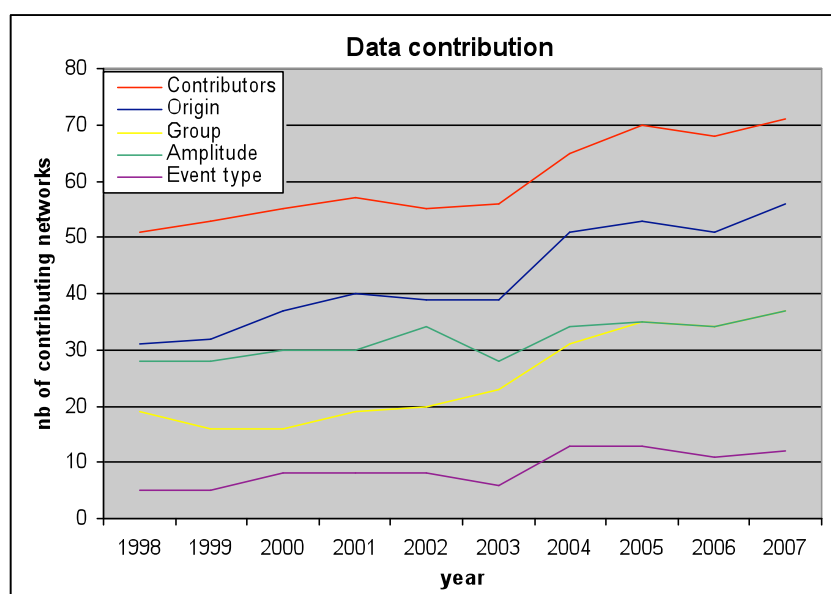


Figure 1: Evolution of the data contribution by the EMSC between 1998 and 2008.

In addition to basic parametric data, 37 networks (in 2007) provide amplitude and period information to the EMSC. These information are crucial to calculate an independent estimation of the magnitude. Since 1998, the number of networks providing amplitude/period information has increased from 28 to 37 over ten years, but still only represents 50% of all contributing networks.

Event type information is provided in the Euro-Med bulletin. It includes earthquake but also non tectonic event information such as rock burst, induced event, mine explosion, experimental explosion, nuclear explosion, landslide using the nomenclature defined in IASPEI (Bormann, 2002). It is becoming a crucial point to avoid misinterpreting the seismicity in a specific region. In particular, if a seismicity catalogue is used for seismic hazard assessment studies, draw-backs can be propagated. However, identifying induced seismicity is only possible when the contributors provide this information. Though the EMSC is devoting a large effort to collect event type description, it is often missing from the data contributions. Since 1998, a total of 15 networks (this values varying over the years) have included event type information in their data exchange (Fig. 1). Seven networks only provide

information on known earthquakes and discard non tectonic events from their contribution to the EMSC. More contributions and detailed event type policy information are needed to further discard non tectonic activity from the Euro-Med Bulletin.

A total of 2,465 stations in the Euro-Med region (Fig. 2) have reported revised parametric data to EMSC since 1998. The distribution of stations in the Euro-Med region shows a good coverage except gaps in Ukraine and parts of the Middle East (Fig. 2).

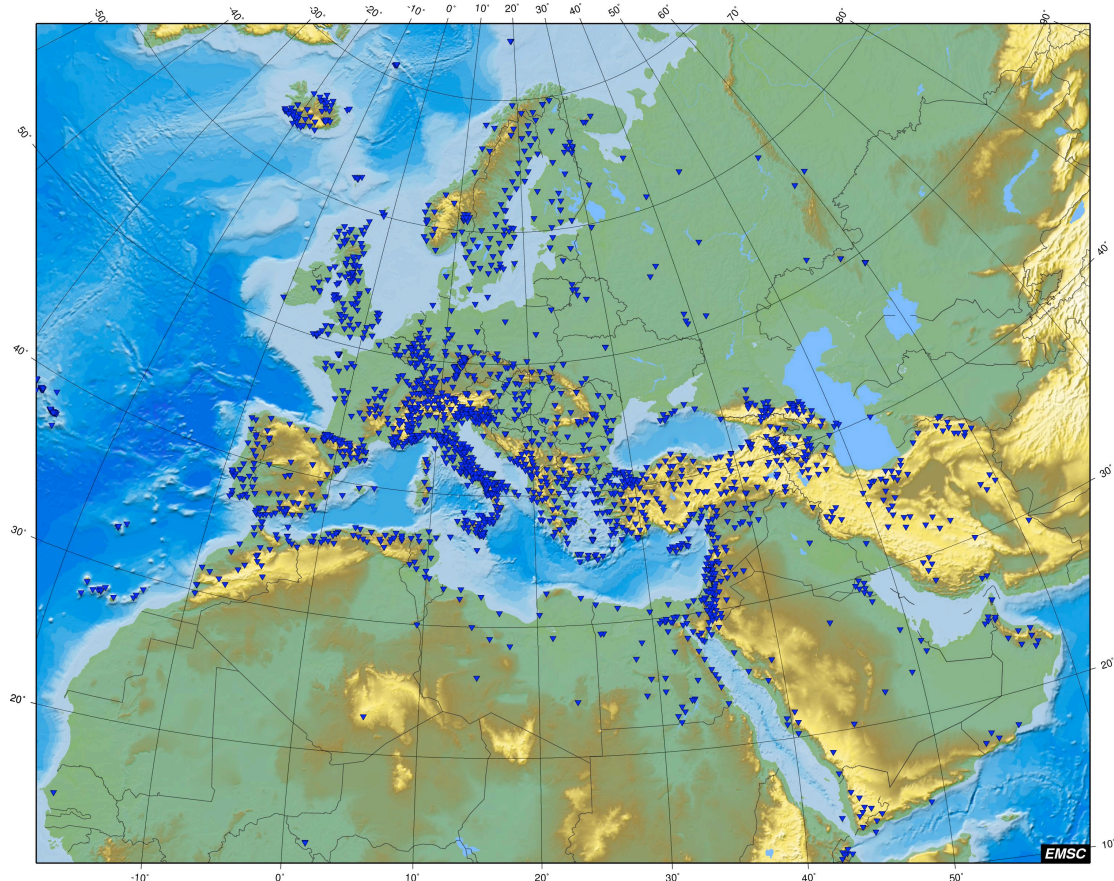


Figure 2: Location of the contributing stations to the Euro-Med bulletin.

Products and Data Access

Three classes of events are defined for the Euro-Med Bulletin.

- Associated events are events for which phase association from several networks is possible. In this case, a new location is computed.
- Reported events are events recorded by a single network in its authoritative region. This region corresponds to the network deployment area, comprising the country and extending into the sea or neighboring countries. In this case, no phase association is possible and the location of the local network is reported without relocation.
- Deprecated events are events recorded by a distant network (outside of its authoritative region). No phase association is possible and the location of the contributing network is reported without relocation and flagged as dubious. These events are discarded from the published Euro-Med Bulletin. Their access is only possible upon specific request.

The Euro-Med catalogue (list of locations) is fully available to the general public on our web site <http://www.emsc-csem.org/index.php?page=data&sub=drm>. Free and full access to the raw bulletins (i.e. original bulletins provided by the contributing networks) database (by autoDRM) and to the Euro-Med Bulletin is given to all data contributors and EMSC members for non commercial uses through our web site <http://www.emsc-csem.org/index.php?page=data&sub=drm>. The requested data are provided in GSE2.0 format. By the end of 2009, all EMB products should become available to all. Since 2006, the Euro-Med Bulletin is also integrated to the ISC bulletin.

Euro-Med Bulletin 1998-2007 Content

For the period January 1998 to December 2007, the Euro-Med bulletin encompasses 102,014 events (corresponding to above 2.5 millions phases). Since 2003, the amount of events in the Euro-Med bulletin has dramatically increased reaching 21,562 events for the year 2007 (Fig. 3). This increase is related to the additional contributions from several networks and to the change of the magnitude threshold (from 3.0 to 2.5) applied in the manual revision. The evolution of the number of phases used in the Euro-Med Bulletin over the years follows a similar trend.

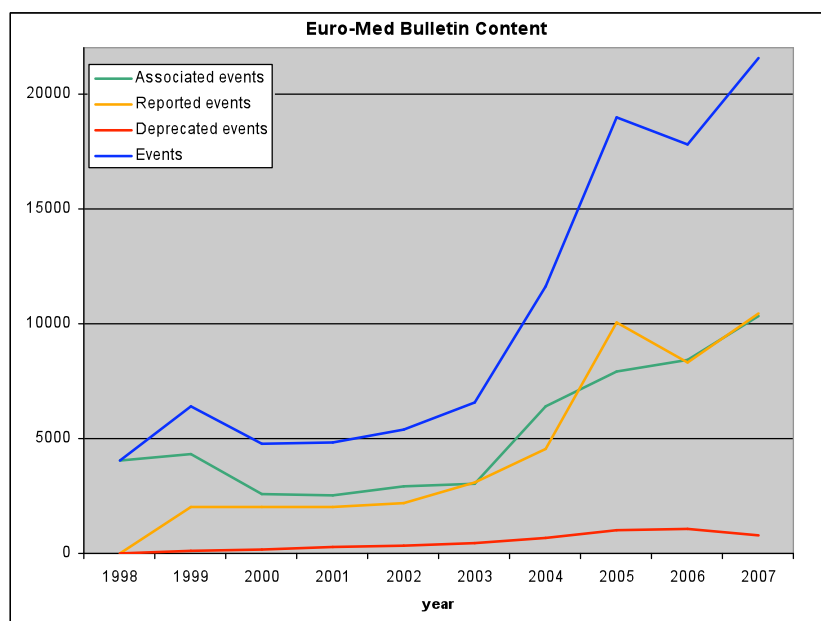


Figure 3: Evolution of the data content of the Euro-Med Bulletin from 1998 to 2007.

Fig. 3 also shows the evolution for each type of classes. The number of reported events has increased in a similar way to the number of associated events in relation with the growing contributions. Those events occurred mostly in the seismically active Aegean region. The higher number of reported events in 2005 is also mainly related to the Greek earthquake sequence of October and November for which smaller events were only reported by the National Observatory of Athens.

Seismicity in the Euro-Med Region between 1998 and 2007

The Euro-Mediterranean region is the scene of highly variable tectonic processes although the African-Eurasian plate interaction dominates the geodynamic regime. Regions with the highest seismicity are related to major faults (North Anatolian fault,

Dead Sea fault) corresponding to shallow earthquakes and subduction zones (Hellenic Arc, Calabria, Vrancea) displaying deeper events. Subcrustal seismicity is also depicted near the Gibraltar Arc and in the South of Spain. Seismicity occurs also along the Mid Atlantic and the Red Sea-Aden Gulf Ridges. Continental collision also generates high subcrustal seismicity in the Zagros region. Other areas of lower seismicity are characterized by diffuse and intermittent activity.

The maps of natural seismicity obtained in the Euro-Med Bulletin (where non tectonic events and deprecated events are discarded) are presented on Fig. 4 and 5 as a function of magnitude and depth.

Both magnitude and hypocentral distributions obtained characterised well the seismicity. Three earthquakes of magnitude greater than 7.0 are observed and 44 events of magnitude greater than 6.0 (Fig. 4). For magnitude lower than 3.5, heterogeneous distribution can be obtained as each network uses different magnitude threshold in their contribution to the EMSC. The threshold applied by the Icelandic network is set to 3.5, whereas it is set to 2.0 in Norway. Seismicity in the Sub-Saharan Africa and part of Russia is under sampled in the Euro-Med Bulletin due to little constraints available in those areas. Low magnitude seismicity may also be missing at the edges of the study areas (Mid Atlantic Ridge, Aden Gulf).

Seismicity related to subduction zones are well characterised in the Euro-Med bulletin (Fig. 5) in the Tyrrhenian Sea and in the Hellenic Arc. The Vrancea is defined by a narrow zone of large depth seismicity. Intermediate seismicity is observed in the Gibraltar, Zagros and Cyprus regions.

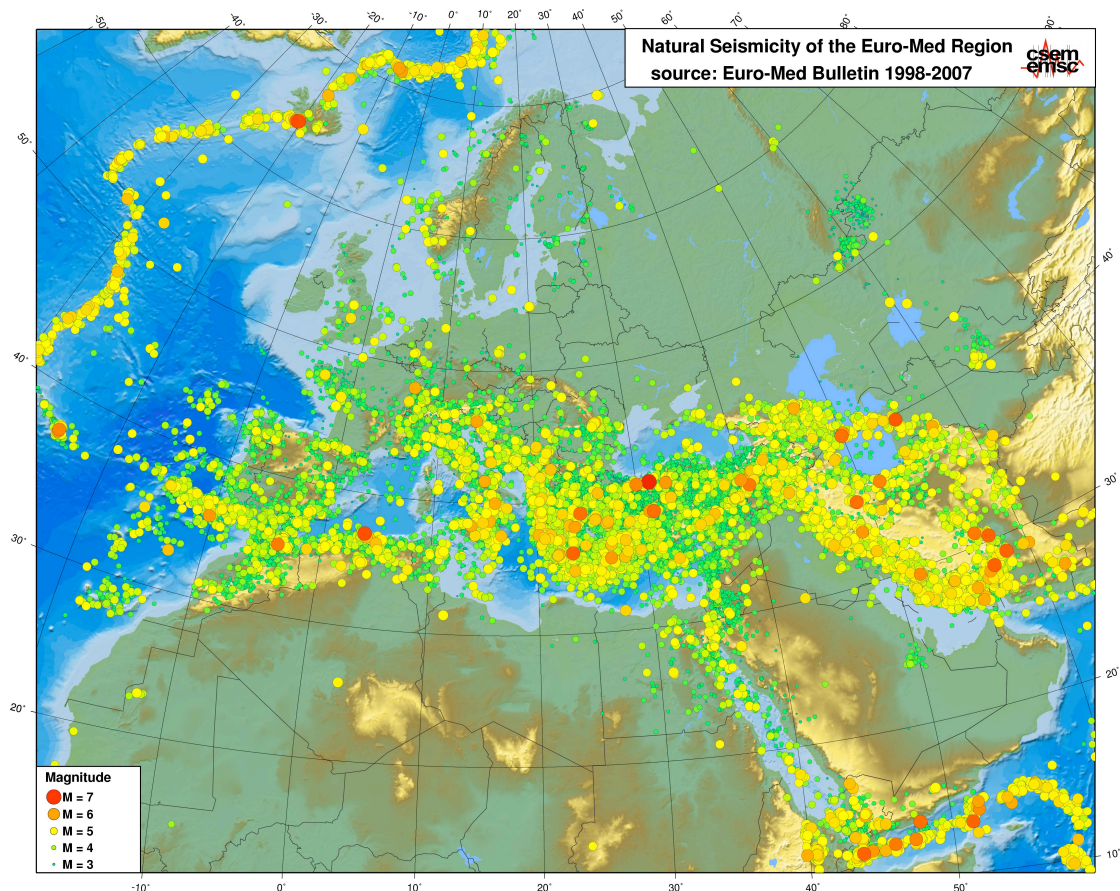


Figure 4: Earthquakes magnitude distribution in the Euro-Med bulletin between 1998 and 2007.

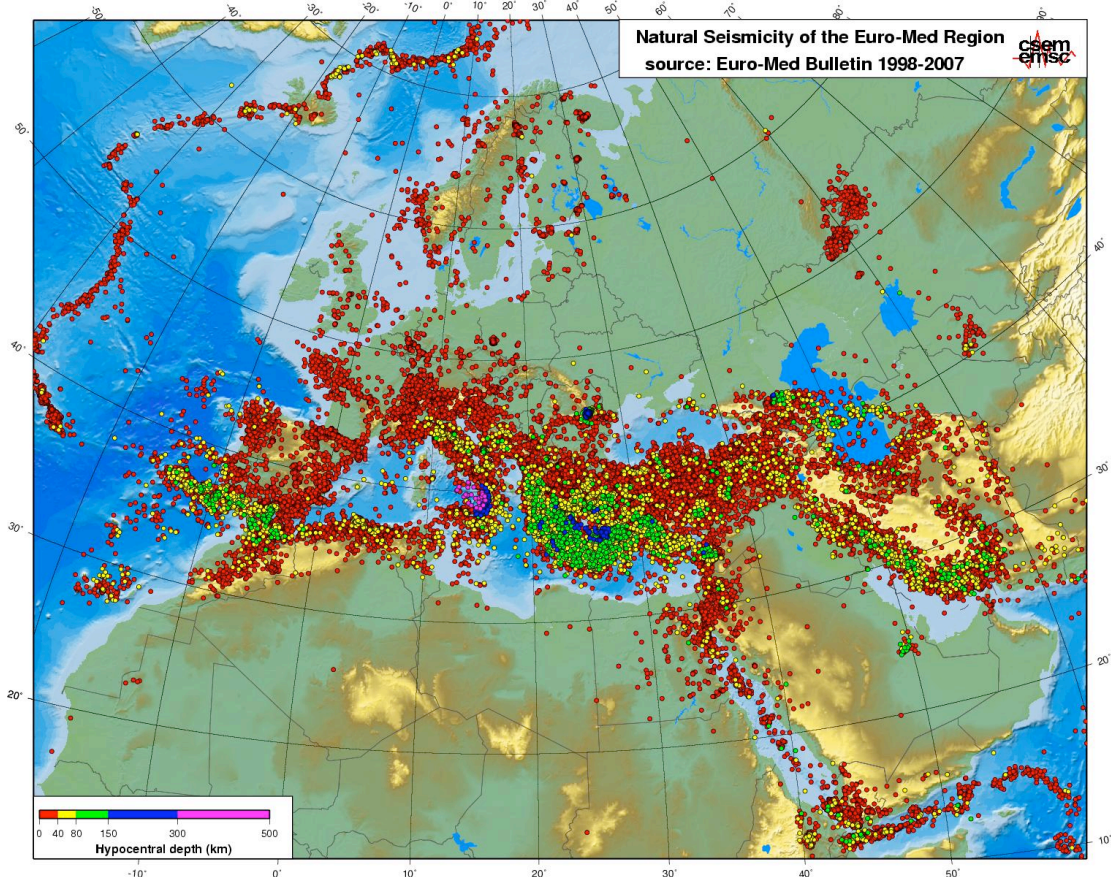


Figure 5: Earthquakes hypocentral distribution in the Euro-Med bulletin between 1998 and 2007.

Euro-Med Bulletin Performances

The Gutenberg Richter law computed for associated and reported events displays a magnitude ML completeness of 2.8 (Fig. 6). The completeness has been improved in the Euro-Med Bulletin since 2006 when the magnitude threshold for reviewing was lowered to 2.5 (Godey et al., 2006). The magnitude completeness is 4.0 for mb magnitude (Fig. 6).

The comparison of 6,266 events reported by the NEIC (PDES) for which mb magnitude are available shows a large agreement of the two bulletins (Fig. 7) with 86% of the events displaying a magnitude difference of less than 0.2. In terms of ML magnitude, 3,068 events could be compared. Again, the two bulletins are largely consistent. However, most ML values included in the EMB and PDES are not independent but reported from the same local networks.

The azimuthal gap provides a first insight on the earthquake location constraint obtained in the Euro-Med Bulletin. The results for the period 1998-2007 are provided on Fig. 8 for associated events. High resolution is observed for most of the Euro-Med region although lower azimuthal gap is obtained at the outskirts of the area and at the coasts (e.g. West of Gibraltar). The active region of Greece and Turkey is well covered, except in the Libyan and Ionian Seas. In this region, improvements are already observed since 2007 thanks to the data contribution from Libya. In the North of the Red Sea, lower resolution is also obtained which should be improved by new data contribution from Saudi Arabia and Egypt.

Over the 10 years for which the Euro-Med Bulletin has been computed, the azimuthal gap has greatly improved. 70% of the events of 2007 display a gap lower than 140° against 45% in 1998 (Fig. 9).

To further assess the accuracy of the earthquakes location included in the Euro-Med Bulletin, we have performed a search of events fulfilling the ground truth (GT)

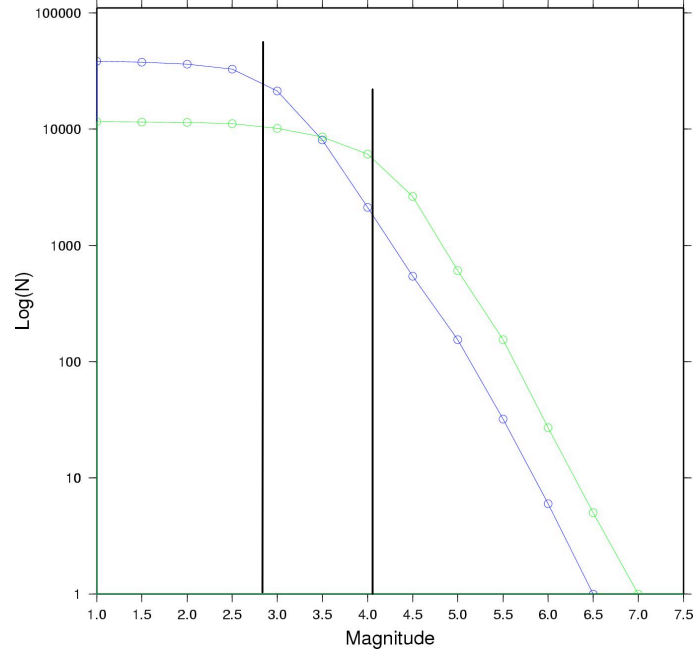


Figure 6: Gutenberg-Richter cumulative distribution for mb (Green) and ML (blue) magnitudes observed in the Euro-Med bulletin.

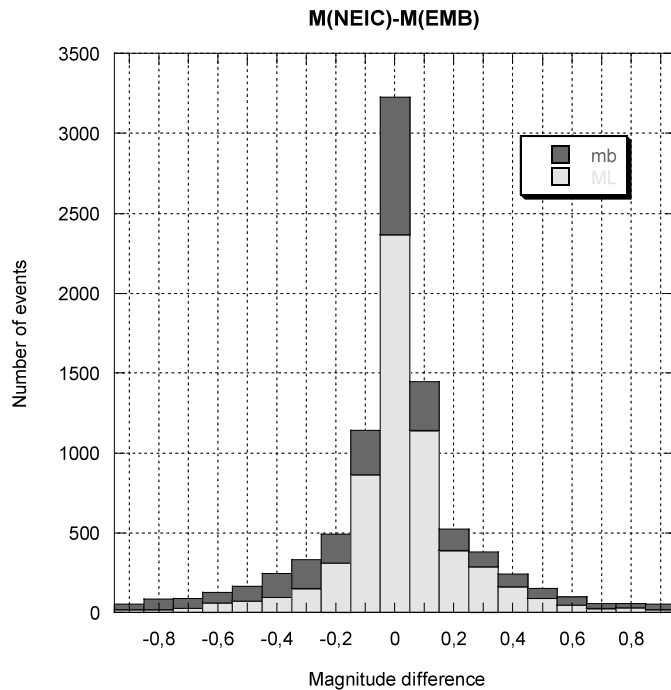


Figure 7: Comparison of mb and ML magnitudes computed at the NEIC and in the Euro-Med bulletin for all associated events. Mean values are -0.06 for mb and 0.02 for ML. Associated standard deviations are 0.49 for mb and 0.27 for ML.

criteria as defined by Bondar et al. (2004). 4,702 events of our bulletin correspond to GT5 events at 95% confidence (Fig. 10). For those events the epicenter information uncertainty is estimated to 5km. Their number has steadily increased over the years, from 200 in 1998 to 1,400 in 2007, showing the ongoing improvements in the data collection and bulletin production at the EMSC. The distribution of GT5 events mainly relies on the station distribution. Most of the GT5 events lay in Western Europe and in Turkey where the station density is the highest.

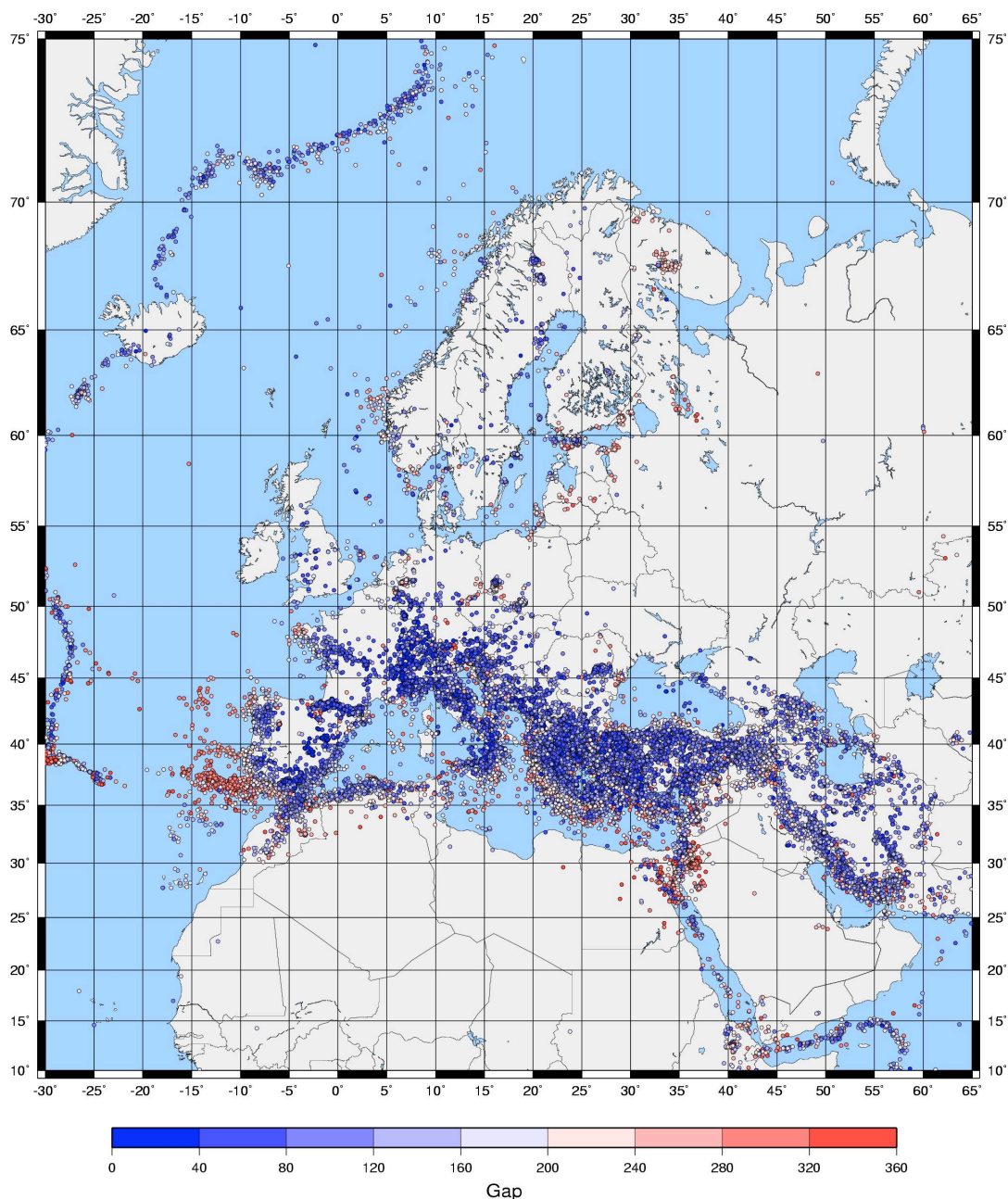


Figure 8: Azimuthal gap distribution of associated events in the Euro-Med Bulletin.

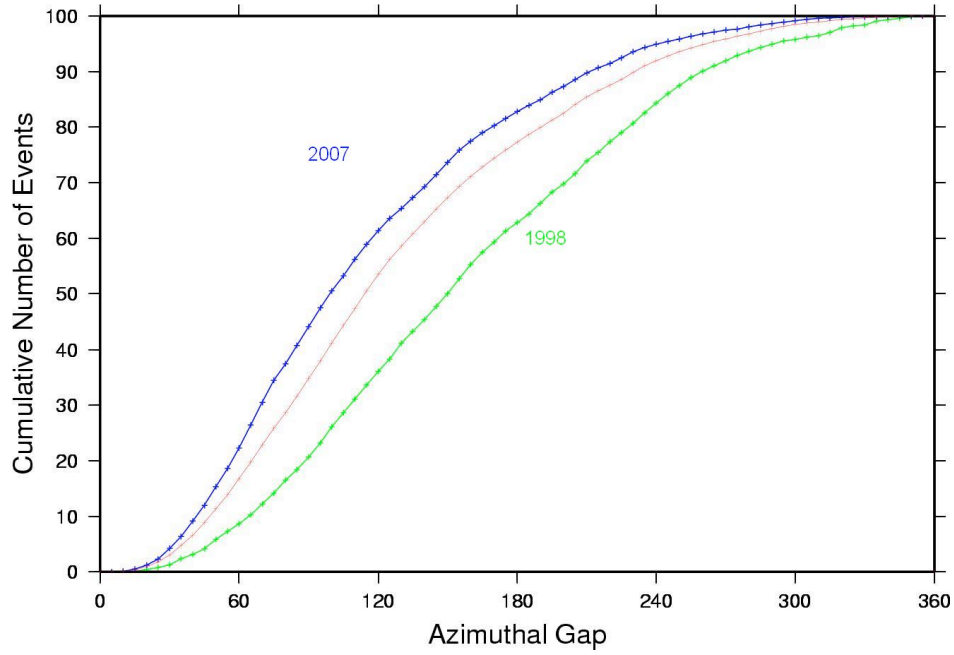


Figure 9: Azimuthal gap obtained in the Euro-Med Bulletin for all associated events. Red: average over the period 1998-2007; Blue: average over the year 2007; Green: average for the year 1998.

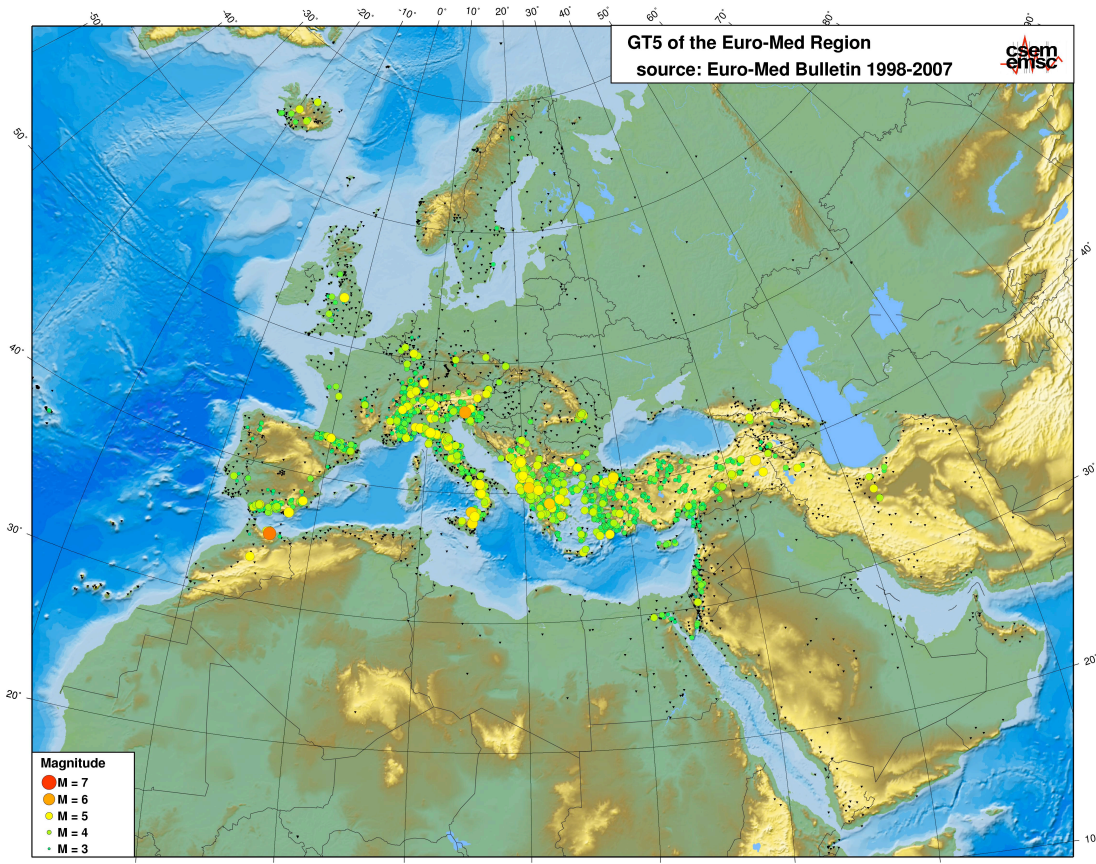


Figure 10: Events fulfilling the GT5 criteria (Bondar et al., 2004) in the Euro-Mediterranean bulletin.

Perspectives

Seeking to improve the Euro-Med Bulletin production and content, the EMSC is working on several aspects: the proper identification of non tectonic events, the inclusion of low magnitude events and the use of a more up-to-date velocity model.

For the period 1998-2007, 3,437 events are currently identified as non tectonic events. Seismicity associated with induced events is observed in Poland at the exploration sites of Lubin and Silesia. Clusters are also observed in Scandinavia, the Middle East and at the border of Germany and the Benelux. However, small clusters of seismicity can be observed in Poland in the natural seismicity map (Fig. 11) which means that identification of mine activity may not be complete. The first improvement to apply on our bulletin is therefore to work in collaboration with the data contributors to fully integrate identification of non tectonic seismicity and to promote the distribution of event type information in the international data exchange.

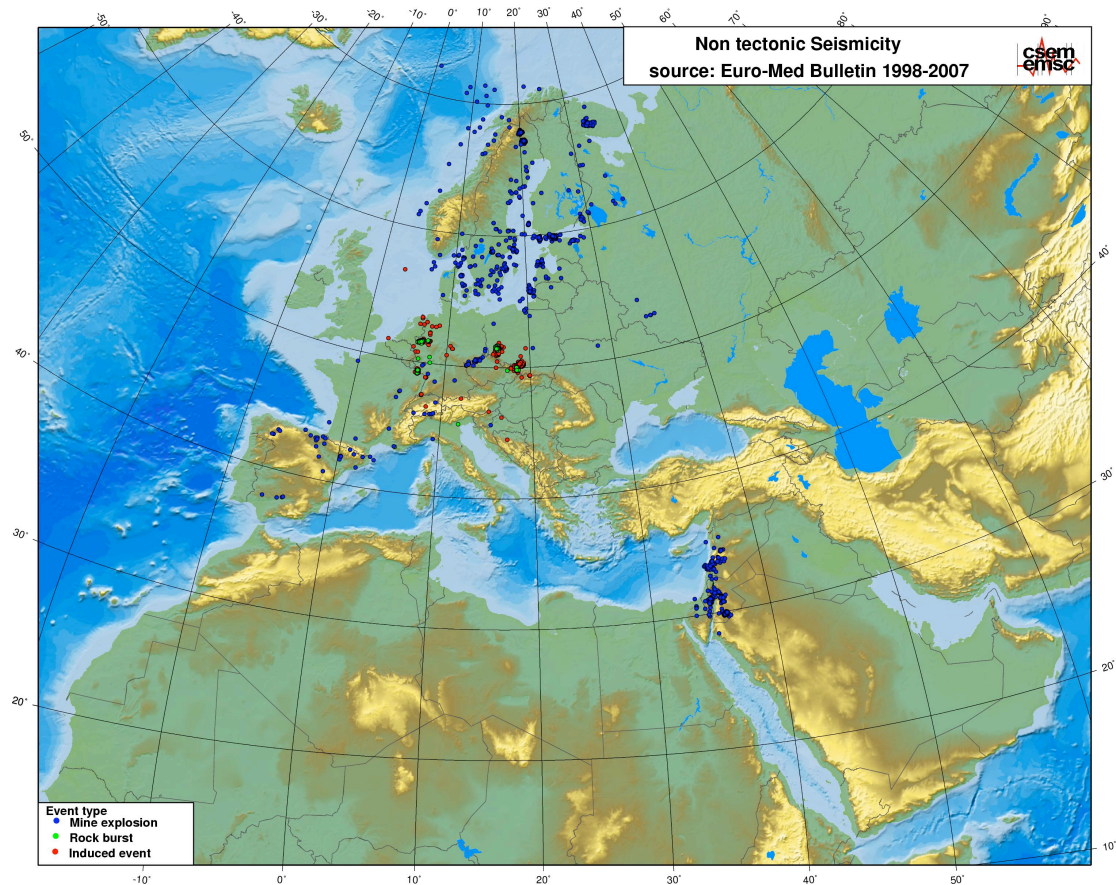


Figure 11: Distribution of identified non tectonic events in the Euro-Med Bulletin 1998-2007.

In the framework of the NERIES (Network of Research Infrastructures for European Seismology) project (<http://www.neries-eu.org/>), all seismological information (waveforms, parametric data, accelerograms, shakemaps, etc) for each event will be available through one single web portal. A reference catalogue of earthquakes is necessary in order to link all information related to a single event. This catalogue should include the most accurate information at any time and therefore should encompass from real time data to past information. To reach this goal, the Euro-Med

Bulletin and the Real Time Information provided by the EMSC are associated. This association not only provides the essential seed of the NERIES portal but also contributes to a detailed analysis of the real time information service based mostly on automatic data in comparison with the Euro-Med Bulletin based on reviewed and more complete information. It will enable us to identify and comment on specific events of the Real Time Catalogue: ghost events generated by local automatic procedures; artificial events or small magnitude events reported in real time but discarded from the revised contributions of the local institutes and poorly constrained real time locations.

The second main improvement to be applied in the Euro-Med Bulletin is the integration of low magnitude events, using all the bulletin data (origins and associated picks) provided by the data contributors. The initial goal of the Euro-Med Bulletin was to include earthquakes greater than magnitude 3.0. However, with the development of the NERIES portal, end-users have requested to include lower magnitude events and to dismiss this threshold. This will be performed for the whole period 1998-2007. It is important to notice that higher discrepancy in the magnitude completeness will then be observed depending on the region.

Another key point of the Euro-Med Bulletin production is the velocity models used. Tests are currently performed at the EMSC to implement the 1D reference ak135 global velocity model (Kennett *et al.*, 1995) which is recommended by the IASPEI working group on earthquake location method. The use of local velocity models will then be withdrawn. The total 10 years of bulletin will be recomputed and analyzed before being published during the year 2009.

Finally the Euro-Med Bulletin will be used to realize an educational seismicity map of the region, dedicated to a general audience, especially targeting schools. The goal of this informative map is to raise public awareness of the seismic risk and its prevention. The Euro-Med bulletin will be displayed in association with the regional tectonic settings and specific information on major events of the region.

Conclusions

Through regular and enhanced collaboration with the seismological institutes of the Euro-Med region, the EMSC is able to produce a comprehensive regional bulletin of the region. It led to continuously increasing data collection and more accurate results. The seismicity presented here spans the period 1998-2007. By merging data from the various local institutes, high azimuthal coverage is obtained for most of the region. The obtained catalogue is consistent with local network knowledge and improved in border regions and off-shore. The Euro-Med Bulletin is now integrated to the ISC bulletin and has become a useful reference for the seismological community, such as the NERIES project. Willing to improve its production, the EMB will be enriched with more accurate event type information and low magnitude events before being recomputed with ak135 global velocity models.

References

- Bondár I., Myers C., Engdahl R. and Bergman E., 2004, Epicentre accuracy based on seismic network criteria, *Geophys. J. Int.*, 156, 483–496 doi: 10.1111/j.1365-246X.2004.02070.x
- IASPEI New Manual of Seismological Observatory Practice* (2002). Peter Bormann, ed. Potsdam: GeoForschungsZentrum Potsdam.
- Godey S., Bossu R., Guilbert and J., Mazet-Roux G., 2006, The Euro-Mediterranean Bulletin: A Comprehensive Seismological Bulletin at Regional Scale *Seismological Research Letters* vol. 77, number 4 July/August 2006
- Jeffreys, H. and K. E. Bullen, 1940, *Seismological tables*, London: British Association for the Advancement of Science, Gray Milne Trust, 50 pp.
- Kennett, B. L. N., E. R. Engdahl, and R. Buland (1995). Constraints on seismic velocities in the Earth from travel times. *Geophysical Journal International* 122, 108–124.
- Storchak, D. A., J. Schweitzer and P. Bormann, 2003, The IASPEI Standard Seismic Phase List, *Seismological Research Letters*, vol 74, n 6, 761-772.
- Geiger, L., 1910, Herdbestimmung bei Erdbeben aus den Ankunftszeiten, *Nachrichten von der Königlichen Gesellschaft der Wissenschaften zu Göttingen* 4, pp. 331-349.

Appendix 1: List of Contributing Networks to the Euro-Med Bulletin

Algeria: Centre de Recherche en Astronomie, Astrophysique et Geophysique
Greece: National Observatory of Athens
Republic of Azerbaijan: Center of Seismic Survey, Azerbaijan Academy of Science
Italy: Osservatorio Sismologico Universita di Bari
Belarus: Center of Geophysical Monitoring
Serbia: Seismological Survey of Serbia
Norway: University of Bergen
Germany: Bundesanstalt für Geowissenschaften und Rohstoffe
United Kingdom: British Geological Survey
Slovakia: Geophysical Institute, Slovak Academy of Science
Romania: Romanian Seismic Network
Hungary: Hungarian Seismic Network
Morocco: Centre National de la Recherche Scientifique et Technique
The Netherlands: Koninklijk Nederlands Meteorologisch Instituut
Turkey: Directorate of Disaster Affairs
Yemen: National Seismological Observatory Center
Ireland: Dublin Institute for Advanced Studies
Denmark: National Survey and Cadastre
Dubai: Dubai Seismic Network
Syria: Higher Institute of Earthquake Studies and Research
Turkey: Marmara Research Center
Italy: Rete Sismica Igg
Czech Republic: Geophysical Institute of the Academy of Sciences
Israel: Geophysical Institute of Israel
Lebanon: Centre National de Recherche Scientifique
Germany: Seismological Central Observatory
Finland: Institute of Seismology

Egypt: National Research Institute of Astronomy and Geophysics
Portugal: Instituto de Meteorologia
Czech Republic: Institute of Physics of the Earth
Turkey: Kandilli Observatory
Iraq: Iraqi Meteorological Organisation and Seismology
Jordan: Jordan Seismological Observatory
Kuwait: Kuwait Institute for Scientific Research
France : Laboratoire de Detection et de Geophysique
Libya: Libyan Center for Remote Sensing and Space Science
Lithuania: Geological Survey of Lithuania
Slovenia: Agencija Republike Slovenije za okolje
Latvia: Latvian Seismic Network, Latvian Environment, Geology and Meteorology Agency
Spain: Instituto Geografico Nacional
Moldova: Institute of Geophysics and Geology
Spain: Institut Cartografic de Catalunya
Norway: Norwegian Seismic Array
USA: National Earthquake Information Center
Cyprus: Geophysical Survey Department
Kazakhstan: National Data Center, Institute of Geophysical Research
Syria: National Syrian Seismological Centre
Armenia: National Survey of Seismic Protection
Russia: Geophysical Survey of the Russian Academy of Sciences
Oman: Earthquake Monitoring Center of Oman
Portugal: Instituto de Meteorologia, Azores University
Montenegro: Montenegro Seismological Observatory
Iceland: Department of Geophysics, Icelandic Meteorological Office
Italy: Istituto Nazionale di Geofisica e Vulcanologia
Saudi Arabia: King Saud University
Tunisia: Institut National de Meteorologie
Spain: Real Instituto y Observatorio de la Armada
Macedonia: Seismological Observatory
Saudi Arabia: Saudian National Seismological Network
Bulgaria: Geophysical Institute of Sofia
Bosnia-Herzegovina Republic: Hydrometeorological Institute
Morocco: Departement de Physique du Globe
France: Reseau National de Surveillance Sismique
Iran: Institute of Geophysics, University of Tehran
Greece: Aristotle University of Thessaloniki
Iran: International Institute for Earthquake Engineering and Seismology
Georgia: Seismic Monitoring Centre of Georgia
Albania: Albanian Seismological Network
Italy: Istituto Nazionale di Oceanografia e di Geofisica Sperimentale
Belgium: Observatoire Royal de Belgique
Sweden: Uppsala seismic network
Greece: University of Patras Seismological Laboratory
Uzbekistan: Institute of Seismology, Uzbekistan Academy of Sciences
Poland: Warsaw seismic network
Croatia: Seismological Survey
Austria: Central Institute for Meteorology and Geodynamics
Switzerland: Swiss Seismological Service

A harmonized seismicity data base for the Euro-Mediterranean region

Gottfried Grünthal and Rutger Wahlström

GFZ German Research Centre for Geosciences, Telegrafenberg, D-14473 Potsdam, Germany, ggrue@gfz-potsdam.de

Abstract

Data from over 50 domestic and regional catalogues, the ISC and NEIC bulletins for the NE Atlantic Ocean, and numerous special studies were used to compile an M_w based earthquake data base for Europe and the Mediterranean region. Non-tectonic, non-seismic and non-existing as well as duplicate events were identified and removed according to our current stage of knowledge. If not given by the original source, M_w was calculated for each event with a specified epicentral location and a given strength measure (i.e., a magnitude of any type or, for onshore events only, an intensity). The investigated area is subdivided into 37 polygons, in each of which one or more catalogues, supplemented by data from the special studies, are used. If more than one catalogue lists an event, one entry was selected according to a priority algorithm specific for each polygon. If the selected catalogue entry contains more than one strength type, one was selected for the M_w calculation according to another priority scheme. A current version of the data base, with events mainly in the area north of latitude 44°N , in the time period 1000-2004, and with magnitudes $M_w \geq 3.50$, has recently been released as the CENEC catalogue (Grünthal et al., 2009b) and its harmonization with respect to M_w has been investigated (Grünthal et al., 2009a). Besides updating this part, an extension to southern Europe and the Mediterranean region is under construction, with a higher threshold magnitude foreseen for the southern part.

Introduction

Earthquakes have caused many major disasters in Europe. The two worst in the past centuries occurred offshore Lisbon in 1755 and in the Strait of Messina in 1908 and caused about 70,000 and 72,000 deaths, respectively, to a large extent by the generated tsunami waves. Including the area immediately to the east of the Mediterranean Sea, the Aleppo earthquake in 1138 with estimated 130,000 fatalities should be noted. An earthquake the year after in Azerbaijan just off the SE corner of Europe caused an estimated 230,000 deaths. Fig. 1 shows the earthquakes in the current data base with M_w magnitudes of 6 and larger, with the most destructive events marked (Table 1). Events with $M_w \geq 8$ are given in Table 2.

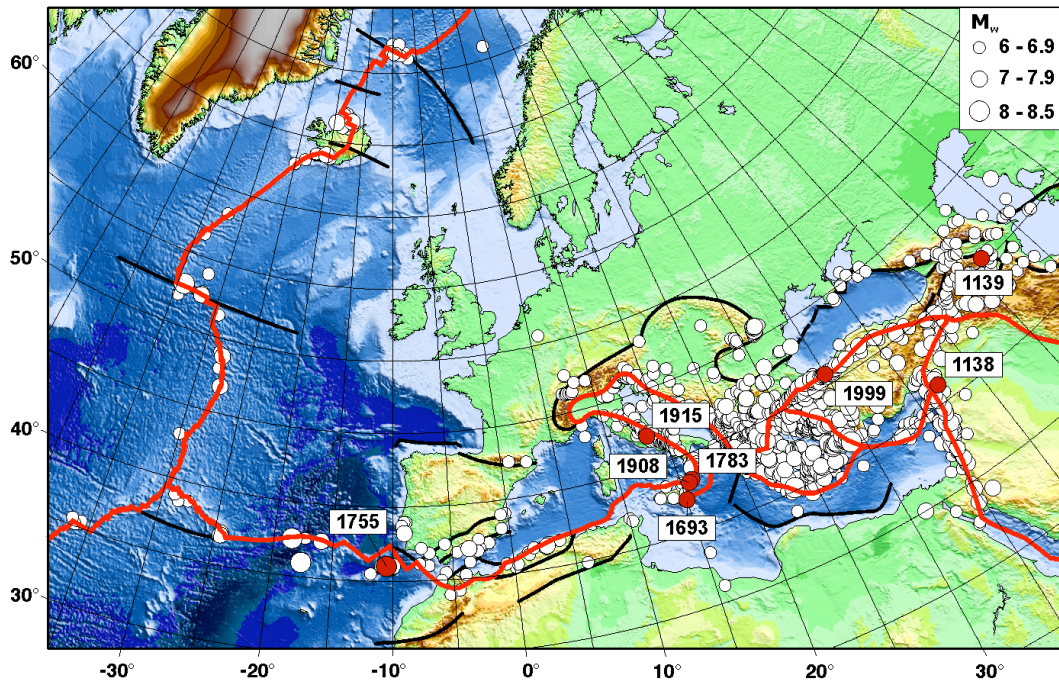


Figure 1. Earthquakes in the data base with $M_w \geq 6$. The most destructive earthquakes are specially marked (see Table 1). The plate boundaries are after Bird (2003), modified and extended by the authors.

Table 1. The most destructive earthquakes in the Euro-Med region (number of fatalities).

Date	M_w	Country	Location	Fatalities ¹⁾
1138 October 11	7.1	Syria	Azrab/Aleppo	130,000
1139 September 30	7.7	Azerbaijan	Ganzak	230,000
1693 January 11	7.4	Italy	Catania	60,000
1755 November 1	8.5	Portugal	Lisbon	70,000
1783 February 5	6.9	Italy	Calabria	35,000
1908 December 28	7.1	Italy	Messina	72,000 ²⁾
1915 January 13	7.0	Italy	Avezzano	35,000
1999 August 17	7.5	Turkey	Kocaeli	45,000 ³⁾

¹⁾ After Musson (2001) and Marza et al. (2003) except 1908

²⁾ Numbers in the literature ranges from 60,000 to 200,000, the more reliable from 65,000 to 110,000; the preferred number, 72,000, is given by USGS (2009)

³⁾ Sum of reported killed (20,000) and missing (25,000) (Marza et al., 2003)

Table 2. Earthquakes with $M_w \geq 8$ in the Euro-Med region.

Date	M_w	Epicentre
365 July 21	8.3	offshore Crete
1303 August 8	8.0	offshore Rhodes
1755 November 1	8.5	offshore Lisbon
1939 December 26	8.0	Erzincan, Turkey
1941 November 25	8.3	Gloria fault, Atlantic Ocean
1967 February 13	8.2	North Atlantic Ridge
1975 May 26	8.1	Gloria fault, Atlantic Ocean

Because strong events in the investigated area are scarce, the entire damaging potential can only be understood when long time spans are considered. It is a requirement from various current EU and other projects to have high-quality, harmonized earthquake catalogues extended over a long period of time. The existing global and European data bases such as ISS/ISC, NEIC, Engdahl et al. (1998), BCIS/EMSC or Kárník (1996) are covering too short time periods and/or have too high threshold magnitudes to be satisfactory, especially in areas of relatively low seismicity such as large parts of Europe. The magnitudes are also not unified in some of these data bases. It is the objective of the current study to create a homogeneous catalogue for Europe and the Mediterranean region.

Tectonically, the study area corresponds to the whole western part of the Eurasian plate, including the adjoining micro-plates, and the corresponding plate boundary zones in the Atlantic Ocean, the Mediterranean region, and the eastward extension of the complicated southern bounds of the Eurasian plate running through the Caucasus and the Caspian Sea.

Data and Method

Our data base is founded on over 50 local or national catalogues and data bases, and numerous special studies on individual events, event series or regions. They represent, in most cases, the optimal completeness of events and precision of their parameters, and together they cover the historical and instrumental time periods of the investigated region. Currently (June 2009), there are over 450,000 entries in the total data base, whereby an event can be represented by entries from several sources. The entries are then lumped together to form a family for this event.

The investigated area is defined by and subdivided into 37 polygons (Fig. 2). The border of these mostly follow the national borders. For each polygon, one or more local catalogues and data bases are accepted as sources from which the representative entry for an event is selected. If there are entries from more than one of the allowed catalogues, a specified hierarchy decides which one to use. Data are also provided by many special studies referring to one or a limited set of events. These data usually have priority over the local catalogues as to picking the preferred entry.

All original data which do not have M_w but another magnitude concept and/or intensity were assigned M_w through conversion algorithms. An error estimate is given for each derived relation by Grünthal et al. (2009b). The regressions for the M_w conversion formulae were carried out using the chi-square maximum likelihood technique described by Stromeyer et al. (2004). For each catalogue, a priority scheme decides from what other strength measure M_w should be calculated. Where an M_w entry is given by Swiss Moment Tensor Solutions (2009) or Pondrelli et al. (2002, 2004, 2007), which are sources providing original M_w from digital data, this was used.

So far a full analysis has been performed and published for the northern part of the Euro-Med region, i.e., basically north of latitude 44°N, the CENEC catalogue (Central, Northern and northwestern European earthquake Catalogue, Grünthal et al., 2009b). This study gives details on the local catalogues, polygons, and the different priority rules. The work continues with the southern part and with updates of the northern part to an extended catalogue, EMEC (Euro-Mediterranean Earthquake Catalogue), covering the whole Euro-Med region.

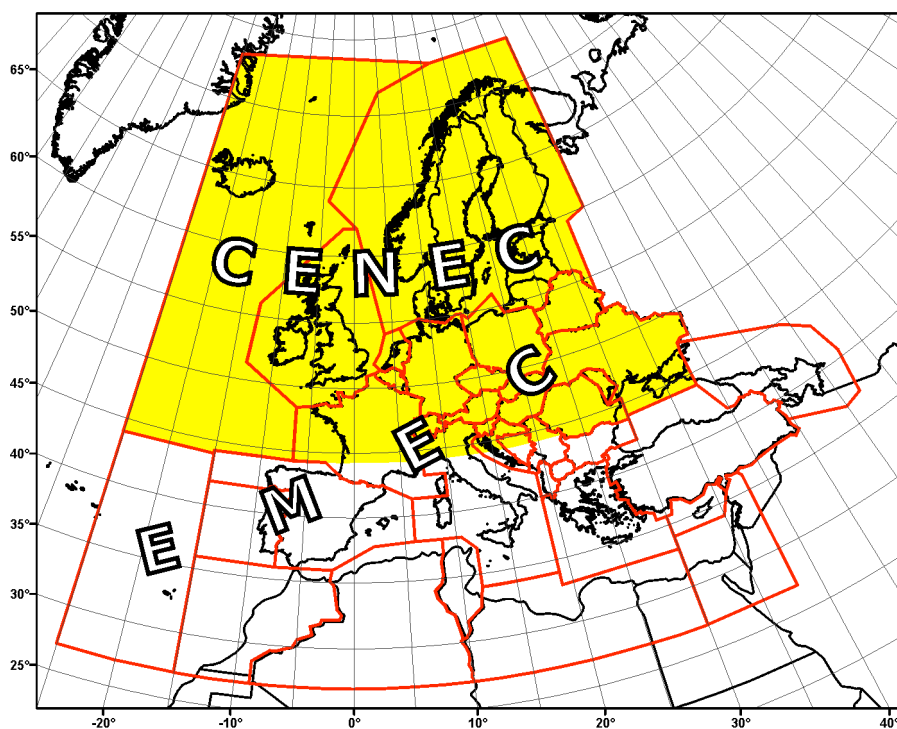


Figure 2. The polygons in each of which one or more of the catalogues and data bases is valid. The EMEC catalogue encompasses all polygons; CENEC covers the yellow-marked area.

Harmonization of M_w (CENEC part)

Even if all entries get M_w , it remains to investigate how compatible they are to each other. This has so far been done for the CENEC entries (Grünthal et al., 2009a). Some inhomogeneity in the M_w obtained from over 40 local catalogues and data files and over 50 special studies is inevitable.

Only about 2% of the data used for CENEC have original M_w magnitudes derived directly from digital data (most of them from the sources mentioned in the previous section). Some of the local catalogues and data files give M_w , but calculated by the respective agency from other strength measures. About 60% of the local data give strength measures other than M_w and these are the ones we have converted.

Two different approaches have been followed to investigate the compatibility of the different M_w sets. The first approach compares original M_w from Swiss Moment Tensor Solutions (2009) and Pondrelli et al. (2002, 2004, 2007) with (1) M_w given in national catalogues and (2) M_w derived by applying different empirical relations developed for CENEC. These high-quality M_w data bases specialize on European and Mediterranean area events. The second approach concerns the vast majority of earthquakes in CENEC, for which no digitally obtained M_w exist. In this case, an empirical relation for the M_w dependence on epicentral intensity (I_0) and focal depth (h) was derived for 41 master events with high-quality data and located all over central Europe (Fig. 3a). To include also the data lacking h , the corresponding depth independent relation for these 41 events was also derived (Fig. 3b). These equations were compared with the different sets of data from which CENEC is composed and the goodness of fit was calculated for each set. The vast majority of the events are

very well or reasonably consistent with the equations so that the data can be said to be harmonized with respect to M_w , but there are exceptions, which are discussed in detail by Grünthal et al. (2009a). In the ongoing study, covering also southern Europe and the Mediterranean region, harmonization checks will be used to improve existing M_w calculating algorithms, striving at a maximum harmonized catalogue.

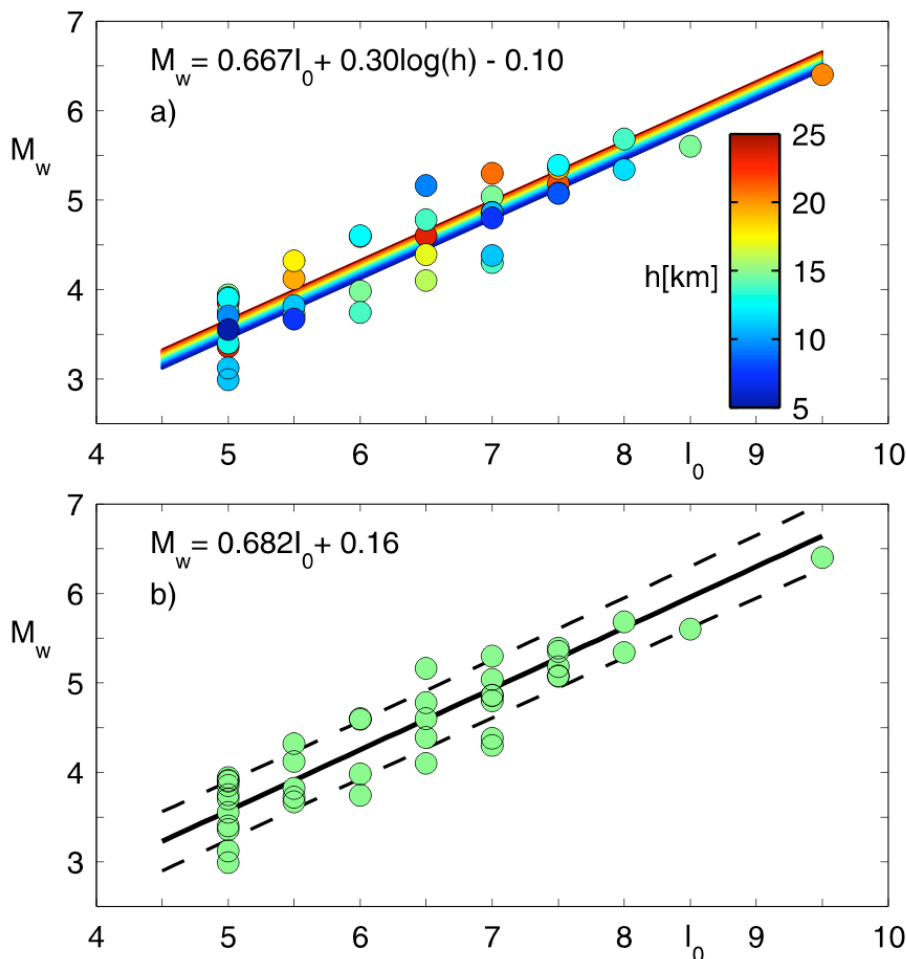


Figure 3. Master event relations and the 41 data points used for their derivation (after Grünthal et al., 2009a). (a) depth-dependent relation and (b) depth-independent relation. The dashed lines in (b) show the 68% confidence bounds, whereas the confidence bounds in (a) cannot be visualized in a simple way.

Conclusions

It is a long and non-trivial work to compile, edit, scrutinize, and homogenize all the data in the large data base and to make the final selection of the entries for the catalogues. An important part of the study considers the identification of duplications and various types of fake events. False locations and dates, and non-tectonic and non-seismic events, were labelled as such and eliminated from the further analysis.

A critical part of any data base compiled from different local sources is the harmonization of magnitudes. The present one contains unified M_w magnitudes, but a full harmonization is hard to achieve. Different quantitative tests showed that a high degree of harmonization exists for M_w from most local catalogues and data bases, but

there are a few notable exceptions. The need for such tests as a part of cataloguing work is urgent, although usually not made.

Fig. 1 shows the excellent correlation of the major seismicity with the plate boundaries and main faults. The intense seismicity in Greece, western Turkey, and Caucasus is connected with the complicated plate- sub-plate pattern. The data base presented here gives more complete and constrained solutions than those presented by the international seismological centres, and it has the added benefit of including historical data. In our data base, parameters from ISC and NEIC provide preferred entries only where a domestic catalogue does not exist, i.e., for Atlantic Ocean events.

Quality data of this kind are important to adequately quantify the seismic and tsunami threats. The historical data show that even if catastrophic events are infrequent these threats must be taken seriously. The CENEC catalogue and the extended catalogue, EMEC, will be useful for applications in many fields of seismicity and in seismic hazard assessment, especially in large-scale projects of probabilistic seismic hazard assessment.

Acknowledgements

We are thankful for comments by the referee, L. Chiaraluce. The financial support for the regional earthquake cataloguing by Aon Benfield is acknowledged. The technical staff of our section contributed in various steps of the data processing.

References

- BCIS/EMSC European-Mediterranean Seismological Centre (previously Bureau Central International Sismologique) bulletins, Strasbourg, France.
<http://www.emsc-csem.org/index.php?page=home>
- Bird P. (2003). An updated digital model of plate boundaries, *Geochem. Geophys. Geosyst.* 4(3), 1027. doi:10.1029/2001GC000252.
- Engdahl, E.R., van der Hilst, R. and Buland, R. (1998). Global teleseismic earthquake relocation with improved travel times and procedures for depth determination. *Bull. Seism. Soc. Am.* 88:722-743.
- Grünthal, G., Stromeyer, D. and Wahlström, R. (2009a). Harmonization check of M_w within the central, northern and northwestern European earthquake catalogue (CENEC). *J. Seismol.* 13(4), 613-632, doi: 10.1007/s10950-009-9154-2.
- Grünthal, G., Wahlström, R. and Stromeyer, D. (2009b). The unified catalogue of earthquakes in central, northern, and northwestern Europe (CENEC) – updated and expanded to the last millennium. *J. Seismol.* 13(4), 517-541, doi:10.1007/s10950-008-9144-9.
- ISC/ISS International Seismological Centre (previously International Seismological Summary) bulletins, Newbury, United Kingdom.
<http://www.isc.ac.uk/search/index.html>
- Kárník, V. (1996). Seismicity of Europe and the Mediterranean. Geophysical Institute, Czech Academy of Sciences, Prague, The Czech Republic, 28 pp (+maps and catalogue).

- Marza, V., Carvalho, J., Barros, L. and Chimpliganond, C. (2003). A look at global seismicity during 1999 in the longer-term time frame. *J. Seismol.* 7:89-98.
- Musson, R.M.W. (2001). Deadliest ever earthquakes, Internet circulation on sci.geo.earthquakes (USENET) and Quake-L list server, 4 pp.
- NEIC National Earthquake Information Center bulletins, U.S. Geological Survey, World Data Center A for Seismology, Boulder, Colorado, USA. <http://neic.usgs.gov/neis/epic>
- Pondrelli, S., Morelli, A., Ekström, G., Mazza, S., Boschi, E. and Dziewonski, A.M. (2002). European-Mediterranean regional centroid-moment tensors: 1997–2000. *Phys Earth Planet Inter* 130:71–101. doi:10.1016/S0031-9201(01)00312-0.
- Pondrelli, S., Morelli, A. and Ekström, G. (2004). European-Mediterranean regional centroid moment tensor catalog: solutions for years 2001 and 2002. *Phys. Earth Planet. Inter.* 145:127–147. doi:10.1016/j.pepi.2004.03.008.
- Pondrelli, S., Salimbeni, S., Morelli, A., Ekström, G. and Boschi, E. (2007). European-Mediterranean regional centroid moment tensor catalogue: solutions for years 2003 and 2004. *Phys. Earth Planet. Inter.* 164:90–112. doi:10.1016/j.pepi.2007.05.004
- Stromeyer, D., Grünthal, G. and Wahlström, R. (2004). Chi-square regression for seismic strength parameter relations, and their uncertainties, with applications to an M_w based earthquake catalogue for central, northern and northwestern Europe. *J. Seismol.* 8:143–153. doi:10.1023/B:JOSE.0000009503.80673.51.
- Swiss Moment Tensor Solutions (2009). Moment tensor solutions from the Schweizerischer Erdbebendienst (SED), Zurich, Switzerland. <http://www.seismo.ethz.ch/mt>
- USGS (2009). Most destructive known earthquakes on record in the world (census data). http://earthquake.usgs.gov/regional/world/most_destructive.php (version of January 29, 2009)

Compiling an earthquake catalogue for Algeria (ECA): Sources and method

Assia Harbi*

Centre de Recherche en Astronomie, Astrophysique et Géophysique, BP. 63, Bouzaréah,
16340, Algiers, Algeria., harbi.assia@gmail.com. *Regular Associate of the Abdusalam
International Centre for Theoretical Physics, Trieste, Italy.

Abstract

The compilation of a comprehensive catalogue is a major need for assessing seismicity and seismic hazard of Algeria. The main purpose of this paper is to present the sources and the methodology used in order to build a reliable database. Results of the first investigations are briefly summarized.

Introduction

The idea to produce a revised earthquake catalogue, for Algeria, arose after the comparison of the earthquake catalogues, published simultaneously, by Mokrane et al. [1] for the period (1365-1992) and Benouar [2] for the period (1900-1990). The north-eastern part of the country was chosen as experimental zone with the aim of merging the two catalogues into a unified one, after verification of the reliability of all the quoted parameters [3]. The obtained results underline the necessity of revising the historical seismicity of Algeria before compiling earthquake catalogue (ECA). In this paper we describe the previous catalogues by reporting the strong and weak points of each catalogue, and the improvements made by the new proposed method. We briefly present *a)* the methodology applied in a compilation of the most homogeneous and reliable database and *b)* some results of the ongoing work.

Sources

The compilation of ECA consists in merging historical and instrumental catalogues, local, regional or global. All the descriptive and parametric catalogues available to us are used. The types of their sources and the periods of time they span are shown in Fig. 1. Fig. 2 summarizes the parameters provided in each earthquake catalogue.

Local catalogues

The *Chesneau* earthquake catalogue [4] is exclusively descriptive and reports seismic events for which only the date and time of occurrence are provided.

Hée [5 and 6] give a list of all the earthquakes felt in Algerian territory, divided in nineteen quadrangles. This method makes it difficult to determine the macroseismic epicentre since an earthquake recorded at a site belonging to the quadrangle n°2, for example, may be also attributed to sites of the quadrangles n°1 and n°3. Therefore, this catalogue should be handled with great caution.

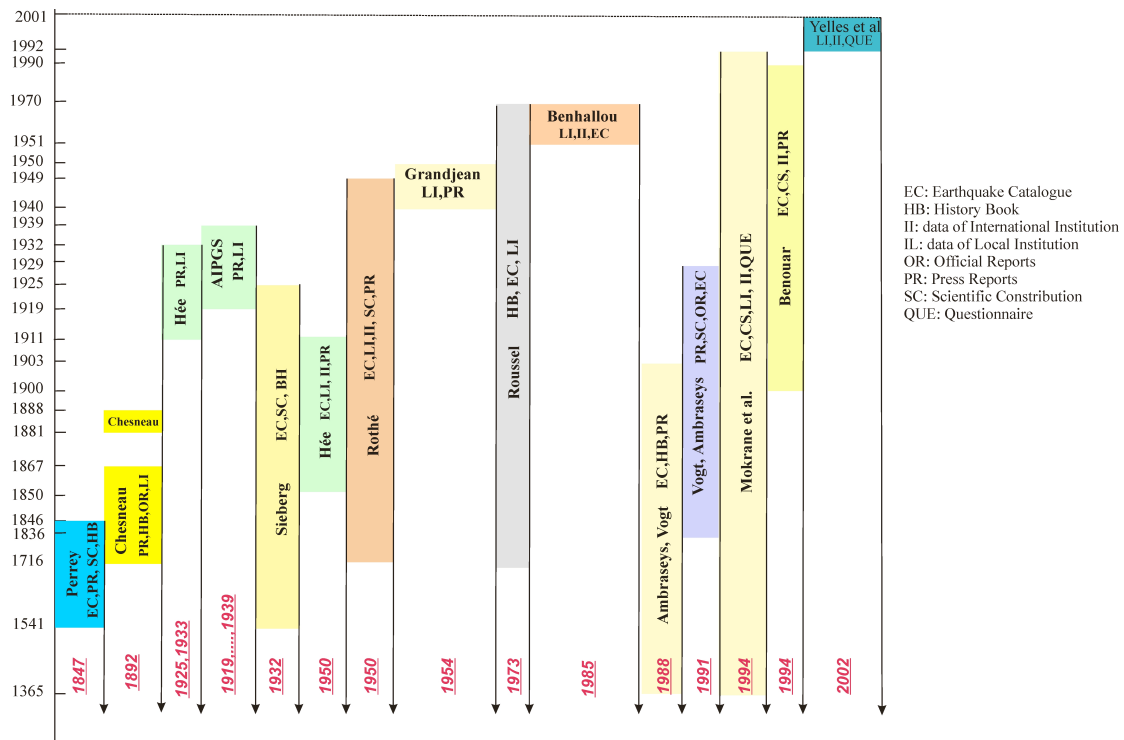


Figure 1: The main sources used in the compilation of ECA. The abbreviations indicate the type of sources used by the authors.

The *Hée* catalogue [7] is produced in the same format as the previous ones.

The *Rothé* memoir [8] is the most used source by many of his followers. It deals with the damaging and destructive events and may be considered as the first local parametric catalogue. Often, Rothé resumes the earthquake descriptions of previous authors, particularly Perrey and Hée (see references), and presents some isoseismal maps.

The *Grandjean* catalogue [9] gives a brief description of the duration and direction of the shock. The epicentre coordinates and instrumental magnitude are sometime included but generally the author does not mention the effects from which an intensity value is estimated. Intensity maps are provided for significant earthquakes.

Roussel [10] produced the first catalogue of major earthquakes which is exclusively parametric. The included observations concern the damage and the numbers of destroyed houses and casualties. Intensity estimates are given without any explanation.

Benhallou [11] continued Roussel work by focusing on all events and presents several intensity maps.

The *Ambraseys and Vogt* descriptive catalogue [12] is a valuable work, covering events of the Algiers region. It is a methodical study underlining the importance of going back to the original sources in order to assess any earthquake parameter. These authors were the first who reported the first known seismic event of Algeria, in 1365. Several earthquakes are extensively described and some intensity maps are presented.

Hée [5, 6, 7]													
Date	Time	Site		OBS	I ₀								
Rothé [8]													
Date	Time	Lat	Long	M	I ₀	Site							
Grandjean [9]													
Date	Time	Lat	Long	M	I ₀	Site	D						
Roussel [10]													
Date	Time	Lat	Long	M	I ₀	OBS							
Benhallou [11]													
Date	Time	Lat	Long	M	DEP	I ₀	Rm	OBS	REF				
Ambraseys and Vogt [12] for the 1365-1811 period													
Date	Time		Site			Effects							
Ambraseys and Vogt [12] for the 1825-1903 period													
Date	Time	Lat	Long	Quality of location		Effects							
Mokrane et al. [1]													
Date	Time	Lat	Long	DEP	M _i	M _m	I ₀	REF					
Yelles et al. [14]													
Date	Time	Lat/Lon (Ins)		Lat/Lon (Mc)		M	I ₀	DEP	Site	REF			
Benouar [2]													
Date	Time	Lat	Long	DEP	M _s	mb	M	M _l	I ₀	NS	OBS	Site	REF

M: 1) Gutenberg magnitude in Rothé, Grandjean, Roussel and Benhallou catalogues;
 2) m_b and/or M_l in Yelles et al. catalogue
 3) unknown type of instrumental magnitude in Benouar catalogue

Figure 2: The parameters provided in the previous earthquake catalogues. D: epicentral distance, Rm: mean radius of perceptibility, OBS: observations, REF: references, Ins: instrumental, Mc: macroseismic.

The *Vogt and Ambraseys* descriptive catalogue [13] is the continuation of the previous work [12]. It is a reliable source of documented information on historical seismicity of western Algeria [1°W-1°E, 35°N-36.25°N].

The *Mokrane et al.* catalogue [1] is the first parametric catalogue published by CRAAG, the institution in charge of seismic monitoring in Algeria. The type of instrumental magnitude M_i is not specified. Several intensity maps are presented in the macroseismic Atlas, including those already drawn by Rothé, Hée, Grandjean, Benhallou, and Ambraseys and Vogt. Generally the earthquakes are studied by means of questionnaires.

The *Yelles et al.* parametric catalogue [14] is the continuation of the earthquake catalogue of Algeria by Mokrane et al. [1]. It is also a CRAAG contribution with a macroseismic Atlas.

Regional and global catalogues

The *Perrey* descriptive catalogue [15] is the first invaluable document for earthquakes of Algeria. It contains a plenty of information, taken from a variety of sources, on 34 earthquakes recorded in Algeria.

Annales de l'institut de physique du globe de Strasbourg (AIPGS) by Hée [16, 17] are annual lists of earthquakes with brief descriptions of the shocks, the date, origin time, intensity and the sites where each event was felt. It contains 1035 earthquakes, felt in Algeria. Except for some destructive shocks for which a detailed report is available, there is no information justifying the estimation of any intensity.

The *Sieberg* descriptive catalogue [18] deals with the most important earthquakes and contains, for Algeria, 16 events with four isoseismal maps.

The *Benouar* compilation [2] for the Maghreb region is the first earthquake catalogue where the epicentre and surface wave magnitude are systematically provided. Macroseismic or/and instrumental studies are devoted to the damaging seismic events (23 for Algeria). All the authors cited above, used the Mercalli Modified intensity scale while Benouar uses the Medvedev-Sponheuer-Karnik (MSK) scale. Concerning the not re-studied earthquakes, the author prefers the ISC localisation and generally provides an intensity value without quoting his source. This implies some uncertainty, particularly when the intensity is higher than VI MSK, suggesting a damaging earthquake.

Catalogues and bulletins of national and international centres: Bureau Central International de Séismologie (BCIS), Centre de Recherche en Astronomie, Astrophysique et Géophysique (CRAAG), Euro-Mediterranean Seismological Centre (EMSC) (<http://www.emsc-csem.org>), Instituto Geografico Nacional (IGN) (<http://www.geo.ign.es>), USGS National Earthquake Information Center (<http://neic.usgs.gov>), International Seismological Center (ISC) <http://www.isc.ac.uk>.

Methodology and structure of ECA

The compilation of a primary catalogue, based on the above sources, gives us a working data file whose entries should be carefully checked (in term of reliability) or reviewed. We have to know how the earthquake parameters were assessed. The first step consists in investigating the primary sources (archives, libraries, documentary materials, questionnaires, etc.). Hence a systematic historical investigation that reaches as far back in time as possible becomes a primary need. The second step consists of building up a new and more reliable database founded on various primary sources of information. Criteria for the determination of parameters are then specified. This includes, where possible, events which previously had no determined parameters (as in the catalogues by Hée) and events for which unreliable or doubtful parameters are assigned. A surface wave magnitude M_s , is systematically calculated using empirical relationships

Aiming at making the ECA as informative and interactive as possible, we present two versions of the catalogue. The *basic version* contains all the compiled events (even the doubtful ones), where each event is defined by the following entries: date (year, month, day); time (h, m, s); epicentre (lat, lon); depth; magnitudes (M_s , m_b , M (M_u for

unknown type, M_w or M_n), M_l , M_{se} (empirical M_s)); intensity, MM or MSK/EMS as given by the author; number of recording stations; observations identifying the event (foreshock, aftershock, macroseismic, offshore, coastal, damaging, destructive, nuclear explosion, availability of macroseismic information, focal mechanism, intensity map); parameter quality rank of the macroseismic information; sites; references as well as the name of the author of the determination of each parameter. The *second simplified version* is obtained after removing doubtful events and keeping only a unified homogeneous parameter (e.g., EMS scale for intensity), allowing a comprehensive analysis of the catalogue content.

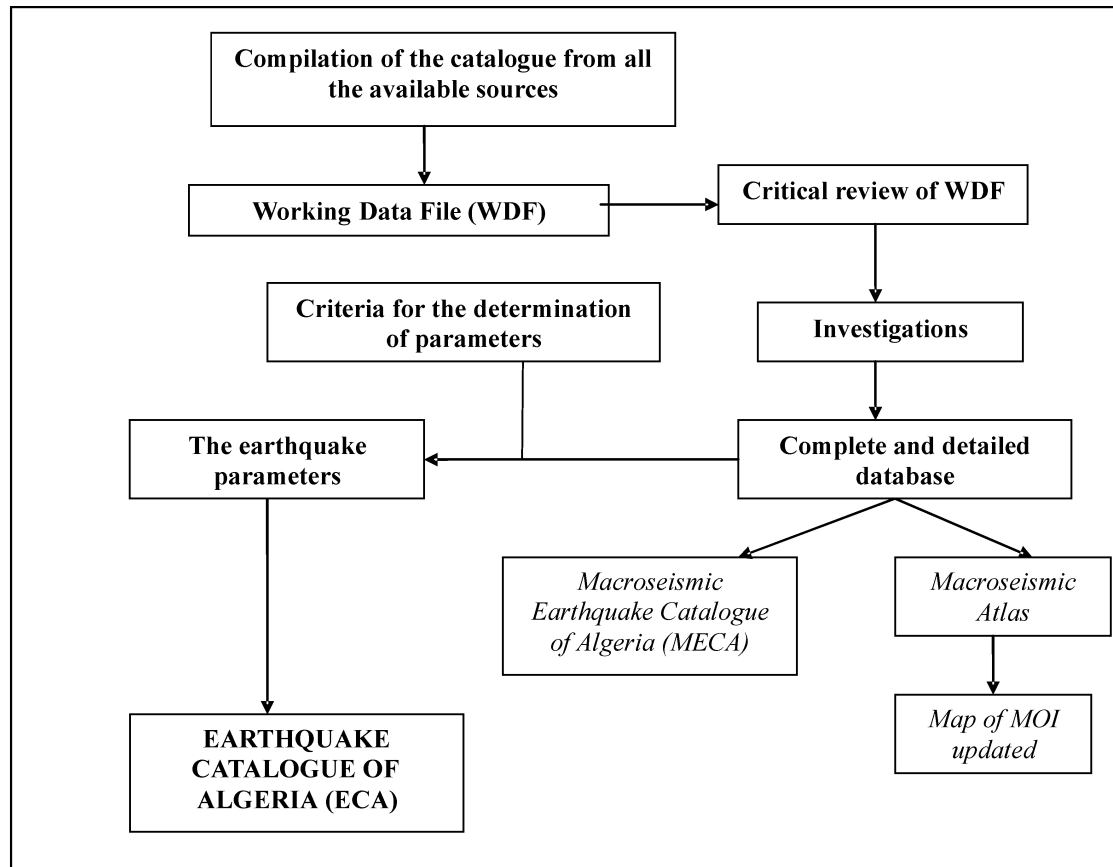


Figure 3: Flow chart describing the procedure for compiling ECA, MOI: Maximum Observed Intensities.

Ongoing work

Eastern Algeria has been chosen as a starting point for this study. According to the flow-chart (Fig. 3), we carried out a re-appraisal of the seismicity of the region [19, 20] and compiled a new revised earthquake catalogue [21]. This catalogue provides a more reliable picture of the seismicity in eastern Algeria than the previous ones [1, 2] as shown by the comparison over the common territory and time span (Fig. 4).

Conclusions

The final driving force to this study is to make available the catalogue on file transfer, along with, a macroseismic atlas, a map of Maximum Observed Intensities (MOI) and a full account of Algeria seismicity, to researchers and decision makers alike. The

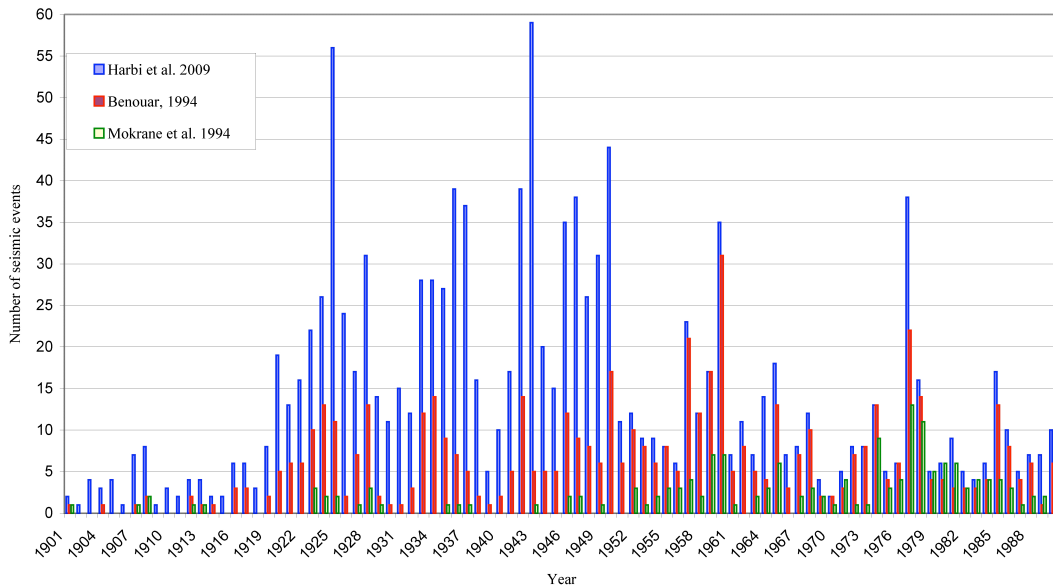


Figure 4: Comparison of the earthquake catalogue of eastern Algeria with the recent previous catalogues over the common territory and time span (modified from 21).

sources used in the compilation of the Algerian earthquake catalogue are more numerous than previously [1, 2]. The proposed method allow to get an earthquake catalogue with a more informative and homogeneous format. Both versions of the catalogue can be easily updated and adapted to the needs of the user. The obtained comprehensive databank on the seismicity, covering a period of time going back as far as possible, will serve in studying the seismicity, seismotectonics and seismic hazard of the country. Some achievements and recommendations can be drawn from the ongoing work:

- 1) The checking of the reliability of all entries by going back to the original sources is important. Some earthquakes of the region have been mislocated in previous catalogues e.g., the earthquake of January 1758 reported at Constantine in three catalogues (8, 11, 15) while the *Journal Historique* of March 1758, to which Perrey (15) referred, mentions destruction and casualties at Tunis (Tunisia) even if the earthquake was strongly felt in Constantine region.
- 2) The intensity should be re-assessed on the basis of the collected information using one intensity scale. The conversion of MM intensities to the EMS ones by using the existing relationships should be avoided. The re-appraisal of seismicity [19, 20] showed that the intensity evaluation may be over or underestimated.
- 3) All the available catalogues should be considered. The data of Hée [5, 6, 7] and Grandjean [9] were not used by Mokrane et al. [1] and Benouar [2]; they supply 122 additional events during the period 1885-1937 and 230 events during 1940-1950 [21].
- 4) Emphasis should be put on the collection of archaeological data which may inform of ancient earthquakes as that of Setifis in 419 [19].
- 5) The retrieval of further documentary data for the pre-Ottoman and Ottoman periods is an essential pre-requisite for enriching the historical dataset. European archives are the so far main examined sources [19, 20, 22, 23].

Acknowledgements

The author is grateful to the reviewers for their suggestions and remarks on an earlier version of the manuscript. This is a CRAAG contribution n° E007/08.

References

- Mokrane A., Ait Messaoud A., Sebai A., Ayadi A., Bezzghoud M., Benhallou H. (1994). Les séismes en Algérie de 1365 à 1992. CRAAG publication, Alger, 277.
- Benouar D. (1994). Materials for the investigation of the seismicity of Algeria and adjacent regions during the twentieth century. *Annali di Geofisica*, XXXVII, 4: 459-860
- (Harbi) A. (2001). Analyse de la sismicité et mise en évidence d'accidents actifs dans le Nord-Est Algérien. Thesis, USTHB, Alger, 177 p
- Chesneau M. (1892). Note sur les tremblements de terre en Algérie. *Mém. Ann. Des Mines, Série 9, t. I.*
- Hée A. (1925). La fréquence des tremblements de Terre en Algérie 1911-1924. *Monogr, Bur. Centr. Seismol. Inter. ; série B (2)*, pp. 111-154.
- Hée A. (1933). La fréquence des tremblements de terre en Algérie, 1911-1932. *Monogr. Bur. Centr. Seism. Intern. ; pp. 99*
- Hée A. (1950). Catalogue des séismes algériens de 1850 à 1911. *Ann. Inst. Phys. Globe, Strasbourg*, 41-49.
- Rothé J.P. (1950). Les séismes de Kherrata et la sismicité de l'Algérie. *Bull. Serv. Cart. Geol. Algérie ; 4ème série, Géophysique, N. 3*
- Grandjean A. (1954). Séismes d'Algérie de 1940 à 1950 inclus, *Ann. Inst. phys. Globe, Strasbourg; 3ème partie, Géophysique, VII, 83 (Le Puy)*.
- Roussel J. (1973). Les zones actives et la fréquence des séismes en Algérie 1716-1970. *Bull. Soc; Hist. Natur. Afrique du Nord. 64 (3), 2*, pp. 11-227.
- Benhallou H. (1985). Les Catastrophes Séismiques de la Région d'Echéliff dans le contexte de la Sismicité Historique de l'Algérie. Thesis, Alger, 294pp.
- Ambraseys N.N, Vogt J. (1988) Material for the investigation of the seismicity of the region of Algiers. *European Earthq. Eng.* 1988; 3, 16-29.
- Vogt J, Ambraseys N.N. (1991). Matériaux relatifs à la sismicité de l'Algérie occidentale au cours de la deuxième moitié du XIXe et du premier tiers du Xxe siècle. *Méditerranée*, 4: 39-45.
- Yelles A. A. Deramchi, A. Ferkoul & K. Aoulaiche. Les séismes en Algérie de 1992 à 2001. Alger : C.R.A.A.G Publication 2002, 216 pp (2002)
- Perrey A. (1847). Note sur les tremblements de terre en Algérie et dans l'Afrique septentrionale, *Mémoires de l'Académie des Sciences, Arts et Belles Lettres de Dijon, années 1845-1846*, pp. 299-323
- Hée A. (1919,, 1935). Les séismes de l'Algérie, *Annales de l'Institut de Physique du Globe de Strasbourg, 2e partie, Séismologie, t, I,, IV.*
- Hée A. (1936,, 1939). Les séismes de l'Algérie, *Annales de l'Institut de Physique du Globe de Strasbourg, 2e partie, Séismologie, t, I,, IV.*

- Sieberg A. (1932). Erdbeben geographie, Handbuch der Geophysik, **4**, 687-1005, Berlin.
- Harbi A., Benouar D., Benhallou H. (2003). Re-appraisal of seismicity and seismotectonics in the north-eastern Algeria Part I: Review of historical seismicity. *Journal of Seismology*, January, 1; 7: 115-136
- Harbi A., Maouche S. (2009). Effets macrosismiques des principaux séismes du nord-est de l'Algérie, Mémoires du Service Géologique National. N° 19, 81 pp. Editions du Service Géologique National, Alger.
- Harbi A., Peresan A., Panza G.F. Seismicity of Eastern Algeria: ECEA the revised and extended earthquake catalogue. Submitted to Natural Hazard. Available as ICTP internal report, IC/IR/2008/011.
- Harbi, A, Maouche S, Vaccari F, Aoudia A, Oussadou F, Panza G F, Benouar D (2007a) Seismicity, Seismic Input and Site effects in the Sahel-Algiers Region (North Algeria). *Soil Dynamics and Earthquake Engineering* vol 27: 427-447.
- Sebaï A., Bernard P. (2008). Contribution à la connaissance de la sismicité d'Alger et de ses alentours au XVIIIe siècle, extraite des archives françaises. *C. R. Geoscience* 340: 495–512

The historical earthquake database of the Royal Observatory of Belgium

Thierry Camelbeek, Elisabeth Knuts, Frédéric Devos and Pierre Alexandre

Royal Observatory of Belgium, Avenue circulaire 3, B-1180 Brussels, Belgium,
thierry.camelbeek@oma.be

Abstract

This paper describes the structure and the contents of the historical earthquake database in development at the Royal Observatory of Belgium. It includes all the original reports of earthquakes and the information on the corresponding historical sources for the seismic activity in Northwest Europe since the earliest known document (circa 700 AD) and in Western Europe before 1527. Part of the database concerning the 20th century earthquakes is already available on our web site [www.seismologie.be] and our objective in a near future is to open freely most of the information.

Introduction

The study of earthquakes that occurred before the development of modern seismic networks is mainly based on the observations of their felt effects or the importance of the damages they caused on buildings. From the geographical location and extension of the damaged areas and/or the felt effects, the earthquake location and magnitude can be evaluated (Ambraseys, 1995; Bakun and Wentworth, 1997). Although often considered, wrongly, as poor or irrelevant this kind of information can actually supply valuable observations on the impact of strong earthquakes worldwide.

The record-offices are full of texts reporting the effects of earthquakes that are unknown to the seismologists. Retrieving those reports is the role of professional historians. For earthquakes before the XIXth century, their involvement in the research is also necessary to apply the historical criticism methods on the earthquake reports, which can be only useful for the seismologists if their origin can be certified. In many regions of Europe, this kind of research is rarely undertaken and the relevance of the pre-instrumental parts of the earthquake catalogues is poor. Even in Northwest Europe, where the historical methodology is used since more than 20 years (Alexandre, 1985, 1990; Vogt, 1984, 1985; Ambraseys and Melville, 1983; Melville, 1982), the richness of historical sources is so important since the 16th century that it should be always possible to improve greatly our knowledge of past earthquakes.

The most critical aspect in historical seismicity studies is the lack of access for the seismologists to the original earthquake reports allowing them to formulate their own hypothesis on specific earthquakes. Therefore, the earthquake reports and the information concerning their source should be opened to the earthquake scientists,

engineers and stakeholders. This is particularly important when considering the relationship between historical earthquakes and seismic hazard assessment.

At the Royal Observatory of Belgium, we have been collecting reports on historical earthquakes for more than 20 years. It spans a period from the earliest available sources (circa 700 AD) to 1527 for Western Europe and up to now for Northwest Europe. The objective of this note is to present the historical earthquake database that has been developed to save these data for the future and to make them accessible by the internet.

The available information for 20th century earthquakes

Most of the information concerning the earthquakes felt in Belgium from 1932 is archived at the Royal Observatory of Belgium, because since that time, after each felt earthquake in Belgium, our institute has conducted an official inquiry, addressing a questionnaire to all city and district authorities in the country. In parallel the ROB archives contain letters from the public describing, sometimes with numerous details, how they felt the earthquake and the damage to their properties. For some of these earthquakes, the archives contain also unpublished internal report resulting from the ROB scientist and technician visits in the affected localities.

Another important source of information is the scientific publications concerning the specific earthquakes. For the period from 1900 to 1932, these works are often the only reports available.

During the recent years, we undertook also a systematic search in the newspapers (Alexandre et al., 2007), which not only supply direct information on the damage and other observed effects of the earthquakes, but also on additional related socio-economic topics.

These different types of reports have been introduced in our database. Presently only newspaper reports are available on our web site [www.seismologie.be]. The other documentation is available on our intranet and allowed already, in cooperation with the Faculté Polytechnique de Mons, to undertake specific research related to seismic risks (Barszez, 2005; Philipront, 2007).

The available information for historical earthquakes before 1900

For the earthquakes that occurred before the instrumental era it is necessary to search original written sources contemporaneous with the seismic events. As seen above, cooperation with professional historians is necessary for those studies.

Works published by Alexandre (1985, 1990), Alexandre and Vogt (1994), Vogt (1984, 1985), Ambraseys and Melville (1983) or Melville (1982) have shown indeed that most of the studies on northwest European historical earthquakes used up to that time were compilations conducted without any sense of source criticism. Even if part of the information in those works is correct they did not mention their sources and therefore it is impossible to assess its veracity. Some recent earthquake catalogues and studies continue to suffer from this lack of report to the original basic information. On the other hand, there are also studies, like the book of Meidow (1995) on the

earthquakes in the Northern Rhine region, that continue to use old compilations but that nevertheless provide also new useful original data.

The use of ancient and medieval narrative sources raises specific problems, because a lot of these documents come from lost original sources; so it is necessary to clearly identify these lost texts. In this respect, the Guidoboni's catalogue (Guidoboni, 1994) is an important contribution to the study of the earthquakes felt in ancient Mediterranean area; for Western Europe area in the Middle Ages, the methodology perfected by Alexandre (1987) concerning the climatic data can be applied to the chronicles and other annalistic sources available in the Royal Observatory of Belgium earthquake database.

The earthquake information database

There are five inputs in the historical earthquake database of the ROB (Fig. 1): the earthquakes, the historical texts, the sources, the bibliography and the localities. Each earthquake is referenced with an ID (identification number) in the catalogue. Each earthquake report is labeled as an historical text, with a specific ID. With each historical text a historical source is associated. The modern scientific studies that published specific historical sources (and discussed their associated historical texts) are also identified in the historical bibliography with a specific ID. The fifth input is the localities where the shocks were reported. The complete description of the data related to each part of the database is given on Fig. 1.

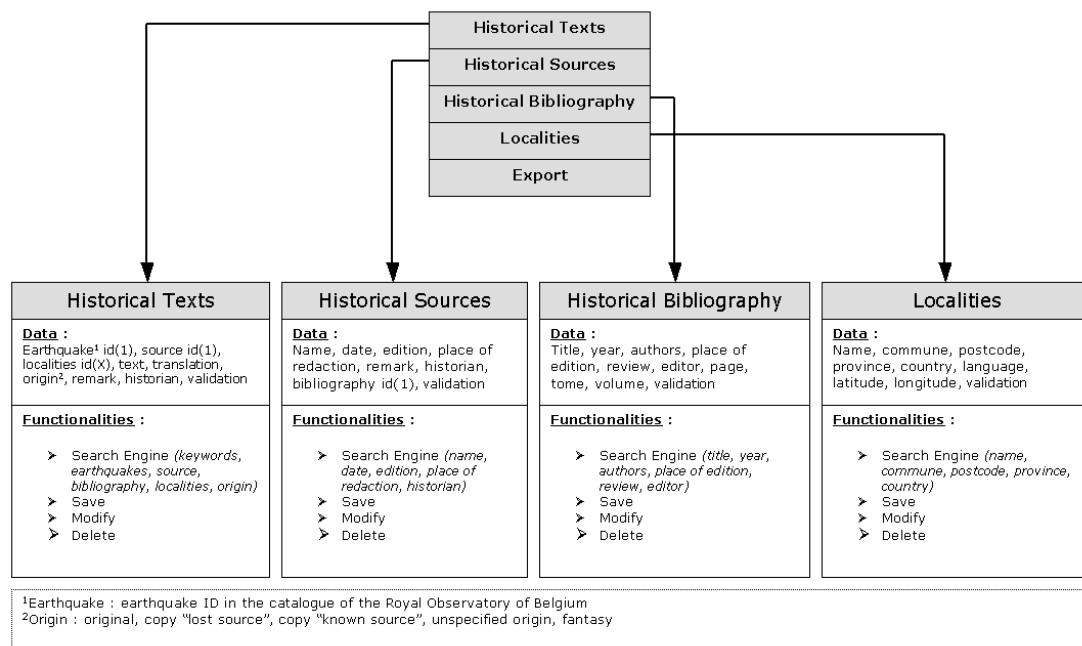


Figure 1: Organigram of the historical earthquake database of the Royal Observatory of Belgium.

The data associated with the historical texts for one specific earthquake are the source, the localities that are mentioned in the text, the text itself in its original language and transcription, in some cases a translation of the text into an other language (French or Dutch), the originality of the source, with relevant remarks if necessary, the name of the historian who conducted the research and a flag describing the validation status of

the text (yes or no). This status confirms only that a scientist validated the information in the database. The same flag exists for the different inputs of the database.

The originality of the text concerns the relevance of the text in terms of historical criticism. It can be a text coming from an «original» contemporaneous historical source, a copy of an original «lost source», a copy of a former «known source», an unspecified origin or a fabrication. It is evident that the texts originated from the last three types of sources have no interest for us. Nevertheless we mentioned them in the database, to mark a false information and so preventing inexperienced persons, lacking of basic knowledge in historical science, from rediscovering the event and reinserting it in the data base. The description of historical sources is fundamental because it is the information that validates the earthquake report from the historical point of view. It should allow anyone to retrieve the original texts in the record-offices. The name of the source is given by the historian, applying specific rules to obtain a homogeneous presentation of the data. The «edition» input is used to help the reader in the search of the original text.

As an example, you will find here a text describing the effects of the 18 Septembre 1692 earthquake at Soiron in Belgium: *«Il at fait un tremblement de terre espouvantable qui a abbatu des maisons, cheminées don't les miennes l'ont esté et le chasteau de Soiron gasté et irréparable.»*. The name of the source is *«Servais Ronval, Notes du registre paroissial de Soiron»* and the edition *«M. Graindor, La vie quotidienne à Soiron au temps jadis, Olne, 1964. »*.

If the text has been not edited by an historian yet, it is described as a manuscript and referenced by the record-office where it has been found with the associated references to the manuscript.

The different developed functionalities provide the people in charge of the introduction of the data in the database with an easy handling of the information as well as the custom with user friendly tools to search for information about a specific earthquake, or report, or locality.

Discussion and Conclusions

The historical earthquake database developed at the Royal Observatory of Belgium intends to put together the original reports of earthquakes in Northwest and Western Europe and to preserve them for the future.

It is also a response to a real need within the seismological community in this part of Europe. The access to the original reports used to infer local intensity is becoming an important topic in earthquake studies related to seismic hazard assessment. Actually, this is the only way to control the validity of the parametric catalogues that are used to model the seismic activity and therefore to evaluate their uncertainties.

In the framework of the Eurocode 8 parasismic norm implementation in the European countries, it will be necessary to provide information to the public, the authorities and the building companies to justify the use of the norm. This database and its open access to the internet is also a part of a more general prevention strategy. Presently, the access is only open to the reports of the newspapers for the 20th century earthquakes. As the data have been introduced during student works, the other parts of

the database will be given accessible as soon as they will be controlled by an historian appointed by the ROB. Nevertheless, for specific investigations, it is possible to have an access to the data when coming at the ROB and consulting our intranet.

In Europe other historical earthquake databases already do exist, for instance in France [www.sisfrance.net] or in Switzerland [www.seismo.ethz.ch], so it would be useful to perfect a European earthquake catalogue, elaborated according to the rules of historical criticism. In this way, this European catalogue would not be the simple addition of different national catalogues, but well a new standardized work, where original sources would be distinguished from the worthless compilations. In this respect, the expertise developed in the ROB database concerning the complex problem of the medieval sources can bring an important contribution to the study of the seismicity of that era.

References

- Alexandre P. (1985). Catalogue des séismes survenus au Moyen Age en Belgique et dans les régions voisines. In « Seismic activity in Western Europe », P. Melchior editor, Reidel, 189-203.
- Alexandre P. (1987). Le climat en Europe au Moyen Age. Contribution à l'histoire des variations climatiques de 1000 à 1425, d'après les sources narratives de l'Europe occidentale. Paris, 827 pp.
- Alexandre P. (1990). Les séismes en Europe Occidentale de 324 à 1259. Nouveau catalogue critique: Série Géophysique, Observatoire Royal de Belgique, 267 p.
- Alexandre P. and Vogt J. (1994). La crise sismique de 1755-1762 en Europe du Nord-Ouest, *in* Albin P. and Moroni A., eds., Historical investigation of European earthquakes, materials of the CEC project: review of historical seismicity in Europe: Milano, CNR, 2, p. 37-76.
- Alexandre P., Kusman D. et Camelbeeck T. (2007). La presse périodique, une source pour l'histoire des tremblements de terre dans l'espace belge, *Archives et Bibliothèques de Belgique*, LXXVIII, 1-4, 257-278.
- Ambraseys N. (1985). Intensity-attenuation and magnitude-intensity relationships for northwest European earthquakes, *Earthquake Engineering and Structural Dynamics*, 13, 733-778.
- Ambraseys N. and Melville C. (1983). *Seismicity of the British Isles and the North Sea*: London, SERC, Marine Technology Centre, 132 p.
- Bakun W. and Wentworth C. (1997). Estimating earthquake location and magnitude from seismic intensity data. *Bulletin of the Seismological Society of America*, 87, 1502-1521.
- Barszez A.-M. (2005). Aléa sismique du Bassin de Mons et vulnérabilité des bâtiments anciens – Analyse du risque sismique pour un quartier du centre historique de Mons. FPMs, Service d'Architecture et de Mines, MSc-thesis.
- Guidoboni E. (1994). Catalogue of ancient earthquakes in the Mediterranean area up to the 10th century, Istituto Nazionale di Geofisica, Roma, 504pp.
- Meidow H. (1995). Rekonstruktion und reinterpretation von historische erdbeben in den nördlichen Rheinlanden unter Berücksichtigung der Erfahrungen bei dem

- erdbeben von Roermond am 13 April 1992. Phd-thesis der Universität zu Köln, 305 pp.
- Melville C. (1982). The seismicity of England : the earthquake of May 21, 1382. *Boll.Geof. Teorica ed Applicata*, 24, 129-133.
- Melville C., Levret A., Alexandre, P., Lambert, J., and Vogt, J. (1996). Historical seismicity of the Strait of Dover-Pas de Calais: *Terra Nova*, v. 8, p. 626-647.
- Philipront A. (2007). Quels sont les effets sur le patrimoine architectural des séismes importants de nos régions ? Applications aux églises de Hesbaye – inventaire, méthodologies et perspectives. FPMs, Service d'Architecture et de Mines, MSc-thesis.
- Vogt, J. (1984). Révisions des deux séismes majeurs de la région d'Aix-la Chapelle-Verviers-Liège ressentis en France: 1504 1692, *in* Tremblements de terre, Histoire et Archéologie: actes du colloque d'Antibes 2-4/11/1983, Valbonne, p. 13-21.
- Vogt, J. (1984). Problèmes de sismicité historique. In « Seismic activity in Western Europe », P. Melchior editor, Reidel, 205-215.

B-FEARS: The Belgian Felt Earthquake Alert and Report System

Thomas Lecocq, Giovanni Rapagnani, Henri Martin, Frédéric Devos, Marc Hendrickx, Michel Van Camp, Kris Vanneste and Thierry Camelbeeck

Royal Observatory of Belgium, Avenue circulaire, 3, B-1180 Brussels, Belgium,
thomas.lecocq@seismology.be

Abstract

An automatic felt earthquake alert and report system, B-FEARS, was developed around the Belgian seismic network allowing seismologists to provide the authorities, the media and the public with information on local felt earthquakes a few minutes after their occurrence. This system is based on the analysis of the connection flow on the website of the Royal Observatory of Belgium (ROB) in parallel to an automatic control of a web macroseismic inquiry based on the “Did you feel it?” of the U.S. Geological Survey (Wald et al., 1999), available on the ROB website since 2002. This information is neither as precise nor as reliable as the one supplied by the analysis of seismic signals, but is efficient thanks to the great population density in Belgium. The alert is supplemented by the analysis of the seismic signals from seven real time seismic stations appearing on the website with a delay of more or less ten minutes.

The alert and report system was successfully tested and improved during the earthquake sequence that started in the southwest of Brussels on 12 July 2008. B-FEARS is now running continuously and warns seismologists in the minutes after the occurrence of a felt earthquake.

Introduction

Belgium has a moderate seismicity, with an average of 50 earthquakes per year during the last 25 years. Some are felt locally or even throughout the country. Under particular circumstances, even very low magnitudes earthquake can be felt. This is the case of one third of the events of the sequence that began on 12 July 2008 in the southwest of Brussels. On 20 March 2009 more than 100 earthquakes were on record. Although the magnitude of the felt events ranges 0.4 to 3.2, this induced a strong demand from the media and the population, who has been worrying about these repeated felt events.

For most of these events, the signal is weakly recorded by the permanent Belgian seismic network and would be very difficult to detect using real time detection algorithms based on the seismogram analysis. This paper presents B-FEARS, the Belgian Felt Earthquake Alert and Report System, which allows warning the

seismologists quickly about the occurrence of small but felt events, in order to inform the authorities and the public.

The Belgian seismic network

A modern seismic monitoring network has been progressively established by the ROB since 1985. Presently, it is formed by 24 seismic and 18 accelerometric stations. Three stations are located in Grand-Duchy of Luxemburg and one is in The Netherlands. These four equipments are managed in cooperation with the ECGS in Luxemburg and the KNMI in the Netherlands.

The traces of seven streaming or quasi real-time stations are displayed at the ROB offices in Uccle, a suburb of Brussels. This allows an immediate reaction during working hours. The signals are also relayed on the ROB website with a delay not exceeding 10 minutes. This allows us, if needed, to confirm the occurrence of an earthquake even outside working hours, when no personnel is present at the ROB.

In the daily routine procedure, the seismic signals from the seven on-line stations are visually processed in order to identify the seismic events recorded the day before and to automatically list the data files that have to be downloaded from the other (off-line) stations during the next night. The phase measurements from all the stations are then made the day after, meaning a delay of two days after the events (four days after a week-end). Of course, when an earthquake is felt, a specific script is applied to quickly retrieve all the data.

The macroseismic inquiry on the web

The first web macroseismic inquiries program "Did you feel it?" was developed by the U.S. Geological Survey (Wald et al., 1999). In 2002, we adapted the USGS web form (in English) and translated it into the three official languages in Belgium: French, Dutch and German. Immediately after the Alsdorf Earthquake ($M_L=5.0$) in Germany that occurred on 22 July 2002 at 05:45 UTC, we were able to open the inquiry on the internet, in the four languages. The internet address was given to the media which relayed the information to the public. In the afternoon after the earthquake, more than 2000 persons had already filled in the form, which allowed elaborating a preliminary map of the effects. In total, more than 6000 persons answered the questionnaire. The data from neighbouring countries were not analyzed and only 20 questionnaires were rejected due to incoherence. This first experience was very successful because it demonstrated (Camelbeeck *et al.*, 2003) that in regions like northwest Europe with a high density of population, web macroseismic inquiry are a real relevant source of information on earthquake ground motion as already demonstrated in more active zones like California (Atkinson and Wald, 2007).

This "Did you feel it?" inquiry is important because it can be used to delineate the epicentral area of any felt or destructive earthquake. This relies on an automatic analysis of the formularies. More advanced statistical and critical analysis can also be performed immediately. Fig. 1 presents the map obtained for the strongest earthquake of the seismic sequence that has occurred since the 12 July 2008 in the district of Court-Saint-Etienne, some 20 km to the southeast of Brussels. This $M_L = 3.2$ earthquake took place on the 13 July. It was felt up to the north of Brussels with a maximal radius of perceptibility of 35 km. The maximal municipality average

Community Internet Intensity (CII: calibrated to be similar, on average, to the Modified Mercalli Intensity) is 3.8 near the epicenter. The statistical distribution of the different answers to the questionnaires in the municipality of Court-Saint-Etienne is presented on Fig. 2.

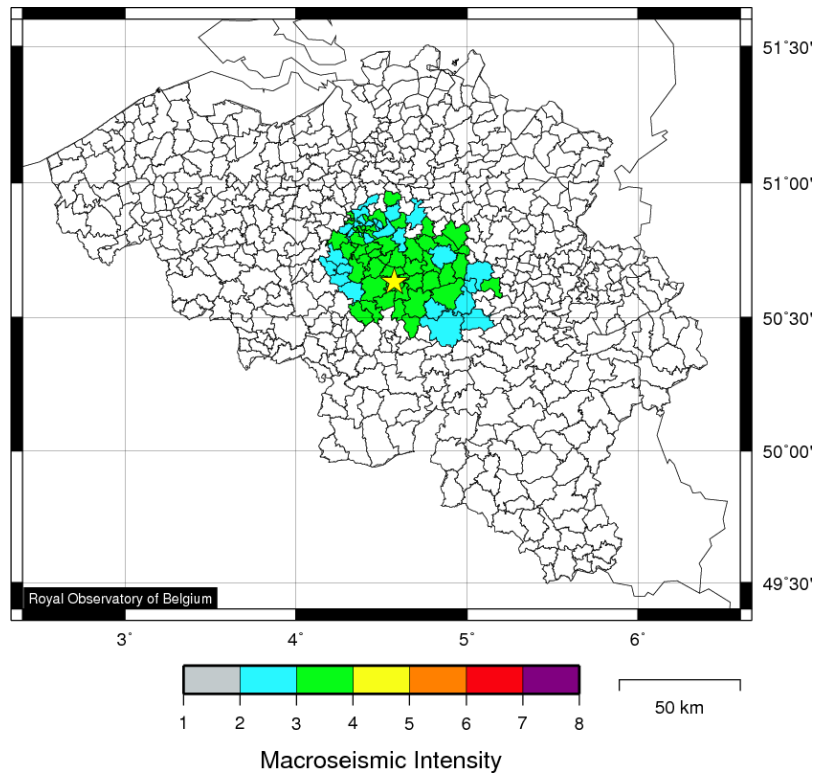


Figure 1: Macroseismic map of the M_L 3.2 earthquake of the 13 July 2008. Intensities (CII) are averaged and rounded to the nearest unit for each municipality. The star corresponds to the epicenter.

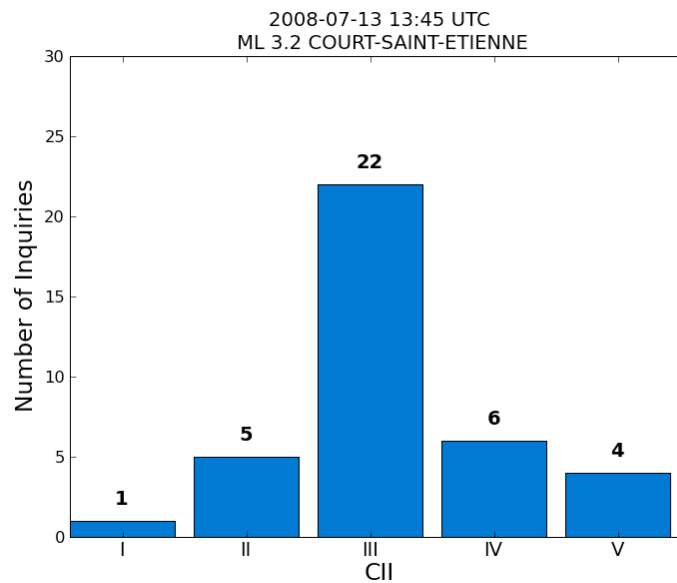


Figure 2: Distribution of the intensities at the municipality of Court-Saint-Etienne where the epicenter of the M_L 3.2 earthquake of the 13 July 2008 is located. Values are rounded down to the nearest unit. This distribution corresponds to an average of 3.8.

The development of an Alert System

Website Connection Flow approach

During the 2008 seismic swarm, it has been noticed that people rushed to the ROB website within minutes following a felt event and spontaneously filled in the web inquiry. This had previously been mentioned by Lisa Wald and Stan Schwartz (Wald and Schwartz, 2000) as they compared the USGS web traffic surge experienced after the 16 October 1999 Hector Mine Earthquake and a famous effect called "The Slashdot Effect". Slashdot.org is a popular website linking to articles around the internet. Whenever a link is posted on this website, the effect is a sudden, large increase in web server traffic. A similar surge happened on the USGS servers that day. Recently, the EMSC published (Bossu *et al*, 2008) a more detailed analysis of the traffic surge to their website when any earthquake occurs. The real-time analysis of the location of Internet Protocol (IP) addresses allows them to roughly know where an event has struck. We are currently working with the EMSC for implementing their "IP to Location" methodology, but as the Belgian internet network is fairly small, one cannot rely too much on the locations provided.

Based on this knowledge, it was decided to elaborate an alert system based on the number of connections to the website and on the number of filled "Did you feel it?" inquiries. The system sends text messages to the seismologists via E-Mail and SMS.

This first system triggers an alert whenever the parameters satisfy the following criteria:

	Visitors online	Number of filled inquiries
ALERT 1	$X \geq 50$	0
ALERT 2	$Y \geq X + 100$	At least 1
ALERT 3	$Z \geq Y + 100$	At least 1

Table 1: Parameters required to trigger an alert.

The "online" value is determined as the number of connections to the website in the last hour. The value of 50 visitors is a solid limit based on the "normal" average number of visitors connected to the ROB website.

In parallel to the SMS being sent, a more complete report is sent via E-Mail. The report contains summary of the "Did you feel it?" filled forms in addition to the same info as in the SMS (date, time, number of visitors, number of spontaneously filled inquiries).

When the alert is given to the seismologists during working hours, the first action is to look at the seismic streams to confirm the occurrence of an event, then to add the event to the database, open the inquiry and to start measuring phase arrival times and amplitudes on the seismograms. Outside working hours, if a seismologist has the opportunity to connect to the internet, the first action is to look at the quasi real-time seismic traces on the ROB website to confirm the occurrence of the earthquake and to estimate its magnitude and origin time. Then, the next action is to add this new event in the database, with the parameters deduced from the summary of the filled forms and the rough analysis of the on-line seismic traces on the website.

As soon as an event is added to the database with an open inquiry, the public connecting to the website will be invited to fill in the forms linked to that event.

Short Term Average / Long Term Average Method

A problem with the alarm being triggered at 50 online visitors is that on a normal day the activity of the website is slowly but surely increasing during the morning, stable during the day and decreasing during the afternoon (or evening). This slow increase can sometimes come very close to 50, and even pass it. Thus, the alarm would be triggered for nothing.

A method already validated (example: Bossu *et al*, 2008) is to compare a short time average (STA) to a long term average (LTA), a common method in signal processing. STA and LTA are the number of connections to the website in the last minute and in the last hour, respectively. To avoid false alarms, only the connections with IP addresses resolved to Belgium or to the neighbouring countries were taken into account. STA and LTA values must be determined in order to trigger alarms, ideally triggering an alert for every felt earthquake and with the lowest number of false alarms. An alert will be triggered when $STA \geq A$ and $STA/LTA \geq B$.

	Date	Time	Place		M_L	Forms	Parameters
1	2008-02-27	00:56	LINCOLNSHIRE	UK	4.9	27	01 – 20
2	2008-07-12	17:47	COURT-SAINT-ETIENNE	BE	2.2	330	03 – 25
3	2008-07-13	13:45	COURT-SAINT-ETIENNE	BE	3.2	1472	13 – 23
4	2008-07-14	01:33	DOUR	BE	2.6	91	03 – 05
5	2008-08-08	09:40	COURT-SAINT-ETIENNE	BE	1.6	33	03 – 07
6	2008-08-08	09:54	COURT-SAINT-ETIENNE	BE	1.7	32	08 – 13
7	2008-08-08	17:52	COURT-SAINT-ETIENNE	BE	1.8	33	08 – 06
8	2008-08-09	03:33	COURT-SAINT-ETIENNE	BE	1.5	26	02 – 60
9	2008-08-09	14:18	COURT-SAINT-ETIENNE	BE	2.2	74	20 – 27
10	2008-08-09	18:31	COURT-SAINT-ETIENNE	BE	2.2	174	36 – 14
11	2008-08-13	22:47	VILLERS-SAINT-GHISLAIN	BE	1.5	4	02 – 09
12	2008-08-22	13:26	COURT-SAINT-ETIENNE	BE	1.1	14	13 – 21
13	2008-08-22	15:38	COURT-SAINT-ETIENNE	BE	1.7	17	26 – 30
14	2008-09-10	08:26	COURT-SAINT-ETIENNE	BE	1.3	37	06 – 12
15	2008-09-12	05:08	COURT-SAINT-ETIENNE	BE	2.2	484	10 – 17
16	2008-09-13	01:14	COURT-SAINT-ETIENNE	BE	2.6	1086	14 – 28
17	2008-09-18	20:57	COURT-SAINT-ETIENNE	BE	0.9	66	10 – 17
18	2008-09-27	16:41	COURT-SAINT-ETIENNE	BE	1.7	104	12 – 23
19	2008-10-06	06:07	COURT-SAINT-ETIENNE	BE	1.2	5	07 – 19
20	2008-10-06	06:14	COURT-SAINT-ETIENNE	BE	2.0	76	08 – 13
21	2008-10-21	02:46	COURT-SAINT-ETIENNE	BE	0.4	3	03 – 20
22	2008-10-30	19:12	COURT-SAINT-ETIENNE	BE	1.6	126	28 – 28
23	2008-12-20	20:53	COURT-SAINT-ETIENNE	BE	2.5	831	45 – 50
24	2008-12-29	03:27	COURT-SAINT-ETIENNE	BE	1.5	126	06 – 51
25	2008-12-29	14:01	COURT-SAINT-ETIENNE	BE	0.8	42	25 – 15

Table 2: The 25 earthquakes felt in Belgium in 2008. The greyed rows correspond to the events for which no obvious traffic increase is observed.

A connection table was created from the connection log of the ROB website for the whole year 2008. For each minute, STA, LTA, STA/LTA values are calculated. Table 2 shows the 25 events felt in Belgium in 2008 and the corresponding traffic statistics. There is no obvious traffic increase for 6 of them. For all 25 cases, the maximum A and B pairs in the 10 minutes following the origin time are shown.

Based on these values, a test was made using $A = 6$ and $B = 12$ (Event 14). This test triggers an alarm for 17 of the 19 events and triggers 1 false alarm. There is a different explanation for not detecting two events:

- Event 2: the first event widely felt in Belgium in 2008, and the very first in the epicentral region (20 km south-east of Brussels) since 1957. Local people were not yet aware of the existence of the ROB website.
- Event 7: it happened on the same day as Event 6. The LTA value was still high (> 1.0), so the STA/LTA value did not reach the trigger value.

The only false alarm happened on the day of the M_L 3.2 earthquake, at 17:36 UTC. It is 19:36 local time, 6 minutes after the beginning of the evening news on the R.T.B.F. ("Radio Télévision Belge Francophone": French speaking Belgian television). The ROB website URL was given to the public in order to invite them to fill in the "Did you feel it?" formularies. This is a Slashdot effect!

This STA/LTA method is now continuously running on the ROB servers.

Alert Example:

On December, 20th, an ALERT 1 was triggered by the servers at 20:54:05 UTC. 66 persons were already online and no inquiries had been filled in yet. ALERT 2 was triggered at 20:55:45 UTC with 183 persons online and 2 inquiries filled. Finally ALERT 3 was triggered at 20:57:45 UTC with 4 inquiries filled.

Event	Location	Origin Time	Latitude	Longitude	Depth	Magnitude
2008-12-20	Estimated	20:53:00	50.6°	4.6°		M_L 2.6
2008-12-20	Measured	20:53:08.26	50.654°	4.566°	2.1 km	M_L 2.5

Table 3: Alert example for one event. Estimated (in the minute following an Alert, based on the inquiries and the seismograms) and measured (after measuring the phases and amplitudes) location and parameters are shown.

No seismologist was present at the ROB (21:57 local time), but some were to access the internet from home. The initial parameters were determined in the minutes following the alerts, based on the forms and the seismograms. Indeed, despite only the low number of forms available, their location and the raw triangulation based on the S-P arrival times were consistent. According to the experience acquired the last months, the magnitude was to be higher than for the 30 October event, at least because of the much faster increase of the connections to the website (Fig. 3) which cannot be only due to the better knowledge of the website existence. In the first minutes after the occurrence of the earthquake, seismologists were warned by the alert system and able to answer the media that were already calling. The initial location was a good approximation of the final location. Finally, 831 inquiries were filled in for this event, with $CII_{max}=IV$.

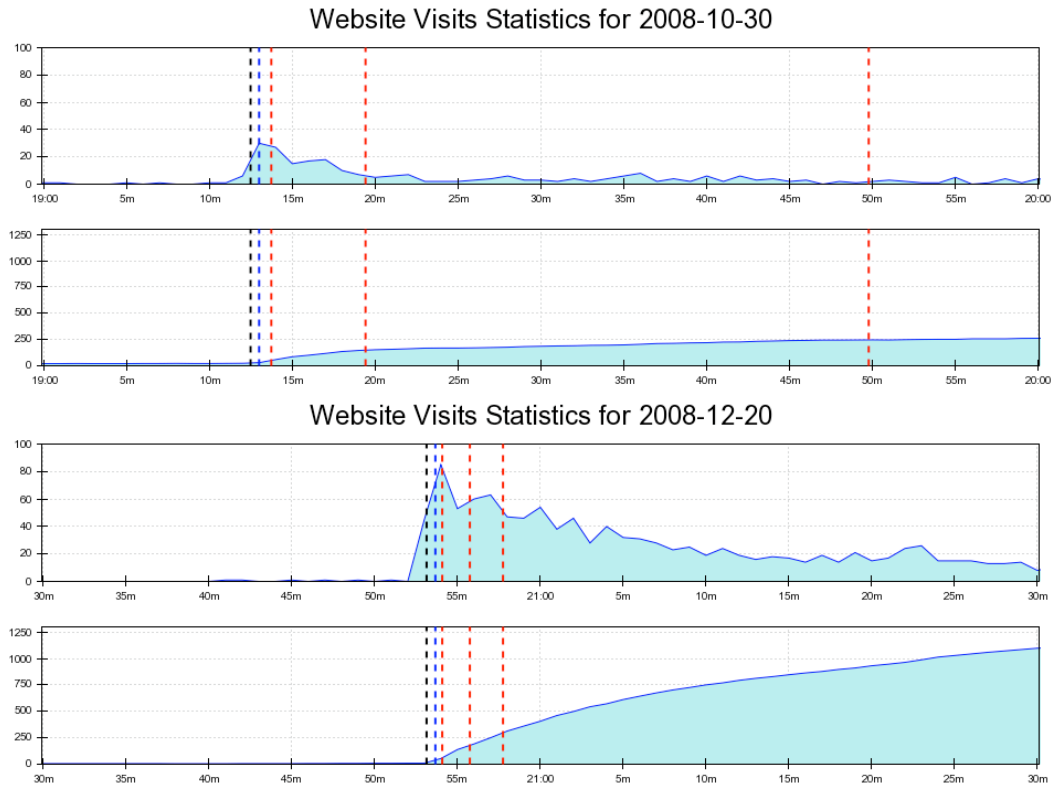


Figure 3: 1-hour website connections graphs for a $M_L1.6$ earthquake (2008-10-30) and for a $M_L2.5$ (2008-12-20). For each date: Above: New connections per minute (STA). Below: New connections in the last hour. The dashed lines represent: the origin time (black), the STA/LTA alert (blue), the ALERT 1, 2 and 3 (red).

Using the STA/LTA method, an alert would have been triggered at 20:53:40 UTC, 20 seconds earlier than ALERT1. This may not sound significant, but every second is important when an earthquake is felt.

Encountered problems & possible pitfalls

The ROB infrastructure supported a simultaneous number of visitors of more than 1000 but accessibility problems to the database were identified. This resulted in a general slowness of the website. The website structure was modified to limit the number of resources needed to print the main web pages. A 10 minute cache was defined for most of the pages. The cache can be manually emptied to allow the seismologists to refresh the content of the website. There has been no major event since these changes were implemented, so it is not yet known if they will be sufficient to overcome a massive flow of visitors.

The system is perfectible, its good-working is depending on a lot of parameters, the most important being all servers working properly. Currently, there is no alternative solution (mirror or external server) available in case of a major power cut. The SMS server is one key element in the system. Its state must be monitored to prevent the alerts being triggered but not sent via the SMS server.

The method presented here works nicely for the present earthquakes in the region south of Brussels, because of the low magnitude of the events, the high density of

population and the awareness of the public that they can find and report information on the ROB website. We cannot predict how the system will react for a larger earthquake. Indeed, if a destructive event happens it makes sense that people would not rush to internet but well on the streets. This could lead to a blind zone on the map produced from the inquiries. Nevertheless, people feeling the earthquake at a larger distance would trigger an alert and moreover, the seismologists would probably feel it too.

Conclusions and Perspectives

The seismic sequence that began in July 2008 20 km to the Southeast of Brussels provided the opportunity to develop and improve the seismic alert system at the ROB. Each of the first 22 felt earthquakes of the sequence allowed testing the modifications, solving specific problems in the procedures and improving the alert and report system.

The first alert system using the online number of visitors was improved and replaced by a more robust solution using STA/LTA values determined by the analysis of one year of connection data. The latter being the one actually running on the ROB servers. The STA/LTA not only triggers alerts sooner than the previous systems, but did not trigger any false alarm in 3 months. Since its migration to STA/LTA, B-FEARS has triggered 15 alerts, each time for a real event.

Three improvements are in development:

- Automatic implementation of the new earthquake in the database, without the intervention of a seismologist. This will allow the visitors of the website to associate the questionnaire they are filling with the event. The advantage is that the automatic results of the inquiry will be available quickly on the website.
- Test of the program SEISCOMP3, a software for seismic data analysis in near-real time developed by the GFZ Potsdam. The purpose would be to combine an alert based on the real-time processing of seismic signals with the one presented in this paper.
- Analyse of the basic information of the “Did you feel it?” inquiry to provide an automatic location of the epicenter and evaluation of the magnitude.

Finally, outside working hours, the ROB alert and report system highly depend on the good will and availability of the seismologists. The system may be working perfectly, but one day could come when no seismologist will be available. This matter has to be discussed with the authorities. One solution would be to establish an on duty service. If no seismologist can be on duty at the ROB 24/7, a realistic and technologically simple solution would be to buy a laptop with a GPRS (or 3G) connection. It would be the responsibility of one person to carry the laptop and to answer any alert outside working hours.

Acknowledgements

We thank Dr. Ronald Van der Linden, director general of the Royal Observatory of Belgium, for supporting and encouraging B-FEARS. Dr. Fabian Roosbeek, D. Herreman, A. Somerhausen are acknowledged for installing and maintaining the SMS server at the ROB, and H. Langenaken for her assistance for the communication with the public. Thomas Lecocq is bursar F.R.I.A., *Fonds pour la formation à la Recherche dans l'Industrie et l'Agriculture*, #FC76908.

References

- Atkinson, G.M. and Wald, D.J. (2007). "Did you feel it?" intensity data: a surprisingly good measure of earthquake ground motion. *Seismological Research Letters*, 78, 362-368.
- Bossu, R., Mazet-Roux, G., Douet, V., Rives, S., Marin, S. and Aupetit, M. (2008). Internet users as seismic sensors for improved earthquake response. *Eos, Transactions, American Geophysical Union*, Vol. 89, N°25, 17 June 2008, pp. 225-226.
- Camelbeeck, T., Van Camp, M., Martin, H., Van de Putte, W., Béatse, H., Bukasa, B., Castelein, S., Collin, F., Hendrickx, M., Petermans, T., Snissaert, M., Vanneste, K., Verbeeck, K., Verbeiren, R. (2003). Les effets en Belgique du tremblement de Terre du 22 juillet 2002. *Ciel et Terre*, 119, 1.
- Camelbeeck, T., Vanneste, K., Alexandre, P., Verbeeck, K., Petermans, T., Rosset, P., Everaerts, M., Warnant, R. and Van Camp, M. (2007). Relevance of active faulting and seismicity studies to assess long term earthquake activity in Northwest Europe, *Continental Intraplate Earthquakes: Science, Hazard, and Policy Issues*. Geological Society of America, S. Stein and S. Mazzotti (eds.) Special Paper 425, 193-224.
- Wald, D.J., Quitoriano V., Dengler L. and Dewey J. (1999). Utilization of the internet for rapid community intensity maps. *Seismological Research Letters*, 70, 680-697.
- Wald, L., and Schwartz, S. (2000). The 1999 Southern California Seismic Network Bulletin, *Seismological Research Letters*, 71-4, 401-413.

Tectonic stress field in rift systems – a comparison of Rhinegraben, Baikal Rift and East African Rift

Andreas Barth (1), Damien Delvaux (2) and Friedemann Wenzel (1)

- 1) Karlsruhe Institute of Technology (KIT), Geophysical Institute, Hertzstr. 16, D-76187 Karlsruhe, Germany, andreas.barth@kit.edu, friedemann.wenzel@kit.edu
- 2) Royal Museum for Central Africa, Leuvensesteenweg 13, B-3080 Tervuren, Belgium, damien.delvaux@africamuseum.be

Abstract

Crustal stress pattern provide important information for the understanding of regional tectonics and for the modelling of seismic hazard. Especially for small rifts (e.g. Upper Rhine Graben) and beside larger rift structures (e.g. Baikal Rift, East African Rift System) only limited information on the stress orientations is available. We refine existing stress models by using new focal mechanisms combined with existing solutions to perform a formal stress inversion. We review the first-order stress pattern given by previous models for the Upper Rhine Graben, the Baikal Rift, and the East African Rift System. Due to the new focal mechanisms we resolve second-order features in areas of high data density. The resulting stress orientations show dominant extensional stress regimes along the Baikal and East African Rift but strike-slip regimes in the Upper Rhine Graben and the interior of the Amurian plate.

Introduction

Stress field orientations are valuable constraints for understanding rift kinematics and rift development. They can be used to deduce boundary conditions for kinematic models (Buchmann & Connolly, 2007; Petit & Fournier, 2005). Moreover, data from regions adjacent to rift structures can reveal spatial changes from the rift-related stress field. Stress data from the inversion of focal mechanism solutions (FMS) of light earthquakes can improve the data coverage especially for intraplate regions with a low seismicity. We use new FMS from earthquakes with $M_w \geq 3.9$ that were determined using the Frequency Sensitive Moment Tensor Inversion (FMTI, Barth et al., 2007). The FMTI allows to invert regional waveform data for automatically determined frequency pass-bands based on a 1D earth model. Combining the new FMS with known FMS, we perform the formal stress inversion (Michael, 1987). After using both nodal planes for inversion, the best fitted plane is chosen for the final inversion. First-order stress pattern are a consequence of sub-lithospheric processes and plate boundary forces, that partly are related to gravitational potential energy as discussed by several authors (Zoback, 1992; Coblenz & Sandiford, 1994). However, this alone cannot explain second and third order pattern as discussed in this work, that result from three-dimensional density variations and deep mantle processes in some cases.

East African Rift System (EARS)

The EARS is a complex example of active continental rifting. Passing for nearly 3000 km through the continent, the EARS separates the Nubian subplate to the west from the Somalian subplate to the east. The eastern part of the African continent, which is dominated by the EARS, is affected by extensional stresses with a general E-W orientation of the minimum horizontal stress S_h , while the Nubian plate is affected by a compressional regime with the maximum horizontal stress S_H oriented E-W (Fig. 1). Barth et al. (2007) determined 38 new focal mechanisms using the FMTI. Delvaux & Barth (2009) combined these solutions with others to a total dataset of 332

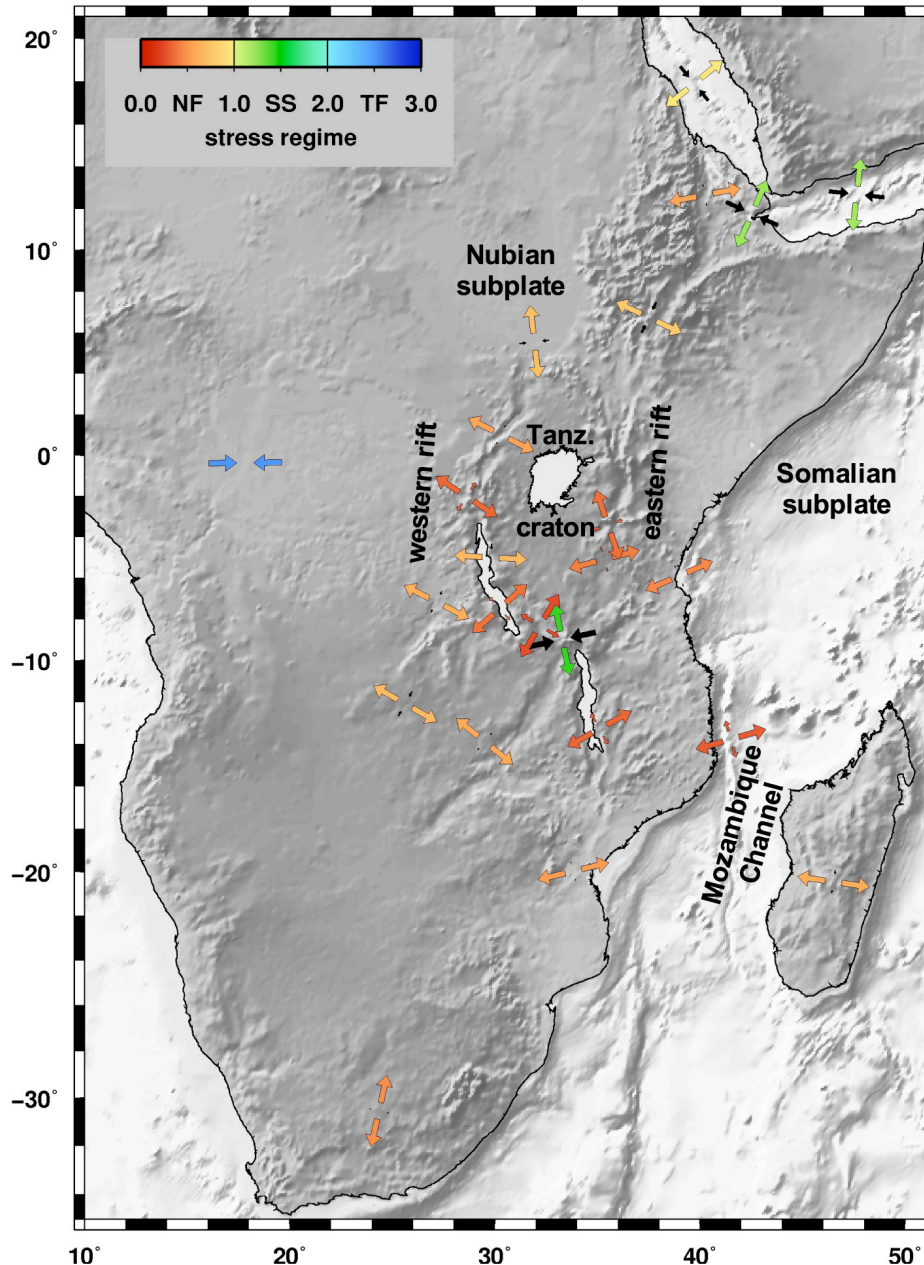


Figure 1: Formal stress inversion of 332 FMS in Africa (Delvaux & Barth, 2009). Colours indicate the stress regime. Vectors give the orientations of max. and min. horizontal compressional stress S_H and S_h , respectively. Stress symbols after Delvaux et al. (1997).

FMS and performed stress inversions for 24 bins. For 12 bins they obtained quality A and B following the *World-Stress-Map (WSM)* quality ranking scheme (Heidbach et al., 2008). They showed that the rift basins that surround the Tanzanian craton mostly have S_h orientations roughly orthogonal to their trend. Two dominant orientations of S_h arise: WNW-ESE extension in the north-western segments of the EARS and in the south-western high plateau region and ENE-WSW extension in the central part of the western rift branch, the southern extremity of the eastern rift branch, the southernmost rift segment, and the continental margin. The overall extensional regime mainly results from plate boundary forces combined with lithospheric gravitational potential energy of the African high plateaus. As the lowlands of the Indian Coast and the Mozambique Channel seem also affected by extensional faulting, the extension might also reflect a combination of complex 3-dimensional crustal structure and deep processes like the spreading of a mantle plume head beneath the Tanzanian craton or mantle flow at the base of the lithosphere (Delvaux & Barth, 2009).

Baikal Rift and Amurian plate

The Amurian plate is situated between the Eurasian and Pacific plates and spans approximately 2500 km in both the north-south and the east-west directions. Since Zonenshain & Savostin (1981) suggested the existence of a distinct Amurian plate, its development, plate kinematics as well as the location of its plate boundaries have been matters of debate (e.g. Petit & Fournier, 2005; Delvaux et al., 1997). Barth & Wenzel (2009) used the FMTI to calculate 41 focal mechanism solutions for earthquakes with magnitudes of $M_w \geq 3.9$ that have not been determined before. Here we combine them with additional data to a set of 272 FMS. Stress inversion is performed for 13 bins along the Baikal Rift, the Transbaikal, and the Amurian plate (6

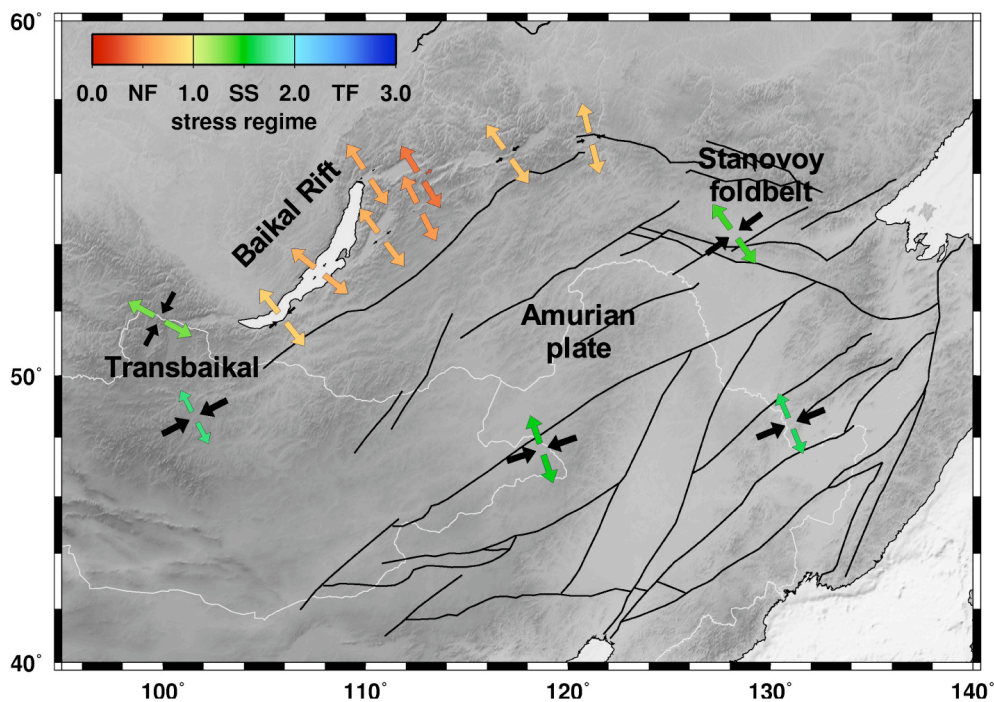


Figure 2: Formal stress inversion of 272 FMS along the Baikal Rift and within the Amurian plate. Symbols as in Fig. 1.

quality A and B). Along the rift itself we obtain normal faulting regimes with S_H oriented NW-SE, mostly orthogonal to the rift trend. For the Transbaikal and interior of the Amurian plate we obtain a strike-slip regime with an NE-SW to ENE-WSW orientation of S_H (Fig. 2). The stress field at the Stanovoy foldbelt shows a slight rotation with respect to the more southern regions and might be influenced by the Baikal Rift extension. The transpressive regime in the eastern part of the Amurian plate responds to far field plate boundary forces from the Pacific plate subducting at the Kuril trench and northern Japan (Barth & Wenzel, 2009).

Upper Rhine Graben (URG)

The URG is part of the European Cenozoic Rift System (ECRS) that extends from the Mediterranean Sea to the North Sea. Within the last 100 years five events of magnitude 4.7 took place in the URG and the largest historic event dates from 1356 when in Basel/Switzerland a major earthquake of maximum intensity IX killed 300 people (Leydecker, 2008). Several studies focused on the stress field in the seismically more active southern part of the URG and its connection to the southern parts of the ECRS (Plenefisch & Bonjer, 1997; Cardozo & Behrmann, 2006; Delacou et al., 2004). However, for the adjacent seismic active regions of the Vosges Mountains and the Swabian Alb no stress inversion of focal mechanism data has been performed so far. In this study we group 83 FMS (Swiss Seismological Service; Bonjer, 1997) in three bins: Southern URG (SURG: 47 FMS), Vosges Mountains (VS: 8 FMS), Swabian Alb (SW: 28 FMS). Figure 3 shows that the stress field of SURG ($S_H = 146^\circ$, B quality) is slightly rotated compared to $S_H = 159^\circ$ of both, VS (B quality) and SW (A quality). While SURG and SW show transtensional strike-slip regimes, VS has a tendency to a transpression. Besides the strong influence of the African-Eurasian collision the regional stress field might be a consequence of the strong gradients in local topography.

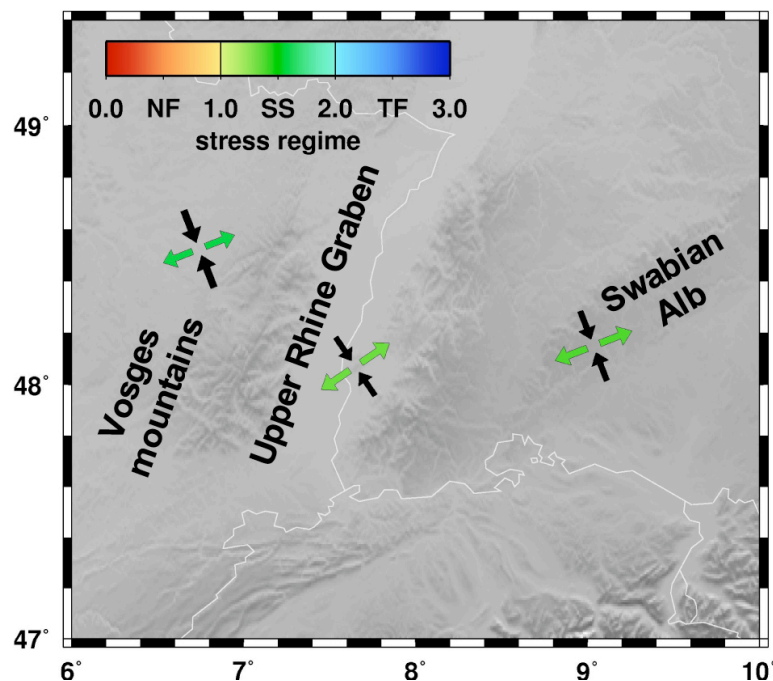


Figure 3: Formal stress inversion of 83 FMS for the URG and adjacent regions. Symbols as in Fig. 1.

Discussion & Conclusions

Both active rifts, the Baikal and the East African Rift System (EARS) show extensional regimes along the main rifts. The adjacent regions to the Baikal Rift reveal strike-slip regimes as a consequence of plate boundary forces. However, the extensional regime of the EARS in combination with topography effects of the high plateaus dominates the stress field in eastern Africa, although local stress variation indicate structural heterogeneities and/or deep processes. In the URG a strike-slip regime has reactivated the main structures that is also apparent in the adjacent Vosges mountains and Swabian Alb. The first-order stress pattern of the presented rifts are in general supported by data of the *WSM Project* (Heidbach et al., 2008), while second and third order effects reveal the influence of local heterogeneities.

We showed that the FMTI (Barth et al., 2007) can be used for the determination of focal mechanisms of earthquakes $M_w \geq 3.9$ and that it is applicable world-wide. It can improve the knowledge of active tectonics and may allow stress inversions in regions where it was not possible before.

References

- Barth, A., Wenzel, F. & Giardini, D. (2007). Frequency sensitive moment tensor inversion for light to moderate magnitude earthquakes in eastern Africa. *Geophys. Res. Lett.* 34, L15302, doi:10.1029/2007GL030359.
- Barth, A. & Wenzel, F. (2009). New constraints on the intraplate stress field of the Amurian plate deduced from light earthquake focal mechanisms. *Tectonophysics*, in press, doi:10.1016/j.tecto.2009.01.029.
- Bonjer, K.-P. (1997). Seismicity pattern and style of seismic faulting at the eastern borderfault of the southern Rhine Graben. In: K. Fuchs, R. Altherr, B. Müller, and C. Prodehl, (Editors), *Stress and Stress Release in the Lithosphere – Structure and Dynamic Processes in the Rifts of Western Europe*. *Tectonophysics* 275, 41–69.
- Buchmann, T.J. & Connolly, P.T. (2007). Contemporary kinematics of the Upper Rhine Graben: A 3D finite element approach. *Global Planetary Change* 58, 287–309.
- Cardozo, G.G.O.L. & Behrmann, J.H. (2006). Kinematic analysis of the Upper Rhine Graben boundary fault system. *Journal Of Structural Geology Pergamon-Elsevier Science Ltd* 28, 1028–1039.
- Coblentz, D.D. & Sandiford, M. (1994). Tectonic stresses in the African plate: Constraints on the ambient lithospheric stress state. *Geology* 22, 831–834.
- Delacou, B., Sue, C., Champagnac, J. & Burkhard, M. (2004). Present-day geodynamics in the bend of the western and central Alps as constrained by earthquake analysis. *Geophys. J. Int.* 158, 753–774.
- Delvaux, D. & Barth, A. (2009). African Stress Pattern from formal inversion of focal mechanism data. *Tectonophysics*, in press, doi:10.1016/j.tecto.2009.05.009.
- Delvaux, D., Moeys, R., Stapel, G., Petit, C., Levi, K., Miroshnichenko, A., Ruzhich, V. & San'kov, V. (1997). Paleostress reconstructions and geodynamics of the

- Baikal region, central Asia, part 2. Cenozoic rifting. *Tectonophysics* 282 (1–4), 1–38.
- Heidbach, O., Tingay, M., Barth, A., Reinecker, J., Kurfeß, D. & Müller, B. (2008). The World Stress Map database release 2008, doi:10.1594/GFZ.WSM.Rel2008.
- Leydecker, G. (2008). Erdbebenkatalog für die Bundesrepublik Deutschland mit Randgebieten für die Jahre 800–2006 – Datenfile <http://www.bgr.de/quakecat>; Bundesanstalt für Geowissenschaften und Rohstoffe (BGR), Stilleweg 2, D-30655 Hannover.
- Michael, A.J. (1987). Use of focal mechanisms to determine stress: a control study. *J. Geophys. Res.* 92 (B1), 357–368.
- Petit, C. & Fournier, M. (2005). Present-day velocity and stress fields of the Amurian plate from thin-shell finite-element modelling. *Geophys. J. Int.* 160 (1), 358–370.
- Plenefisch, T. & Bonjer, K.-P. (1997). The stress field in the Rhine Graben area inferred from earthquake focal mechanisms and estimation of frictional parameters. In: K. Fuchs, R. Altherr, B. Müller, and C. Prodehl, (Editors), *Stress and Stress Release in the Lithosphere - Structure and Dynamic Processes in the Rifts of Western Europe*. *Tectonophysics* 275, 71–97.
- Zoback, M.L. (1992). First- and second-order patterns of stress in the lithosphere: The World Stress Map project. *J. Geophys. Res.* 97, 11,703–11,728, doi:92JB00132.
- Zonenshain, L. & Savostin, L. (1981). Geodynamics of the Baikal rift zone and plate tectonics of Asia. *Tectonophysics* 76 (1–2), 1–45.

First step toward realistic ground-motion prediction for SW-Germany

Vladimir Sokolov and Friedemann Wenzel

Geophysical Institute, Karlsruhe Institute of Technology (KIT) / University of Karlsruhe,
Hertzstr. 16, 76187 Karlsruhe, Germany, vladimir.sokolov@gpi.uni-karlsruhe.de

Abstract

Although seismic hazard in Germany is not high, as compared with countries such as Italy and Greece, earthquakes here have been known since the Middle Ages. The state of Baden-Württemberg, which is located in the South-Western part of Germany, is characterized by the highest seismic activity in the country. Among the strongest earthquakes, which shook the territory, we can mention the Basel (Switzerland), 1356, earthquake (M_W 6.4), the Ebingen, 1935 (M_W 5.4), and the Albstadt, 1978 (M_W 5.2), earthquakes (Swabian Alb). The last event caused economic losses of more than EUR 250 million. The requirements of aseismic design, seismic losses and risk management, as well as the Shakemap and Early Warning techniques, dictate the necessity of estimation of seismic hazard in terms of various parameters of ground motion that include seismic intensity. Such estimations, in turn, need the correspondent site-dependent ground-motion prediction models. However, due to the extreme shortage of the observed data, the seismic hazard estimations for the region had been performed using the global European, or even worldwide, models. The models do not consider the regional peculiarities of local site conditions and they are limited in terms of the used ground motion parameters (only peak ground acceleration and response spectra). We describe the first step of development a realistic model for estimation of site-dependent engineering strong ground-motion parameters in South-Western Germany. The model is based on the regional earthquake ground-motion data, site amplification parameters, and stochastic simulation. We analyzed the attenuation models recently developed for Europe and the observed earthquake ground motion effect in Baden-Württemberg. The observed data include macroseismic observations collected after the Albstadt earthquake and strong-motion records obtained during the recent Waldkirch, 2004, earthquake (M_W 4.9). The resulting model (a) fits the observations and (b) it is compatible with European-wide attenuation models developed recently. In future, the model allows constructing correspondent ground-motion prediction equations to be used in deterministic and probabilistic seismic hazard assessment, Shakemap generation and Early-Warning systems.

Introduction

Although seismic hazard in Germany is not high, as compared with countries such as Italy and Greece, earthquakes here have been known since the Middle Ages (Leydecker 1999; Grünthal and Waldström 2003; Grünthal 2004). The state of Baden-Württemberg, which is located in the South-Western part of Germany (Fig. 1), is characterized by the highest seismic activity in the country (e.g. Abrahamczyk et al. 2005; Keintzel 2005; Tyagunov et al. 2006) and several seismic zones had been outlined here (Leydecker and Aichele 1998). The strongest earthquakes, which shook the territory are the Basel (Switzerland), 1356, earthquake (M_W 6.4, epicentral intensity up to IX MSK) (see review in Gisler et al. 2006) the Ebingen, 1935 (M_W 5.4, epicentral intensity VII-VIII MSK), and the Albstadt, 1978, (M_W 5.2, epicentral intensity VII-VIII MSK) earthquakes in Swabian Alb (e.g. Amstein et al. 2005; Schwarz et al. 2005, see the global CMT catalog, <http://www.globalcmt.org>, for the moment magnitude values). The last event caused economic losses of more than EUR 250 million.

Grünthal et al. (1999) used global European, or even worldwide, models (Ambraseys et al. 1996; Sabetta and Pugliese 1996; Spudich et al. 1997) for seismic hazard estimations for the region due to extreme shortage of observed data. These models do not consider the regional peculiarities of local site conditions and are limited in terms of the used ground motion parameters - only peak ground acceleration and amplitudes of pseudo-spectral acceleration can be evaluated.

In this article we describe the first step towards a realistic model for estimation of site-dependent strong ground-motion parameters, based on regional ground-motion models, site amplification parameters, and stochastic simulation. We analyzed ground-motion models recently developed for Europe and available information of distribution of ground motion effect in Baden-Württemberg. The observed data include macroseismic observations collected after the Albstadt, 1978 (M_W 5.2), earthquake and 12 strong-motion records obtained during the recent Waldkirch, 2004, earthquake (M_W 4.7 from global CMT catalog, or M_W 4.9 based on $M_W - M_L$ relationship, see Hintersberger et al. 2007). The resulting model (a) fits the observations and (b) it is compatible with European-wide attenuation models developed recently.

Description of the approach and the input data

For regions with a lack of instrumental strong-motion data, an indirect approach can be used for developing ground-motion prediction equations. They are developed on the basis of Fourier Amplitude Spectrum (FAS) source scaling, attenuation models, and generalized site amplification functions. The scheme of the approach is shown in Fig. 2.

The peak amplitudes of ground acceleration (PGA) and velocity (PGV), as well as the pseudo-spectral acceleration (PSA), are calculated from the site-dependent spectra using a stochastic technique (Boore 2003). The attenuation models for seismic intensity in this indirect approach may be evaluated using the relations between intensity and FAS (Chernov and Sokolov 1999; Sokolov 2002), or peak amplitudes of ground motion (Wald et al. 1999). Accelerograms are generated for many magnitudes and distances and the data are used to derive the prediction equations.

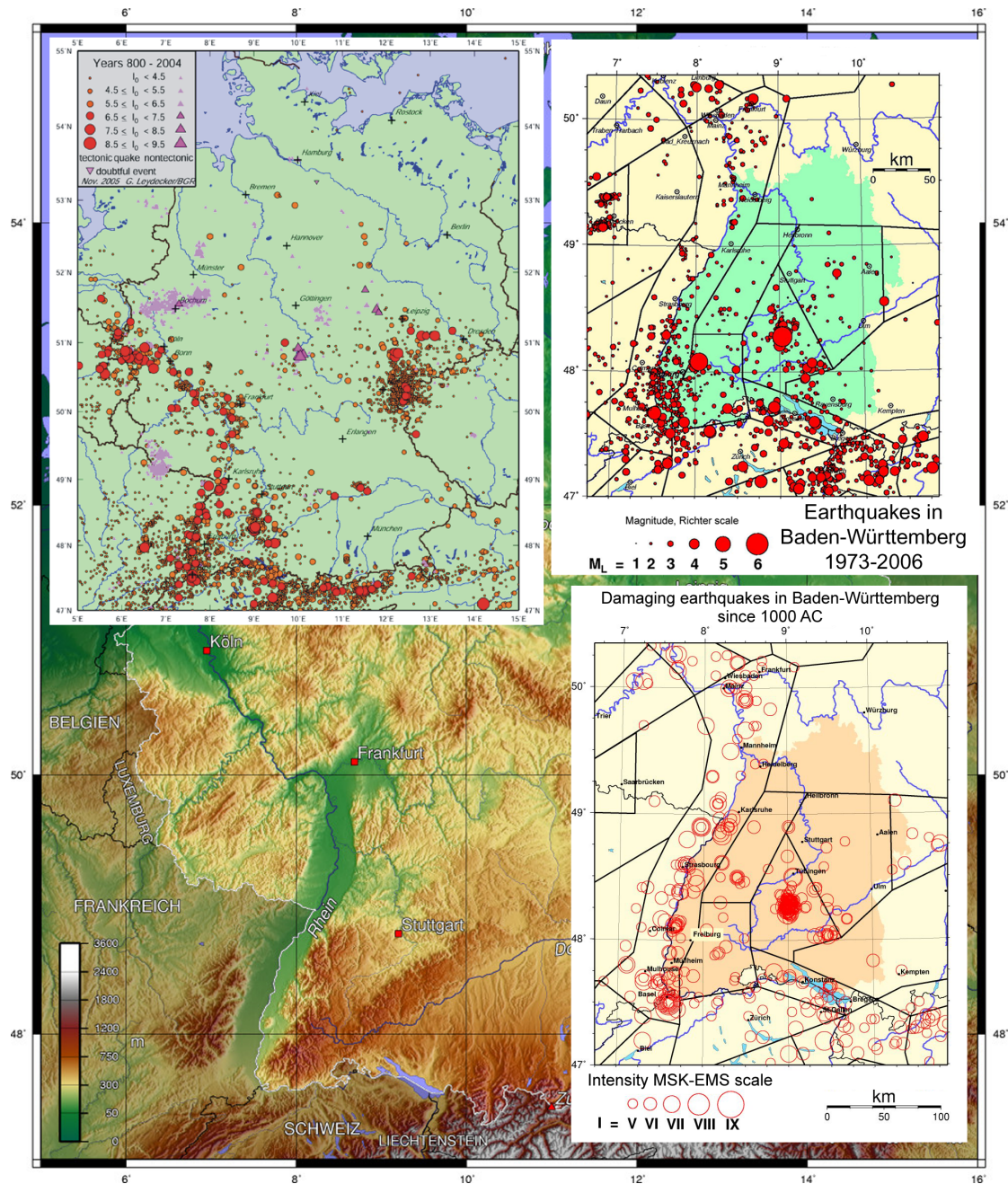


Figure 1. Seismicity of Germany and Baden-Württemberg. Map of earthquake epicenters with estimated epicentral intensity I_0 in the Federal Republic of Germany and adjacent areas for the period from AD 800 to 2004 is taken from (Leydecker, 2005).

Reviews of recent applications of the technique in various regions of the world may be found in Boore (2003). Sokolov and Wenzel (2007) and Sokolov et al. (2008) used the technique for the case of intermediate-depth earthquakes in the Vrancea (Romania) region.

The approach requires FAS models and a ground-motion database for calibration and testing of the model. As reference we selected three spectral models developed for Europe. The characteristics of the models are summarized in Table 1. Malagnini et al.

Table 1. Seismological parameters of the spectral models considered in this study.

Parameter*	Description
Fourier acceleration spectrum $A(f)$	$A(f) = (2\pi f)^2 CS(f)D(R, f)$
The scaling factor C	$C \sim R^N / (4\pi\rho\beta^3)$
Geometric attenuation R^N	$R^{-0.8}$ (0-140 km), $R^{-1.5}$ (140-180 km), $R^{0.0}$ (180-220 km), $R^{-0.5}$ (> 220 km) (Malagnini et al., 2000); $R^{-1.1}$ (0-50 km), $R^{-0.6}$ (50-70 km), $R^{0.2}$ (70-100 km), $R^{-0.5}$ (>100 km) (Bay et al., 2003, 2005); $R^{-0.8}$ (0-30 km), $R^{-1.0}$ (30-65 km), $R^{-0.5}$ (> 65 km) (Hintersberger et al., 2007).
Source spectrum $S(f)$	Brune (1970) ω -square, point source $S(f) = M_0 / [1 + (f / f_0)^2]$
Corner frequency f_0	$f_0 = 4.9 \times 10^6 \beta (\Delta\sigma / M_0)^{1/3}$
Stress parameter $\Delta\sigma$	30 bars (Malagnini et al., 2000); $\Delta\sigma = f(M)$ (Bay et al., 2003, 2005)
Density, ρ (gm/cm ³)	2.8
Shear velocity, β (km/sec)	3.8
Frequency-dependent attenuation $D(R, f)$	$D(R, f) = \exp[-\pi f R / Q(f)\beta]P(f, f_{\max})$
Path attenuation $Q(f)$	$400 f^{0.42}$ (Malagnini et al., 2000); $52 f^{0.78}$ (Hintersberger et al., 2007); $270 f^{0.5}$ (Bay et al., 2003, 2005)

(2000) obtained their model using records from 67 earthquakes in Central Europe obtained by German Regional Seismic Network. Records from about 300 earthquakes with magnitude from 2.0 to 5.2 occurred in Switzerland were analyzed by Bay et al. (2003, 2005). The data from the Waldkirch, 2004, earthquake were used by Hintersberger et al. (2007).

The soil classification, which is used in German Seismic Codes (DIN 4149 2005, see also description, for example, in Ref. [Keintzel 2005]), includes three generalized classes for deep geology (depth more than 20 m), namely: A (rock); B (thin sediments); C (thick sediments); and three generalized classes for shallow soil conditions, namely: 1 (hard soil); 2 (stiff soil); 3 (soft soil). The deep-geology class for a particular site may be found in the correspondent maps (e.g. "Karte der geologischen Untergrundklassen für Baden-Württemberg 1:350.000") and the shallow soil conditions have to be determined *in situ*. Brüstle and Stange (1999) calculated frequency-dependent site amplification functions of possible combinations of the deep geology and shallow soil classes using geotechnical characteristics (Table 2) that are typical for Baden-Württemberg. The generalized site amplification functions for the soil classes are shown in Fig. 3.

The observational data which we have considered include two earthquakes: (1) a number of strong motion records obtained during the recent 2004 Waldkirch

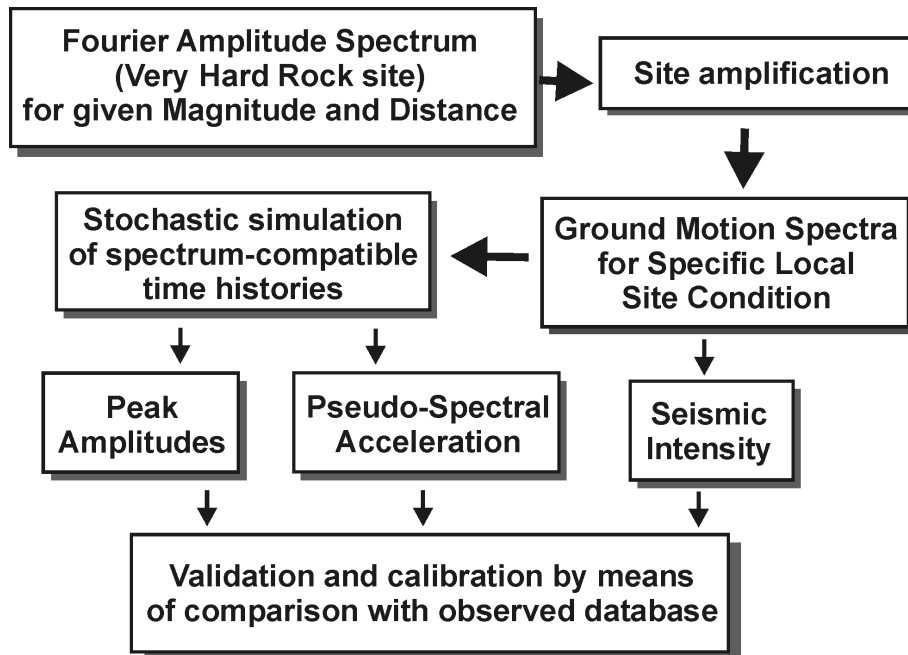


Figure 2. Scheme of evaluation of the ground-motion parameters based on the Fourier amplitude spectra and stochastic simulation.

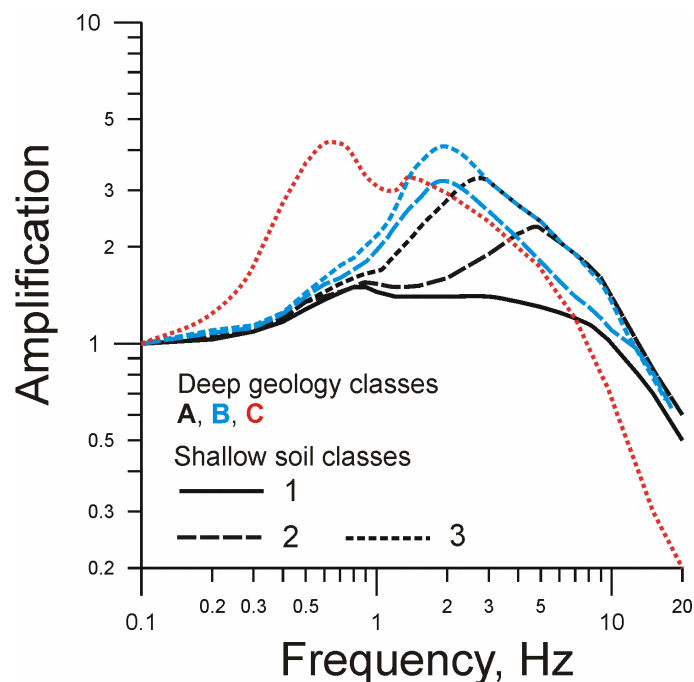


Figure 3. Generalized site-amplification functions for typical site classes in Baden-Württemberg (Brüstle and Stange 1999).

earthquake; (2) macroseismic intensity observations collected after the 1978 Albstadt earthquake (Prochazkova et al. 1979). We develop spectral models starting from the 3 available ones discussed before and adapt them to both observations. In addition we assure that these models are compatible with recently proposed attenuation relations for Europe (Table 3).

Table 2. Geotechnical characteristics of typical geological classes in Baden-Württemberg

Class description	Shear wave velocity, m/s *	Quality factor *	Density, g/cm ³ *
Bedrock	3300	200	2.7
Deep geology			
A (rock)	1600 ± 200	50 ± 10	2.3
B (thin sediments)	600 ± 100	25 ± 6	1.85
C (thick sediments)	350 ± 50	15 ± 4	1.75
Shallow soil			
1 (hard soil)	1100 ± 200	30 ± 4	2.1
2 (stiff soil)	550 ± 100	20 ± 4	1.8
3 (soft soil)	270 ± 50	10 ± 2	1.7

* The values of geotechnical characteristics for the “deep geology” rock classes gradually increase to the correspondent “bedrock” values at depth of 1000 m (Brüstle and Stange, 1999)

Table 3. Characteristics of empirical ground-motion prediction models

Model	Source	Database	Magnitude	Soil	Distance
AMB1996	Ambraseys et al., 1996	Italy, Greece and the Former Yugoslavia	M_S	Rock ($V_S > 750$ m/s) Stiff soil ($360 < V_S < 750$ m/s) Soft soil ($V_S < 360$ m/s)	fault rupture distance
SP1996, maximum horizontal component	Sabetta and Pugliese, 1996	Italy	M_W (4.6 – 6.8)	Stiff soil, shallow and deep alluvium	fault rupture or epicentral distance (< 100 km)
SPU1999	Spudich et al., 1999	Worldwide, extensional regime	M_W (5.0 – 7.7)	Rock and soil	fault rupture distance (< 70 km)
B-T2003	Berge-Thierry et al., 2003	ESM database	M_S (4.0 – 7.9)	Rock ($V_S > 800$ m/s) Soil ($V_S < 800$ m/s)	Hypocentral distance (< 330 km)

First, we analyzed the ground motion records obtained during the Waldkirch earthquake. The dataset contains 12 records at epicentral distances 25 km – 150 km. The values of recorded peak acceleration amplitudes were compared with the amplitudes of the motion, which were calculated using stochastic technique (Fig. 2) on the basis of the available spectral (source scaling and attenuation) models (Table 1) and the generalized site amplification functions (Fig. 3). The duration model, in which it is assumed that most (90%) of the spectral energy is spread over a duration $t_{0.9}$ of the accelerogram, consisted in two terms as follows: $\tau_{0.9} = \tau_S + \tau_P$, where $\tau_S = 1/f_0$ is the source duration (f_0 is the corner frequency) and $\tau_P = 0.06R$ is the path duration

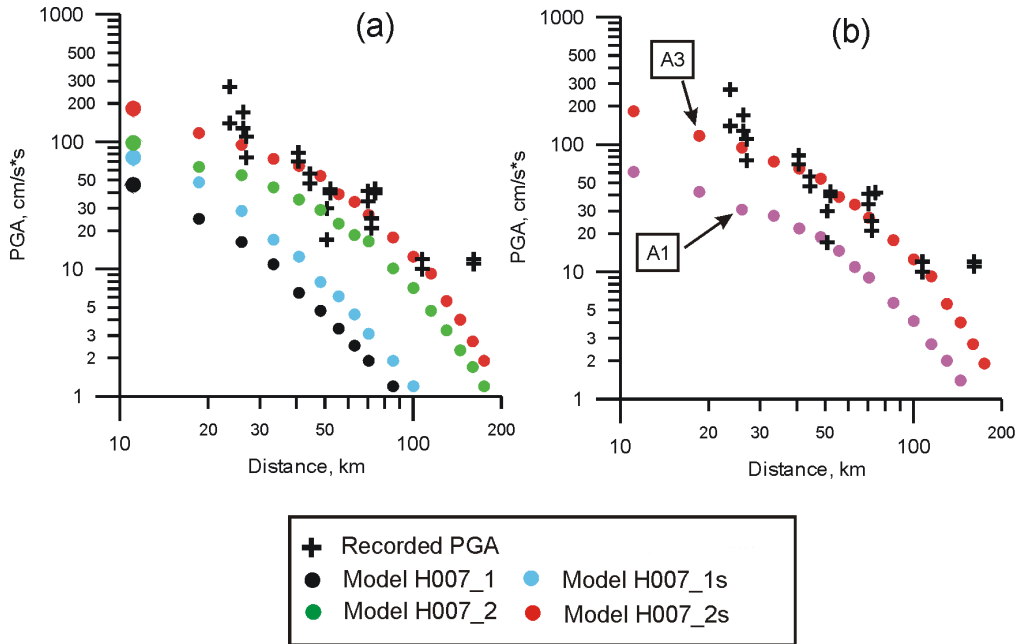


Figure 4. The Waldkirch earthquake (December 5, 2004, M_W 4.9). Distribution of the observed and modeled (Hintersberger et al. 2007) ground motion parameters versus epicentral distance. See text for the description of the model variants. (a) The parameters were modeled for generalized site condition A3. (b) Comparison between results of the modeling (model H007_2s) for two generalized site conditions A1 and A3.

(Hintersberger et al. 2007). Second for the Albstadt earthquake we analysed the observed macro-seismic data (Prochazkova et al. 1979) and compared them with computed intensities from our spectral model.

Analysis of the ground-motion models

The spectral model developed by Hintersberger et al. (2007) utilized the strong motion records of the Waldkirch earthquake and optimized the parameters for their stochastic model (spectral source scaling and attenuation) aiming at a good match for the pseudo-acceleration spectra.

Initially, the modeling in our study has been performed using the original models of geometric and anelastic (path) attenuation suggested by Hintersberger et al. (2007) (see Table 1) and two values of stress parameter namely: (1) stress parameter is evaluated as a function of magnitude (Bay et al. 2003, 2005), the parameter is equal to 15 bars for M_W 4.9 (the model is called H007_1); and (2) stress parameter of 30 bars, as suggested by Malagnini et al. (2000) (the model is called H007_1s). The site attenuation parameter has been taken as $\kappa = 0.005$ (Hintersberger et al. 2007).

As can be seen from Fig. 4 the application of the original attenuation parameters [three-segment geometric attenuation as: $R^{-0.8}$ (0-30 km), $R^{-1.0}$ (30-65 km), $R^{-0.5}$ (> 65 km); and $Q(f) = 52 f^{0.78}$], even with combination with the generalized site class A3 (rock covered by soft soil) resulted in lower (more than 3 times at small distances) PGA values than the recorded amplitudes. The stochastic model would match the

Spectral model of Malagnini et al., 2000

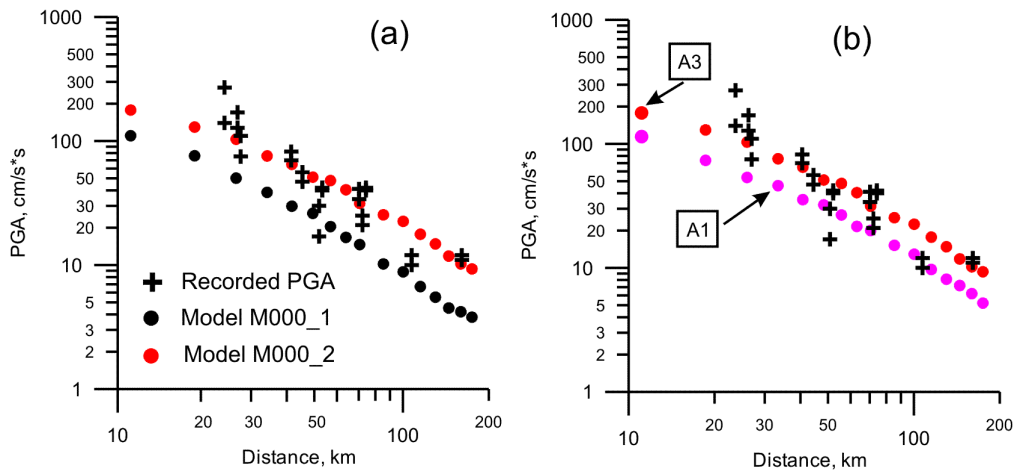


Figure 5. The Waldkirch earthquake (December 5, 2004, M_W 4.9). Distribution of the observed and modeled (Malagnini et al. 2000) ground motion parameters versus epicentral distance. See text and Table 1 for the description of the spectral model. (a) The parameters were modeled for generalized site condition A3. (b) Comparison between results of the modeling (model M000_2) for two generalized site conditions A1 and A3.

Spectral model of Bay et al., 2003, 2005

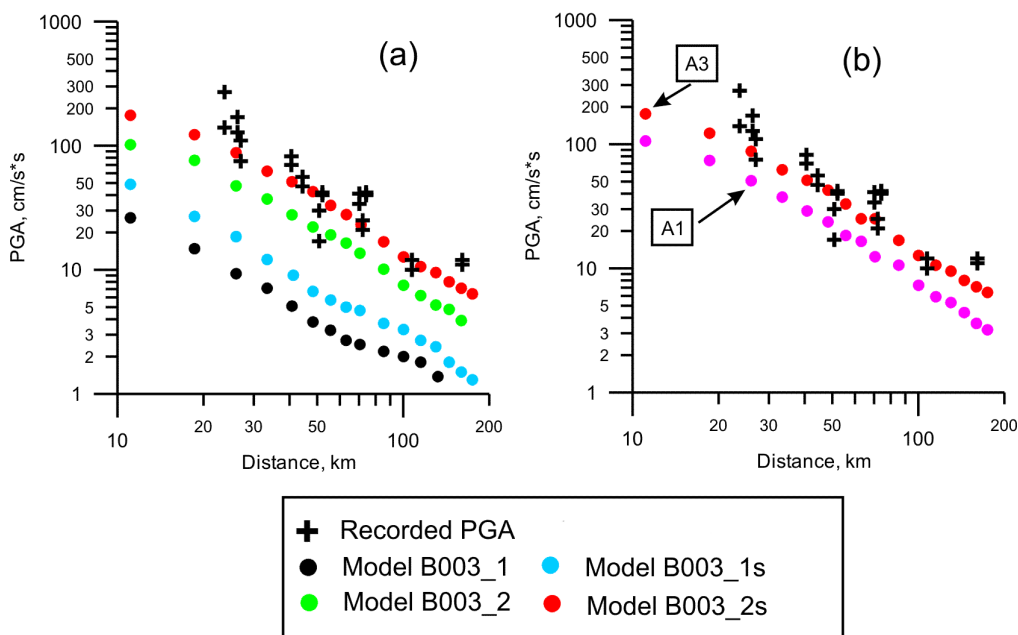


Figure 6. The Waldkirch earthquake (December 5, 2004, M_W 4.9). Distribution of the observed and modeled (Bay et al. 2003, 2005) ground motion parameters versus epicentral distance. See text and Table 1 for the description of the spectral model. (a) The parameters were modeled for generalized site condition A3. (b) Comparison between results of the modeling (model B003_2s) for two generalized site conditions A1 and A3.

observations much better when changing the attenuation parameters. We face a trade-off between geometrical spreading and Q factors (anelastic attenuation) so that the determination of attenuation functions is not unambiguous. In this study we did not change the original Q -models and considered only geometric attenuation. The model H007_2 has been constructed by the change of geometric attenuation as $R^{-0.5}$ (0-20 km), and $R^{0.0}$ for $R > 20$ km. Again, two variants of stress parameter were used: the magnitude-dependent stress (the model H007_2) and the value of 30 bars (the model H007_2s). The last variant provided a good fit with the observed data. At this point the conclusion can be made that the Hintersberger et al. (2007) model should be modified in order to match the observations. The modifications include the stress parameter (30 bar) and the geometric attenuation.

The results of application of two generalized spectral models, which were developed for Central Europe (Malagnini et al. 2000) and Switzerland (Bay et al. 2003, 2005), are shown in Figs. 5 and 6. Bearing in mind the necessity of adjustment of the attenuation model, as revealed when using the region-dependent spectral model (Hintersberger et al. 2007), we also used the changed parameters of geometric attenuation together with the original models of geometric and anelastic (path) attenuation.

For the spectral model developed by Malagnini et al. (2000) (Fig. 5), the original geometric attenuation [$R^{-0.8}$ (0-140 km), $R^{-1.5}$ (140-180 km), $R^{0.0}$ (180-220 km), the model M000_1] resulted in the slightly lower PGAs than the observed values. However, a simpler two-segment geometrical attenuation [$R^{-0.6}$ (0-140 km), $R^{-0.2}$ (140-220 km), the model M000_2] provides a good fit to the observed data.

The model proposed by Bay et al. (2003, 2005) (Fig. 6) is characterized by magnitude-dependent stress parameter. Therefore we used four variants of the model, namely: (a) original attenuation with a complex four-segment geometric attenuation [$R^{-1.1}$ (0-50 km), $R^{-0.6}$ (50-70 km), $R^{0.2}$ (70-100 km), $R^{-0.5}$ (>100 km)] and magnitude-dependent stress (the model B003_1); (b) original attenuation and stress of 30 bars (the model B003_1s); (c) the three-segment geometric attenuation [$R^{-0.6}$ (0-10 km), $R^{-0.8}$ (10-100 km), $R^{-0.2}$ (> 100 km), the model B003_2]; (d) the three-segment geometric attenuation and stress of 30 bars (the model B003_2s). The last variant provides results that are consistent with observations.

The comparison between the empirical and the modeled pseudo-spectral acceleration (5% damped) for the Waldkirch earthquake is shown in Figure 7. The modeled PSA values were calculated for the centers of the selected distance intervals using three models of the input Fourier spectra and two generalized models of site amplification (A1 and A3). For station KRW (distance about 110 km), the C3 model of site amplification is used because the station is located on deep deposits of Rhine graben (city of Karlsruhe). The modeled response spectra show a good agreement with the empirical spectra. However it seems that the H007_2S model underestimates the PSA amplitudes at distances more than 100 km.

Two major conclusions can be drawn from the comparison. First, for the stochastic modelling of the Waldkirch earthquake occurred in South-Western Germany, the stress parameter should be taken equal, at least, to 30 bars. Second, the geometric attenuation should differ from that suggested in the spectral models recently proposed

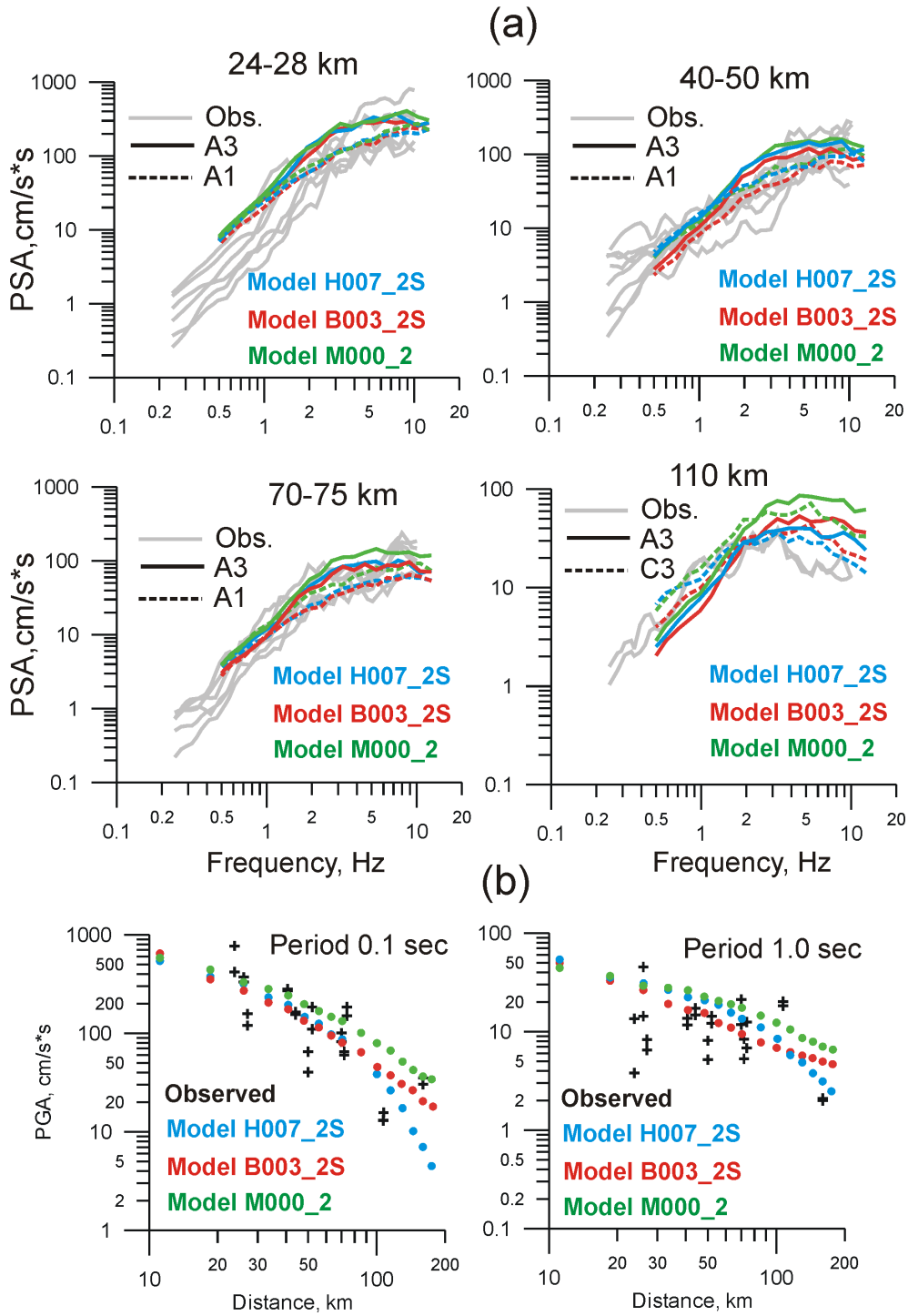


Figure 7. The Waldkirch earthquake (December 5, 2004, M_W 4.9). Comparison of the observed (horizontal components) and the modeled pseudo-spectral acceleration. See text and Table 1 for the description of the models.

for Europe (Malagnini et al. 2000; Bay et al. 2003, 2005; Hintersberger et al. 2007). Note, that here we did not perform a special study (e.g. inversion of the observed data) to find the solution for the parameters of geometric attenuation that reveal the best fit with the observation. We tested several models of the attenuation and show here one of the most suitable variants.

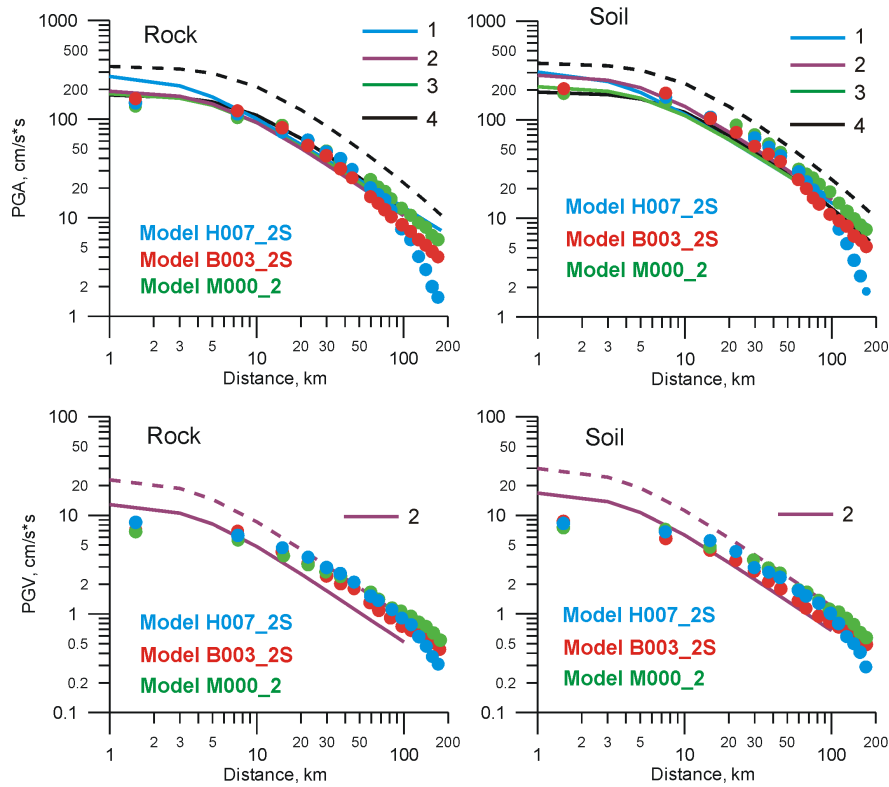


Figure 8. The Albstadt earthquake (September 3, 1978, M_W 5.2). Comparison of distribution of ground motion parameters (peak ground acceleration and velocity) versus epicentral distance estimated using different models. Lines represent the ground-motion equations (Table 3), solid lines – mean amplitude, dashed lines – mean plus 1 standard deviation: 1 – model AMB1996; 2 – model SP1996; 3 – model SPU1999; 4 – model B-T2003. See text for the description of the stochastic models (symbols). The geological class A1 was used for “rock” condition and class A2 – for “soil”.

As the developed model is only constrained by two data sets we wanted to make sure that it is compatible with the attenuation relations developed for European strong motion data (Table 3). In our comparison we assume that the ‘rock’ site category in the attenuation relation corresponds to class A1 in the stochastic model and the ‘soil’ site category corresponds to class A2. Figure 8 and 9 show the results of ground motion modelling for the Albstadt (September 3, 1978, M_W =5.2, depth 8 km) and the Basel (October 18, 1356, M_W 6.5, depth 10 km) earthquakes. We compare the distribution of peak amplitudes of ground acceleration and velocity versus epicentral distance.

All used ground-motion prediction equations (Table 3) produced approximately the same values of peak ground acceleration. The results of stochastic modeling ($\Delta\sigma = 30$ bars) reveal a good fit to the predictions. The model H007_2S, which is based on the highest rate of path attenuation $Q = 52 f^{0.78}$ (Hintersberger et al. 2007), underestimates the ground motion parameters at distances more than 100 km.

Among the considered strong-motion models (see Table 1), only the SP1996 model (Sabetta and Pugliese 1996) allows estimating peak ground velocity. The stochastic modeling, showing a good agreement with the SP1996 model when considering the

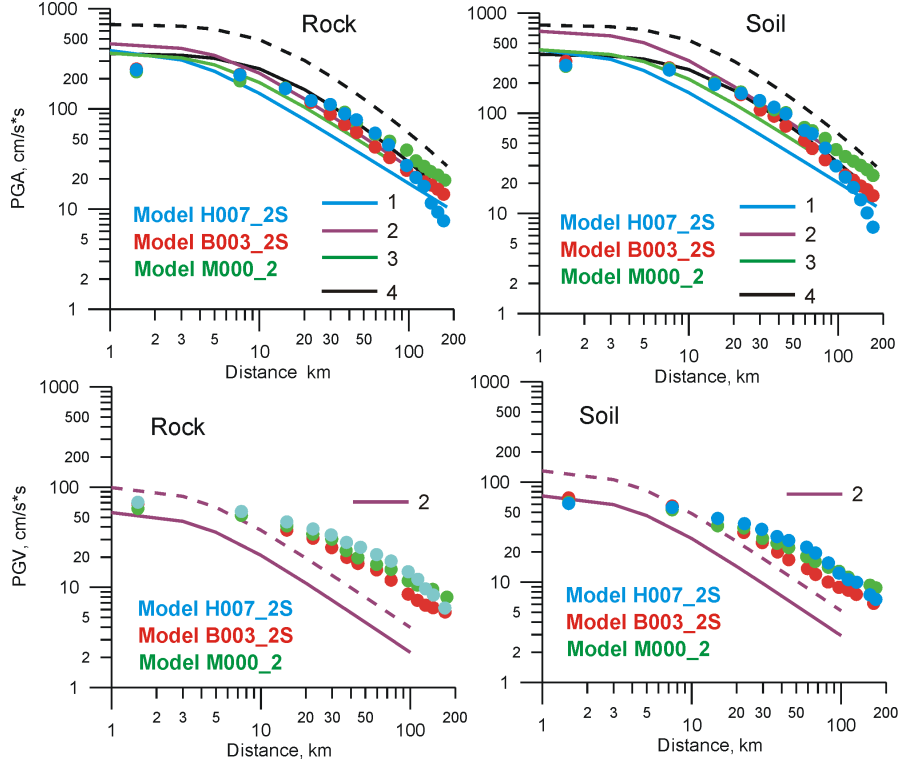


Figure 9. The Basel earthquake (October 18, 1356, M_W 6.5, depth 10 km). Comparison of distribution of ground motion parameters (peak ground acceleration and velocity) versus epicentral distance estimated using different models. See text for the description of the stochastic models (symbols). Lines represent the ground-motion equations (Table 3), solid lines – mean amplitude, dashed lines – mean plus 1 standard deviation: 1 – model AMB1996; 2 – model SP1996; 3 – model SPU1999; 4 – model B-T2003. The geological class A1 was used for “rock” condition and class A2 – for “soil”.

event of M_W 5.2, resulted in the higher PGV values distances more than 20-30 km for large event (M_W 6.5) At present state of knowledge we only suggest that the difference is caused by peculiarities of the empirical ground-motion database used by Sabetta and Pugliese, which contains records from only two large ($M > 6.0$) earthquakes occurred in Italy.

For the Albstadt earthquake (Fig. 10a) the modeled MSK intensity values were compared with the observed intensity (Prochazkova et al. 1979). We do not show the particular macroseismic observations, but the intervals of epicentral distances at which the given level of intensity has been observed. The observed intensities were reported as integer (e.g. VI or VII MSK) or mixed integer (e.g. VI-VII MSK) numbers. Therefore we represent the observations in the figure with step of 0.5 MSK units so the reported intensity V-VI MSK, for example, is shown as the 5.5 MSK level. We also modelled macroseismic intensity using the well-known intensity attenuation function of Sponheuer (1960) based on Kövesligethy (1907), namely

$$I_{SITE} = I_{EPIC} - 3\log_{10}(R/H) - 3\alpha(R - H) \quad (1)$$

where I_{EPIC} is the epicentral intensity; R is the hypocentral distance (km); H is the depth (km); and α is the region-dependent absorption coefficient, here 0.001 km^{-1} .

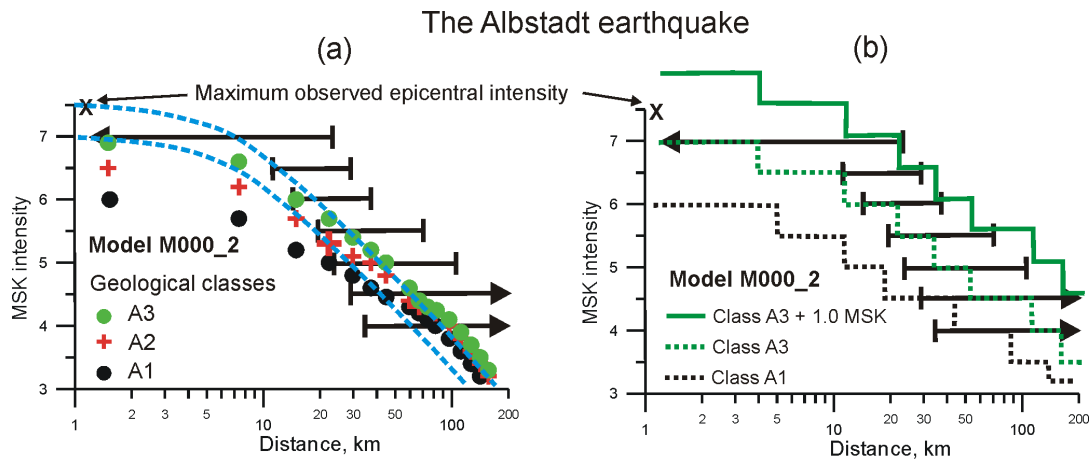


Figure 10. Modeling of macroseismic intensity for the Albstadt earthquake. The bounded segments represent intervals at which the particular level of intensity had been observed during the Albstadt earthquake. The dashed curves at plots (a) and (c) shows estimations that are based on epicentral intensity (see text, Eq. 1).

For the Albstadt earthquake we selected two values of epicentral intensity, namely: 7.0 MSK, as reported by Prochazkova et al. (1979), and 7.5 MSK (Leydecker 1999).

The values of modeled intensity I_M that were calculated directly from the site-dependent spectra (site class A3, soft soil) show a good agreement with the observations and with the independent estimations that were based on epicentral intensity. Note that our estimations of I_M values were obtained using generalized site-amplification functions (Fig. 3). Therefore they should be considered as the “average” values. The averaged intensity, obviously, does not reflect damage of a particular structure under specific unfavorable local ground conditions, e.g. narrow-band high-amplitude amplification or influence of ground water (see examples in Schwarz et al. 2005). In reality, the particular values of observed intensity may vary up to 1-2 MSK units even within a small area. Thus, we have to bear in mind that, using any modeling technique, the average value of intensity assigned to one locality (e.g. village or medium size town) can be determined within an uncertainty of 0.5 - 1 MSK unit (see Sokolov and Wald 2002).

Conclusions

We developed a spectral ground motion model for Southwest Germany that allows the computation of stochastic seismograms on the basis of two available data sets (Waldkirch earthquake 2004; Albstadt earthquake 1978). We did this analysis in recognition of a number of models that refer to larger areas: three spectral models have been developed recently for Europe and on a global scale; in addition four attenuation models for Europe are available.

We find that if we modify the Hintersberger et al. (2007) model, which has been recently developed using the instrumental data from earthquakes in western Europe, with respect to the geometric attenuation and the stress drop we can achieve (a) that the spectral model fits the observations in terms of acceleration with regard to the Waldkirch event and in terms of intensities with regard to the Albstadt event. In

Table 4. Seismological parameters of the spectral model for earthquakes in South-Western Germany.

Parameter*	Description
Fourier acceleration spectrum $A(f)$	$A(f) = (2\pi f)^2 CS(f)D(R, f)$
The scaling factor C	$C \sim R^N / (4\pi\rho\beta^3)$
Geometric attenuation R^N	$R^{-0.6}$ (0-140 km), $R^{-0.2}$ (140-200 km),
Source spectrum $S(f)$	Brune (1970) ω -square, point source $S(f) = M_0 / [1 + (f / f_0)^2]$
Corner frequency f_0	$f_0 = 4.9 \times 10^6 \beta (\Delta\sigma / M_0)^{1/3}$
Stress parameter $\Delta\sigma$	30 bars
Density, ρ (gm/cm ³)	2.8
Shear velocity, β (km/sec)	3.8
Frequency-dependent attenuation $D(R, f)$	$D(R, f) = \exp[-\pi f R / Q(f)\beta]P(f, f_{\max})$
Path attenuation $Q(f)$	$400 f^{0.42}$
High-frequency filter $P(f)$	$P(f) = \exp(-\pi \kappa f)$ (Anderson and Hough 1984)
Site attenuation, κ (sec)	$\kappa = f(M)$

addition this model is compatible and compares well to the attenuation models developed for Europe for PGA and PGV. Parameters of the models are given in Table 4.

We thus believe that this new model has to capability to serve as a starting point for ground motion modelling in Southwest Germany. Among the future tasks we should mention the analysis of available macroseismic data from small earthquakes in South-Western Germany for testing and calibration of the model.

Acknowledgments

The authors would like to thank Wolfgang Brüstle for providing the necessary data and for thoughtful suggestions. The comments from Gottfried Grünthal allowed improving of the initial version of manuscript.

References

- Abrahamczyk L, Langhammer T, Schwarz J (2005). Earthquake regions in Germany – a statistical evaluation, Bautechnik 82 (8): 500-507 (in German).
- Ambraseys NN, Simpson KA, Bommer JJ (1996). Prediction of horizontal response spectra in Europe, Earthquake Engineering and Structural Dynamic, 25: 371-400.
- Amstein S, Lang DH, Schwarz J (2005). Shaking effects of historical earthquakes and novel applications in the scientific field of earthquake engineering, Bautechnik 82 (8): 641-655 (in German).

- Anderson J, Hough S (1984). A model for the shape of the Fourier amplitude spectrum of acceleration at high frequencies. *Bull Seism Soc Am* 74: 1969-1993.
- Bay F, Fäh D, Malagnini L, Giardini D (2003). Spectral shear-wave ground-motion scaling in Switzerland. *Bull Seism Soc Am* 93: 414-429.
- Bay F, Wiemer S, Fäh D, Giardini D (2005). Predictive ground motion scaling in Switzerland: best estimates and uncertainties. *Journal of Seismology* 9: 223-240.
- Berge-Thierry C, Cotton P, Scotti O, Griot-Pommeroy D-A., Fukushima Y (2003). New empirical response spectral attenuation laws for moderate European earthquakes. *Journal of Earthquake Engineering* 7 (2): 193-222.
- Boore DM (2003). Simulation of ground motion using the stochastic method. *Pure Appl Geophys* 160: 635-676.
- Brüstle W, Stange S (1999). Geologische Untergrundklassen zum Entwurf von Normspektren für DIN 4149 (neu), Landesamt für Geologie, Rohstoffe und Bergbau Baden-Württemberg, Freiburg im Breisgau.
- Chernov Y, Sokolov V (1999). Correlation of seismic intensity with Fourier acceleration spectra. *Physics and Chemistry of the Earth, Part A: Solid Earth and Geodesy* 24(6): 522-528.
- DIN 4149 (2005). Bauten in deutschen Erdbebengebieten- Lastannahmen_ bemessung und ausführung üblicher Hochbauten. Vorgesehen als Ersatz für DIN 4149-1:1981-04 und DIN 4149-1/A1:1992-12. Normenausschuss in Bauwesen (NADau) im DIN Deutsches Institut für Normung e.V., Berlin
- Gisler M, Schwarz-Zanetti G, Fäh D, Masciadri M, Rippmann D (2006). The 1356 Basel earthquake from a historical point of view: old wine in new wineskins? New data to gain new insight? Proc. First European Conference on Earthquake Engineering and Seismology, Geneva, Switzerland, 3-8 September, 2006, paper 24.
- Grünthal G (2004). The history of historical earthquake research in Germany, *Annali di Geofisica*, 47(2/3): 631-643.
- Grünthal G, Wahlström R (2003). A M_w based earthquake catalogue for central, northern and northwestern Europe using a hierarchy of magnitude conversions. *Journal of Seismology* 7: 507-531
- Grünthal G, GSHAP Region 3 Working Group (1999). Seismic Hazard Assessment for Central, North and Northwest Europe: GSHAP Region 3, *Annali di Geofisica* 42 (6): 999-1011.
- Hintersberger E, Scherbaum F, and Hainzl S (2007). Update of likelihood-based ground-motion model selection for seismic hazard analysis in western central Europe. *Bull. Earthquake Eng.* 5: 1-16.
- Keintzel E (2005). About the way to the new German Seismic Code DIN 4149: 2005-04. *Bautechnik* 82 (8): 475-485 (in German).
- Kövesligethy R (1907). Seismischer Stärkegrad und Intensität der Beben, *Gerlands Beiträge zur Geophysik, Band VIII*, Leipzig.
- Leydecker G, Aichele H (1998). The Seismogeographical Regionalisation of Germany: The Prime Example for Third-Level Regionalisation. *Geol. Jb.*, E 55: 85-98.

- Leydecker G (1999). Erdbebenkatalog für die Bundesrepublik Deutschland mit Randgebieten für die Jahre 800 bis 1994 (für Schadensbeben bis 1998). Datenfile. Bundesanstalt für Geowissenschaften und Rohstoffe, Hannover (see also http://www.bgr.bund.de/cln_011/nn_331926/DE/Themen/Seismologie/Erdbeben/historisch/germany.html)
- Malagnini L, Herrmann RB, Koch K (2000). Regional ground-motion scaling in Central Europe. *Bull Seismol Soc Am* 86(2): 1052-1061.
- Prochazkova D, Schneider G, Schmedes E, Drimmel J, Fiegweil E, Lukeschitz G, Vogt J, Courtot P, Godefroy P, Grünthal G, Mayer-Rosa D, Berger R (1979). Macroseismic field of the earthquake of September 3, 1978, in the Swabian Jura. *J Geophys* 46: 343-347.
- Sabetta F, Pugliese A (1996). Estimation of response spectra and simulation of nonstationary earthquake ground motions. *Bull Seismol Soc Am*. 86(2): 337-352.
- Schwarz J, Langhammer T, Kaufmann Ch (2005). Assessment of damage and loss potentials due to earthquake (1) reconstruction of the “Albstadt”-quake in the Swabian albs in September 03, 1978. *Bautechnik* 82 (8): 520-531 (in German).
- Sokolov V (2002). Seismic intensity and Fourier acceleration spectra: revised relationship. *Earthquake Spectra* 18: 161-187.
- Sokolov V, Wald DJ (2002). Instrumental Intensity Distribution for the Hector Mine, California, and the Chi-Chi, Taiwan, Earthquakes: a Comparison of Two Methods. *Bull Seismol Soc Am* 92(6): 2145-2162.
- Sokolov V, Wenzel F (2007). Seismic hazard assessment for areas with a lack of empirical strong ground motion data: a case of Romania. *Proceedings of 3rd Indian-German Workshop on Seismic Safety of Structures, Risk Assessment and Disaster Mitigation, Mumbai India 12-14 March 2007*: 1-10.
- Sokolov V, Bonjer KP., Wenzel F, Grecu B, Radulian M (2008). Ground-motion prediction equations for the intermediate depth Vrancea (Romania) earthquakes, *Bull. Earthquake Eng* 6(3): 367-388 (DOI:10.1007/s10518-008-9065-6)
- Sponheuer W. (1960). Methoden zur Herdtiefenbestimmung in der Makroseismik. (Methods for depths estimation in macroseismic), Akademie Verlag Berlin, Freiburger Forschungs-Hefte C 88, 117 pp.
- Spudich PJ, Fletcher B, Hellweg M, Boatwright J, Sullivan C, Joyner WB, Hanks TC, Boore DM, McGarr A, Baker LM, Lindh AG (1997). SEA96-A new predictive relation for earthquake ground motions in extensional tectonic regimes, *Seismol Res Lett* 68(1): 190-198.
- Tyagunov S, Grünthal G, Wahlström R, Stempniewski L, Zschau J (2006). Seismic Risk mapping for Germany. *Nat. Hazards Earth Syst Sci.* 6: 573-586.
- Wald DJ, Quitoriano V, Heaton TH, Kanamori H (1999). Relationships between peak ground acceleration, peak ground velocity and Modified Mercalli intensity in California. *Earthquake Spectra* 15: 557–564.

Structure of the East Anatolian Fault zone at the Hazar Basin, Eastern Turkey

D. Garcia Moreno (1, 2), A. Hubert-Ferrari (1,3), J. Moernaut (2), J. G. Fraser (1), X. Boes (1), U. Avsar (1, 2), M. Van Daele (2), E. Damci (4), N. Çağatay (4), M. De Batist (2).

- 1) Royal Observatory of Belgium, section of seismology. 3 Av. Circulaire, 1180 Brussels. Belgium. David.GarciaMoreno@oma.be
- 2) Renard Centre of Marine Geology, Ghent University. 281 Krijgslaan (S. 8), B-9000, Ghent. Belgium.
- 3) Ecole Normale Supérieure, Laboratoire de géologie UMR 8538. 24 rue Lhomond, 75231. Paris, CEDEX 5. France.
- 4) Eastern Mediterranean Centre for Oceanography and Limnology, Istanbul Technical University. Maslak 34469 Istanbul, Turkey.

Abstract

The Hazar Basin is a transtensional structure located on the central part of the East Anatolian Fault in eastern Turkey. This basin is interpreted as a large pull-apart basin because of its onshore geomorphology and fault geometry. However, the structure of the basin beneath Lake Hazar, which occupies almost the entire basin, has never been studied in detail. This study presents and discusses a new structural map of the Hazar basin based on a high-resolution seismic survey undertaken at Lake Hazar during summer 2007. This structural map reveals that the main strand of the East Anatolian Fault is continuous across the Hazar Basin. Therefore, contrary to many pre-existing studies, the East Anatolian Fault extends from Palu to Sincik forming a continuous segment of about 130 km.

Introduction

The left-lateral East Anatolian Fault zone (EAFZ) extends for about 600 km trending NE-SW. It forms the boundary between the Arabian and Anatolian plates linking the North Anatolian Fault with the Dead Sea Fault (Fig. 1). The EAFZ is characterized by a segmented fault trace (Barka & Kadinsky-Cade, 1988; Şaroğlu et al., 1992) with a slip rate of 10 – 11 mm/yr (Çetin et al., 2003; Reilinger et al., 2006), a total offset of 15 – 30 km (Şaroğlu et al., 1992; Westaway, 1994, 2003) and an estimated age of 3 – 4 Ma (Barka, 1992; Şaroğlu et al., 1992; Westaway & Arger, 1996; Hubert-Ferrari et al., 2008). The EAFZ has ruptured over most of its length during the 19th century producing several earthquakes of magnitudes ~7 (Ambraseys, 1989; Ambraseys, 1997; Nalbant et al., 2002). Two of these events occurred in the vicinity of Lake Hazar in 1874 and 1875 of magnitudes 7.1 and 6.7, respectively (Ambraseys, 1989; Ambraseys & Jackson, 1998). Both earthquakes uplifted the south-eastern outlet of Lake Hazar by several metres ending the outflow of the lake into the Tigris River (Ambraseys, 1989).

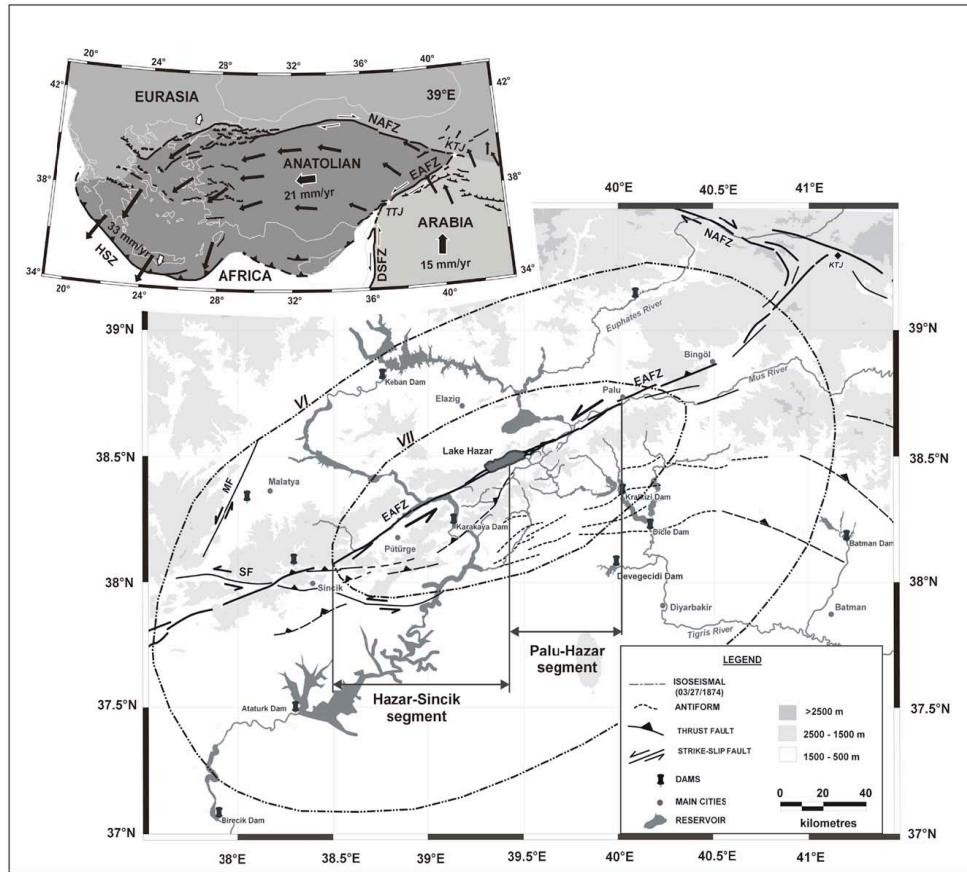


Figure 1: Tectonic map of the East Anatolian Fault zone (north-eastern part) showing fault segmentation according to Şaroğ lu et al. (1992) and Çetin et al. (2003). Isoseismals VII and VI of the March 27, 1874 earthquake are indicated (Ambraseys, 1989). Dams, main rivers and cities are shown. The arrows indicate relative fault motions. **Inset:** schematic diagram of the continental extrusion of the Anatolian block away from the Arabia-Eurasia collision zone including GPS vectors relative to Eurasia (McClusky et al., 2000; Reilinger et al., 2006). NAFZ: North Anatolian Fault Zone; EAFZ: East Anatolian Fault Zone; DSFZ: Dead Sea Fault Zone; MF: Malatia Fault; SF: Sürgü Fault; HSZ: Hellenic Subduction Zone; KTJ: Karliova Triple Junction; TTJ: Türkoglu Triple Junction. Projections: Lat/Long-WGS84.

The Hazar Basin is located on the central part of the EAFZ and occupies an elongate area of about 175 km^2 (Hempton et al., 1983). It is predominantly overlain by Lake Hazar, which covers about 100 km^2 of the basin area. The Hazar Basin is described as a pull-apart basin with a left-lateral stepping separation of $\sim 3 \text{ km}$ between the Havri and South-western faults (Fig. 2a) (Hempton, 1982; Hempton et al., 1983; Mann et al., 1983; Hempton & Dunne, 1984; Ş engör et al., 1985; Şaroğ lu et al., 1992; Westaway, 1994; Çetin et al., 2003). This interpretation is generally accepted, although some authors have suggested that both segments of the EAFZ may be continuous through Lake Hazar (Muehlberger & Gordon, 1987; Barka & Kadinsky-Cade, 1988). An alternative interpretation of the Hazar basin structure has been proposed by Aksoy et al. (2007), who suggest that the Hazar Basin is the result of a negative flower structure. Nevertheless, all these hypotheses are based on the onshore fault geometry and geomorphology, as, until the present study, there was no information about the structure underneath Lake Hazar. In order to better understand the structure of the Hazar Basin and its influence as a segmentation boundary, Lake

Hazar was the locus of a high-resolution seismic survey during summer 2007. In this paper, we will discuss the structure of the Hazar Basin revealed from that seismic survey and the implications of this structure for our understanding of the EAFZ.

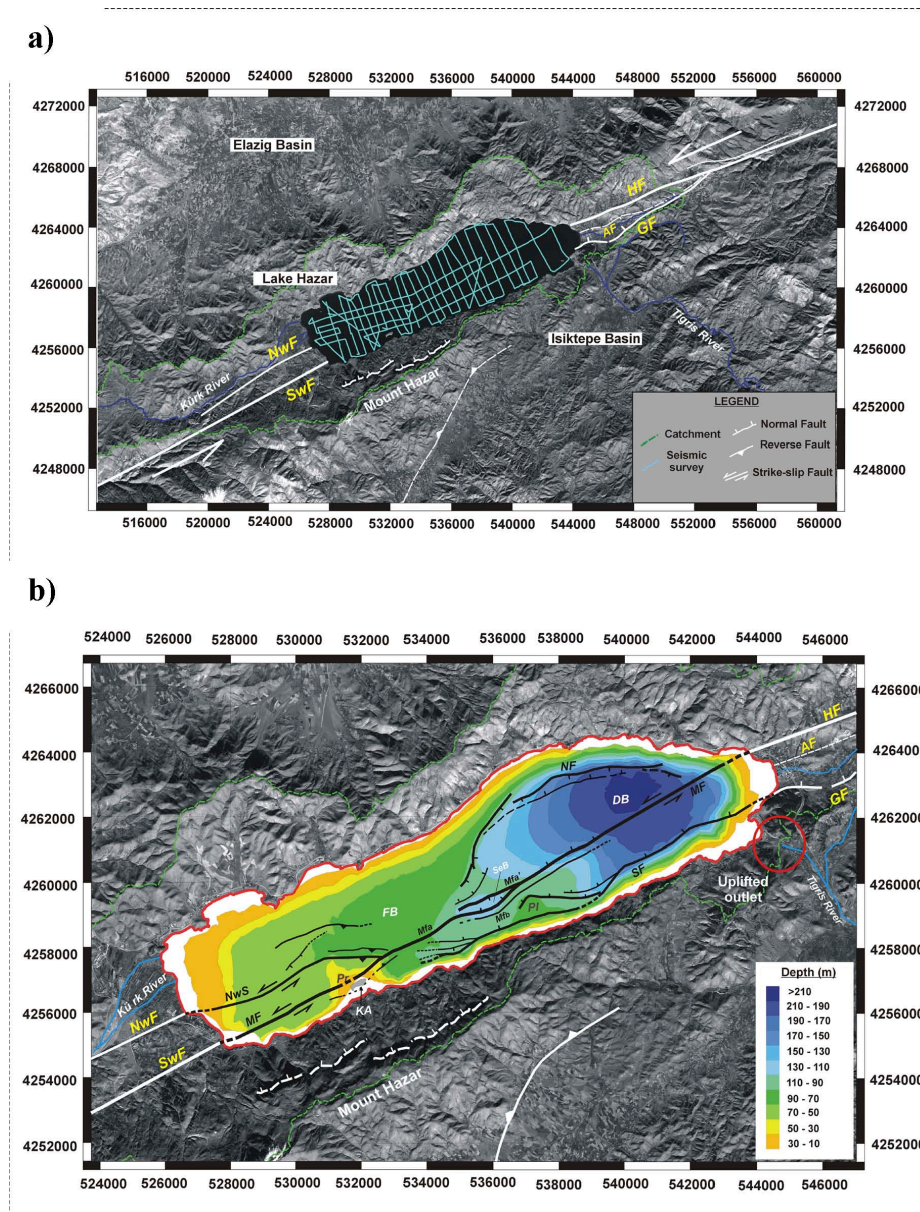


Figure 2: (a) Onland fault map of the Hazar Basin area plotted on SPOT image showing the seismic survey grid of the 2007 geophysical campaign. HF: Havri Fault; GF: Gezin Fault; AF: Aidin Fault; NwF: North-western Fault; SwF: South-western Fault. (b) Bathymetry and fault map of Lake Hazar obtained from the seismic survey. The uplifted outlet of Lake Hazar during the 1874 and 1875 earthquakes (Ambraseys, 1989) is marked by a red circle. MF: Master Fault; NF: Northern Fault; SF: Southern Fault; NwS: North-western Splay; DB: Deep Sub-basin; FB: Flat Sub-basin; SeB: Small elongated Sub-basin; Pr: promontory; Pl: plateau; KA: Kilise Adasi Island. Projections: UTM-WGS 84, 37N.

Methods and results

The seismic survey consisted of 44-high-resolution seismic profiles along a 500 m spaced grid (Fig. 2a). The acquisition system comprised a “centipede” multi-electrode sparker (300 J and main frequency of 400 – 1500 Hz) as acoustic source and a 10-hydrophone streamer, with an active length of 2.7 m, as receiver.

The bathymetry map (Fig. 2b) shows two distinct areas: an irregular 216 m deep sub-basin (DB) in the north-eastern half of the lake and a much flatter and shallower sub-basin (FB) in its south-western half. Three additional bathymetric features stand out, which are from east to west: 1) a plateau (PI) locally separating the deep sub-basin from the southern lake margin, 2) a small 140 m deep elongated sub-basin (SeB) located northwest of the plateau and southwest of the deep sub-basin and 3) a promontory (Pr) situated south of the flat sub-basin, from which Kilise Adasi Island (KA) emerges.

We describe the structure revealed by the seismic investigation from west to east (Fig. 2). Onshore, two main faults approach the lake: the North-western Fault (NwF), which may accommodate some dip-slip displacement, and the South-western Fault (SwF), which shows mainly strike-slip motion (Hempton, 1982; Hempton et al., 1983). In the lake, these strands correlate respectively with the North-western Splay (NwS) and Master Fault (MF). Both faults converge at the north-eastern corner of the promontory giving rise to shortening features associated with the bend of the North-western Splay. To the southeast of their junction a northwardly dipping fault (SF) is recognized and extends NE-wards along the southern margin of the lake with several complex splays. This fault (SF) correlates onshore to the Gezin Fault described by Çetin et al. (2003) defining a 24 km long fault strand. Near the centre of the lake a splay of the master fault forms a sag-pond depression (SeB in Fig. 2b). In the northern quartile of the lake an apparently normal, down to the south, fault (NF) arcs around the northern side of the deep sub-basin. This fault has a conjugate strand in places and forms localised graben structures. At the north-eastern end of the lake the Northern Fault converges with the Master Fault, which correlates to a clear terrestrial fault trace named the Havri Fault (Çetin et al 2003). Therefore, the South-western, Master and Havri faults are in fact the same continuous fault strand. In the northeast half of the lake the Master Fault strikes at 6° rotated counter-clockwise relative to its onshore continuation, the Havri Fault. This change in strike constitutes a subtle releasing bend and explains the location of the largest subsidence in the northern part of the deep sub-basin (Fig. 2b).

Discussion and Conclusions

According to the new data shown in this study, the main strand of the EAFZ is currently continuous across the Hazar Basin as was already suggested by Barka & Kadinsky-Cade (1988) and Muehlberger & Gordon (1987). Therefore, the Hazar Basin does not constitute a segmentation boundary and the Palu-Hazar and Hazar-Sincik segments are one – the 130 km long Palu-Sincik segment. Consequently, high-magnitude earthquakes, as the 1874 (M_s 7.1), are probably produced by ruptures of this Palu-Sincik segment. In fact, a fault segment of this length may be capable of generating a maximum moment magnitude of 7.5 ± 0.3 (Wells & Coppersmith, 1994), what suggest that the magnitude of the 1874 earthquake may have been underestimated.

References

- Aksoy, E., Inceöz, M., Koçyiğit, A. (2007). Lake Hazar Basin: A Negative Flower Structure on the East Anatolian Fault System (EAFS), SE Turkey. *Turkish Journal of Earth Sciences*, **16**, 319 – 338.
- Ambraseys, N. N. (1989). Temporary seismic quiescence: SE Turkey. *Geophysical Journal*, **96**, 311 – 331.
- Ambraseys, N. N. & Jackson, J. A. (1998). Faulting associated with historical and recent earthquakes in the Eastern Mediterranean region. *Geophysical Journal International*, **133**, 390 – 406.
- Ambraseys, N. N. (1997). The little-known earthquake of 1866 and 1916 in Anatolian (Turkey). *Journal of Seismology*, **1**, 289 – 299.
- Barka, A.A. & Kadinsky-Cade, K. (1988). Strike-slip fault geometry in Turkey and its influence on earthquake activity: *Tectonics*, **7**, 663 – 684.
- Barka, A. A. (1992). The North Anatolian fault zone. *Annales Tectonicae (Suppl.)*, **6**, 164 – 195.
- Çetin, H., Güneşli, H., Mayer, L. (2003). Paleoseismology of the Palu-Lake Hazar segment of the East Anatolian Fault Zone, Turkey. *Tectonophysics*, **374**, 163 – 197.
- Hempton, M. R. (1982). Structure of the northern margin of the Bitlis Suture Zone near Sivrice, southeastern Turkey. Ph.D. Thesis, State University of New York at Albany. pp. 383.
- Hempton, M. R., Dunne, L. A., Dewey, J.F. (1983). Sedimentation in an active strike-slip basin, south-eastern Turkey. *Journal of Geology*, **91**, 401 – 412.
- Hempton, M. R. & Dunne, L. A. (1984). Sedimentation in pull-apart basins: active examples in Eastern Turkey. *Journal of Geology*, **92**, 513 – 530.
- Hubert-Ferrari, A., King, G., Van Der Woerd, J., Villa, I., Altunel, E., Armijo, R. (2008). Long-Term Evolution of the North Anatolian Fault: New Constraints from its Eastern Termination. In 'Geodynamics of Collision and Collapse at the Africa-Arabia-Eurasia Subduction Zone'. Geological Society, Special publication. Editors: Douwe van Hinsbergen, Mike Edwards, Rob Govers.
- Mann, P., Hempton, M.R., Bradley, D.C., Burke, K. (1983). Development of pull-apart basins. *Journal of Geology*, **91**, 529 – 554.
- McClusky, S., Balassanian, S., Barka, A., Demir, C., Ergintav, S., Georgiev, I., Gurkan, O., Hamburger, M., Hurst, K., Kahle, H., Kastens, K., Kekelidze, G., King, R., Kotzev, V., Lenk, O., Mahmoud, S., Mishin, A., Nadariya, M., Ouzounis, A., Paradissis, D., Peter, Y., Prilepin, M., Reilinger, R., Sanlı, I., Seeger, H., Tealeb, A., Toksöz, M. N., Veis, G. (2000). GPS constraints on plate motion and deformation in the eastern Mediterranean: Implication for plate dynamics. *Journal of Geophysical Research*, **105**, 5695 – 5719.
- Muehlberger, W. B. & Gordon, M. B. (1987). Observations on the complexity of the East Anatolian Fault, Turkey. *Journal of Structural Geology*, **9** (7), 899 – 903.
- Nalbant, S. S., McCloskey, J., Steacy, S. & Barka A. A. (2002). Stress accumulation

and increased seismic risk in eastern Turkey. *Earth and Planetary Science Letters*, **195**, 291 – 298.

- Reilinger, R., McClusky, S., Vernant, P., Lawrence, S., Ergintav, S., Cakmak, R., Ozener, H., Kadirov, F., Guliev, I., Stepanyan, R., Nadariya, M., Hahubia, G., Mahmoud, S., Sakr, K., ArRajehi, A., Paradissis, D., Al-Aydrus, A., Prilepin, M., Guseva, T., Evren, E., Dmitrotsa, A., Filikov, S.V., Gomez, F., Al-Ghazzi R., Karam G. (2006). GPS constraints on continental deformation in the Africa-Arabia-Eurasia continental collision zone and implications for the dynamics of plate interactions. *Journal of Geophysical Research*, **111**, B05411, doi: 10.1029/2005JB004051.
- Şaroğlu, F., Emre, Ö. and Kuşçu, İ. (1992). The East Anatolian fault zone of Turkey. *Annales Tectonicae*, **99** – 125 (Special Issue-Supplement to Volume VI).
- Şengör, A.M.C., Görür, N., Şaroğlu, F. (1985). Strike-slip faulting and related basin formation in zones of tectonic escape: Turkey as a case study. In: Biddle, K.T. & Christie-Blick, N. (eds) *Strike-slip faulting and Basin formation*. Society of Economic Paleontologists and Mineralogist, Special Publication, **227** – 267.
- Westaway, R. (1994). Present-day kinematics of the Middle East and eastern Mediterranean. *Journal of Geophysical Research*, **99**, 12071–12090.
- Westaway, R. & Arger, J. (1996). The Gölbaşı basin, southeastern Turkey: a complex discontinuity in a major strike-slip fault zone. *Journal of the Geological Society*, **153**, 729 – 744.
- Westaway, R. (2003). Kinematics of the Middle East and Eastern Mediterranean Updated. *Turkish Journal of Earth Sciences*, **12**, 5 – 56.
- Wells, D. L. & Coppersmith, K. J. (1994). New Empirical Relationships among Magnitude, Rupture Length, Rupture Width, Rupture Area, and Surface Displacement. *Bulletin of the Seismological Society of America*, **88**, 974 – 1002.

Time-dependent analysis of the earthquake rates in the Dead Sea Fault Zone

Amir Hakimhashemi, Holger Schelle and Gottfried Grünthal

GFZ German Research Centre for Geosciences, Telegrafenberg, D-14473 Potsdam, Germany, hakim@gfz-potsdam.de

Abstract

The aim of this study is to analyse the temporal changes of the seismicity rate of large earthquakes ($M_w \geq 6$) in the Dead Sea Fault Zone (DSFZ). Therefore, four parametric statistical distributions, including Weibull, Gamma, Lognormal and Brownian Passage Time (BPT), are applied as well as the Poisson process (exponential distribution) as the classically applied time-independent model. The next step is to find which model can explain the seismicity rate better. In order to estimate the model parameters, we use a modified Maximum Likelihood Estimation (MLE). This method considers both inter-event times and censored time in the estimation process. These data are extracted from the earthquake data file assembled at the GFZ (cf. Grünthal and Wahlström, this volume). The last step is the best model choice and validation. This is performed using two criteria, the Bayesian Information Criterion (BIC) and the Kolmogorov-Smirnov goodness-of-fit test. The results of our study show a significant time-dependency, at least for the northern part of the DSFZ.

Introduction

The seismicity of the Middle East coupled to the Dead Sea Fault Zone (DSFZ) and other tectonic features is significant (Fig. 1). The list of earthquakes, which extends far back into history, includes many cases of severe destructions. The classical Poissonian based (time-independent) analysis of earthquake rates applied for Probabilistic Seismic Hazard Assessment (PSHA) has been repeatedly applied in the past for the DSFZ.

The idea of time-dependent earthquake modeling is traditionally more involved with the aftershock modeling. Omori's law (Omori 1894) is probably the first time-dependent model for describing earthquake rates. Utsu (1961), Reasenbergs and Jones (1989) and Ogata (1988) made use of Omori's law for their new methods to model aftershock sequences.

In order to estimate the rate of large repeating earthquakes on a single fault or fault segment, time-to-failure modeling is the mostly used statistical method. This method considers the earthquake process as a renewal process, such that the earthquake inter-event times are independently identically distributed. The most commonly used

parametric distributions for the time-to-failure modeling of mainshocks are Weibull (Nishenko 1985), Gamma, Lognormal (Nishenko & Buland 1987; Michael & Jones 1998) and inverse Gaussian - known as Brownian Passage Time, BPT – (Ellsworth et al. 1998). Recently, several studies have combined these statistical parametric models, as well as pure physical models like the rate-and-state model (Dietrich 1992; 1994). Parsons (2004, 2005) presented a combination of the rate-and-state model and a BPT distribution, and Gomberg et al. (2005) applied the rate-and-state model and a Lognormal distribution. Hardebeck (2004) discussed the superposing or double counting of the two models, and proposed a method to calculate interaction probabilities.

In this study four distributions, Weibull, Gamma, Lognormal and BPT as time-dependent models, are tested besides the Poisson process, as time-independent model, to estimate the rate of earthquakes with $M_w \geq 6$ in the DSFZ. Then, the results obtained from each model are compared and the time-dependence of the earthquake rate in the study area is discussed.

Method

The parametric statistical distributions used in this study are:

- Weibull distribution (with β and η as the scale and the shape parameters)

$$f_{\beta,\eta}(t) = \left(\frac{\beta}{\eta}\right) \left(\frac{t}{\eta}\right)^{\beta-1} \exp\left(-\left(\frac{t}{\eta}\right)^\beta\right)$$

- Gamma distribution (with k and θ as the scale and the shape parameters)

$$f_{k,\theta}(t) = t^{k-1} \frac{\exp\left(-\frac{t}{\theta}\right)}{\theta^k \Gamma(k)}, \quad \Gamma(k) = \int_0^{\infty} x^{k-1} \exp(-x) dx$$

- Lognormal distribution (with σ and μ as the scale and the shape parameters)

$$f_{\mu,\sigma}(t) = \frac{1}{t\sigma\sqrt{2\pi}} \exp\left(-\frac{(\ln t - \mu)^2}{2\sigma^2}\right)$$

- BPT distribution (with λ and μ as the scale and the shape parameters)

$$f_{\mu,\lambda}(t) = \sqrt{\frac{\lambda}{2\pi t^3}} \exp\left(-\frac{\lambda(t - \mu)^2}{2\mu^2 t}\right)$$

- Exponential distribution (Poisson process, time-independent, with λ as the rate and $1/\lambda$ as the scale parameter)

$$f_{\lambda}(t) = \lambda \exp(-\lambda t)$$

The first four distributions are time-dependent. It means that while the rate functions corresponding to these distributions are functions of elapsed time since the last mainshock, the rate of the exponential distribution is time-independent.

In order to estimate the parameters of each model, a modified Weighted Maximum Likelihood Estimation (WMLE) is used for two reasons. The first is the intrinsic uncertainty of historical earthquake data. Uncertainties in the earthquake parameters, especially for the older ones, are neither recognizable, nor calculable. The second reason is the fact that earthquake rates probably change with time. Therefore, the estimation process requires higher weights for earthquakes occurring in the recent time. In the WMLE method, the role of the more recent earthquakes is considered to be more important than that of the older ones. The log-likelihood function of WMLE reads as:

$$l(\Theta | T, t_c, W, w_c) = \log(L(\Theta | T, t_c, W, w_c)) = \sum_{i=1}^n w_i \log(f_{\Theta}(t_i)) + w_c \log(S_{\Theta}(t_c)),$$

where $T = \{t_1, \dots, t_n\}$ is the set of inter-event times, $W = \{w_1, \dots, w_n\}$ is the set of corresponding weights, t_c is the censored time; i.e. the time since the last event, w_c is the weight corresponding to the t_c , Θ is the set of parameters of the corresponding distribution, and f_{Θ} and S_{Θ} are probability density and survivor functions of the corresponding distribution:

$$S_{\Theta}(t) = \int_t^{\infty} f_{\Theta}(x) dx.$$

The best parameter estimates result from the solution of the following optimization problem:

$$\hat{\Theta} = \arg \max_{\Theta} l(\Theta | T, t_c, W, w_c).$$

Two different methods are applied to select the best distribution. The first is the Bayesian Information Criterion; $BIC = k \ln(n) - 2 \ln(L)$ (Volinsky et al. 1999), where n is the number of records involved in the estimation process, k is the number of parameters and L is the maximum likelihood of the corresponding distribution. The model with smaller corresponding BIC fits the data better. The other method is the Kolmogorov-Smirnov goodness-of-fit test (KS-test, Chakravart et al. 1967). A modified weighted version of one-sample KS-test is used in this study.

Data

The dataset (Fig. 1a) is extracted from available special studies and catalogues for the Middle East area according to the procedure described in Grünthal & Wahlström (2009 and in this volume). It contains, amongst others, all known earthquakes with $M_w \geq 6$ along the DSFZ, with a width of about 20 km (Fig. 1b). The completeness of this dataset starts at about 300 AD. A declustered dataset is used.

The study area along the DSFZ is divided into three sub areas, a southern, a central and a northern area (Fig. 1a). The approach is not applied for the southern part of the DSFZ, because in this part there is just one mainshock with $M_w \geq 6$ since 300 AD. This is of course not sufficient for a rational statistical analysis. In the followings, earthquakes of $M_w \geq 6$ are referred to as large earthquakes.

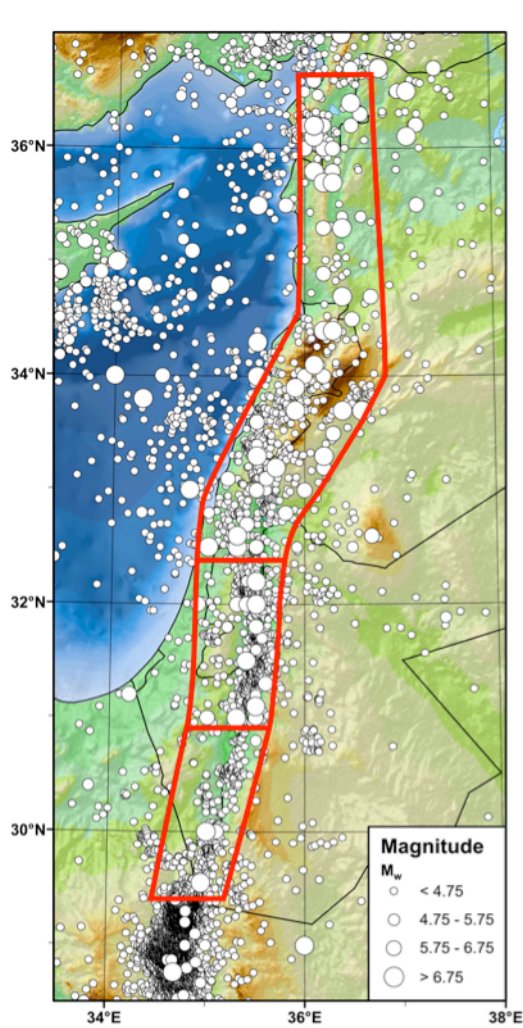


Figure 1a. Seismicity in the study area including the subdivision of the Dead Sea Fault Zone (DSFZ) into a southern, central and northern segment according to the datafile described in Grünthal & Wahlström (this volume).

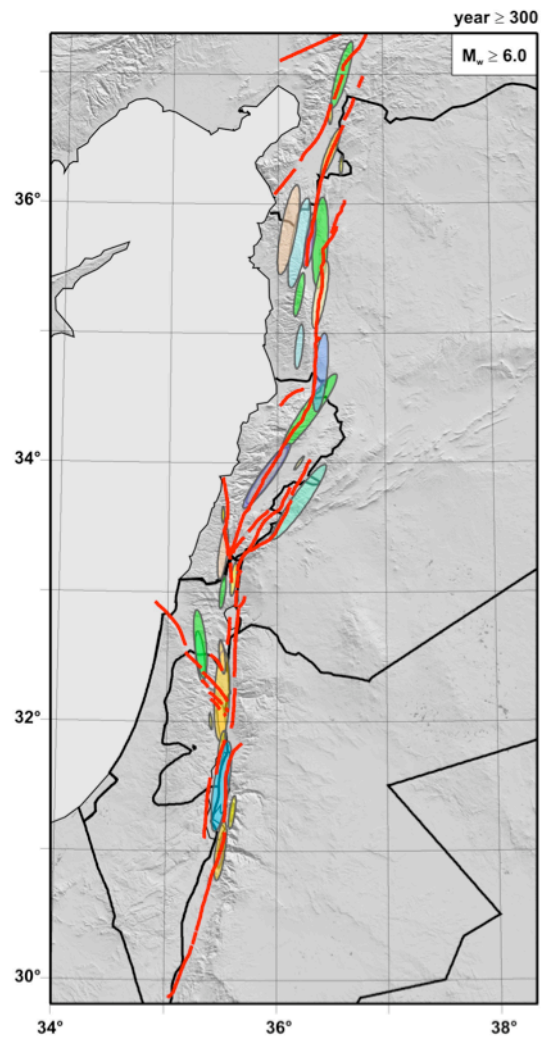


Figure 1b. Rupture areas of the $M_w \geq 6.0$ earthquakes in the DSFZ since 300 AD.

Results

The methods are applied for both the central and the northern sub areas. For the central area there could be found no significant time-dependence for the rate of the large earthquakes. Here it is preferred to apply a Poisson process to estimate the earthquake rate, because the Poisson process (with inter-event times exponentially distributed) is simpler than the time-dependent distributions. For the northern area, there is a significant time-dependence for the earthquake rate (Table 1).

Characteristic	Model	Scale parameter	Shape parameter	Log-ML	BIC	KS-test P-value	Probability of exceedence during the next 100 years	Weight in the combined model
Time-independent	Exponential	111.64		-	203.15	0.06	0.88	
Time-dependent	Weibull	61.70	0.90	-93.79	193.47	0.94	0.97	0.15
	Gamma	85.86	0.91	-93.63	193.15	0.49	0.95	
	Lognormal	41.68	3.39	-92.55	191.00	0.91	0.92	0.15
	BPT	86.36	28.37	-92.36	190.60	0.99	0.92	0.70

Table 1. Results of the method for the northern part of the DSFZ.

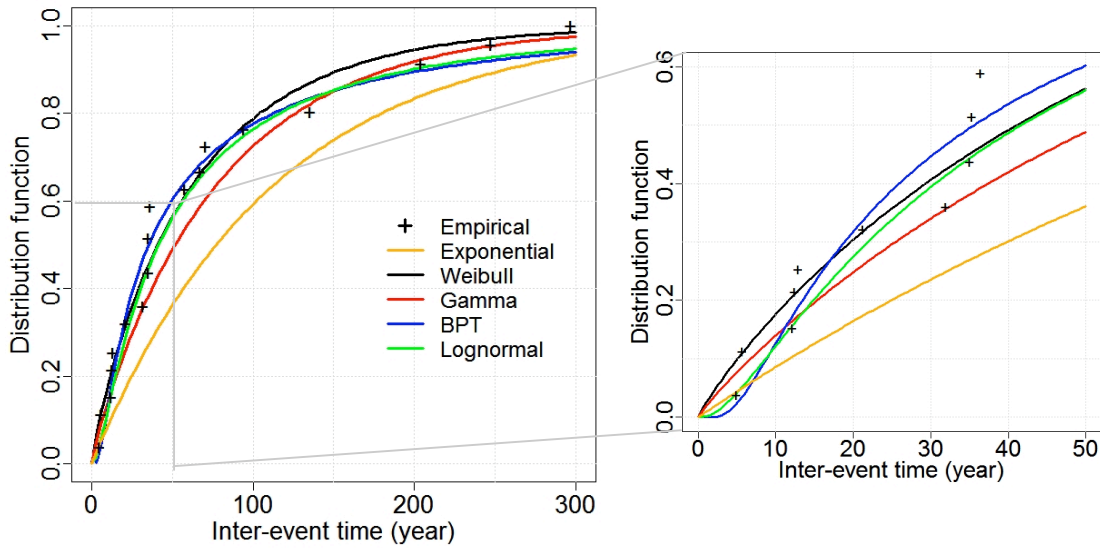


Figure 2. Inter-event times and distributions. Three distributions, i.e. BPT, Lognormal and Weibull fit the data very well. On the right: Enlargement of an inter-event time range up to 50 years.

From Table 1 and Fig. 2, it is clear that the BPT distribution is the best model; however two other distributions, the Weibull and Lognormal, provide good fits as well. All these three models have very significant KS-test p-values, which results in significant estimates. Among these three models, only BPT, as a physical based model, considers the steady tectonic loading process which is superposed by Brownian perturbations (Matthews et al. 2002). In order to estimate the probability of exceedence of a big earthquake in the northern area, a combined model is designed using the three models. Because of the physical base of the BPT and the higher KS-test p-value and lower BIC, the weight for the BPT in the combined model is considered as 0.7, as well as 0.15 for each Weibull and Lognormal estimates. Fig. 3 shows the probability of exceedence of a big earthquake within a generic time t since the last earthquake based on each of the three mentioned models as well as the combined model and the time-independent model (Poisson process).

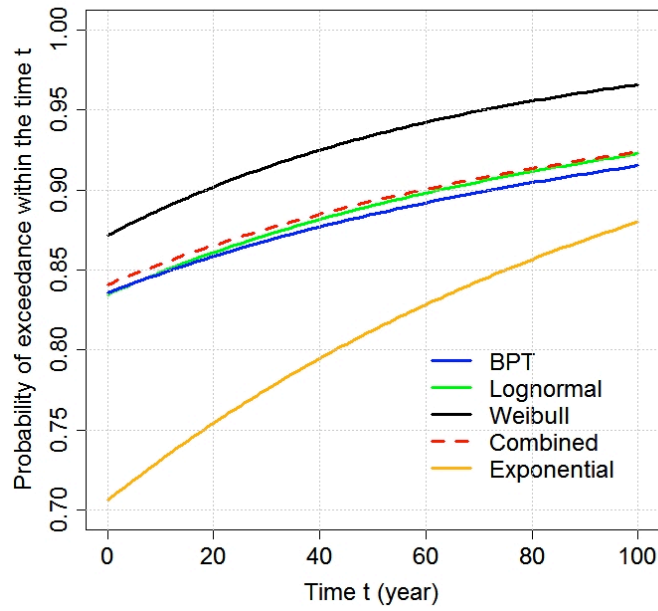


Figure 3. Probability of exceedance of a $M_w \geq 6$ earthquake within time t .

Conclusions

The rate of the earthquakes with $M_w \geq 6$ in the northern part of the DSFZ is significantly time-dependent. Not only the higher KS-test p-values and the lower BIC corresponding to the time-dependent models, but also the very low KS-test p-value and the high BIC corresponding to the exponential distribution confirm the time-dependence of the earthquake rates in the northern part of the DSFZ.

On the other hand, the cumulative seismic release curve for this area reconfirms this result (Fig. 4). This curve indicates an obviously periodic behavior of seismicity with time in this area. For the central part of the DSFZ, we could not show a significant difference between time-dependent models and the time-independent one, i.e. the Poisson process is as good as the time-dependent models. Because of lack of data in the southern part the time-dependence of earthquake rates could not be investigated in this segment.

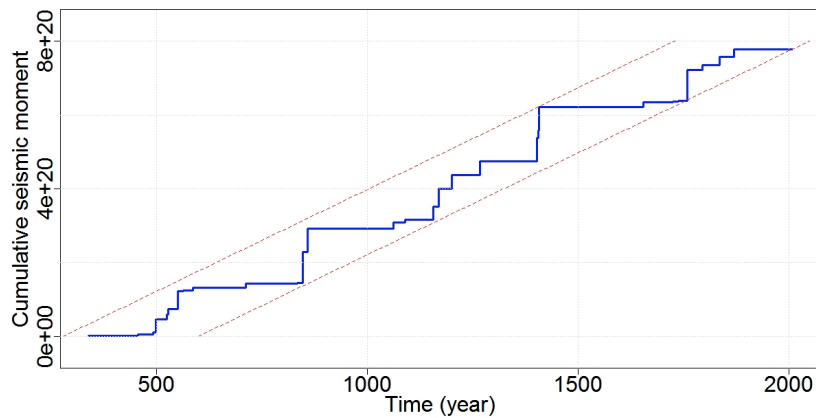


Figure 4. Cumulative seismic moment release in the northern part of the DSFZ, which seems to indicate a periodic behaviour of seismicity.

Acknowledgements

We appreciate the support from the German Research Centre for Geosciences, GFZ. This study is part of the Dead Sea Integrated Research project, DESIRE, funded by the Deutsche Forschungsgemeinschaft (German Research Foundation).

References

- Chakravarti, Laha & Roy (1967). Handbook of Methods of Applied Statistics. Volume I, John Wiley and Sons, pp. 392-394.
- Dieterich J. (1994). A constitutive law for rate of earthquake production and its application to earthquake clustering. *J. Geophys. Res.*, 99, 2601–2618.
- Dieterich J.H. (1992). Earthquake nucleation on faults with rate- and state-dependent friction. *Tectonophysics*, 211, 115-134.
- Ellsworth W.L., Matthews M.V., Nadeau R.M., Nishenko S.P., Reasenberg P.A. & Simpson R.W. (1998) A physical based earthquake recurrence model for estimation of long-term earthquake probabilities. Proceedings of the Second Joint Meeting of the UJNR panel on Earthquake research, 135-149. Geographical Survey Institute.
- Gomberg J., Belardinelli M.E., Cocco M. & Reasenberg P. (2005) Time-dependent earthquake probabilities. *J. Geophys. Res.*, 110, B05S04, doi:10.1029/2004JB003405.
- Grünthal G., Wahlström R. & Stromeier D. (2009) The unified catalogue of earthquakes in central, northern, and northwestern Europe (CENEC) – updated and expanded to the last millennium. *J. Seismol.* 13(4), 517-541, doi:10.1007/s10950-008-9144-9.
- Hardebeck, J.L. (2004). Stress triggering and earthquake probability estimates. *J. Geophys. Res.*, 109, B04310, doi:10.1029/2003JB002437.
- Matthews M.V., Ellsworth W.L. & Reasenberg P.A. (2002). A Brownian model for recurrent earthquakes. *Bull. Seismol. Soc. Am.*, 92, 2233– 2250.
- Michael A.J. & Jones L.M. (1998). Seismicity alert probabilities at Parkfield, California, revisited. *Bull. Seism. Soc. Am.*, 88, 117-130.
- Nishenko S.P. (1985). Seismic potential for large and great interplate earthquakes along the Chilean and Southern Peruvian margins of South America: a quantitative reappraisal, *J. Geophys. Res.*, 90, 3589-3615.
- Nishenko S.P. & Buland R.A. (1987). A generic recurrence interval distribution for earthquake forecasting. *Bull. Seism. Soc. Am.*, 77, 1382-1399.
- Ogata Y. (1988). Statistical models for earthquake occurrences and residual analysis for point processes. *J. Am. Stat. Ass.*, 83, 9-27.
- Ogata Y. & Zhuang J. (2006) – Space-time ETAS models and an improved extension. *Tectonophysics*, 413, 13-23.
- Omori F. (1894). On the aftershocks of earthquakes, *Journal of the College of Science, Imperial University of Tokyo*, 7, 111–200.

- Parsons T. (2005). Significance of stress transfer in time-dependent earthquake probability calculations. *J. Geophys. Res.*, 110, B05S02, doi:10.1029/2004JB003190.
- Parsons T. (2004). Recalculated probability of $M \geq 7$ earthquakes beneath the Sea of Marmara, Turkey. *J. Geophys. Res.*, 109, B05304, doi:10.1029/2003JB002667.
- Reasenber P.A. & Jones L.M. (1989). Earthquake hazard after a mainshock in California. *Science* 243, 1173-1176.
- Utsu T.,(1961). A statistical study on the occurrence of aftershocks. *Geophys. Mag.*, 30, 521-605.
- Volinsky C.T. & Raftery A.E. (2000). Bayesian information criterion for censored survival models. *Biometrics*, 56, 1, ProQuest Medical Library, p. 25.

Expansion of the Istanbul Earthquake Early Warning System – Performance tests

Nina Köhler (1), Friedemann Wenzel (1), Mustafa Erdik (2), Hakan Alçik (2), Aydin Mert (2) and Maren Böse (3)

- 1) Karlsruhe Institute of Technology (KIT), Geophysical Institute, Hertzstr. 16, D-76187 Karlsruhe, Germany, Email: nina.koehler@gpi.uni-karlsruhe.de
- 2) Kandilli Observatory and Earthquake Research Institute, Bogazici University, 81220 Cengelkoy, Istanbul, Turkey
- 3) California Institute of Technology, 1200 E. California Blvd., Mail Code 252-21, Pasadena, CA 91125, USA

Abstract

The Turkish mega-city Istanbul is exposed to high seismic risk due to its vicinity to the Main Marmara Fault, the western continuation of the North Anatolian Fault, one of the most active faults in the world. Due to this high seismic risk, earthquake early warning is an important task concerning the safety of millions of people living in and around Istanbul.

We investigate the contribution of a planned expansion of the *Istanbul Earthquake Rapid Response and Early Warning System (IERREWS)* to the early warning performance of the system by applying PreSEIS, an artificial neural network based approach for early warning. Due to the lack of real earthquake observations, a set of 280 simulated earthquake scenarios is used for the investigations.

The planned expansion of the network clearly improves the early warning performances. The PreSEIS source parameter estimates become more accurate within a shorter time, leading to larger warning times for Istanbul.

Introduction

In this work we study the possible contribution of the planned expansion of the *Istanbul Earthquake Rapid Response and Early Warning System (IERREWS)* [Erdik et al., 2003; Alçik et al., 2009] to its early warning performance for the Turkish mega-city Istanbul. The city is exposed to high seismic risk due to its direct vicinity to the Main Marmara Fault, a dextral strike-slip fault system intersecting the Sea of Marmara, which is the western continuation of the North Anatolian Fault [Le Pichon et al., 2001]. Recent estimates by Parsons [2004] give a probability of more than 40% of a $M \geq 7$ earthquake that will affect Istanbul until the year 2034. Due to this high seismic risk, earthquake early warning (EEW) is an important task concerning the safety of millions of people living in and around Istanbul.

EEW systems provide real-time estimates of earthquake source and ground motion parameters to users before strong shaking occurs at these sites [Kanamori et al., 1997; Kanamori, 2005]. They make use of the fact that the most destructive ground shaking

during an earthquake is caused by S- and surface waves which travel much slower than electromagnetic signals carrying warnings to potential users.

IERREWS is a dense network of strong ground motion stations installed in and around Istanbul by the Kandilli Observatory and Earthquake Research Institute. The current network includes a set of 10 strong motion stations used for EEW purposes, which are installed in on-line data transmission mode as close as possible to the fault. Implemented is a simple and robust early warning algorithm which is based on the exceedance of filtered peak ground acceleration (PGA) as well as cumulative absolute velocity (CAV) threshold values [Erdik et al., 2003; Alcik et al., 2009]. Figure 1 shows the locations of the current 10 early warning station sites. In context of the research project EDIM (Earthquake Disaster Information System for the Marmara Region, Turkey), the network is planned to be expanded in the near future to regional scale by installing an additional set of 10 stations around the Sea of Marmara (Fig.1).

For the performance tests presented in this study we make use of the EEW methodology PreSEIS as benchmark system. PreSEIS is an artificial neural network based approach to EEW which uses the incoming information on seismic ground motion from a seismic network to estimate the most likely hypocentral location and magnitude of the earthquake. The source parameter estimates start as soon as the first station triggers by including the information about not-yet-triggered stations to confine the possible range of solutions. The estimates are continuously updated every 0.5 s. As input parameters, PreSEIS uses the P-wave arrival time differences at the stations as well as the CAV values of the incoming signal [Böse, 2006; Böse et al., 2008]. Since PreSEIS has the advantage of using the full seismic signals, it is highly valuable for investigating the performance differences between the current and the expanded network. It can detect differences in the trigger order of the stations quicker and can therefore start the source parameter estimations as soon as the P-waves arrive, instead of waiting for the later arriving stronger ground motion.

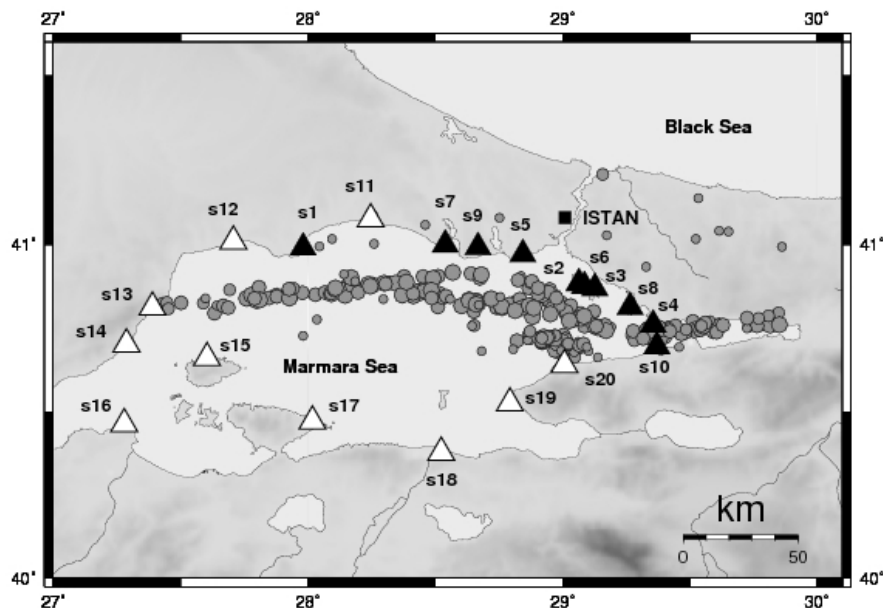


Figure 1: Map of the Marmara region, Turkey. The black triangles represent the present 10 EEW stations, the white triangles show the locations of the 10 additionally planned stations. The gray circles show the distribution of the 280 simulated earthquakes. ISTAN defines a user site within the city of Istanbul.

Due to a lack of local earthquake data recorded at the early warning stations, a set of 280 simulated earthquake scenarios is used for this study. The expected ground motions for these events are simulated for both the station locations of the original and the expanded early warning network. The simulated earthquakes are mainly located along the segments of the Main Marmara Fault (Fig. 1) with moment magnitudes between 4.5 and 7.5 at depths between 5.1 and 18.3 km [Böse, 2006; Böse et al., 2008].

Results

When comparing the PreSEIS performances of the current network and the planned expanded network, a clear improvement in the estimation process of the source parameters can be obtained by expanding the network around the Sea of Marmara. The average duration from the time at which the P-waves reach the first station until the time at which three stations trigger can be reduced by 1 second from 5 s for 10 stations to 4 s for the expanded case of 20 stations (Figure 2).

This leads to a reduction of the theoretical warning times for all 280 events, as displayed in Figure 3. The warning time is defined as the time difference between the initial P-wave detection at the first station and the S-wave arrival at a selected user site ISTAN in Istanbul. Using the current 10 stations, the theoretical warning times range between -0.6 s and 32.3 s with an average value of 12.6 s. For 20 stations, warning times between -0.6 s and 37.7 s can be obtained, with an average of 13.1 s. Although the average warning times only increase by 0.5 s, it can be clearly seen in Figure 3 that the distribution of warning times for the expanded network is more consistent, with a less distinct maximum shifted to larger warning times.

Figure 4 displays the source parameter estimates obtained by PreSEIS for all 280 simulated earthquakes. The black curves in Figure 4 represent the results obtained for the original network of 10 stations, whereas the red curves give the results using the expanded network of 20 stations. The sub-figure on the left hand side shows the absolute hypocenter location errors of all 280 events, defined as the differences between the true and the estimated hypocenter locations at each time step. The estimation process starts when the P-wave of an earthquake triggers the first station.

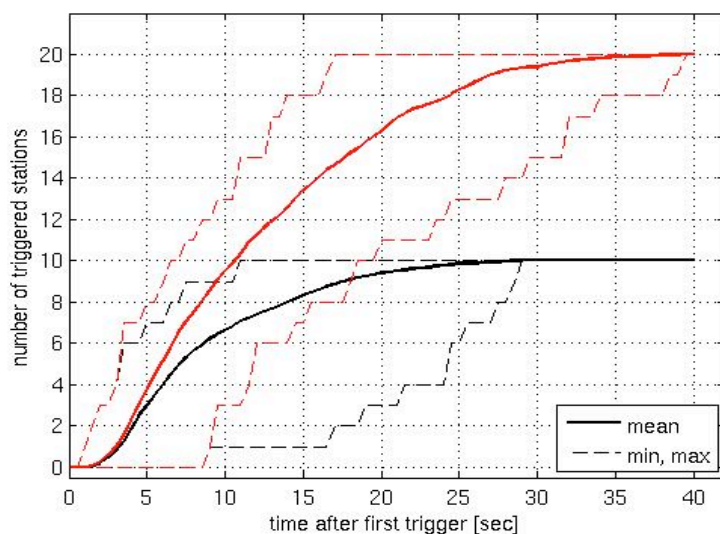


Figure 2: Average number of triggered stations with progressing time. The solid lines represent the means of all 280 earthquakes for the 10 current early warning stations (black curve) and for the expanded network of 20 stations (red curve). The dashed lines represent the minimum and maximum values, respectively.

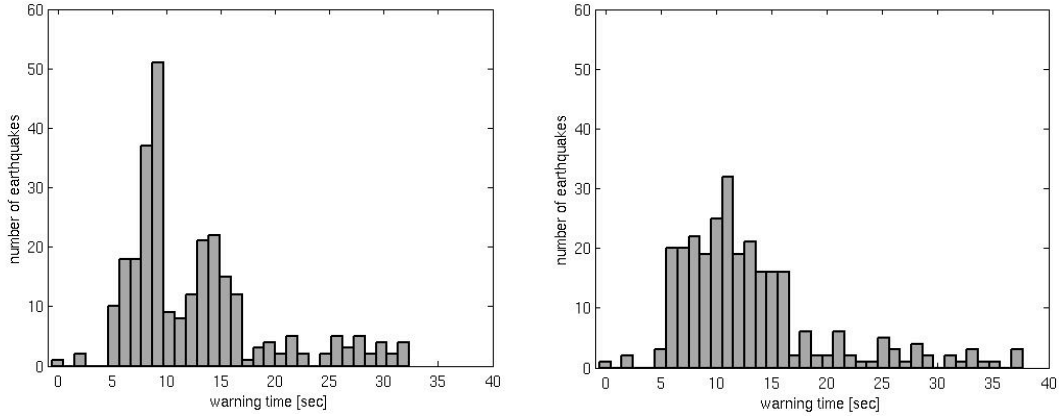


Figure 3: Warning times of all 280 earthquake scenarios using 10 (left) and 20 (right) stations. The warning time is defined as the time difference between the P-wave detection at the first station and the S-wave arrival at the user site ISTAN in Istanbul.

The location errors are divided into their 25th, 50th, 75th, and 95th percentiles, whereas the 50th percentiles (solid lines) represent the medians. The sub-figure on the right hand side shows the mean magnitude errors of all 280 events (circles) plus their standard deviations (bars) for each time step after the first trigger.

The localisation and magnitude errors both decrease when using 20 stations instead of 10 stations. While the initial estimates are similar, the median of the localisation errors becomes after 2.5 s significantly smaller for 20 stations, by about 2 – 3 km.

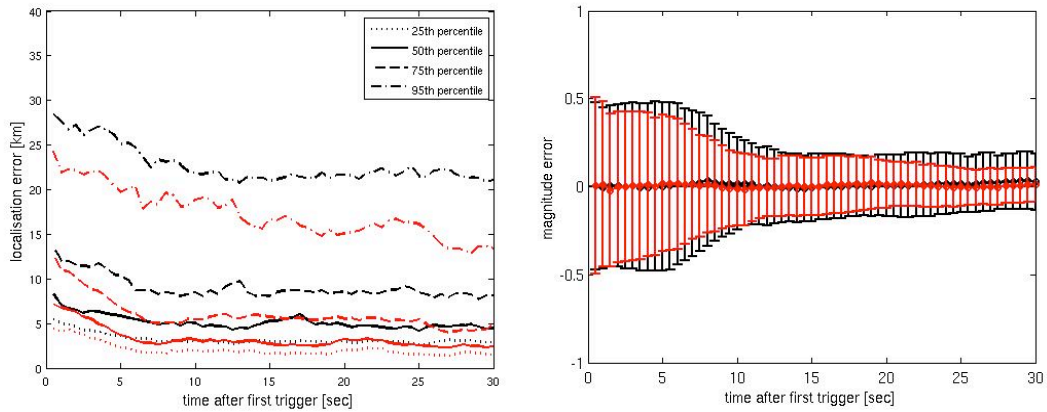


Figure 4: Absolute hypocenter location errors (left) and mean magnitude errors (right) with progressing time after the P-wave arrival of each event at the first station, obtained by PreSEIS for all 280 events. The location errors are defined as the differences between the true and the estimated hypocenter locations. The black curves give the results from using the original seismic network of 10 stations, whereas the red curves give the results obtained by using the expanded network of 20 stations.

The magnitude estimates for 20 stations start to become smaller than for 10 stations already after the second time step (1 s). For example after 2 s, the errors obtained by using all 20 stations are already 8% smaller than for 10 stations, and after 5 s the errors are already 19% smaller. With further time steps and more seismic information

becoming available, the localisation and magnitude errors using the expanded network decrease consistently.

Conclusions

The planned expansion of the earthquake early warning network as part of the *Istanbul Earthquake Rapid Response and Early Warning System* by installing additional 10 stations located around the Sea of Marmara shows a clear improvement in the early warning performances of the network. When applying the early warning algorithm PreSEIS, the source parameter estimates become more reliable – the hypocenter locations and magnitudes of 280 simulated earthquakes can be estimated more accurate within a shorter time. The warning times until the destructive S- and surface waves reach the city of Istanbul can be reduced due to the earlier recognition of the earthquakes. The results of this study show that the network expansion would contribute positively to the early warning capability of the Istanbul earthquake early warning system.

Acknowledgements

This work was funded by the research project EDIM (Earthquake Disaster Information System for the Marmara Region, Turkey), as part of the GEOTECHNOLOGIEN programme of the German Federal Ministry of Education and Research (BMBF) and the German Research Foundation (DFG), as well as by the EU-SAFER project.

References

- Alcik, H., Ozel, O., Apaydin, N., and M. Erdik (2009). A study on warning algorithms for Istanbul earthquake early warning system, *Geophys. Res. Lett.*, *36*, L00B05, doi: 10.1029/2008GL036659.
- Böse, M. (2006). Earthquake Early Warning for Istanbul using Artificial Neural Networks, Ph.D. thesis, Karlsruhe University, Karlsruhe, Germany.
- Böse, M., Wenzel, F., and M. Erdik (2008). PreSEIS: A Neural Network-Based Approach to Earthquake Early Warning for Finite Faults, *Bull. Seismol. Soc. Am.*, *98*(1), 366-382, doi: 10.1785/0120070002.
- Erdik, M., Fahjan, Y., Ozel, O., Alcik, H., Mert, A., and M. Gul (2003). Istanbul Earthquake Rapid Response and the Early Warning System, *Bull. Earthquake Eng.*, *1*, 157-163.
- Kanamori, H., Hauksson, E., and T. Heaton (1997). Real-Time Seismology and Earthquake Hazard Mitigation, *Nature*, *390*, 461-464.
- Kanamori, H. (2005). Real-Time Seismology and Earthquake Damage Mitigation, *Annu. Rev. Earth Planet. Sci.*, *33*, 195-214.
- Le Pichon, X., Şengör, A.M.C., Demirbağ, E., Rangin, C., Imren, C., Armijo, R., Görür, N., Çagatay, N., Mercier de Lepinay, B., Meyer, B., Saatçılar, R., and B. Tok (2001). The active Main Marmara Fault, *Earth Planet. Sci. Lett.*, *192*, 595-616.
- Parsons, T. (2004). Recalculated probability of $M \geq 7$ earthquakes beneath the Sea of Marmara, Turkey, *J. Geophys. Res.*, *109*, B05304, doi: 10.1029/2003JB002667.

Probabilistic seismic hazard assessment in eastern Algeria

Y. Bouhadad

National Center of Earthquake Engineering (CGS), 1 rue Kadour Rahim H. dey, Algiers,
Algeria, bouhadad_y@yahoo.com

Abstract

Northern Algeria is a part of the Eurasia-Africa plate boundary where seismic threat is a challenge. This paper presents results of the probabilistic seismic hazard analysis carried out in the Constantine (eastern Algeria) region. The probabilistic approach is used in order to take into account uncertainties. Seismic sources have been identified on the basis of field geological investigations. Source parameters such as b-values, activity rate and maximum magnitude are assessed for each seismic source. Attenuation relations which fit Algerian strong motion records have been used. Results are presented as annual frequencies of exceedance versus peak ground acceleration (PGA) values in hard rock as well as map of hazard for a return period of 500 years.

Key words: probabilistic analysis, Algeria, hazard map, hard rock, seismic source parameters, attenuation relations, PGA.

Introduction

The first step in reducing the risk of the society from natural disasters is an assessment of the hazard. This means that the reduction of earthquake risk, whether it depends on other aspects such as the vulnerability of the exposed population, could be based on the knowledge about the expected level of ground motion that may be experienced in the area within a given mean return period. Algeria belongs to the plate boundary between the African and Eurasian tectonic plates which are converging in the NW-SE direction (Fig. 1). The rate of shortening is 3-6 mm/yr (De Mets et al., 1990). Therefore, earthquake hazard constitutes a constant threat to human lives and properties. During the last two decades several moderate-sized and strong earthquakes have occurred (Fig. 1). Big damage is often associated with these earthquakes due to the vulnerability of constructions and the shallow character of the seismicity. As an inter-plate area earthquakes are directly related to active reverse faults which may be blind or not. Sometimes we have strike slip faulting as in the case of Constantine, eastern Algeria area. In this work we aim to present the seismic hazard analysis for the area of Constantine located in eastern Algeria.

Methodology

The probabilistic approach of seismic hazard analysis used in this study was proposed by Cornell (1968) and developed in its computer form by Mc Guire (1978) and

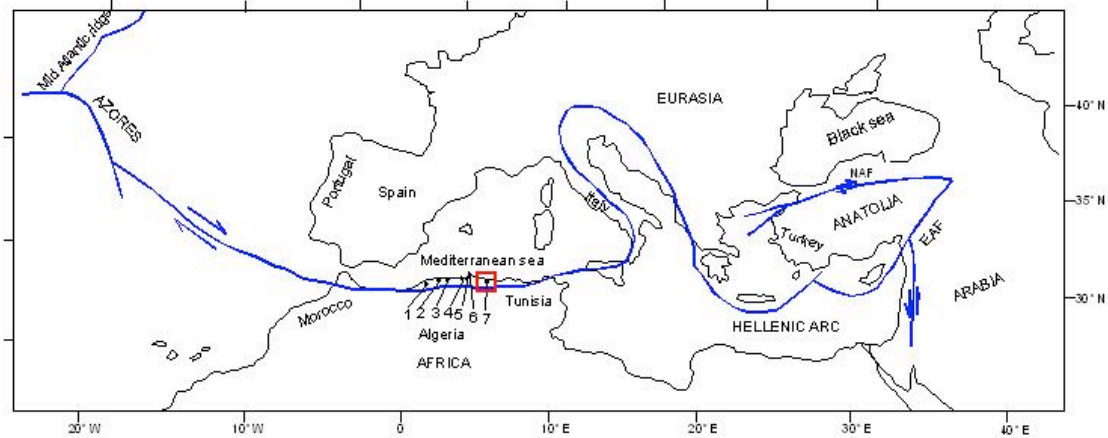


Figure 1. Schematic interface (blue line) between Africa and Eurasia plates (redrawn and modified from Kiratzi & Papazachos (1995)). Numbers 1 to 7 indicate respectively earthquake epicenters of 1= Ain Témouchent December 22, 1999, $M_S=5.6$; 2= Béni-Chougrane August 18, 1994, $M_S = 5.6$; 3= El-Asnam October 10, 1980, $M_S = 7.3$; 4= Chenoua October 29, 1989, $M_S = 5.7$; 5= Ain Benian September 5, 1996, $M_S = 5.4$; 6= Boumerdes May 21, 2003, $M_w = 6.8$; 7= Constantine October 27, 1985, $M_S = 5.7$. The red rectangle indicates the studied area.

Geomatrix Consultants (1993). It is assumed that the occurrence of earthquakes in a seismic source is a Poisson process. Then, the probability that at a given site a ground motion parameter, Z , will exceed a specified level, z , during a specified time, T , is represented by the expression:

$$P(Z > z) = 1.0 - e^{-v(z)T} \leq v(z)T,$$

where $v(z)$ is the average frequency during time period T at which the level of ground motion, Z , exceeds the level z at a given site. The values of the parameters and the attributed weights are analyzed within a logic tree model, the details of which are given in Fig. 2.

Seismic source model

In examining the seismicity pattern in the Constantine region one may observe that earthquakes are not distributed randomly but are directly related to geological structures. Four seismic source zones have been defined on the basis of geological and seismicity data. These sources are indicated as Z1, Z2, Z3, and Z4 (Fig. 3). S1 is the main segment of the Ain Smara dextral strike slip fault which was recognized as the source of the $M_S = 5.7$ earthquake of 27 October 1985 with clear surface breaks.

Source parameters

The assessed seismic source parameters are shown in Table 1. The maximum magnitude is assessed on the basis of the Wells & Coppersmith (1994) formulas and the Kijko & Sellevoll (1992) method. Due to the lack of geological data we are limited to the seismicity parameters. The used seismicity parameters are: (i) Seismicity rate (λ) associated to the "a" parameter of the Gutenberg & Richter (1954) relation. The relation between "a" and λ is: $a = \log_{10} \lambda + b M_{min}$. "a" describes the

seismic activity of the studied area and depends on the size of the zone and the observation period. (ii) the *b-value* representing the relation between earthquakes of different magnitudes.

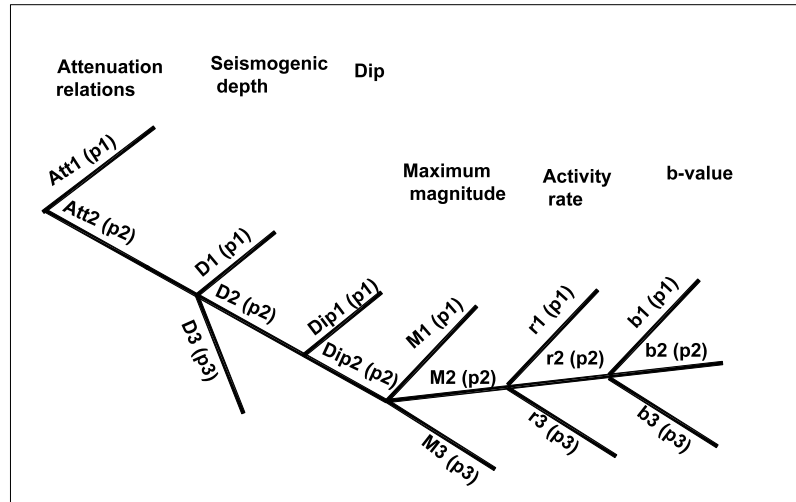


Figure 2. The used logic tree model. p_1, p_2, p_3 indicate the attributed weights.

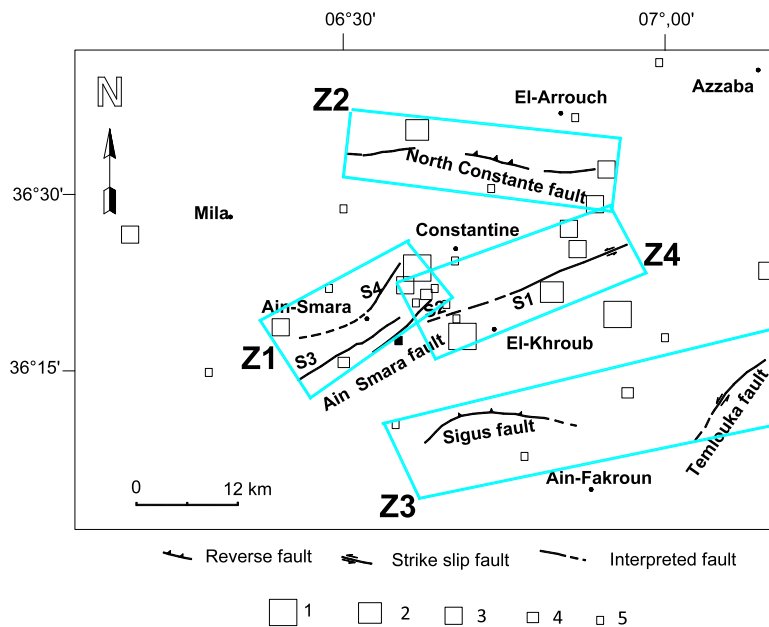


Figure 3. Seismic source model for the studied area. Z1 to Z4 are the defined seismic sources, S1 to S4 represent the different segments of the Ain Smara fault. 1 = $M_S > 5$; 2 = $4 < M_S \leq 5$; 3 = $3 < M_S \leq 4$; 4 = $2 < M_S \leq 3$; 5 = $M_S \leq 2$.

Table 1. Source parameters used in the logic tree model. Numbers in brackets represent the attributed weights for each parameter. The two used attenuation laws are given the same weight of 0.5.

Source	Depth (km)	Dip (°)	Maximum magnitude	Activity rate	b-value
Z1	10	85 SE	6.5 (0.6)	0.11 (0.6)	0.86 (0.2)
	15	75 SE	6.3 (0.2)	0.18 (0.3)	0.36 (0.4)
	18		5.7 (0.2)	0.03 (0.1)	0.61 (0.4)
Z2	10	70 NW	6.4 (0.5)	0.028 (0.6)	0.87 (0.7)
	15	80 NW	5.7 (0.5)	0.03 (0.2)	0.59 (0.2)
	18			0.026 (0.2)	0.31 (0.1)
Z3	10	65 NW	6.6 (0.2)	0.096 (0.6)	0.87 (0.7)
	15	75 NW	6.3 (0.6)	0.051 (0.4)	0.59 (0.2)
	18		5.7 (0.2)		0.31 (0.1)
Z4	10	85 SE	7.0 (0.2)	0.07 (0.2)	0.46 (0.4)
	15	75 SE	6.6 (0.6)	0.10 (0.6)	0.69 (0.4)
	18		6.2 (0.2)	0.04 (0.2)	0.27 (0.2)

Attenuation of ground motion

Strong ground motions produced by earthquakes are influenced by the characteristics of the earthquake source, the crustal wave propagation path, and the local site geology. There is no already developed attenuation relation for Algeria. Therefore, two worldwide developed relations are used in this work, Ambraseys & Bommer (1991) and Sadigh et al. (1993). These two relations fit the strong motion recordings of the Béni-Chougrane August 18th earthquake ($M_S = 5.6$) (Fig. 4), furthermore, the Ambraseys & Bommer 1991 relation includes Algerian data from three earthquakes (El-Asnam, 1980, $M_S = 7.3$, Constantine, 1985 $M_S = 5.7$ and Chenoua, 1989, $M_S = 5.7$).

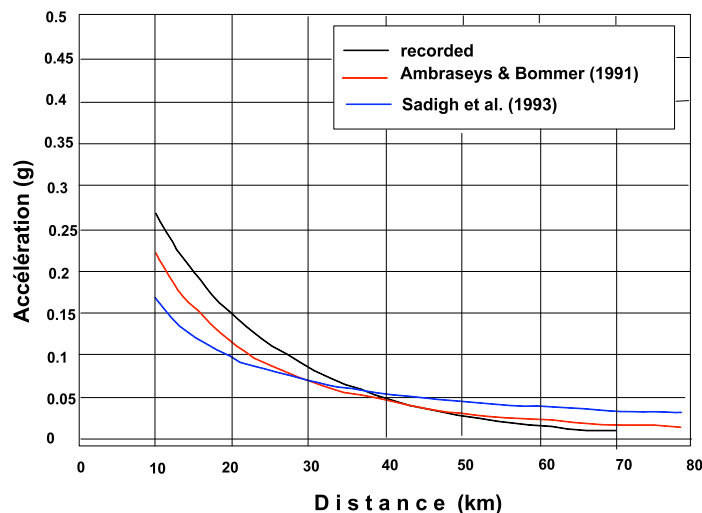


Figure 4. Comparison of the used attenuation relations with Algerian strong motion records obtained during the Béni-Chougrane August 18th, 1994 earthquake ($M_S = 5.6$).

Results and Conclusions

Results of the seismic hazard assessment are presented for Constantine city (6,673 E, 36.435 N) as graphs showing the annual frequency of exceedence and return period ,

respectively as a functions of the peak ground acceleration (Fig. 5). Uncertainties due to the choices of parameter values and attenuation are presented as the mean, median (50% percentile), 15%, and 85% values. It appears that the seismic hazard in the studied region is dominated by the Ain Smara fault, where the mean values of peak ground acceleration are close to 0.4g for a return period of 500 years (Fig. 6).

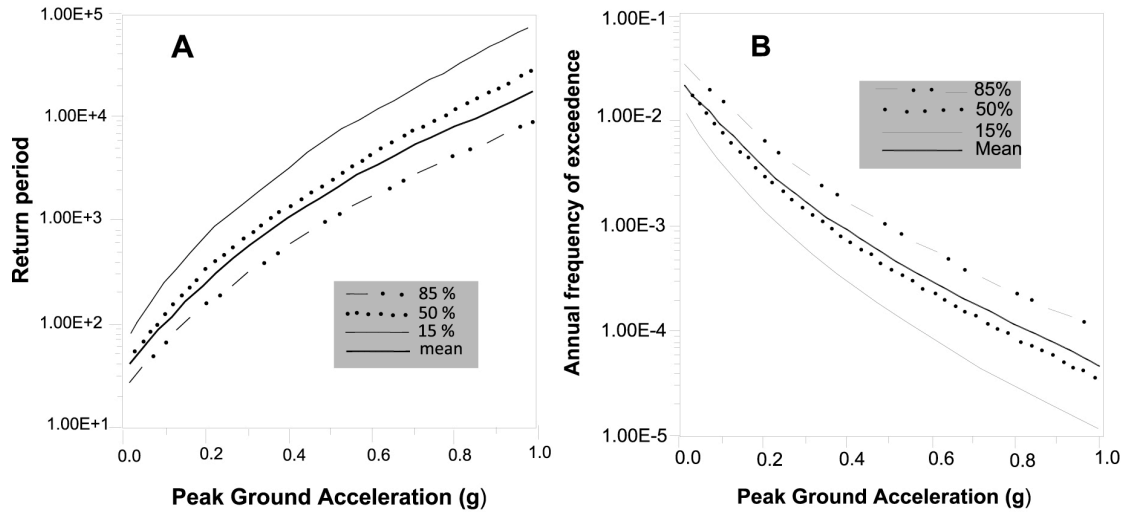


Figure 5. Annual frequency of exceedance (A) and return period (B) versus peak ground acceleration.

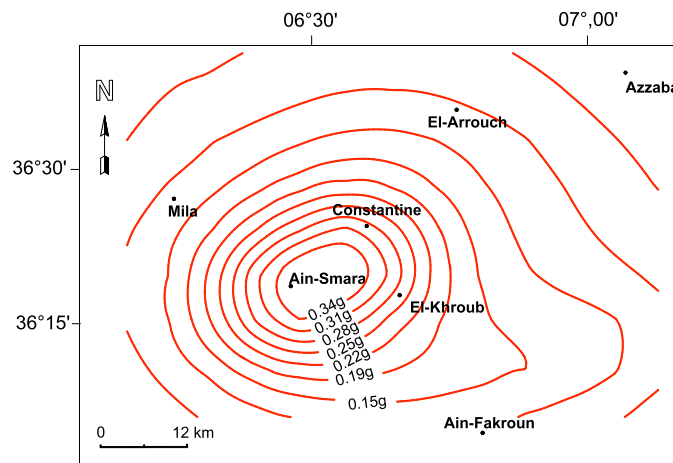


Figure 6. Seismic hazard map (mean PGA values) for a return period of 500 years.

References

- Ambraseys, N.N. & Bommer, J.J.: 1991, The attenuation of ground accelerations in Europe, *Earthquake Eng. Struct. Dyn.*, 20, 1179-1202.
- Cornell, C.A.: 1968, Engineering seismic risk analysis. *Bull. Seismol. Soc. Am.*, 58, 1583-1606.
- De Mets, C.R., Gordon, R.G., Argus, D.F., Stein, S.: 1990, Current plate motions, *Geophys. J. Inter.*, 101, 425-478.
- Geomatrix Consultants: 1993. Probabilistic seismic hazard analysis computer program: A user manual.
- Gutenberg, B. & Richter, C.F.: 1954, *Seismicity of the earth and associated phenomena*, Princeton Univ. Press, New Jersey, pp. 310.
- Kijko, A. & Sellevoll, M. A. 1989. Estimation of earthquake hazard parameters from incomplete data files. Part II. Incorporation of magnitude heterogeneity, *Bull. Seismol. Soc. Am.* 82, 1, 120-134.
- Kiratzi, A. & C.B. Papazachos (1995): Active deformation of the shallow part of the subducting lithospheric slab in the southern Aegean, *J. Geodyn.*, 19, 65-78.
- Mc Guire, R.K.: 1978, FRISK: computer program for seismic risk analysis using faults as earthquake sources. U.S. Geological Survey. Open file report 78-1007.
- Sadigh, K., Chang, C.Y., Abrahamson, N.A., Chiou, S.J., Power, M.S.: 1993, Specification of long period ground motion. Updated attenuation relationships for rock site conditions and adjustment factors for near fault effects. Proceedings of ATC-17-1 seminar on seismic isolation, passive energy dissipation, and active control. March 11-12 San -Francisco, California, 59-70.
- Wells, D.L. & Coppersmith, K.J.: 1994, Updated empirical relationships among magnitude, rupture length, rupture area, and surface displacement. *Bull. Seismol. Soc. Am.*, 84, 974-1002.

Ground motion simulations for the Taipei basin (Taiwan) for shallow and deep seismicity

J. Miksat (1), V. Sokolov (1), K-L. Wen (2), F. Wenzel (1) and Ch-T. Chen (2)

- 1) Geophysical Institute, Karlsruhe University, Hertzstr. 16, 76187 Karlsruhe, Germany, joachim.miksat@gpi.uni-karlsruhe.de
- 2) Institute of Geophysics, National Central University, No. 300, Jhongda Rd., Jhongli City, Taoyuan County 32001, Taiwan (R.O.C) wenkl@earth.ncu.edu.tw

Abstract

The city of Taipei in northern Taiwan is located on a sedimentary basin and was affected by several destructive earthquakes in the past (April 15, 1909, $M_L = 7.3$; November 15, 1986, $M_L = 6.8$; September 21, 1999, $M_L = 7.3$; March 31, 2002, $M_L = 6.8$). As the seismicity of Taiwan is very high and the Taipei basin area is covered with a dense strong motion network, a detailed analysis of observed ground motion can be performed. Recent analysis of recorded earthquakes shows significant differences between records for deep and shallow events. We apply 3D finite-difference (FD) modeling of wave propagation through the basin in order to describe the observed basin response. By comparison with observed data we found that numerical modeling reproduces the main characteristics of the Taipei basin response. Therefore the method could be applied to other basins, especially when basin response cannot be derived from observed data because of the lack of records.

Introduction

The city of Taipei in northern Taiwan is located on a sedimentary basin and was affected by several destructive earthquakes in the past (April 15, 1909, $M_L = 7.3$; November 15, 1986, $M_L = 6.8$; September 21, 1999, $M_L = 7.3$; March 31, 2002, $M_L = 6.8$). The Taipei basin is covered with a dense strong motion network, which is operated in the frame of the TSMIP (Taiwan Strong Motion Instrumentation Program) conducted by the CWB (Central Weather Bureau). Recent analysis of recorded data shows significant difference between records for deep and shallow events. Spectral amplification factors derived by Sokolov et al. (2009, 2008) and Chen et al. (pers. comm., 2009) show that amplifications in the central part of the basin are larger for shallow earthquakes than for deep ones in the low frequency range ($f < 2$ Hz - 3 Hz). For stations located directly along the basin edges, no clear amplitude difference is observable. Furthermore, amplification factors for shallow earthquakes of different azimuths differ clearly at some stations.

In order to understand the observed ground motion characteristics, we perform 3D FD simulations of incident S-wave fronts for different azimuths and incidence angles corresponding to deep and shallow earthquakes. The simulations are performed for

the 3D basin structure and a homogeneous model. The P- and S-wave velocities of the homogeneous model are 3 km/s and 1.5 km/s, which correspond to the found bedrock velocities for the Taipei basin (Wang, 2004). The comparison of the results for both models enables us to examine the relative influence of the 3D basin structure and to calculate spectral amplifications up to 1 Hz. As bridges and high-rise buildings are very sensitive within the 1 Hz frequency range, a detailed understanding and quantification of amplification effects is critical. Numerical modeling is capable to resolve these issues and consequently to improve hazard assessment. Especially, as the data base of observed earthquakes can be extended by numerical modeling because observations do not exist for all possible source regions around the Taipei basin.

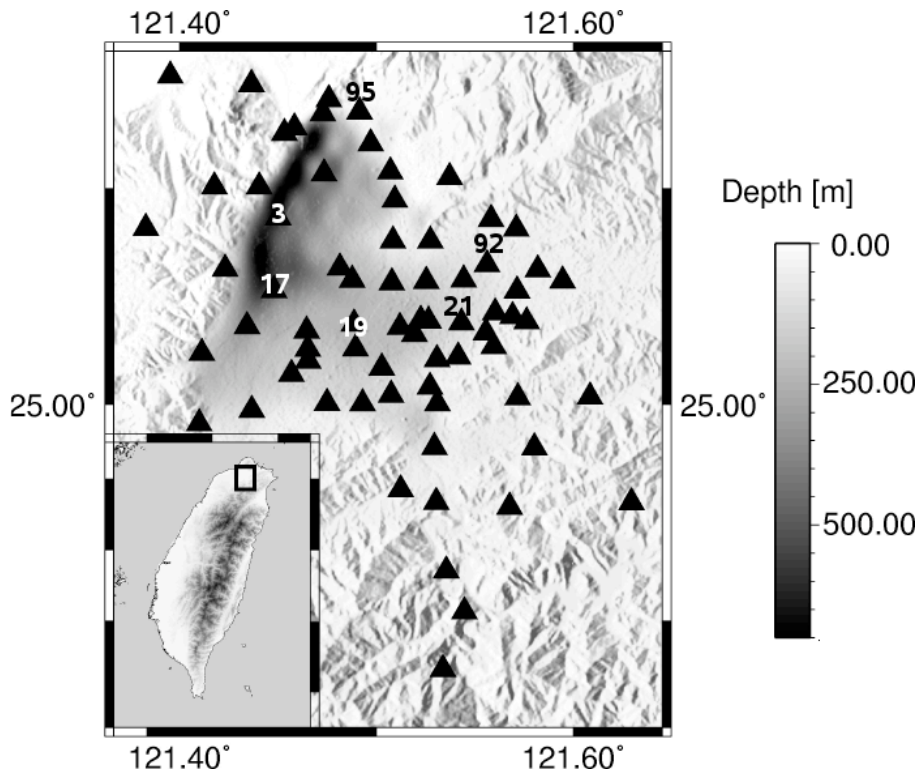


Figure 1: Map of the triangle shaped Taipei basin in northern Taiwan. The depth to the Tertiary basement is indicated by the gray scale. Triangles mark strong motion stations of the TSMIP network operated by the CWB (Central Weather Bureau). Station numbers are given for stations that are evaluated in this paper.

Subsurface Structure

The city of Taipei is located on a sedimentary basin, which can be divided in a deep western part, with steep dipping edges, and a shallow eastern part (see Fig. 1). Maximum depth to the Tertiary basement is about 750 m in the NW. The basin structure is well known and based on reflection seismic experiments and borehole data (Wang et al., 2004). Fig. 2 shows cross-sections through the generated Taipei basin velocity model. The structure and velocities are adopted from Wang et al. (2004) and topography is taken from the SRTM data base (CIAT, 2004). Minimum P- and S-wave velocities of the uppermost layer (the so called Sungshan formation) are 450 m/s and 170 m/s, respectively. Seismic velocities of the Tertiary basement are: $v_p = 3.0$ km/s and $v_s = 1.5$ km/s. The horizontal extension of the model is about 30 km

by 30 km. The spatial discretization applied for modeling is 50 m in horizontal direction and 25 m in vertical direction.

Finite-Difference Method

We use a 3D FD method (Furumura and Chen, 2005; Furumura et al., 2003) in order to simulate wave propagation for the Taipei basin. The code is of 4th (vertical direction) to 16th (horizontal direction) order in space and second order in time. Three grid points per minimum wavelength in horizontal and 6 grid points per minimum wavelength in vertical direction are sufficient in order to obtain accurate results (Furumura et al., 2003).

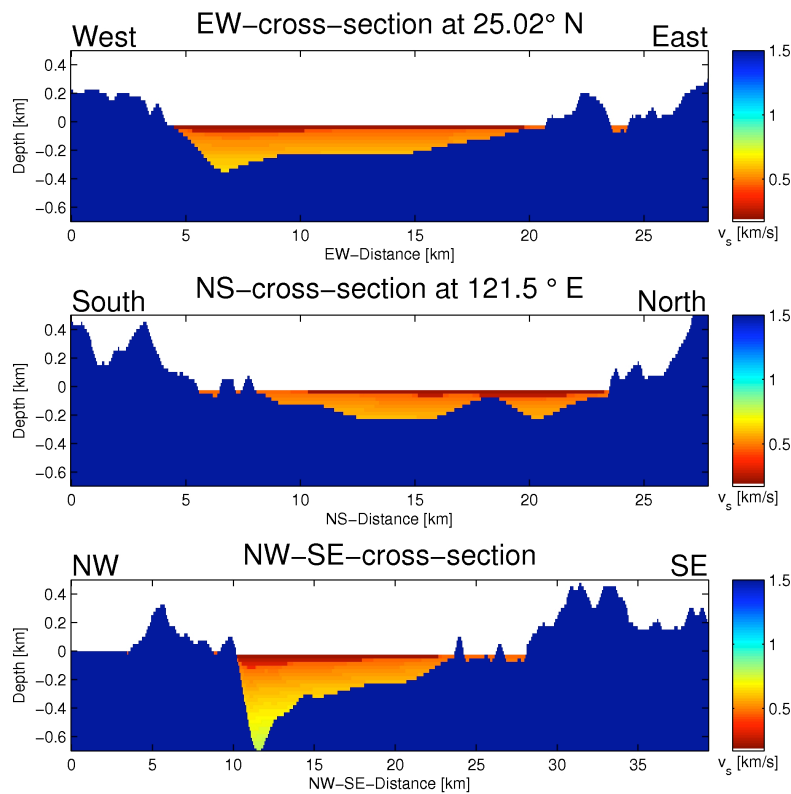


Figure 2: Three cross sections through the Taipei basin model that show shear wave velocities. The generated model is based on Wang et al. (2004).

Consequently, based on the minimum shear wave velocity and grid spacing, the maximum frequency reached by our simulations is 1 Hz. The simulations are carried out on a HP XC 6000 system at the Karlsruhe Scientific Supercomputing Center (SSC).

In order to explore the Taipei basin response, we simulate planar S-wave front incidence on the basin for different incidence angles, which correspond to different earthquake depths (Fig. 3). We also explore the azimuth dependence of the basin response by simulating S-wave front incidence from the East and South. Deep earthquakes are described by a wave front incident from the bottom and shallow earthquakes are simulated by incidence for two different azimuths (East and South). The incident S-wave fronts are SH polarized.

Simulations are performed for two different subsurface structures, the 3D Taipei basin model (Fig. 2) and a homogeneous model with $v_p = 3$ km/s and $v_s = 1.5$ km/s. Frequency dependent spectral ratios are calculated by dividing the calculated Fourier amplitude spectra (FAS) of the simulation with the 3D basin structure by the FAS resulting from the simulation for the homogeneous model. Consequently, the calculated spectral amplifications show relative effects (amplification or deamplification) of the basin structure on incident waves. These effects could be superimposed on existing standard hard rock attenuation relations in order to calculate absolute ground motion values within the basin.

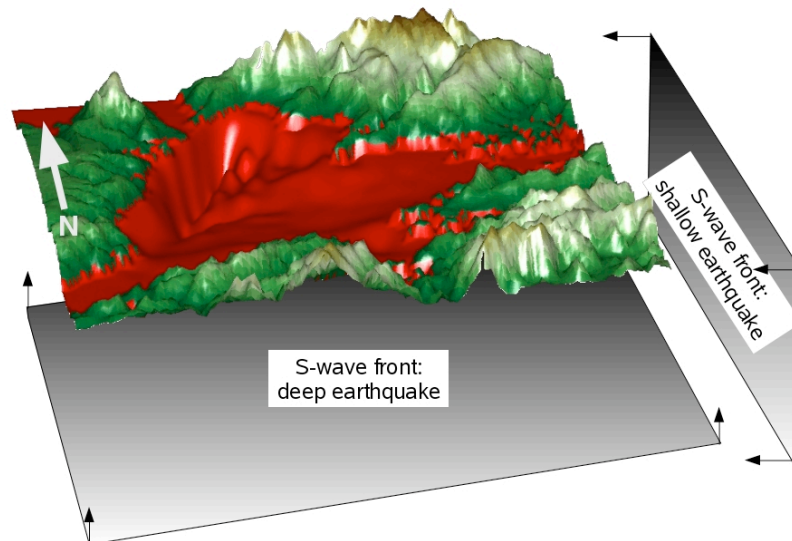


Figure 3: Topography-basement layer of the Taipei basin. We simulate distant deep earthquakes by S-wave front incidence from the bottom and shallow earthquakes by S-wave front incidence from the East and South.

Results

We examine the spectral amplifications (Fig 4 top) for stations which are located in the deepest part of the basin (TAP 17, TAP 3), in the eastern shallow part (TAP 19, Tap 21, TAP 92) and near the basin edge (TAP 95). In general, we obtain larger spectral ratios for the shallow earthquakes than for the deep earthquake at stations within the basin. However, for TAP 95 near the basin edges the spectral amplifications are similar for the deep and shallow scenarios east of the basin. This general difference between stations within the basin and near the basin edges and between shallow and deep earthquakes is described for many stations of the TAP network in Miksat et al., (2009, 2008). Looking at the dominant frequency, maximum ratios change from about 0.3 Hz for stations located in the western deep part of the basin to 0.3 - 0.6 Hz for the central and eastern part. Along the basin edges the maximum is obtained for frequencies larger than 0.6 Hz. The above described main characteristics of simulated spectral amplifications for the Taipei Basin were also found from analysis of empirical data (Sokolov et al., 2009, 2008; Chen et al, 2009, Chen et al., pers. comm., 2009).

Next, we look at snapshots of the wave field for all three scenarios (Fig. 4). The velocities are scaled to the maximum velocity at the marked hard rock (HR) station outside the basin (black triangle). The snapshots show clearly the generation of

surface waves at the southern and eastern basin edge for both shallow scenarios. For the earthquakes in the South, strongest surface waves amplitudes are generated in the south-western edge of the basin and guided along the deep part of the basin to the North (black ellipse). When the earthquake occurs east of the basin, strong surface waves are excited at the eastern edge and at the eastern rim of the northern embayment of the basin and travel to the western deepest part of the basin (black ellipses). The waves generated at the easternmost edge of the basin are guided to the West along a deep channel through the center of the basin. Compared to the deep scenario both shallow scenarios produce stronger surface waves and significant longer ground motions.

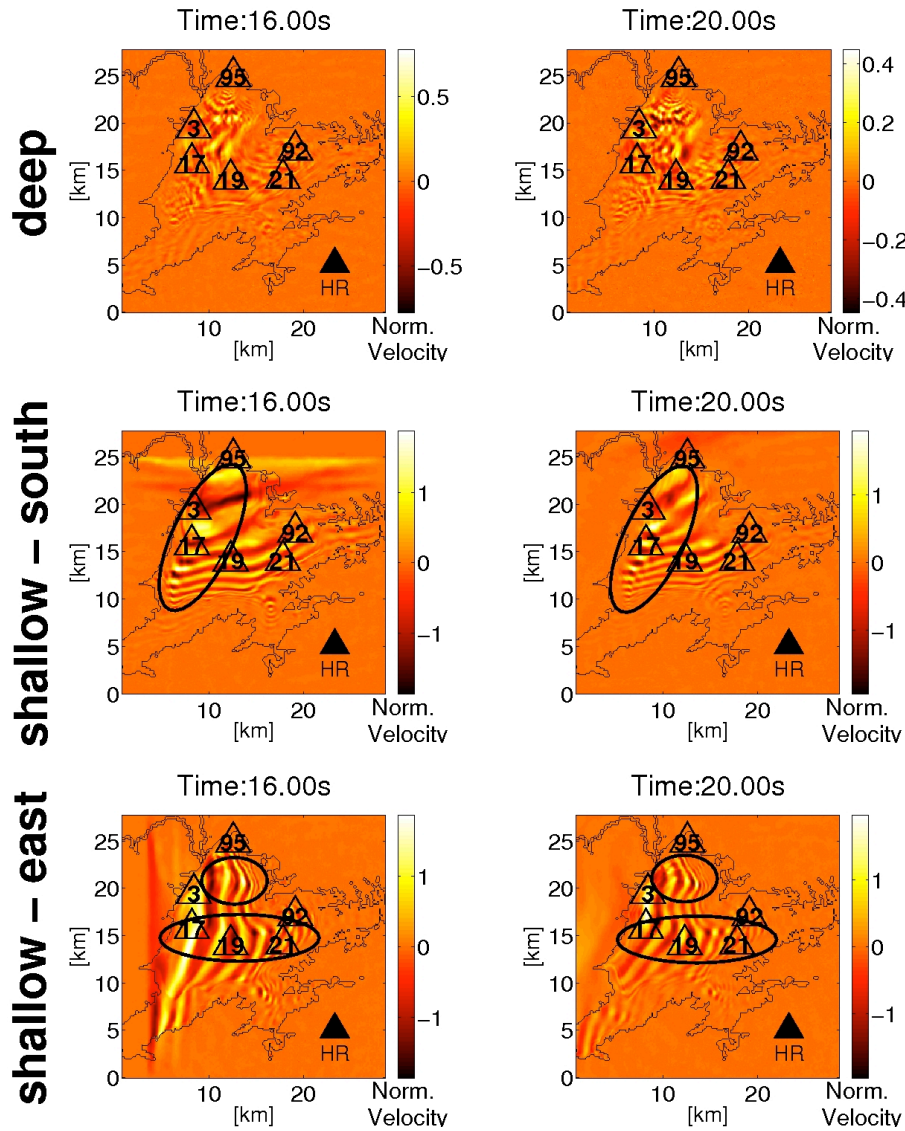


Figure 4: Snapshots of the wave field after 16 s and 20 s with wave incidence for a deep (top) and shallow earthquakes in the South (middle) and East (bottom). The velocities are scaled to the maximum velocity at the marked hard rock (HR) station outside the basin (black triangle).

Therefore, the larger spectral amplifications (Fig. 5) for shallow earthquakes can be explained by the generation of surface waves at the basin margins. The azimuth dependence of surface wave generation and main travel paths through the basin yield

to azimuth dependent spectral amplifications at some stations. For TAP 17, which is located in the southwest of the basin, earthquakes south of the basin produce large amplitudes and long ground shaking. On the other hand, station TAP 92 in the eastern part of the basin shows larger spectral amplifications for earthquakes east of the basin because of surface waves generated along the eastern basin margin. For TAP 95 near the basin edge spectral amplifications are similar for deep and shallow earthquakes. This can be explained by the absence of low frequency surface waves near the basin edges where the sediment thickness is very thin.

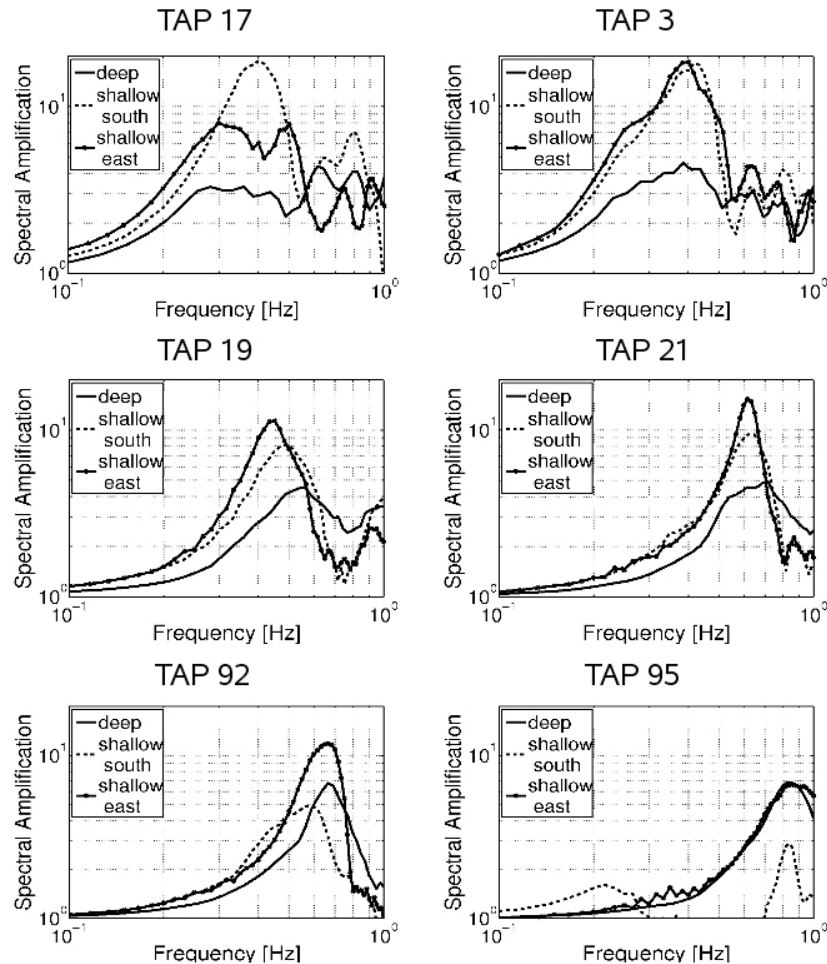


Figure 5: Spectral amplifications for stations in the western deep part of the basin (TAP 17, TAP 3), stations in the eastern shallow part (TAP 19, TAP 21, TAP 92) and at the basin edge (TAP 95).

Summary

We calculated the Taipei basin response by simulating planar S-wave front incidence in order to describe the observed effects in a qualitative way. These effects result from shallow or deep sources as well as the wave pattern they generate, particularly the surface wave effects once shallow earthquakes are involved. Future simulation will focus on the quantitative comparison between modeling and observation of spectral amplifications and a calibration of the modeling procedure for many different azimuths and incidence angles. This will allow the quantitative utilization of 3D modeling for hazard assessment. We found in this study that even by utilizing only

three scenario wave fronts the calculated absolute amplification values in the range of 5 to 10 are comparable with amplification values found from empirical studies (Wen and Peng, 1998).

Our simulations show that the large spectral amplifications of shallow earthquakes compared to deep earthquakes can be attributed to the generation of strong surface waves at the basin edges. Furthermore, our simulations show that the complex basin structure generates ground motion response that depends on earthquake azimuth. Consequently, the implementation of earthquake azimuth is of high importance for hazard assessment for the Taipei basin. As the strong motion database does not contain records from all potential earthquake azimuths, spectral amplifications derived from recorded earthquakes may be biased. Therefore, numerical modeling can extend the data base and improve hazard assessment by incorporating earthquakes of all azimuths. Furthermore, our simulations for the Taipei basin suggests that the applied procedure may be a very valuable tool for other basin structures. Especially, if the basin response cannot be evaluated from observed data because of the lack of observations.

References

- CIAT (2004). Void-filled seamless SRTM data V1 (2004). International Centre for Tropical Agriculture (CIAT), available from the CGIAR-CSI SRTM 90m Database: <http://srtm.csi.cgiar.org>.
- Furumura, T., and L. Chen (2005). Parallel simulation of strong ground motions during recent and historical damaging earthquakes in Tokyo, Japan. *Parallel Comput.*, 31, 149–165.
- Furumura, T., B.L.N. Kennett, and K. Koketsu (2003). Visualization of 3D wave propagation from the 2000 Tottori-ken Seibu, Japan, earthquake: observation and numerical simulation, *Bull. Seism. Soc. Am.*, 93, 870–881.
- Miksat, J., K.-L. Wen, V. Sokolov, Ch.-T. Chen, and F. Wenzel (2009). Simulating the Taipei basin response by numerical modeling of wave propagation. *Bulletin of Earthquake Engineering*, submitted.
- Miksat, J., K.-L. Wen, Ch.-T. Chen, V. Sokolov, and F. Wenzel (2008). Numerical modeling of basin effects for the Taipei basin. *European Seismological Commission ESC 2008, 31st General Assembly, Hersonissos, Crete, Greece, 7 – 12 September*, pp. 271-279.
- Sokolov, V., Wen, K.-L., Miksat, J., Wenzel, F., Chen C.-T. (2009). Analysis of Taipei basin response on earthquakes of various depth and location using empirical data. *Terr. Atmos. Ocean. Sci.* (in press).
- Sokolov, V. , K.-L. Wen, J. Miksat, F. Wenzel, and Ch.-T. Chen (2008). Analysis of Taipei basin response on earthquakes of various depth and location using empirical data. *European Seismological Commission ESC 2008, 31st General Assembly, Hersonissos, Crete, Greece, 7 – 12 September*, pp. 435-442.
- Wang C.-Y., Lee Y.-H., Ger M.-L., and Chen Y.-L. (2004). Investigating subsurface structures and P- and S-wave velocities in the Taipei Basin. *Terr. Atmos. Ocean. Sci.*, 15 (4), 609–627.
- Wen K.-L., and Peng H.-Y. (1998). Site effect analysis in the Taipei basin: Results from TSMIP network data. *Terr. Atmos. Ocean. Sci.* 9(4):691–704.

Seismic monitoring of structures - An important element of seismic hazard reduction

Vladimir Mihailov and Dragi Dojcinovski

Institute of Earthquake Engineering and Engineering Seismology, Skopje, R. Macedonia,
mihailov@pluto.iziis.ukim.edu.mk, dragi@pluto.iziis.ukim.edu.mk

Abstract

Seismic monitoring of structures is one of the activities within the scope of seismology and earthquake engineering, which, has lately been paid considerable attention. This is not without reason, since the results obtained by this monitoring are of multi-fold purpose in the protection against earthquake effects. Apart from this, they are also the basic data for the design of earthquake resistant structures, which directly affects the general efforts for reduction of the existing seismic risk in urban areas.

The seismic instrumentation of the structures should provide exact information on the seismic input and the structural response during the earthquake. The distribution of the instruments is therefore of crucial importance.

In this paper, some of our experiences and results from the investigations performed by the authors will be discussed and presented.

Introduction

The seismic monitoring of structures mainly refers to engineering aspects of the structure. The main objective in seismic monitoring of structures (high-rise buildings, dams, power plants, bridges etc.) is to facilitate response studies that lead to improved understanding of the dynamic behavior and potential for damage to structures under seismic loading.

Data on ground motion during earthquakes to which structures are exposed and behaviour of structures are fundamental for seismic hazard evaluation, definition of design parameters and criteria and for all other dynamic investigations in earthquake engineering. Without such data all investigations and analysis that follow would be based on assumptions. The irregularity in earthquake occurrence makes it difficult to obtain enough data in a short period of time. One of the possible ways to tackle these problems is to establish a network of a greater number of instruments for recording a maximum of data during the rare strong earthquakes.

As a result of the understanding of structural response to seismic loading, design and construction practices can be modified so that future earthquake damage is minimized. Therefore, there are significant implications in (a) risk reduction, (b) improvement of codes, (c) identification of seismic response characteristics of

structural system that may be used in determination of strategies for improvement of their performances.

The application of the results is equally important both for theoretical and fundamental investigations in the field of earthquake engineering and for application and practical investigations in the earthquake engineering. Presented in this paper shall be some ideas and results from the projects realized by the Institute of Earthquake Engineering and Engineering Seismology (IZIIS), Skopje (R.Macedonia).

Strong motion network in Macedonia

The territory of Republic of Macedonia is characterized by a high seismic activity (Fig. 1.). This particularly refers to the area of the city of Skopje where the concentration of residential, administrative, industrial and cultural-historic structures of particular importance for the Republic of Macedonia strongly increases the level of seismic risk.

The earthquake phenomenon almost always involves numerous problems which cannot be solved exactly due to the lack of instruments for recording ground shaking and response of structures. Without such recordings, damage and behavior of structures during strong earthquakes cannot be compared to the seismic design criteria nor proper decisions concerning rational repair and reconstruction could be made.

The installation of networks for recording of strong earthquakes and the results which are obtained from them, has become an increasing need in earthquake engineering and has considerably contributed to the overall activities for seismic risk reduction of existing urban areas and for the minimization of the damage to these structures under the effect of disastrous earthquakes.

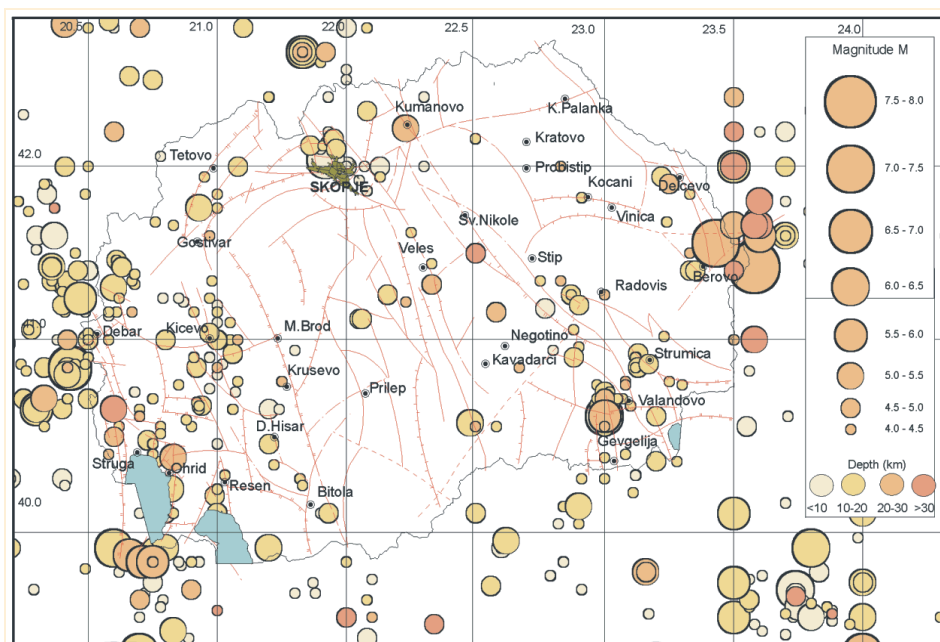


Figure 1: Map showing the epicenters of earthquakes occurring in the R. of Macedonia for the period 1990-1996 with $ML > 4.0$.

The strong motion network in Macedonia (Fig.2) were developed with corresponding density in order to study the following seismological and earthquake engineering aspects: (1) earthquake source mechanism, (2) wave propagation effects, (3) effect of local topography, (4) free-field soil response at different soil conditions, (5) site amplification factors, and (6) structural response of different types of buildings and structures including soil-structure interaction.



Figure 2: Strong motion network in Macedonia.

In areas of potentially unstable soils, strong motion records will help to determine the characteristics of the ground motions which might indicate landslides, subsidence, slumping and liquefaction.

Basic concept of the Macedonian network

The strong motion network installed in 1972 on the territory of Macedonia consists of 115 accelerographs type SMA-1, K-2 with episensors, GNC-CR12 with accelerometers type SSA-320 and quake data recorder QDR .

The selection of detailed locations for establishment of these instruments (Fig.3.) makes it possible to obtain records on 1) bedrock, 2) on a surface of characteristic

soils (alluvial and deluvial sediments), 3) on structures (multistorey buildings, dams, etc.). The instrument distribution, of both accelerographs and seismoscopes was made following this basic concept (Table 1).

Until 1991, the Macedonian strong motion instrument network had been part of the instrument network of former Yugoslavia. It consisted of 106 accelerographs and 54 seismoscopes.

The strong motion network installed on the territory of former Yugoslavia (Fig 2.4.) was one of the largest in Europe. It consisted of over 250 accelerographs of type SMA-1 and about 130 seismoscopes type WM-1.

The strong, motion program consists of five subactivities: (1) network design, (2) network operation, (3) data processing, (4) network management and (5) research as well as application. All this activities are under the responsibility of IZIIS - Skopje.

Table 1. Distribution of instruments

Location	Accelerographs
On bed rock	9
On characteristic soil	47
On structure	59
Total	115

Seismic monitoring of structures

One of the main purposes of the strong motion network is to provide data on the dynamic behaviour of structures under the effect of earthquakes. To achieve this, instruments have been installed at previously defined points.

Seismic monitoring of structures is planned, designed, carried out and organized for each structure taken separately. The parameters for elaboration of a seismic monitoring project can be defined on the basis of:

- (1) Seismic regime of the micro- and the macro-region;
- (2) Dynamic and strength characteristics of the local soil;
- (3) Mode of foundation;
- (4) Type and dynamic characteristics of the structure;
- (5) Soil-foundation-structure interaction and
- (6) Geometrical shape of the structure.

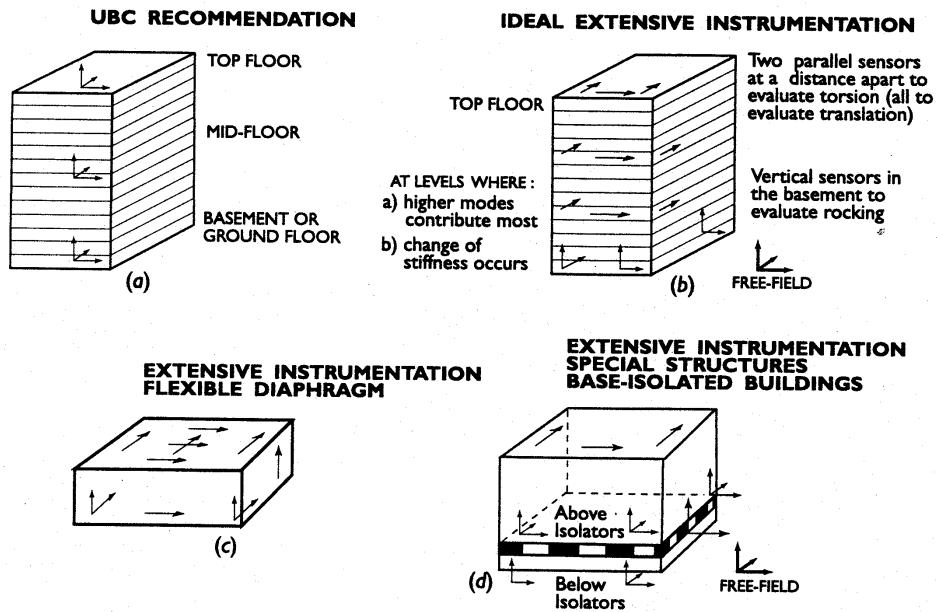
Accordingly, it is necessary to elaborate a separate project for seismic monitoring of each structure in order to:

- establish an optimal system of seismic monitoring instruments and
- obtain practically usable and compatible data in case of an earthquake.

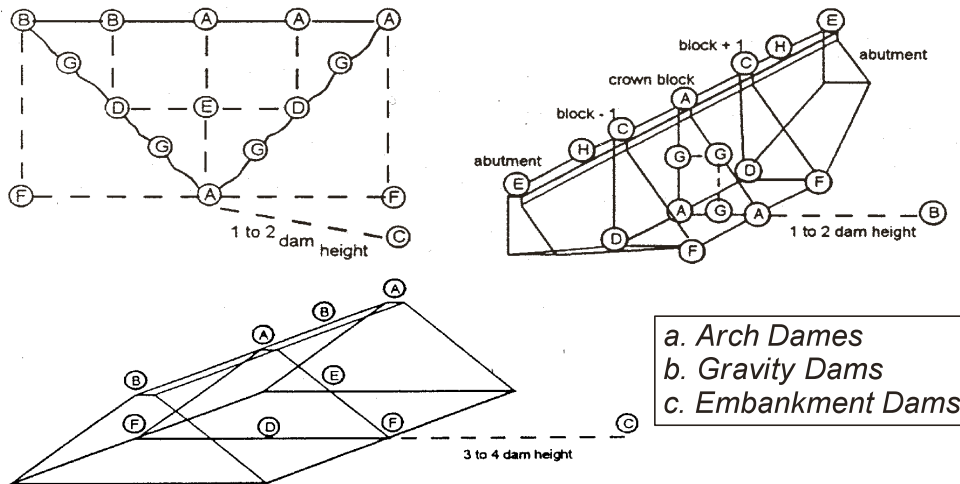
Data obtained by means of the seismic monitoring equipment may serve for multiple purposes, first of all, they are very useful for: (1) verification of previous computations and analyses; (2) analysis of the stress state and level of safety of the structure after the earthquake effect and (3) optimization of the process of design of future structures.

Table 2. Instrumented structures

Structures	No. of Instruments
High-rises building	30
Dams	50
Bridges	20
Total	100



a) Buildings (taken from M. Celebi)



b) Dams (taken from G.R.Darbre)

Figure 3: Typical instrumentation schemes.

An important element of the strong motion instruments installed on the structures are their output information. It is desirable that these be in such a form that they could provide an information on the intensity of an earthquake immediately after its occurrence. Based on this, a decision could be made regarding further exploitation of

the structure. For instance, if the structure is designed for $a = 0.25$ g as a design parameter, and the maximum amplitude of recorded ground acceleration is less than this value, a decision can be made, with great reliability, for further exploitation of the structure with no particular repair or strengthening. However, when the recorded acceleration is greater than 0.25 g, it is desirable, in case when there are no visible signs of damage, to perform a special study and define the stresses and strains in the structure caused by the forces from the recorded earthquake.

The seismic instrumentation of the structures should provide exact information on the seismic input and the structural response during the earthquake. The distribution of the instruments is therefore of crucial importance.

Some results

Since the beginning of 1972, a number of slight ($M \geq 3.0$) and about ten stronger earthquakes with $M \geq 5.2$ have occurred in the territory of former Yugoslavia and neighboring countries. All these earthquakes were mainly recorded by the strong motion instruments of the former Yugoslav network.

A great number of accelerogrammes have been obtained, processed and stored in the databank of the Strong Motion Laboratory of the Institute of Earthquake Engineering and Engineering Seismology (IZIIS), Skopje. Most of the records, i.e., all the records with $a_{\max} \geq 0.05$ g are presented on the IZIIS' web site.

The databank contains 1206 accelerogrammes out of which 823 have been obtained by instruments installed at free field and 383 by instruments installed on different engineering structures (high rises, dams, bridges and power plants). Mentioned here are only the recorded accelerogrammes of stronger earthquakes that have been widely applied in everyday engineering practice for the preceding years. Their wide application in aseismic design of different kinds of structures, seismic hazard analysis and even in the technical regulations for aseismic design is also evident. The more important recorded accelerogrammes refer to the following earthquakes:

- Montenegro earthquake, 1979, with $M = 7.2$
- Kopaonik earthquake, 1980, with $M = 6.3$
- Banja Luka earthquake, 1981, with $M = 6.4$
- Negotino earthquake, 1985, $M = 5.1$
- Gevgelia - Gumenica (Greece) 1990, with $M = 5.5$
- Bitola earthquake, 1994, with $M = 5.2$

as well as earthquakes that occurred in the neighboring countries of former Yugoslavia:

- Friuli, Italy, 1976, with $M = 6.5$
- Vrancea, Romania, 1977, with $M = 7.2$
- Thessaloniki, Greece, 1978, with $M = 6.3$

Accelerograms have been obtained by instruments located at different locations, i.e., not only locations in the immediate vicinity of the epicentral area but also locations at a distance of $L \geq 150$ km.

The above mentioned list of occurred and recorded earthquakes points to increased seismic activity in the territory of former Yugoslavia and neighboring countries in the course of the seventies of the last century. All of these accelerograms have later been extensively applied in engineering practice.

Due to the lack of space for more detailed information on the results obtained by the Macedonian strong motion network, only the records of the strong earthquake occurred in Banja Luka 1981 and Negotino 1985, will be considered in the further text. Accompanied by tables and figures shall be the main characteristics of the recorded accelerogrammes.

The basic information about the buldings and locations of instruments in Banja Luka, together with the characteristics of the obtained records (a_{\max} and spectars) are given in table 3 and fig. 4.

In Banja Luka, we had installed 9 accelerographs on four buldings with different heights. Buldings were located on diferrent geological characteristics. The obtained results show big differences in a_{\max} , that is due to very different geological conditions on the sites. Namely, the instrument located at IMB Institute is on extremely soft soil ($V_s=150$ m/s, depth= 2 m; $V_s=350$ m/s, depth=6m; $V_s=990$ m/s, depth=150m), at the location BK-2 with soft soil ($V_s=150$ m/s, depth= 2 m; $V_s=300$ m/s, depth=6m; $V_s=1200$ m/s, depth=650m), at the location BK-9 with soft soil ($V_s=150$ m/s, depth= 2 m; $V_s=350$ m/s, depth=8m; $V_s=1200$ m/s, depth=650m) and at the location Seismological observatory on bedrock ($V_s=1200$ m/s, depth= 15 m; $V_s=1750$ m/s, depth>15m). We would like to note that the presented values of maximum acceleration (a_{\max}) were obtained directly from the record, that is not utterly correct. The comparison should be made between the data from corrected records. Also, the instruments were placed in ground floor objects on special fundaments, so that there is no significant influence of the object's structure on the measured maximum acceleration. More detailed results from the analysis of the recorded earthquakes can be found in the IZIIS publications.

Table 3. Data obtained from the instrumented 12 Story Building in Banja Luka.

Site	Location of instrument	Max. acc. (cm/s ²)		
		N-S	V	E-W
IMB Institute	ground	506.4	257.4	386.8
Seismological station	ground bedrock	65.2	43.6	72.3
Apartment building "BK-2"	basement	307.2	91.5	268.9
	VI floor	371.1	242.0	269.7
	XII floor	367.1	280.0	197.4
Apartment building "BK-9"	basement II entr.	368.8	120.5	225.4
	IV floor I entr.	382.4	214.9	352.7
	IV floor II entr.	419.2	222.4	364.7
	IV floor III entr.	416.2	162.4	351.1

Table 4. Tikvesh Dam: Data on record 28-09-1985 $M=5.1$

Location	Component N 150 S	Component N 60 S	Component Up.
	cm/s ²	cm/s	cm
Dam Crest	-46.7	40.4	-33.3
Cent. Part	-20.0	17.0	14.2
Lover Part	-12.8	12.4	6.2
Free Field	5.3	-3.6	-4.0

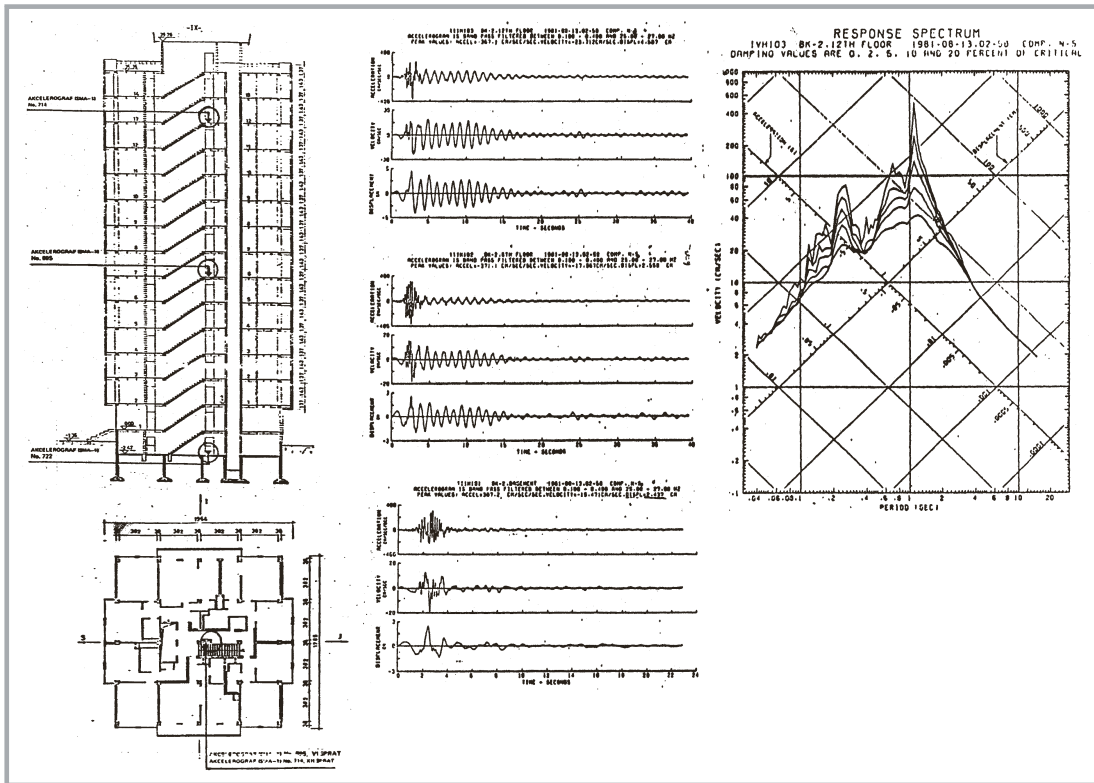


Figure 4: Seismic monitoring on 12 storey building, Banja Luka earthquake of August 13, 1981, $M = 5.7$.

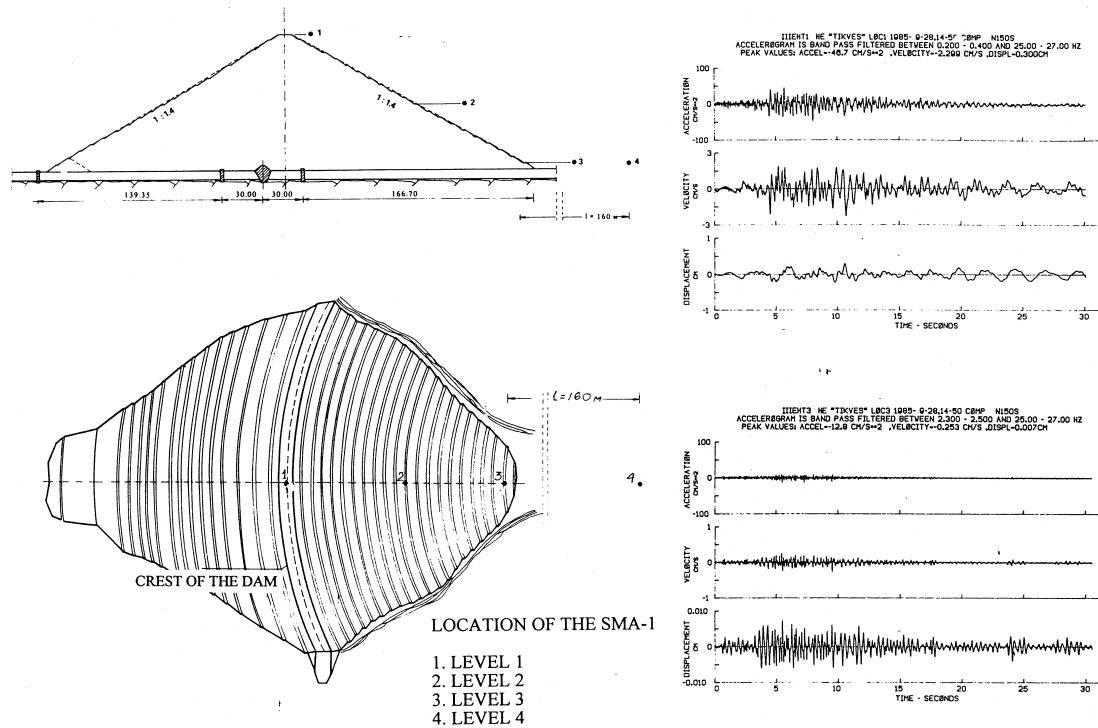


Figure 5: Seismic monitoring on Tikvesh Dam. Negotino Earthquake of Sept. 28, 1985, $M=5.1$

Conclusions

The seismic monitoring of structures is still an actual problem in earthquake engineering. The results from processed earthquake records make a considerable contribution to experimental and analytical studies of the dynamic behaviour of structures. All these contribute, directly, towards optimization of the process of design and construction of aseismic structures.

The existing number of instrumented structures is relatively small, even on world scale. Its increase is necessary by instrumentation of structures, particularly those constructed by the application of newer technologies and methods of design. It is technically and economically justified, since the cost of the instruments, compared to the total investment value of the structures is symbolic.

Data on the ground motion during earthquakes to which structures are exposed and behavior of structures are fundamental for seismic hazard evaluation, definition of design parameters and criteria and for all other dynamic investigations in earthquake engineering. Without such data all investigations and analysis that follow would be based on assumptions.

Significant efforts are required to provide rational protection of structures against seismic effects. Seismic instrumentation is one of the most rational ways of protection.

Instrumentation of structures as part of risk reduction programs is very beneficial, as studies of this type will help to better predict the performance of structures in future earthquakes.

References

- Mihailov, V., D. Petrovski , & T. Kirijas , (1975). "Strong Motion Instrument Network in Yugoslavia " Bulletin No. 1, IZIIS Publication No. 47, Skopje.
- Mihailov, V. (1977). "Strong Motion Instrumentation of Structures", Publication No. 51, IZIIS, Skopje.
- Mihailov, V. (1985). "Yugoslav Strong Motion Network", Physics of the Earth and Planetary Interiors 3:110-122, Elsevier Science Publishers B.. Amsterdam.
- Mihailov, V., Trnkoczy A., (1990). "Installation of Network of Instrument for Recording of induced Seismicity and Dynamics Behavior of Body Dams", Cahiers du Centre Européen de Géodynamique et de Séismologie. Volume 1, pp. 103-112, Walferange, Luxemburg.
- Mihailov, V., Dojcinovski D. & D. Mamucevski (1995). "Seismic monitoring on structures: Some experience and related problem", 10th European conference on Earthquake Engineering. Volume 1, pp. 223-227, Vienna, Austria.
- Mihailov, V., Celebi M. (2001). "Seismic monitoring of structures an important element in seismic hazard mitigation for urban media", Macedonian - US Joint Project Number 126/USGS, Report IZIIS 2001-61, Skopje.

Rupture zones of large earthquakes and seismic potential in the Hellenic Arc and Trench

E. Daskalaki and G.A. Papadopoulos

Institute of Geodynamics, National Observatory of Athens, Greece, edaskal@gein.noa.gr

Abstract

The Hellenic Arc and Trench (HAT) system generates large earthquakes of $M \sim 7.5$. Historical seismicity data indicate that earthquakes of $M \sim 8$ also occur in HAT, like the earthquakes of 21 July 365 and 8 August 1303. They had very large areas of perceptibility and generated catastrophic tsunamis which propagated in remote places of the Mediterranean Sea. The 365 and 1303 events very possibly constitute the maximum earthquake that may rupture the western and eastern segments of HAT, respectively. No other similar events are known to have taken place in the two segments of HAT. This implies that they are of very long return period. To investigate the present seismic potential along the HAT we mapped the lateral distribution of rupture zones of (a) the two big earthquakes, (b) the large earthquakes (M over 7) of the last 400 yrs and (c) the strong earthquakes (M over 6.5) of the last 100 yrs. Our analysis may indicate that the segments ruptured by the 365 and 1303 earthquakes are strongly coupled, failing to rupture by large earthquakes in last centuries, which may imply that big earthquakes are under preparation in the western and eastern HAT segments, respectively.

Introduction

The seismotectonics in the Hellenic Arch and Trench (HAT) is controlled by three main processes (e.g. McKenzie, 1970; LePichon and Angelier, 1979; Papazachos and Papadopoulos, 1979; Jackson and McKenzie, 1988; Reilinger et al., 2006 and references therein): (i) subduction of the African lithosphere from SSW to NNE at mean dip of 35° beneath the Aegean Sea along the overriding southern boundary of Eurasia; (ii) counterclockwise rotation of the African lithosphere relative to Eurasia along the trench at rates of 20-30 mm/yr; (iii) rollback of the subducting lithosphere. The subduction process started at least 13 Myrs BP.

The seismicity is very high along the entire arc, which is dominated by thrust faulting with a NE-SW direction of the axis of maximum compression. A particularly damaging, large ($M \sim 8-8.5$) tsunamigenic earthquake occurred in 365 AD and ruptured the western HAT segment offshore Crete Island. Taking into account that the history of seismicity in this region is fairly known for large-magnitude earthquakes, which can be dated as back as the 5th century B. C., there is no indication that this segment of plate boundary was fully ruptured since 365 AD. Similarly, the eastern

HAT segment was ruptured by the large ($M \sim 8$) tsunamigenic earthquake of 1303 but no such a large earthquake occurred there in most recent times. However, both segments were repeatedly affected by earthquakes of about one order of magnitude less than those of 365 and 1303 (e.g. Papazachos and Papazachou, 1997). Therefore, it is of substantial importance to investigate the repeat times of large earthquakes along the HAT system. This paper is a preliminary approach to that very important goal.

Methodology

The earthquake data used were taken from the instrumental catalogues of the Institute of Geodynamics, National Observatory of Athens (NOA) and the Geophysical Laboratory of the University of Thessaloniki (GLUT). They cover the time interval of the instrumental period from 1910 to 2008. Earthquakes occurring in the historical past before 1910 were taken from the GLUT catalogue revised by the second author on the basis of several publications, the most important being those of Guidoboni et al. (1994) and Guidoboni and Comastri (2005), Papadopoulos et al. (2007, 2009) and Papadopoulos (2009). The list of earthquakes used is available on request.

The HAT seismic events considered in our analysis are only shallow and interplate mainshocks (depth ≤ 60 km) of magnitude $M \geq 6.0$. After testing the data completeness (Fig. 1), we concluded that the catalogue is vastly incomplete before 1600, while from 1600 to 1750 the cut-off magnitude is around $M=7.0$. For the 1750-1909 time interval the cut-off magnitude is $M=6.8$. The earthquake data of the instrumental period, that is from 1910 to 2008, are complete for $M=6.0$.

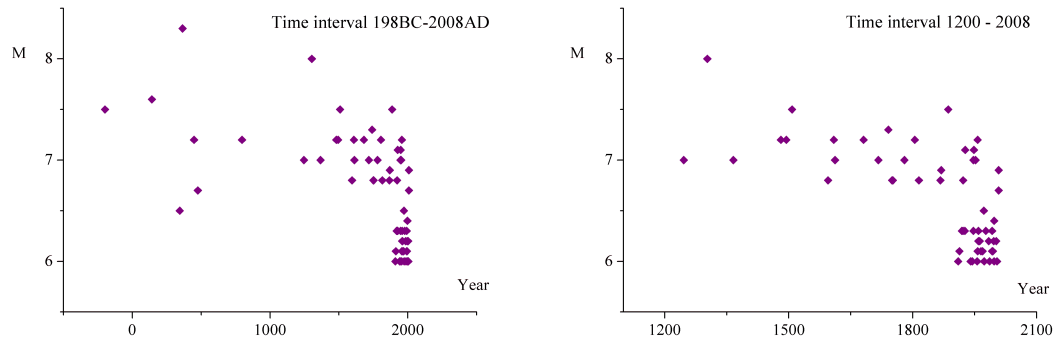


Figure 1. Time plots of the strong ($6.0 \leq M < 6.5$) and large $M \geq 6.5$ earthquakes which occurred in the Hellenic Arc and Trench.

We determined the lateral extension of the seismic rupture zones by assume that their shape is elliptical. To calculate the rupture zone geometry and dimensions we need to know the orientation of the major axis as well as the length, L , and width, W , of the ellipse, which coincide with the lengths of the major and minor axis of the ellipse, respectively. L and W were calculated from the following equations:

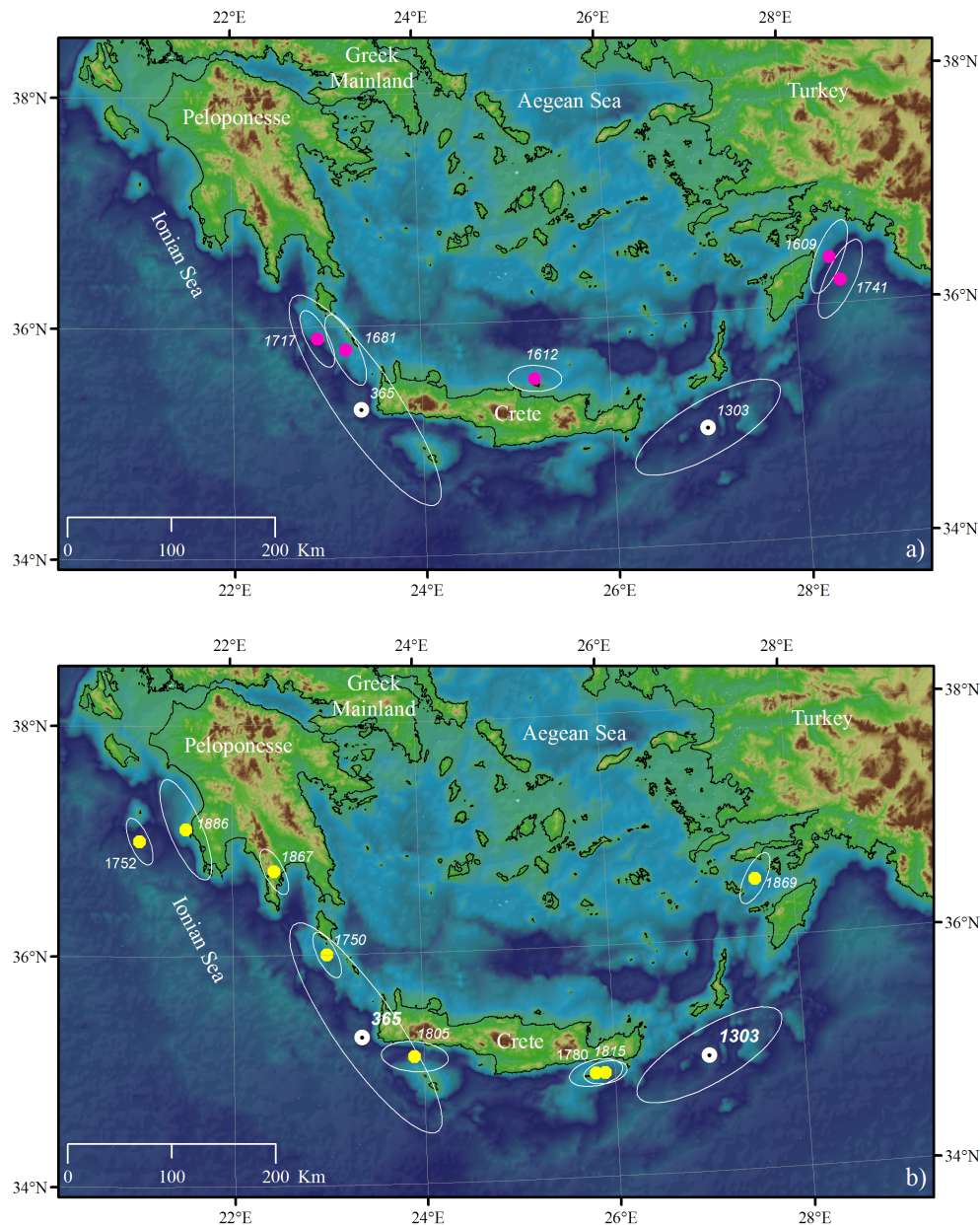
$$\log L = -1.49 + 0.47 M_w \quad (1)$$

$$\log W = -1.07 + 0.34 M_w \quad (2)$$

introduced by Konstantinou et al. (2005) on the basis of the spatial distribution of well-determined aftershock areas of the Mediterranean region, where L is the fault

length and W is the fault width in km; M_w is moment magnitude. The determined lateral extents of rupture zones were plotted in three different maps (Figs. 2a, 2b, 2c) corresponding to the three time periods of different magnitude completeness. Earthquakes of relatively small magnitude ($6.0 \leq M < 6.5$) of the instrumental era are plotted only as dots given that the dimension of their rupture zones are small enough as compared with those of the larger earthquakes. For reasons of comparison in each map we also plot the rupture zones of the 365 and 1303 earthquakes.

One may observe that since 1600 AD only small part of the rupture zones of the big 365 and 1303 earthquakes were ruptured again by strong or large earthquakes. On the contrary, the areas that bound the two big rupture zones were ruptured up until 70's. This indicates that possibly the two rupture zones make seismic gaps where high strain has been accumulated. This working hypothesis should be explored further by different methodologies, such as calculation of the strain accumulation and the degree of lithospheric coupling, as well as statistical and probabilistic approaches.



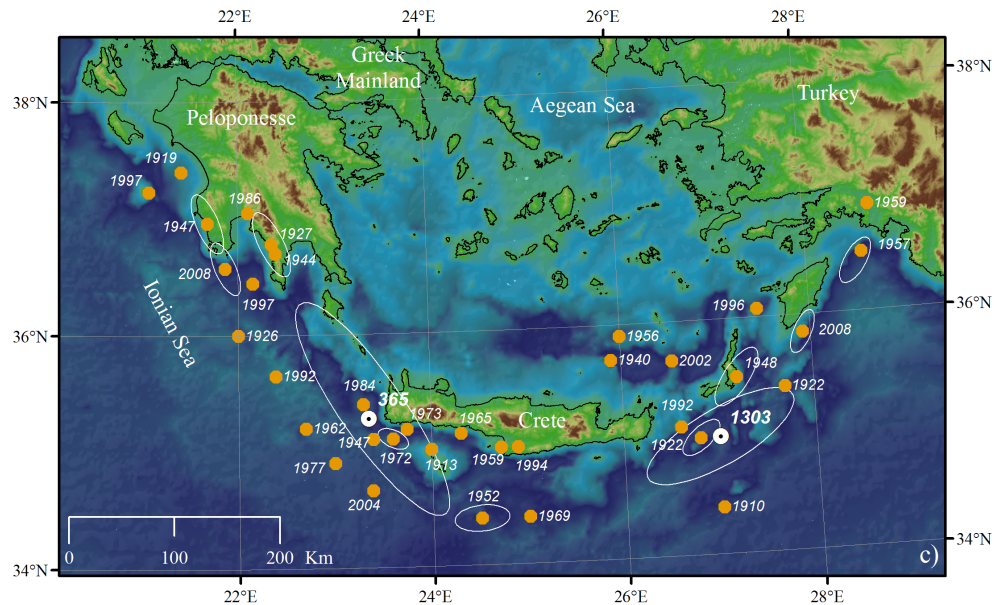


Figure 2. Lateral extent of rupture zones (ellipses) of (a) large earthquakes ($M \geq 7.0$) which occurred in the HAT in the time interval 1600-1750, (b) large earthquakes ($M \geq 6.8$) which occurred in the HAT in the time interval 1750-1909, (c) large earthquakes ($M \geq 6.5$) which occurred in the HAT in the time interval 1910-2008. The epicenters of strong earthquakes ($6.0 \leq M < 6.5$) of the time period (c) are plotted as dots. The rupture zones of the 365 and 1303 large earthquakes are also plotted.

Discussion & Conclusions

In the Hellenic Arc and Trench large earthquakes of $M \sim 8$ occur from time to time, such as the extreme earthquakes of 21 July 365 and 8 August 1303. The 365 earthquake ruptured the western segment while the 1303 earthquake ruptured the eastern segment of HAT. Taking into account that the historical catalog in this region is fairly complete for such magnitude earthquakes, there is no indication that the two segments of plate boundary were ruptured again by big earthquakes in the subsequent time. However, it should be taken into account the rupture zones of those large earthquakes are quite uncertain due to little historical information available.

In addition, the rupture zones of the two large earthquakes were not ruptured by large earthquakes since about 1750 and by strong earthquakes since 1900 if not earlier. However, the areas that bound the two rupture zones were ruptured up until 70's. This indicates that the segments ruptured by the 365 and 1303 earthquakes possibly are strongly coupled failing to rupture by large earthquakes in last centuries, which may imply that large earthquakes are under preparation there.

The repeat of large tsunamigenic seismic events such as those of 365 and 1303 in the future may cause dramatic consequences in many regions of the east Mediterranean Sea. Therefore, there is urgent need to study more systematically the western and eastern HAT segments with the aim to estimate the mean repeat time of such large earthquakes. Of equal importance is also to organize special countermeasures against future large earthquakes and tsunamis regardless the time they may occur.

References

- Jackson, J. and McKenzie, D.P. (1988). The relationship between plate motion and seismic moment tensors, and the rates of active deformation in the Mediterranean and Middle East, *Geophys. J.* 93, 45–73, 1.
- McKenzie, D.P. (1970). Plate tectonics of the Mediterranean region, *Nature* 226, 239–243, 2.
- Guidoboni, E., and Comastri, A. (2005). Catalogue of earthquakes and tsunamis in the Mediterranean area, 11th - 15th century, Istituto Nazionale di Geofisica e Vulcanologia, Rome, 1037.
- Guidoboni, E., Comastri, A., and Traina, G. (1994). Catalogue of ancient earthquakes in the Mediterranean area up to the 10th century, Publications of Istituto Nazionale di Geofisica, Rome, 504.
- Konstantinou K., Papadopoulos G.A., Fokaefs A. & Orfanogiannaki K. (2005). Empirical relationships between aftershock dimensions and magnitude for earthquakes in the Mediterranean Sea region. *Tectonophysics*, 403, 95-115, 3.
- LePichon, X. and Angelier, J. (1979). The Hellenic arc and trench system: A key to the neotectonic evolution of the Eastern Mediterranean area, *Tectonophysics* 60, 1–42, 4.
- LePichon, X., Chamot-Rooke, N. and Lallemand, S. (1995). Geodetic determination of the kinematics of central Greece with respect to Europe: Implications for Eastern Mediterranean tectonics, *J. Geophys. Res.* 100, 12675–12690, 5.
- Papadopoulos, G. A., (2009). A Seismic History of Crete: the central segment of the Hellenic Arc and Trench. *Earthquakes and Tsunamis: 2000 BC – 2008 AD*, Athens.
- Papadopoulos, G. A., Daskalaki, E., Fokaefs, A., and Giraleas, N. (2007). Tsunami Hazard in the Eastern Mediterranean: Strong Earthquakes and Tsunamis in the East Hellenic Arc and Trench System, *Nat. Hazard Earth Sys. Sc.* 7, 57–64.
- Papadopoulos, G. A., Daskalaki, E., Fokaefs, A., and Giraleas, N. (2009) (in press). Tsunami Hazard in the Eastern Mediterranean: Strong Earthquakes and Tsunamis in the West Hellenic Arc and Trench System, *J. of Earthquakes & Tsunamis*.
- Papazachos, B.C. & Papadopoulos, G.A. (1979). Deep tectonic and associated ore deposits in the Aegean area. *Proc. 6th Colloq. Geology Aegean Region*, Athens, Sept. 1977, 3, 1071-1080.
- Papazachos, B.C., Papazachou, C.C. (1997). *The Earthquakes of Greece*, Ziti Publication Co., Thessaloniki, 6.
- Reilinger, R., et al., (2006). GPS constraints on continental deformation in the Africa-Arabia-Eurasia continental collision zone and implications for the dynamics of plate interactions, *J. Geophys. Res.*, 111, B05411, doi: 10.1029/2005JB004051.

Co-seismic stress transfer in northern Africa through 1980-2008

M.S. Boughacha and M. Ouyed

USTHB,FSTGAT, BP 32-16123, Bab-Ezzouar, Algiers, Algeria, m_sboughacha@yahoo.com, mkouyed@yahoo.com

Abstract

In Northern Africa a sequence of nine $M \geq 6$ earthquakes occurred between 1980-2007. We investigate whether this sequence is controlled by the co-seismic stress transfer from one earthquake to the next. We calculate the co-seismic change of Coulomb Failure Stress and find that a fair correlation exists between the location of the events and areas where the previous events induced a positive change of Coulomb Failure Stress. Another map based on the period 1980-2008 indicates that the region of Capital Algiers is located in an area of positive Coulomb Failure Stress due to the combined effect of the El-Asnam earthquake (1980, $M=7.3$, Algeria) and Zemmouri earthquake (2003, $M=6.8$, Algeria).

Key words: Coulomb Failure Function (ΔCFF), Northern Africa, static stress.

Introduction

The hypothesis of earthquake triggering through stress transfer has been investigated for several earthquake sequences in the last decades (King et al., 1994; Nostro et al., 1994; Harris, 1998; Cocco et al., 1999; Stein, 1999; Stein, 2003a,b). The governing idea is based on the fact that earthquakes induce co-seismically stress changes in their surroundings. In terms of Coulomb Failure Stress changes (ΔCFS), positive ΔCFS indicates an enhanced probability of future seismicity whereas sites with negative ΔCFS indicates areas with a decreased probability of future events. Among the prominent papers that put the emphasis on this point of view, in addition to the above-mentioned authors, we can cite Harris et al. (1995), Caskey and Wesnousky (1997), Stein et al. (1997), Papadimitriou et al. (2001), Anderson (2003).

The physical process is based on the Coulomb Failure Function (CFF) (Deng and Sykes, 1997) consisting in a combination of normal and tangential stress calculated on the plane of interest. We are interested in static stress, involving the permanent or co-seismic deformation. As main initiators of this topic, we can refer to Harris, King, Stein. The Landers (King et al., 1994) and the Izmit (Stein et al., 1997) earthquakes played a great part in promoting the idea that an earthquake can trigger another. Nevertheless, it is worth mentioning that the pioneer works on the earthquake

triggering go back to the beginning of the 1980s (Roth, 1988) and the essential of the theory, to the 1960s.

In our study we investigate the triggering hypothesis using an earthquake sequence from the period 1980-2008 in Northern Africa. It refers to the region lying between 34°N-38°N, and 12°W-12°E, which experienced one major event ($M=7.3$), ten strong ($6 \leq M < 7$), and 38 moderate events ($5 \leq M < 6$). The corresponding epicenters are exhibited on Fig. 1.

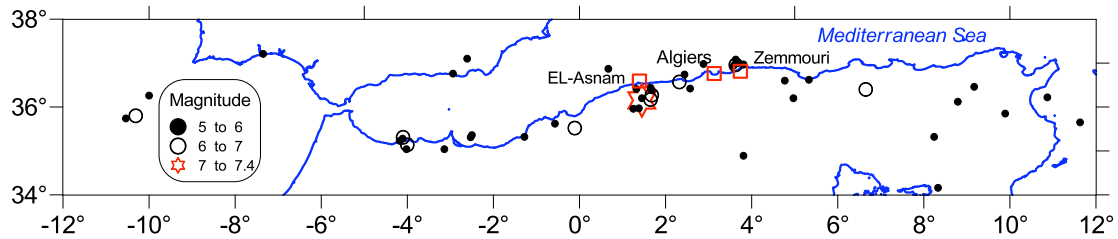


Figure 1: Epicenter map of the earthquakes (1980-2008) used in this study. (Data are from USGS).

Calculation of the Coulomb Failure Function

Stress transfer calculations are based on the work of Okada (1985, 1992). Here, we use the Okada's DC3D subroutine which is on the basis of the computation of displacement and strain fields in a rectangular co-ordinate system attached to the causative fault. The stress tensor is deduced from Hooke's law for a Poisson's solid. Coulomb Failure Function variation is defined as follows: $\Delta CFF = \Delta\tau + \mu' \Delta\sigma$ (King et al., 1994; Deng and Sikes, 1997) where $\Delta\tau$ is the shear stress change resolved on a given receiving plane (assumed positive in the direction of fault slip of the future event); $\Delta\sigma$ is the normal stress change (negative if compressive) on the same plane. μ' is the effective coefficient of friction, usually equal to 0.6 (Deng and Sykes, 1997). Studies of Deng and Sykes (1997) and Ziv and Rubin (2000) conclude that even small values of ΔCFF are meaningful in their role of seismicity triggering.

Date	Lat (°)	Lon (°)	M_w	L (km)	W (km)	ΔU (cm)	Strike (°)	Dip (°)	Rake (°)	Zone
1980 10 10	36.20	1.36	7.3	66	22	173	240	30	105	2
1980 10 10	35.70	1.31	6.2	12	12	30	240	30	105	2
1985 10 27	36.86	6.87	6.0	8	11	22	213	71	-20	3
1989 10 29	36.79	2.45	6.0	8	11	22	240	30	105	2
1994 05 26	35.37	-3.90	6.0	8	11	22	2	84	-10	1
1994 08 18	35.60	0.36	6.0	8	11	22	240	30	105	2
2003 05 21	36.93	3.58	6.8	30	17	78	240	30	105	2
2004 02 24	35.29	-4.00	6.4	16	14	42	2	84	-10	1
2007 02 12	35.90	-10.37	6.0	8	11	22	2	84	-10	1

Table 1: Fault parameters used for calculating ΔCFF .

Fig. 1 and Table 1 show the map of the earthquake sequence and the parameters needed to calculate the co-seismic stress transfer. The calculations of the ΔCFF are made on a horizontal plane at 7 km depth as this is an appropriate mean depth of the earthquake sequence (see Table 1). We use for all $M \geq 6$ events, converting the moment magnitude M_w , the empirical relations of Wells and Coppersmith (1994),

where S and L are respectively the surface and the length of the fault, and ΔU is the dislocation magnitude.

$$\text{Log}_{10}L_{\text{km}} = -3.22 + 0.69 M_w, \text{Log}_{10} S_{\text{km}} = -3.49 + 0.91 M_w, \text{Log}_{10}\Delta U_m = -4.80 + 0.69 M_w$$

We investigate two questions: (1) Are the $M \geq 6$ earthquakes triggered by the sum of the co-seismically induced stress changes? (2) Is the location of events with $5 \leq M < 6$, in relation with the induced ΔCFF ? For this reason, we chose to compute the stress changes on a horizontal plane in order to correlate the epicentres with ΔCFF values. The 7 km depth of this plane may be justified by the fact that the majority of the events in this study are located in Algeria where the mean depth of the earthquakes corresponds to this depth.

ΔCFF Mapping

To determine the ΔCFF values we use the regionalization provided by a regional tectonic model (Pondrelli, 1999) exhibited on Fig. 2: a strike tectonic regime (with a dip component) corresponding to Z1 zone, dominates between 8°W and 0° ; the region extending from 0° to 5°E corresponds to Z2 zone and is characterised by a pure compressive regime; between 5°E to 10°E lies Z3 zone where a strike regime (with a dip component) prevails; beyond 10°E (Z4 zone), it is found a pure compressive regime.

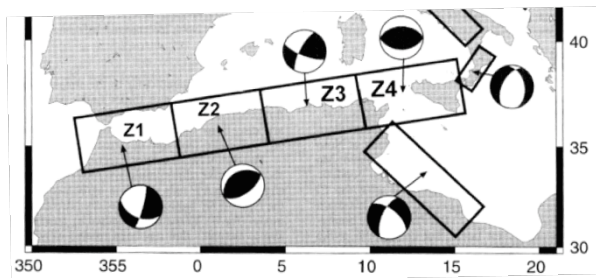


Figure 2: Tectonic model (Pondrelli, 1999) slightly modified, used for calculating ΔCFF .

On the basis of field studies, the ambiguity between nodal planes is removed as follows: the first zone is attributed the El-Hoceima fault parameters (Calvert et al., 1997; Bezzeghoud and Buforn, 1999); the second one is attributed the reverse El-Asnam fault parameters (Ouyed et al., 1983); the third one is attributed those of the Constantine fault (Bounif et al., 1987); the last one is attributed a pure reverse fault with a 270° azimuth (Table 1). In this manner, each zone is attributed a characteristic fault defined by its orientation parameters: strike, dip, slip. For a receiving point pertaining to zone Z_i , the target fault takes the parameters (strike, dip, slip) of the characteristic fault located in Z_i (Table 1); the sources are all the faults where earthquakes occurred, each one having the characteristics of the zone where it is located. They are required strike, dip, slip, length, width, dislocation, depth of upper middle border (Table 1). Exploring the grid, the faults play the role of targets and sources. Values of ΔCFF are cumulated until the day before the subsequent quake. For practical use, ΔCFF mapping needs to be returned into a geographical frame by coordinate transformations. Two maps are produced.

Cumulative ΔCFF maps

The $M \geq 6$ earthquakes are considered as sources. Starting from 1980 (occurrence date of the El-Asnam earthquake, $M=7.3$), and by degrees, the cumulative ΔCFF is

computed at nodes of a horizontal grid of 1x1 km, on a 7 km depth, for the period 1980- *date*. Then a correlation is made between sign of ΔCFF , the location of the $M \geq 6$ event just before *date*, and the subsequent seismicity ($5 \leq M < 6$) occurred between *date* and the occurrence time of the previous $M \geq 6$ event. By cumulating ΔCFF , the process continues with the successive earthquakes, and ends by the action of all events (cumulative effect through 1980-2007). Fig. 3 depicts the results obtained for the different stages.

The examination of each picture reveals that the expected earthquake ($6 \leq M < 7$ labelled with star) and the subsequent seismicity (labelled with open circles) are located in regions where ΔCFF has been enhanced, reinforcing the idea underlying the meaning variations of the Coulomb failure function.

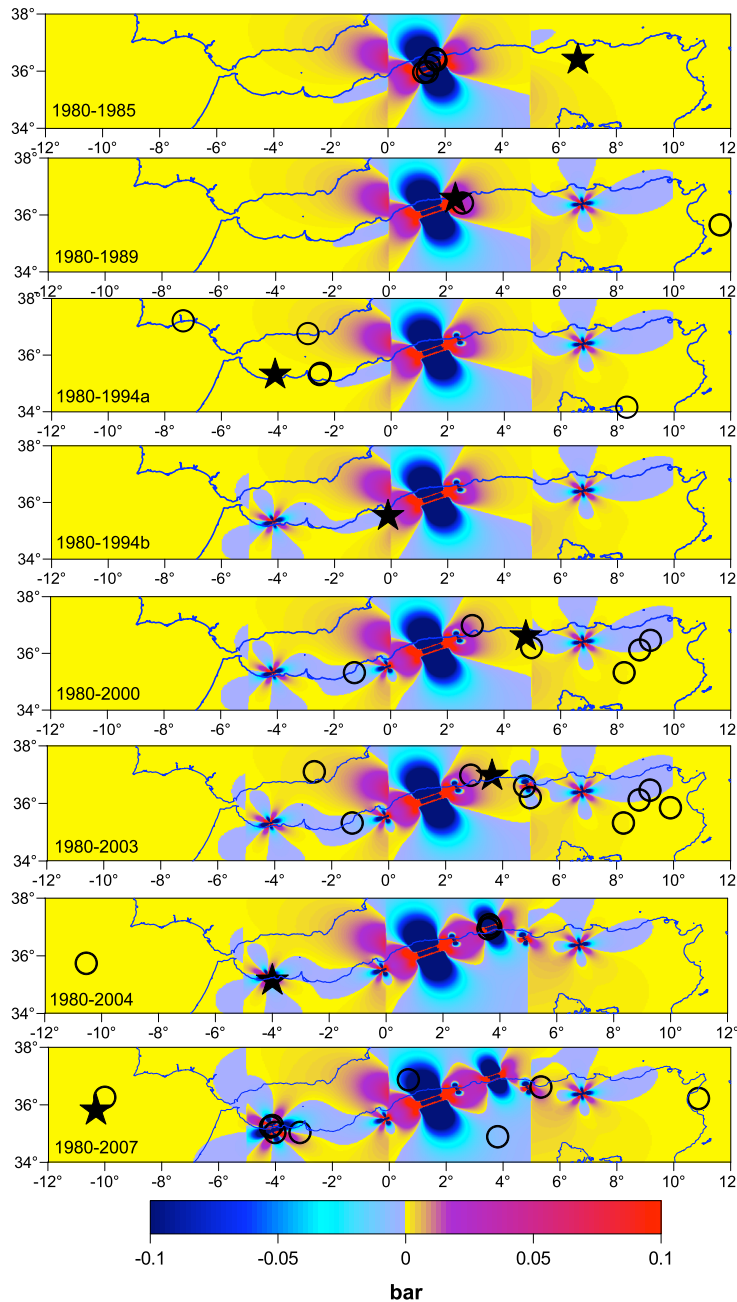


*Figure 3: Pattern of stress transfer illustrated by degrees for the period 1980-2007. The label 1980-*date* refers to the interval time of cumulative ΔCFF from 1980 (occurrence of the $M=7.3$ event) to *date*. Star refers to the event ($6 \leq M < 7$) occurred just before *date*; open circles ($5 \leq M < 6$) refer to the subsequent seismicity (events occurred before *date* and just after the previous one with $M \geq 6$). A fair correlation between $\Delta CFF > 0$ and sites of $M \geq 5$ events may be observed.*

Map foreshadowing the future seismicity

Fig. 4 displays a map of the cumulative values of ΔCFF through 1980-2008, considering all the sources with $M \geq 6$. At first sight, the most prominent aspect of Fig. 4 is that the region of Capital Algiers is located in the area where the combined effect of the El-Asnam earthquake (1980, $M=7.3$, Algeria) and Zemmouri earthquake (2003, $M=6.8$, Algeria) (see Fig. 1 for locations) induced a positive ΔCFF indicating that this area has been brought closer to failure.

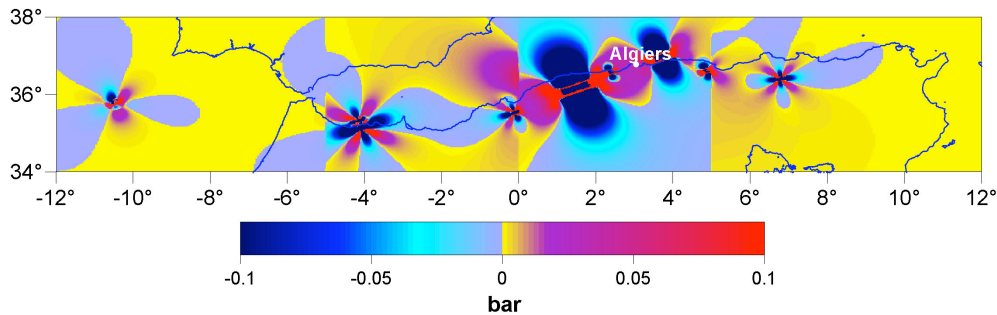


Figure 4: Mapping of cumulative ΔCFF for the period 1980-2008 foreshadowing the future seismicity: regions with $\Delta CFF > 0$ would be the sites of expected seismicity.

Discussion and Conclusions

The results obtained in the present work should be considered prudently. They are strongly controlled by the validity of the formulation underlying the theory, the validity of the tectonic model, and the base line arbitrarily fixed at 1980. The success of the approach or its failure will appear through the observations between the future seismicity and the ΔCFF maps obtained. On the basis of a valid assumption, this issue may lead us to reconsider our perception in seismic hazard assessment. A base line involving the past major earthquakes of the region (like those of 1365, 1716, 1790 occurred in Algeria) and a more refined model involving tectonic loading, should improve the stress pattern of the region.

Acknowledgements

We appreciate the remarks of Dr A. Hubert-Ferrari and Dr O. Heidbach who contributed to improving our manuscript.

References

- Anderson, G.J.C. (2003). Static stress transfer during the 2002 Nenana Mountain Denali Fault, Alaska, earthquake sequence. *Geophysical Research Letters*, 30(6), 1310.
- Bezzeghoud, M., Buforn, E. (1999). Source parameters of the 1992 Melilla, (Spain, $M_w=4.8$), Alhoceima (Morocco, $M_w=5.8$), and 1994 Mascara (Algeria, $M_w=5.7$) earthquakes and seismotectonic implications. *Bull. Seism. Soc. Am.* 89,2, 359-372.

- Bounif, A., Haesler, H., Meghraoui, M. (1987). The Constantine (North Algeria) earthquake of October 27, 1985: surface ruptures and aftershock study. *Earth and Planetary Science Letters*, 85, 451-460.
- Calvert, A., Gomez, F., Seber, D., Barazangi, M., Jabour, N., Ibenbrahim, A., Demnati, A. (1997). An integrated geophysical investigation of recent seismicity in the El-Hoceima region of North Morocco. *Bull. Seism. Soc. Am.*, vol 87, N°3, pp 637-651.
- Caskey, S.J., Wesnousky, S.G. (1997). Static stress changes and earthquake triggering during the 1954 Fairview Peak and Dixie Valley earthquakes, Central Nevada. *Bull. Seism. Soc. Am.* 87, 521-527.
- Cocco, M., King, G.C.P., Nostro, C. (1999). Report for the F.A.U.S.T Project-Fault Interaction Changes. *Recent Advances and New Horizons, Alicante*.
- Deng, J., Sykes, L. R. (1997). Stress evolution in Southern California and triggering of moderate-, small-, and micro-size earthquakes. *J. Geophys. Res.*, 102, 411-435.
- Harris, R.A., Simpson, R.W., Reasenber, P.A. (1995). Influence of static stress on earthquake locations in Southern California. *Nature*, 375.
- Harris, R.A. (1998). Introduction to special section: Stress triggers, stress shadows, and implications for seismic hazard. *Journal of Geophysical Research*, 103, B10, 347-358.
- King, G. C. P., Stein, R., Lin., J. (1994). Static stress change and the triggering of earthquakes. *Bull. Seism. Soc. Am.* 84, 935-953.
- Nostro C., Cocco M., Belardinelli, M. E. (1997). Static stress changes in extensional regimes: an application to Southern Apennines (Italy). *Bull. Seism. Soc. Am.* 87, 234-48.
- Okada, Y. (1985). Surface deformation due to shear and tensile faults in a half-space. *Bull. Seism. Soc. Am.* 75, N°4, 1135-1154.
- Okada, Y. (1992). Internal deformation due to shear and tensile faults in a half-space. *Bull. Seism. Soc. Am.* 82, 1018-1040.
- Ouyed M., Yielding, G., Hatzfeld, D., King, G.C.P. (1983). An aftershock study of the El Asnam (Algeria) earthquake of 1980 October 10. *Geophys. J.R. astr. Soc.*, 73, 605-639.
- Papadimitriou E.E., Karakostas, V.G., Papazachos, B.C. (2001). Rupture zones in the area of the 17.08.99 Izmit (NW Turkey) large earthquake (Mw 7.4) and stress changes caused by its generation. *J. Seismology*, 5, 269-276.
- Pondrelli, S. (1999). Pattern of seismic deformation in the Western Mediterranean. *Annali de Geofisica*, 42, 1, 57-70.
- Roth, F. (1988). Modelling of stress pattern along the western part of the North Anatolian fault. *Tectonophysics*, 152, 215-226.
- Stein, R., Barka, A., Dietrich, J.H. (1997). Progressive failure in the North Anatolian fault since 1939 by earthquake stress triggering. *Geophys J. Int*, 128, 594-604.
- Stein, R. (1999). The role of stress transfer in earthquake occurrence. *Nature* 402, 605-609.

- Stein, R. (2003a). Conversations entre séismes. *Pour la Science*, 26-33, 306, avril 2003.
- Stein, R. (2003b). An Interview with Ross S. Stein, *Special Topics*, December 2003.
- Wells, D.L, Coppersmith, K.J. (1994). New empirical relationships among magnitude, rupture length, rupture area and surface displacement. *Bull. Seism. Soc. Am.*, vol. 84, N°4, 974-1002
- Ziv, A., Rubin, A.M. (2000). Static stress transfer and earthquake triggering: No lower threshold in sight? *J. Geophys. Res.*, 105, 631-642.

Seismicity analysis of Algeria and adjacent regions through 1972-2007

M. Ouyed and M.S. Boughacha

Houari Boumediene University of Sciences and Technology, El Alia, Algiers, Algeria,
mkouyed@yahoo.fr, m_sboughacha@yahoo.com

Abstract

Using USGS catalogue as input data, and ZMAP software (Wyss et al., 2001), we investigate the seismicity pattern of Algeria and adjacent regions between 9°W-12°E and 31°N-38°N through 1972-2007. The catalogue is composed by ~8500 events with a M_c of 2.2. Reasenbergs method of declustering is used in order to remove aftershocks, reducing the number of earthquakes by half. The analysis of the delclustered catalogue shows that the major 1980 El Asnam earthquake ($M=7.3$) may have triggered six $M>5.5$ events within a radius of 300 km.

Introduction

The purpose of this study is to analyze the earthquake catalogue of Algeria and the adjacent regions from 1972 to 2007 using data from the U.S. Geological Survey. The analysis of the catalogue is conducted using the ZMAP code (Wyss et al., 2001) in order to standardize the data.

Seismicity and main structural features of Algeria

Fig. 1 shows the seismicity of Algeria from 1790 to 2000. We can note the absence of seismicity on the Saharan Platform and the High Plateaus, and a moderate to high seismicity in the northern part, on the Tellian Atlas, whereas the Saharan Atlas exhibits low activity. The seismicity clusters observed in the northern part of the map (Fig. 1) correspond to the aftershocks of the largest earthquakes which occurred in the area. We can note that the May 21, 2003 Boumerdes (M_w 6.9) earthquake (represented by a white star on Fig. 1) occurred in an area where very low seismicity was observed.

Seismicity map obtained from the US Geological Survey catalogue

The catalogue of US Geological Survey used in this study contains more than 8500 earthquakes. The corresponding seismicity map and magnitude histogram are represented on Fig. 2 and 3. The seismicity is primarily concentrated in the northern part (Tellian Atlas) and its distribution is comparable with that of the 1790-2000 period (Fig. 1).

We can notice, starting from Fig. 2 that most of the seismicity corresponds to the main earthquakes aftershocks, among which we may cite: El Asnam (October 10, 1980,

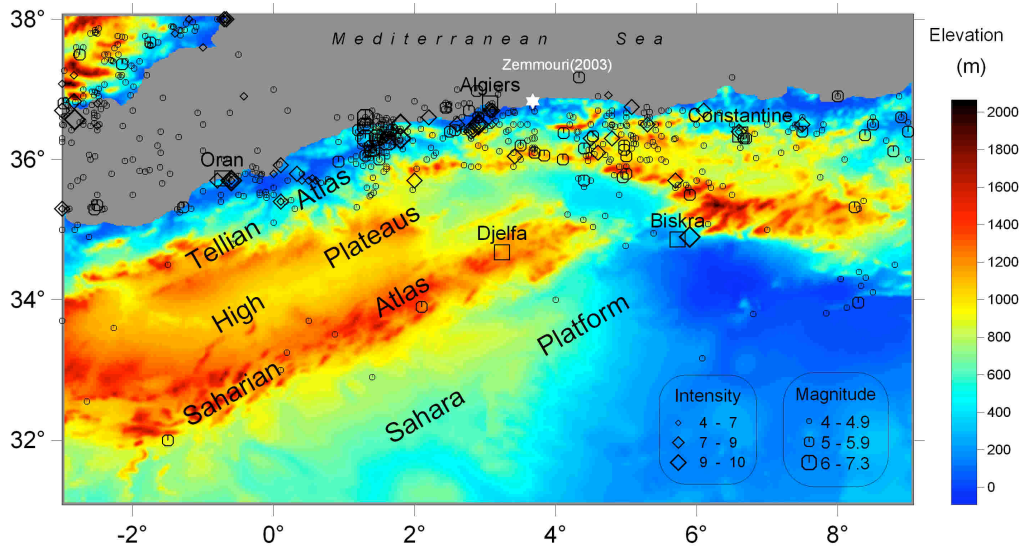


Figure 1: Main structural features and seismicity of Algeria (modified from Boughacha et al., 2003). The white star represents the relocated epicenter of May 21, 2003 Boumerdes earthquake (Bounif et al., 2004). Historical and instrumental epicenters are represented on the map.

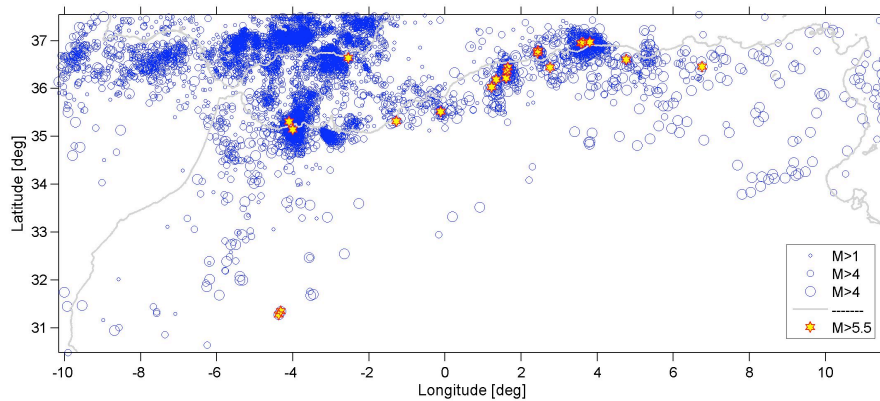


Figure 2: Seismicity map from USGS earthquake catalogue. Earthquakes with $M > 5.5$ are represented by yellow stars.

$M=7.3$, longitude= 1.3°), El Hoceima (February 24, 2004, $M=6.4$, longitude= -4.0°) and Boumerdes (may 21, 2003, $M=6.8$, longitude= 3.6°).

Fig. 2 also shows that the low magnitude earthquakes are especially recorded in the north-western part, and we can assume this is due to the geometry of the seismological stations network, which does not allow the recording of low magnitude earthquakes which occur in the southern and eastern parts of the study area.

Fig. 3 represents the magnitude distribution, which shows for the whole catalogue that the earthquakes of magnitude lower than 2.2 are not all recorded.

Declustering the catalogue

Declustering the catalogue consists in separating the dependent (aftershocks) from the independent seismicity. The procedure uses time and spatial window length versus

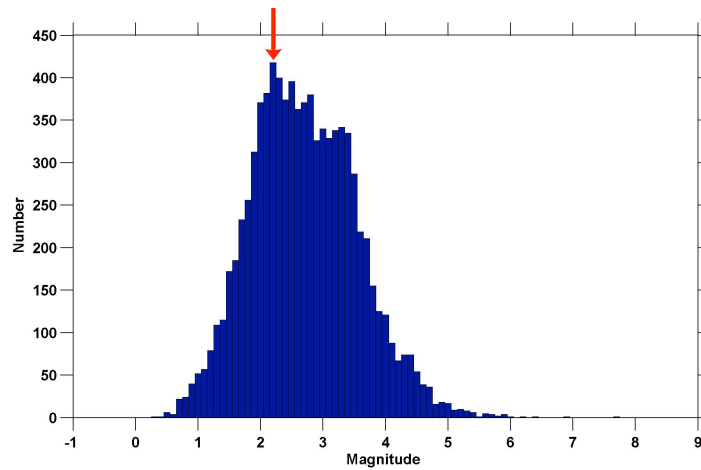


Figure 3: Magnitude histogram of the data. Red arrow indicates the magnitude of completeness computed using ZMAP ($M=2.2$).

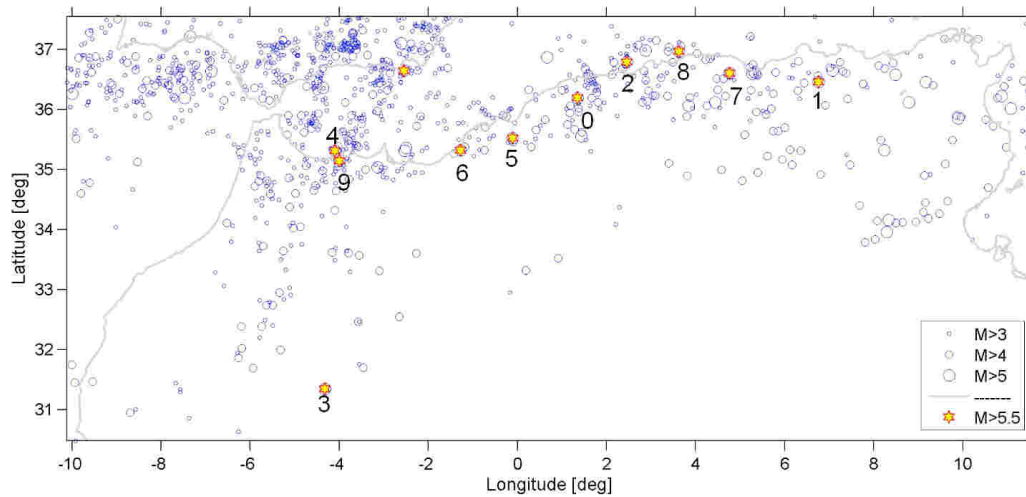


Figure 4: Seismicity map of the declustered catalogue. Main shocks ($M>5.5$) are represented by yellow stars. The numbers correspond to different events classified in the chronological order. The labels 0-9 relate respectively to: El Asnam earthquake (10/10/1980, $M=7.3$), Constantine (27/10/1985, $M=5.9$), Chenoua (29/10/1989, $M=5.9$), Southern Morocco (23/10/1992, $M=5.6$), El Hoceima (26/5/1994, $M=6.0$), Mascara (18/8/1994, $M=5.9$), Ain Temouchent (22/12/1999, $M=5.7$), Beni Ouartilane (10/11/2000, $M=5.8$), Boumerdes (21/10/2003, $M=6.8$), El Hoceima (24/2/2004, $M=6.4$).

magnitude to identify the aftershocks and thus to eliminate them from the earthquake catalogue. The decluster algorithm used in ZMAP is developed by Reasenber (Reasenber, 1985), and the used time and spatial window length versus magnitude curves are those of Gardner and Knopoff (1974). Indeed, these curves are in agreement with the spatial and temporal variations of the aftershocks of the October 1980 El Asnam earthquake (Ouyed et al., 1983). The deletion of the dependent events makes it possible to highlight the faults interaction and to better study the spatial and temporal variations of the seismicity. Fig. 4 represents the map of the declustered earthquake catalogue of magnitude greater or equal to 3, for which only 1100 out of 3400 are regarded as main earthquakes. The threshold magnitude fixed at 3.0 makes it possible to better take into account the seismicity of the eastern part of the study area and thus to standardise the catalogue.

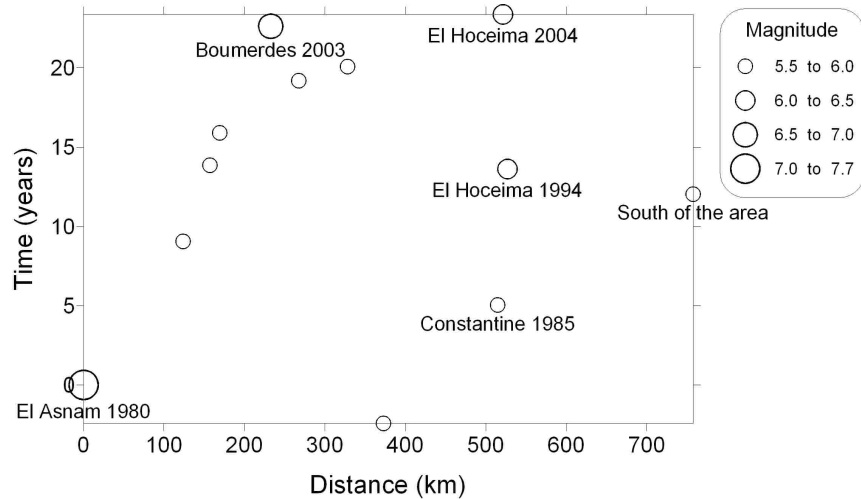


Figure 5: Time elapsed since the El Asnam earthquake according to the distance from each event.

Spatio-Temporal distribution of earthquakes $M > 5.5$

In order to study the interaction effect of the October 10, 1980 El Asnam earthquake ($M_s = 7.3$) with other faults in the region, we identify by numbers (Fig. 4) in a chronological order all earthquakes of magnitude exceeding 5.5. We can assume that the El Asnam earthquake changed the seismicity rate in the region. Indeed, it is recognized that significant variations in seismicity behavior have been observed before and after occurrence of large earthquakes (Papadimitriou et al., 2005; Mantovani et al., 2008).

Fig. 5 represents the time elapsed since the 1980 El Asnam earthquake for each event of magnitude greater than 5.5 versus the distance between the reference earthquake (El Asnam) and each event. We can infer from this graph that the time between each event and the reference earthquake is proportional to the distance when less than 300 km. If we consider that the triggering effect is produced by the post-seismic relaxation induced by the 1980 El Asnam earthquake, then the induced strain-rate peaks move at about 10 km/year. However, earthquakes located at distances greater than 300 km do not appear to be influenced by this phenomenon. Such post-seismic relaxation results from the coupling between a brittle upper crust and a viscoelastic lithosphere (Nur and Mavko, 1974; Rydelek and Sacks, 1990). This feature is also reported by Cenni et al. (2008) concerning the major Northern Apennines earthquakes.

Conclusions

In this study we analysed the USGS earthquake catalogue for Algeria and surrounding regions. The configuration of the worldwide seismic stations does not allow to locate the events of low magnitude. Tests were performed and the obtained threshold magnitude is 3.0, resulting in a uniform database. Declustering the catalogue leads to a file without dependent events, which led us to study the interaction of the El Asnam earthquake with other seismogenic faults. It seems that the $M > 5.5$ earthquakes have been induced by the occurrence of the major 1980 El Asnam event, whereas, those located at distances from the reference event (El Asnam) greater than 300 km were not influenced.

Acknowledgements

We would like to thank Dr. Lauro Chiaraluce for his valuable remarks and suggestions.

References

- Boughacha, M.S., Ouyed, M., Benhallou, H., Djeddi, M., Hatzfeld, D. (2003). Carte de sismicité de l'Algérie de 1790 à 2000. Etude des mécanismes au foyer des principaux séismes en corrélation avec la direction de rapprochement interplaques. *Bull. Serv. Géol. Alg.* Vol. 14 n° 2, 65-77.
- Bounif, A., et al. (2004). The 21 May 2003 Zemmouri (Algeria) earthquake Mw = 6.8: Relocation and aftershocks sequence analysis. *Geophys. Res. Lett.*, 31, L19606, doi:10.1029/2004GL020586.
- Cenni N, Viti M, Baldi P, Mantovani E, Ferrini M, D'Intinosante V, Babbucci D, Albarello D (2008) Short-term (geodetic) and long-term (geological) velocity fields in the Northern Apennines. *Boll Soc Geol Ital* 127(1):93–104.
- Gardner, J. K. and Knopoff, L. (1974). Is the sequence of earthquakes in Southern California, with aftershocks removed, Poissonian?. *Bull. Seism. Soc. Am.* 64, 1363–1367.
- Mantovani, E., Viti, M., Babbucci, D., Albarello, D., Cenni, N., Vannucchi, A. (2008). Long-term earthquake triggering in the Southern and Northern Apennines. *J. Seismol.* doi 10.1007/s10950-008-9141-z.
- Nur A and Mavko G. 1974. Postseismic viscoelastic rebound [J]. *Science*, 183, 204-206.
- Ouyed, M., Yielding, G., Hatzfeld, D. and King, G.C.P. (1983). An aftershock study of the El Asnam (Algeria) earthquake of 1980 October 10, *Geophys. J.R. astr. Soc.* , 73, 605-639.
- Papadimitriou, E., Sourlas, G., and Karakostas, V. (2005). Seismicity variations in the Southern Aegean, Greece, before and after the large (m7.7) 1956 Amorgos earthquake due to evolving stress. *Pure Appl. Geophys.* 162: 783–804. doi 10.1007/s00024-004-2641-z.
- Reasenber, P. A. (1985). Second-order moment of central California seismicity. *J. Geophys. Res.* 90, 5,479–5,495.
- Rydelek P A and Sacks I S. 1990. Asthenospheric viscosity and stress diffusion: A mechanism to explain correlated earthquakes and surface deformation in NE Japan [J]. *Geophys J Int*, 100, 39-58.
- Wyss, M., Wiemer, S. and Zúñiga, R. (2001). Zmap: a tool for analyses of seismicity patterns. Typical applications and uses: a cookbook, 64 pp.

Comparison between seismic hazard assessments using Poisson's and Markov's process - Skopje (Republic of Macedonia) and lower Rhine (Belgium) case studies

Dragi Dojcinovski and Vladimir Mihailov

Institute of Earthquake Engineering and Engineering Seismology, Skopje, R. Macedonia,
dragi@pluto.iziis.ukim.edu.mk, mihailov@pluto.iziis.ukim.edu.mk

Abstract

According to the nature of their occurrence and manifestation upon the surface, earthquakes are very complicated phenomena containing a potential hazard of largescale destruction within a short period of time. The occurrence of earthquakes in space and time belongs to the general category of stochastic processes. Several stochastic processes can be used for probabilistic prediction, i.e. generation of synthetic earthquakes. Most commonly used are: Poisson's model and improved double Poisson's model, equivalent Poisson's model, Markov's model, semi-Markov's chains, Baysov's model and the renewal processes.

In this paper, an attempt is made to present the applicability of the Markov's process as a probabilistic model of earthquake generation. The available data on Skopje epicentral area (one of the seismically most active areas in the Republic of Macedonia) and the earthquakes that have occurred in the Lower Rhine Graben area (Belgium) are examined. The obtained results have been correlated with those previously obtained using the Poisson's model. This provided the possibility for comparison and critical review of the appropriateness and applicability of the Markov's model as a model for earthquake generation.

Introduction

The objective of the presented investigation is to define the applicability and the accuracy of a number of probabilistic models for earthquake generation, their application to and comparison of certain earthquake sources. The most general and most frequently used process is the Poisson's model. It is based on several assumptions according to which the earthquakes are treated as space- and time-independent events, which means that this model does not involve "memory". To overcome this shortcoming, the Poisson's model has been improved into a double Poisson's model (1979), equivalent Poisson's model (1992) and new models like the Markov's (1983), the semi-Markov's chains (1980), the Bayesian model as well as renewal processes have been developed.

In this paper, an attempt is made to test the applicability of the Markov's process as a probabilistic model for earthquake generation. The available data on the Skopje

epicentral area (one of the seismically most active areas in the Republic of Macedonia) and the earthquakes that have occurred in the Lower Rhine Graben area (Belgium) are examined. This way, it was made possible to compare and critically review the appropriateness and applicability of the Markov's model as a model of earthquake generation. According to the nature of their occurrence and manifestation upon the surface, earthquakes are very complicated phenomena containing a potential hazard of large scale destruction within a short period of time.

Poisson and Markov models of seismic occurrences

The recurrence relationship for a given seismic source summarizes the past seismic data in the form of mean number of occurrences per unit of time and source area. To extend or extrapolate this past information into future forecasting, stochastic models are needed.

Assessing future earthquake hazard can be approached through defining an appropriate stochastic model, capable of estimating the probability of occurrence of forthcoming seismic events.

The earthquake occurrences in space and time belong to the general category of stochastic processes. Therefore, some of the stochastic models from the probability theory are used for their modeling. The two most commonly applied stochastic models for generation of the number of earthquake occurrences are the Poisson's and the Markov's models that are quite different one from another in the physical sense.

Poisson's model

A Poisson's process assumes that earthquake occurrences represent processes that are independent of time and space and have no "memory of time".

Once the seismic source regions have been identified, it is assumed that earthquake occurrences on each source form a Poisson process with a mean rate of occurrence independent of magnitude. Earthquake events whose inter arrival times are exponentially distributed are said to follow a Poisson stochastic process. The Poisson model can be written as

$$P_n(t) = \frac{e^{-\lambda t} (\lambda t)^n}{n!}$$

where $P_n(t)$ = Probability of having n events in future time period t ,
 n = number of events,
 λ = mean rate of occurrence.

If λ is independent of time, then the process is called homogeneous. If λ varies with time, the process is called non-homogeneous.

For earthquake events to follow the Poisson model, the following assumptions must be valid:

1. Earthquakes are spatially independent of each other;
2. Earthquakes are temporarily independent of each other;
3. The probability that two seismic events will take place at the same place and at the same instant of time approaches zero.

The first assumption implies that occurrence or non-occurrence of a seismic event at one site does not affect the occurrence or non-occurrence of another seismic event at some other site. The second assumption implies that the seismic events do not have memory in time. The third assumption implies that for a small time interval Δt , no more than one seismic event can occur. This assumption is considered to be realistic and fits the physical phenomenon reasonably well. In spite of many short-comings of the model in terms of its physical interpretation and matching the actual earthquake occurrence phenomenon, this is the most widely used model in the literature.

Markov's model

The Markov's process assumes that earthquake occurrences depend, in a certain sense, on the processes in the past. The main characteristic of the Markov's process is the memory of successive events that is used to describe the dependence of future events on past events, but since the main principles of Markov's processes are generally known they will not be discussed in this paper. Because of the possibility for thorough following of the application of these processes as probabilistic models of earthquake generation, further on will be presented only some of the main, more important formulae used in this study. The Markov's model for the number of earthquakes with a given magnitude in a given time period used in this study is given by the following formula

$$P\{X_I(n\Delta t) \geq 1 | X(0) = 0\} = 1 - P\{X_I(n\Delta t) = 0 | X(0) = 0\} = 1 - (1 - \lambda_I \Delta t)^n \quad (1)$$

where $X_I(n\Delta t)$ is the number of earthquakes exceeding level I in time $t = n\Delta t$, while λ_I is the frequency of earthquake occurrence for each level.

When the events consist of several classified intensity (magnitude) levels, the probability for occurrence of these levels and transition from one level to another can be expressed by application of the Markov's chains.

$$P\{I(n\Delta t) = j | I(0) = i\} = Q_j^n - Q_{j-1}^n, \quad (j > i) \quad (2)$$

$$P\{I(n\Delta t) \leq i | I(0) = i\} = Q_i^n \quad (3)$$

Equation (2) presents the probability for transition from a lower intensity level (Q_{j-1}) to a higher intensity (Q_j), while equation (3) presents the probability that the same intensity level is preserved.

It is important to know the recurrence time and the probability for recurrence of an earthquake below a given level (magnitude or intensity). The probability of recurrence time in $t = n\Delta t$ is represented as follows:

$$f_{ii}^{(n)}(i) = \lambda_i \Delta t (1 - \lambda_i \Delta t)^{n-1} \quad (4)$$

$$f_{ii}^{(n)}(i) = \lambda_i \Delta t (1 - \lambda_i \Delta t)^{n-1} \quad (5)$$

$f_{ii}^{(n)}(s)$ indicates the probability for the return level i for the first time after $t = n\Delta t$ and is defined as a return time probability.

Results from the analysis of Skopje and Lower Rhine graben seismogene areas

The practical applicability of these processes will be presented through the results obtained for the Lower Rhine Graben epicentral area. In the period 1900 - 2006 36 earthquakes with magnitude of $M \geq 3.3$ occurred in the study area (data from web site: www.seismologie.be; and catalogue from Bensberg network: <http://www.seismo.uni-koeln.de/>). Table 1 shows the number of occurred earthquakes per magnitude and the percentage that they cover (from the catalogue). The earthquakes are grouped according to magnitude with an interval of $\Delta M = 0.5$.

Table 1. Number of earthquakes that occurred in the Lower Rhine Graben in the period 1900 – 2006

Magnitude	3.3	3.8	4.3	4.8	5.3	5.8	6.3	Total
Number	14	14	2	3	0	2	1	36
%	38.889	38.889	5.556	8.333	0	5.556	2.778	100

The mean rate of occurrence of earthquakes (λ_0) with $M \geq 3.3$ in the course of 106 years is 0.030/per month. Based on data given in Table 1, obtained is a regression curve presenting the relationship between the Richter magnitude scale and the percentage of earthquakes for which the following relation holds:

$$\ln N = 6.2557 - 0.8354M, \quad (6)$$

where M: Richter magnitude; N: percentage of earthquake occurrence.

From equation (6), the total probability function and the average frequency of occurrence of earthquakes can be computed. This is shown in Table 2 where C_i is the probability as a summarized function of magnitude, whereas λ_I is the frequency of occurrence of earthquakes with intensity exceeding I.

Table 2. Total distribution and average frequency of occurrence of earthquakes

Magnitude	3.3	3.8	4.3	4.8	5.3	5.8	6.3	Total
C_i	0.355	0.228	0.153	0.104	0.072	0.051	0.037	1.0
$\lambda_i = \lambda_0 C_i$	0.0107	0.0068	0.0046	0.0031	0.0022	0.0015	0.0011	0.0300
λ_I	0.0300	0.0194	0.0125	0.0079	0.0048	0.0026	0.0011	

Using the data from Table 2 and substituting in formula (1), one can compute the probability of exceedence of a certain magnitude M, with the Poisson's model and the Markov's model for $\Delta t = 1$ month (Fig. 1a). The probability of exceedence of a certain magnitude in the Markov's model is represented by a blue line, whereas that in the Poisson's model is represented by a black line. The figure clearly shows that earthquakes of different magnitude are characterized by a different probability of exceedence of magnitude when computation is done by different models. Within the framework of the same model, the difference depends on the selected interval Δt . These differences are the smallest for the Markov's and Poisson's model with $\Delta t = 1$ month, whereas these two models approach each other with the increase in magnitude. The difference between the blue and the black line depends on the errors between the

discrete model of the Markov's chains and the continuous model of the Poisson's process. With the increase in Δt from 1 to $\Delta t = 12$ months, there is an increase in the differences between the Poisson's and the Markov's model.

Fig. 1a shows that there is 90% probability that earthquakes with magnitude over 3.3, 3.8, 4.3, 4.8, 5.3 and 5.8 according to the Markov's model will occur at each 7, 13, 19, 30, 57 and 89 years. The black line is representing Poisson's model for the same probability. The difference in the probabilities for Markov's chains and Poisson's process increases with increase of λ and Δt , with greatest difference occurring when $\Delta t=1$ and $M=3.3$. Also it can be noted that the usage of both models results in similar probability estimates for earthquake occurrence for large magnitudes.

Markov's chains are used to calculate the probability of earthquake occurrence with transition from lower to higher magnitude, meaning that greatest probability for occurrence in x years has an earthquake with magnitude M under condition that no earthquake with magnitude $>M$ occurred. The Markov's model could be used to compute the probability of transition from a lower earthquake intensity level toward a higher intensity level. This has been done by using the data from Table 2 and computing equations 2 and 3. The numerical computation of these equations is given in Fig. 1b for time intervals of $\Delta t = 1$ month. The solid lines in the figures show the probability of transition from a lower to a higher intensity level which is given in equation 2. Thus as time period increases the probability for earthquakes with magnitude M is getting smaller and the probability for earthquakes with magnitude $>M$ increases. The probability for occurrence of an earthquake with a magnitude of 5.3 (Fig.1.b) has its maximum in the period of 18.3-25.4 years, and after that it is exceeded by the one for magnitude 5.8. In practice, this means that if one wishes to build a structure with a serviceability period of 18.3 to 25.4 years in Low Rhine Graben area, it will be more economically sound to design it for an earthquake of magnitude 5.3. For each magnitude level, this period is given in Table 3.

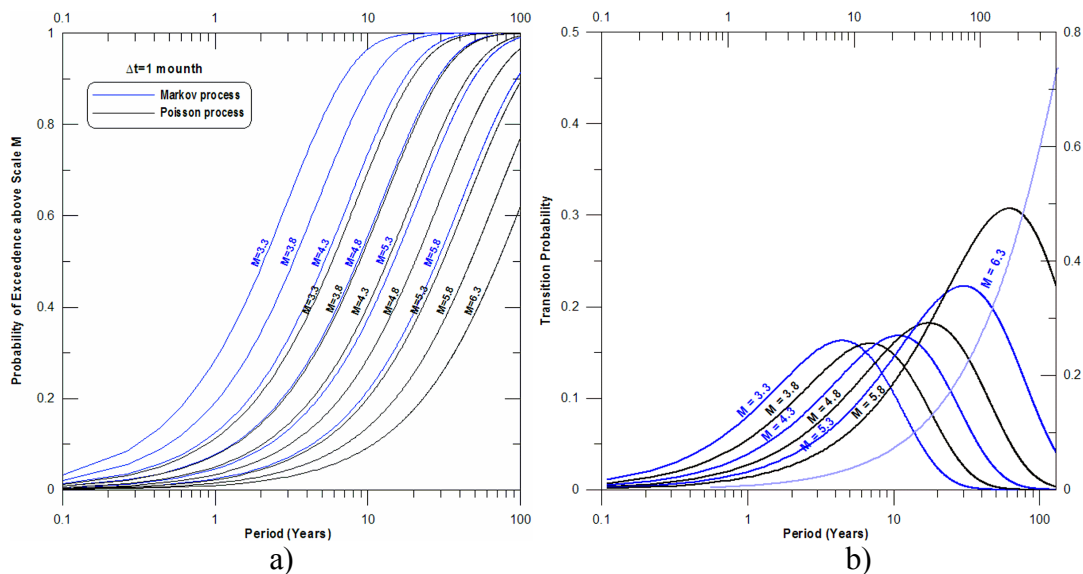


Figure 1: Probability of exceedence and transition probability of earthquake occurrence.

Table 3. Serviceability period of a structure in comparison with a magnitude level

Magnitude	3.3	3.8	4.3	4.8	5.3	5.8	6.3
Economical period	-	5.8years	7.9years	13.5years	18.3years	25.4years	73.1years
	5.8years	7.9years	13.5years	18.3years	25.4years	73.1years	-

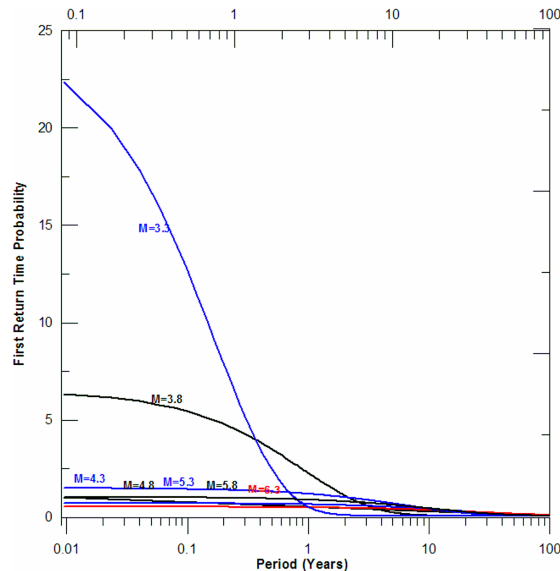
Figure 2: First return time probability of earthquake ($\Delta t=1$ month).

Fig. 2 shows that probability of earthquake occurrence with a magnitude level of 3.3, 3.8, 4.3, 4.8, 5.3, 5.8 and 6.3 will approach 0 after 4, 11, 30, 40, 55, 70 and more than 100 years. This means that an earthquake exceeding the level of 3.3, 3.8, 4.3, 4.8, 5.3, 5.8 and 6.3 will most probably not occur in Low Rhine Graben area after 4, 11, 30, 40, 55, 70 and more than 100 years.

Conclusions

The main objective of this paper is to present another attempt of applying Markov's processes as probabilistic models of earthquake generation. Considered is the Low Rhine Graben epicentral area on which a number of original data exist. The investigations and analyses performed for Low Rhine Graben area were compared with existing analysis made for Skopje region. The results represent a good basis for assessment of the practical applicability of the Markov's model.

On the basis of the obtained results, the following is concluded:

1. The homogeneous Poisson's model is appropriate for seismic hazard assessment for regions characterized by earthquakes of moderate or slight magnitude with a uniform rate of occurrence;
2. The Markov's and the semi-Markov's model describe the occurrence of big rare events - earthquakes of a higher magnitude more realistically than the simple Poisson's model;
3. The probability of occurrence of earthquakes formulated by the Markov's model is closely connected with that of the Poisson's process. When one defines the time interval Δt in the Markov's process precisely, this deviation is minimum, particularly for higher magnitudes;
4. For an area like the Low Rhine Graben where there is no long-lasting accumulation of energy and its abrupt release through earthquakes of large

magnitudes but is released by weaker earthquakes, the probabilistic models of earthquake generation that involve accumulation of energy and time memory (equivalent Poisson's, Markov's and semi-Markov's models) do not have an advantage over the classical Poisson's model.

5. For computation by using the probabilistic models including time, a large number of parameters and seismological data collected in the course of a longer time period are necessary. This is hardly achieved, particularly from the aspect of reliability of parameters. Therefore, the probabilistic computation using the Poisson's model is quite satisfactory for the Low Rhine Graben seismogenic area.

References

- Ashok S. P., R.B.Kulkarni & D.Tocher., (1980). "A Semi-Markov Model for Characterizing Recurrence of Great Earthquakes", *Bulletin of the Seismological Society of America*, vol. 70, no. 1, pp. 323-347.
- Dojcinovski, D., (1995). "Probabilistic Models of Earthquake Generation - Comparative Analysis and Application", Master Thesis, IZIIS, Skopje.
- Kameda H. and Y. Ozaki, (1979). "A renewal Process Model for Use in Seismic Risk Analysis", *Memories of the Faculty of Engineering Kyoto University*, Vol. XLI, Part 1, pp. 11-35, Kyoto.
- Lee V. W., (1992) "On strong- motion uniform risk functional computed from general probability distributions of earthquake recurrence", *Soil Dynamics and Earthquake Engineering*", vol. 11, pp. 357-367, Elsevier Science Publishers Ltd.
- Nishioka T. & H. Shah, (1983). "A Comparison between the Poisson and the Markov processes in modeling seismic occurrences", *Proceeding of review meeting of U.S.-Japan cooperative research on generalized seismic risk analysis and development of a model seismic format*, East-West center, Honolulu.
- Sheldon M. Ross, (1983). "Stochastic processes", University of California, Berkeley, John Wiley & Sons, Inc., USA.

Energy release patterns in aftershock sequences of north Aegean Sea (Greece) through stochastic modeling

D. Gospodinov (1), E. Papadimitriou (2), V. Karakostas (2) and B. Ranguelov (1)

- 1) Geophysical Institute of the Bulgarian Academy of Science, "Akad. G. Bonchev" bl.3, 1113 Sofia, Bulgaria, drago_pld@yahoo.com (Gospodinov, D.), branguelov@gmail.com (Ranguelov, B.)
- 2) Geophysics Department, Aristotle University of Thessaloniki, GR54124 Thessaloniki, Greece, ritsa@geo.auth.gr (Papadimitriou, E.), vkarak@geo.auth.gr (Karakostas, V.)

Abstract

A stochastic model for the study of Benioff strain release during aftershock sequences is suggested. Three datasets are analyzed concerning aftershock sequences in North Aegean Sea, with main shocks of $M_w = 7.2$ in 1981; $M_w = 7.0$ in 1982 and $M_w = 6.8$ in 1983. The stochastic model is elaborated after a compound Poisson process and uses data on which the restricted epidemic type aftershock sequence (RETAS) model was earlier applied. The results reveal that the suggested model makes a good fit of the aftershock Benioff strain release and permits a more detailed study by identifying possible deviations between data and model.

Introduction

Seismic hazard analysis studies usually do not take into account aftershock activity. This tendency is implemented by carrying out different declustering algorithms that remove aftershocks from a catalog. Recently this tendency is replaced by the application of a number of stochastic processes for fitting the clustering behavior of a sequence. Such an approach permits making use of all available information in a seismic catalog and thus aftershock data can in many cases contribute in the detection of anomalous seismicity changes and provide stochastic grounds for seismic hazard analysis (Ogata et al., 2003; Drakatos, 2000).

Researchers oftentimes study the temporal or spatio-temporal relaxation patterns after a strong earthquake by elaborating adequate stochastic models of aftershock occurrences (Ogata, 1988, 1998; Ogata et al., 2003; Gospodinov and Rotondi, 2006). Much fewer papers consider the energy distribution of aftershocks, most often exploring their recurrence law. It is, however, also important to know the aftershock energy release in time. In this study we offer a stochastic process to model Benioff strain in a single sequence. The model is elaborated on the basis of a compound Poisson process based on two main assumptions: a) there is no relation between the magnitude and the occurrence time of an event; b) there is no relation between the magnitude of a certain event and magnitudes of previous events. These assumptions seem reasonable in the lack of a physical theory underlying the relaxation process. We implement the presented stochastic process to model Benioff strain release of three aftershock sequences in North Aegean. Comparison between data and model allows

identifying and interpreting possible deviations thus making possible to explore the aftershock process in more detail.

Methodology

For the development of a Benioff strain release model we apply an analog of a counting process for marked point processes, which is sometimes termed as a mark accumulator process and is defined as follows: let's have a Poisson process $\{N(t) : t \geq 0\}$ with a rate $\lambda > 0$ and suppose that the time T_i of each event is associated to a realization of a random variable Y_i , where $\{Y_n : n > 0\}$ is a family of independent and identically distributed random variables sharing the distribution $G(y) = Pr\{Y_k \leq y\}$. One more requirement is that they have also to be independent of $\{N(t) : t \geq 0\}$, and then the stochastic process

$$Z(t) = \sum_{k=1}^{N(t)} Y_k \quad \text{for } t \geq 0 \quad (1)$$

is said to be a compound Poisson process (Taylor and Karlin, 1984).

If μ and ν^2 are the common mean and variance for the marks Y_1, Y_2, \dots then the moments of $Z(t)$ (mean and variance) are given by:

$$E[Z(t)] = \lambda \mu t \quad (2)$$

$$Var[Z(t)] = \lambda(\nu^2 + \mu^2)t \quad (3)$$

Considering the assumptions made for the elaboration of the compound Poisson process, we see that they coincide with the ones made earlier for the aftershocks' magnitudes. Thus this stochastic process could be used as a model process of random behavior in case a sequence of occurrence times and size of events is to be analyzed.

In the most general treatment of marked point processes $\{N(t) : t \geq 0\}$ is an inhomogeneous Poisson process with an intensity function $\lambda = \lambda(t) : t \geq 0$ and neither the marks $\{Y_n : n > 0\}$ need to form an independent sequence of random variables. Nor it is required for the marks to be independent of the counting process or the occurrence time sequence (Snyder and Miller, 1991).

If we restrict ourselves to consider an inhomogeneous compound Poisson process with a rate $\lambda = \lambda(t)$ then formulae (2) and (3) would be translated into:

$$E[Z(t)] = \mu \int_{t_0}^t \lambda(s) ds \quad (4)$$

$$Var[Z(t)] = (\nu^2 + \mu^2) \int_{t_0}^t \lambda(s) ds \quad (5)$$

following (Snyder and Miller, 1991). The formula (4) mean models the cumulative Benioff strain release and the square root of the variance provides the error bounds.

Formulae (4) and (5) reveal that the intensity function $\lambda = \lambda(t)$ is needed in order to employ the Benioff strain release model. The aftershock intensity decay function is most widely analyzed starting with the Modified Omori Formula (MOF) which

follows the idea that the aftershocks are conditionally independent and follow a nonstationary Poisson process (Utsu, 1970). Multiple strong events and complex aftershock sequences led Ogata (1988) to the formulation of the Epidemic Type Aftershock–Sequence (ETAS) by which each aftershock can trigger its own secondary events.

Gospodinov and Rotondi (2006) proposed the Restricted Epidemic Type Aftershock Sequence (RETAS) model, which is based on the assumption that only aftershocks with magnitudes larger than or equal to a threshold M_{th} can induce secondary seismicity. It has the advantage that it includes the MOF and the ETAS models as limit cases. The conditional intensity function for this model is:

$$\lambda(t | H_t) = \mu + \sum_{\substack{t_i < t \\ M_i \geq M_{th}}} \frac{K_0 e^{\alpha(M_i - M_0)}}{(t - t_i + c)^p} \quad (6)$$

In this equation μ is the background seismicity rate, t_i is the occurrence time of the i^{th} event, p is a coefficient of attenuation, c and K_0 are constants and α measures the effect of magnitude in the production of ‘descendants’. The summation in equation (6) occurs over all events with occurrence times $t_i < t$ and magnitudes $M_i \geq M_{th}$. For the analyzed Aegean aftershock sequences the intensity was assessed by the method of Gospodinov et al. (2007) through the RETAS model and the estimated parameters are presented in Table 1. In the present paper we use the latter results to model the seismic release rate in an aftershock sequence. We have chosen Benioff strain, ε , as a measure of seismic release which is the square root of the seismic energy, and then the cumulative Benioff strain is $\varepsilon(t) = \sum_{i=1}^N \varepsilon_i = \sum_{i=1}^N \sqrt{E_i(t)}$. This measure is particularly useful when smaller events are also considered as in the current case (Tzanis and Vallianatos, 2003). In the above formula $E_i(t)$ is the energy of the i^{th} event and N is the total number of events at time t .

Data and Results

We analyzed data of three aftershock sequences taking place in North Aegean Sea in three successive years, and for which a brief description is given.

NA81, 19 Dec 1981, ($M_w=7.2$). The main shock is associated with a NE–SW right lateral strike–slip fault (Kiritzi et al., 1991) parallel to the orientation of the North Aegean Trough (NAT) (Fig. 1). Analysis is based on a complete catalog of 297 aftershocks with $M_w \geq 3.7$.

NA82, 18 Jan 1982, ($M_w = 7.0$). The main shock is located in the central part of the western branch of the NAT (Fig. 1). The focal mechanism indicates NE–SW striking dextral strike–slip faulting (Kiritzi et al., 1991). We study 158 aftershocks with a cut-off magnitude of $M_\sigma=3.7$, above which the data were assessed to be complete.

NAT83, 6 Aug 1983 ($M_w = 6.8$). The main shock of this sequence took place on a neighboring fault segment of the one associated with the 1982 event, along the NAT (Fig. 1). The dextral strike–slip focal mechanism is similar to the 1982 earthquake

(Kiritzi et al., 1991). The 187 aftershocks which are stronger than the determined magnitude of completeness, $M_0 = 3.8$, are considered for a period of one year after the main earthquake.

<i>Model</i>	M_{th}	<i>AIC</i>	μ	K	α	c	p
		<i>North Aegean 1981; $M=7.2$; $M_0=3.7$</i>					
RETAS (best)	4.4	-376.068	0	0.043	1.759	0.051	1.023
		<i>North Aegean 1982; $M=7.0$; $M_0=3.7$</i>					
RETAS (best)	4.2	-119.535	0	0.046	1.713	0.037	1.049
		<i>North Aegean 1983; $M=6.8$; $M_0=3.8$</i>					
ETAS (best)	3.8	-208.244	0	0.0181	2.270	0.071	1.145

Table 1. RETAS model parameters (see formula (6)) taken from Gospodinov et al. (2007)

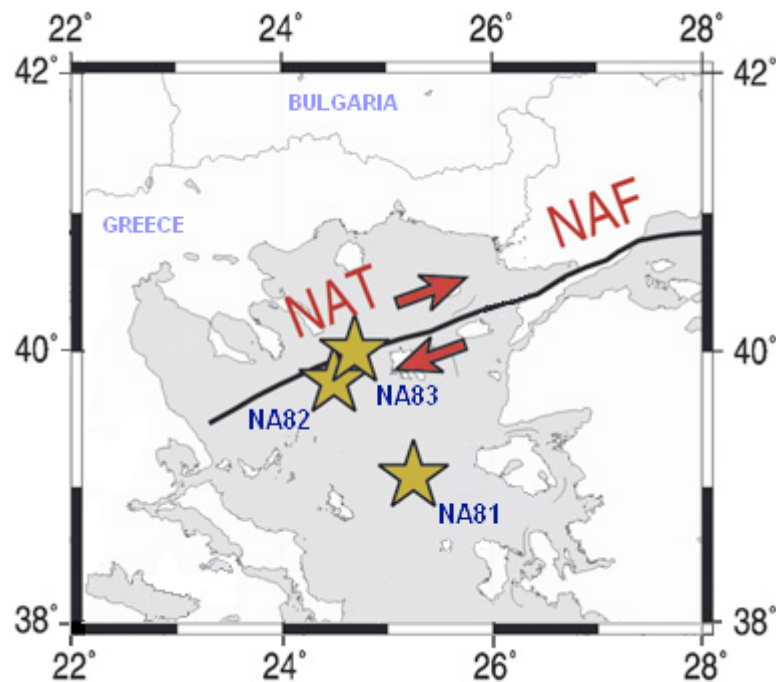


Figure 1. Epicenters of the main shocks in the Aegean Sea (stars) whose aftershock sequences are analyzed in this paper: NA81 – North Aegean seismic sequence, 19 December 1981; $M_w=7.2$; NA82 – North Aegean seismic sequence, 18 January 1982; $M_w=7.0$; NA83 – North Aegean seismic sequence, 6 August 1983; $M_w=6.8$.

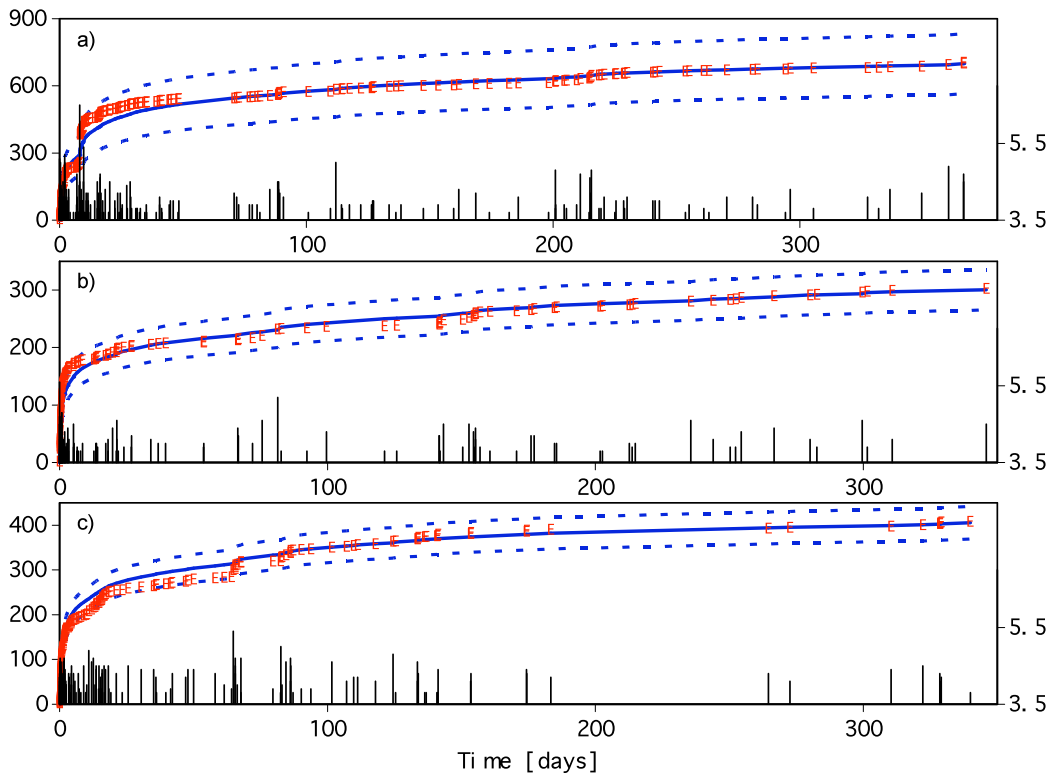


Figure 2. Cumulative Benioff strain as a function of time for the three sequences. Values are normalized to the one of the weakest aftershock in each sample $\varepsilon_i = 10^{(0.75(M_i - M_0))}$. Blue thick line stands for the estimated model values following formula (4), dashed lines are the error bounds by formula (5) and red circles reveal the real cumulative Benioff strain, released in each sequence: a) NA81; b) NA82; c) NA83.

In fact we analyzed the same data which was examined by Gospodinov et al. (2007) through the RETAS model and we used the intensity parameters $\lambda = \lambda(t)$ presented in Table 1 to model stochastically Benioff strain release in each sequence.

The results are presented graphically in Fig. 2. The thick blue line corresponds to the calculated cumulative Benioff strain model after formula (4) with the referent error bounds (dashed lines) and the red circles denote the real Benioff strain released by the aftershocks. As can be seen, the presented stochastic model allows identifying relative deviations of real data. The strongest $M_w 6.5$ aftershock (eight days after the main shock) in the 1981 sequence (Fig. 2a) is preceded by a six days period of decreased strain release while after this aftershock an increased release rate is observed for about 30 days. For the 1982 sequence (Fig. 2b) the relative increase in Benioff strain release starts after the main shock and continues for about 8 days after which model and data fit very well. A relative rate decrease of about 50 days precedes the strongest $M_w 5.4$ aftershock of the 1983 sequence; its occurrence time is about 65 days after the main shock (Fig. 2c).

Altogether the proposed stochastic model makes a good fit of aftershock Benioff strain release; Fig. 2 evidences that real values are in between the model error bounds nearly for the total periods of investigation of the three sequences. These results support the initial suggestions, which were made about the Benioff strain release

process: no relation between magnitudes and the corresponding occurrence times; no relation between magnitudes of different aftershocks. There are some deviations between data and model, however, and they allow a more detailed view of Benioff strain release by relating them to specific strong aftershocks. For two of the sequences (NA81 and NA83), an ‘energy release quiescence’ is observed before the strongest aftershocks. The outcomes from this analysis reveal that the proposed stochastic process can successfully be applied to model aftershock Benioff strain release and to study some of its specific features in time.

References

- Drakatos, G., (2000). Relative seismic quiescence before large aftershocks. *Pure Appl. Geophys.* 157, 1407–1421.
- Gospodinov, D. and Rotondi, R., (2006). Statistical analysis of triggered seismicity in the Kresna Region of SW Bulgaria (1904) and the Umbria–Marche Region of Central Italy (1997). *Pure Appl. Geophys.* 163, 1597–1615.
- Gospodinov D., Papadimitriou E., Karakostas V. and Ranguelov, B., (2007), Analysis of relaxation temporal patterns in Greece through the RETAS model approach, *Phys. Earth Planet. Inter.*, 165/3-4, pp 158-175, doi: 10.1016/j.pepi.2007.09.001
- Kiratzi, A., Wagner, G. and Langston, C., (1991). Source parameters of some large earthquakes in northern Aegean determined by body waveform inversion. *Pure Appl. Geophys.* 135, 515–527.
- Ogata, Y., (1988). Statistical models for earthquake occurrences and residual analysis for point processes. *J. Am. Stat. Assoc.* 83, 9–27.
- Ogata, Y., (1998). Space–time point–process models for earthquake occurrences. *Ann. Inst. Stat. Math.* 50, 379–402.
- Ogata, Y., Jones, L. M. and Toda, S., (2003). When and where the aftershock activity was depressed: contrasting decay patterns of the proximate large earthquakes in southern California. *J. Geophys. Res.* 108, 2318, doi:10.1029/2002JB002009.
- Snyder, D. and Miller, M., (1991). *Random point processes in time and space*: Springer–Verlag, 481 pp.
- Taylor, H. and Karlin, S., (1984). *An introduction to stochastic modeling*: Academic Press, Inc., 399 pp.
- Tzanis, A. and Vallianatos, F., (2003) . Distributed power-law seismicity changes and crustal deformation in the SW Hellenic arc, *Natural Hazards and Earth System Sciences*, 3, 179-198.
- Utsu, T., (1970). Aftershocks and earthquake statistics (II): further investigation of aftershocks and other earthquake sequences based on a new classification of earthquake sequences. *J. Fac. Sci., Hokkaido Univ., Ser. VII (Geophys.)* 3, 198–266.

Seismicity patterns in Vrancea region as revealed by revised historical and instrumental catalogues

M. Popa, M. Radulian, N. Mandrescu and D. Paulescu

National Institute for Earth Physics, Magurele, Romania, mihaela@infp.ro

Abstract

Seismicity patterns characteristic for the Vrancea intermediate-depth source are investigated on a revised catalog spanning one hundred years. Clustering and alignments seem to be stationary and to reflect the structural and rheological inhomogeneities in the high-velocity descending lithosphere. They seem also to be genetically linked to the triggering process of the major shocks that close the seismic cycles. Almost 2D shearing zones are emphasized with significant changes in two active segments located in the upper and respectively lower part of the slab. Apparently, successive major earthquakes occur alternatively in one segment after the other, and the preparation process is like an accelerating type in the lower segment, while decelerating type in the upper segment.

Introduction

The south-eastern extremity of the Carpathians, located in the Vrancea region (Romania), where the mountain chain suddenly turn to the west, looks like the last remaining seismic active area along the entire Carpathians belt. The seismicity is enhanced in the intermediate-depth interval (60 – 180 km depth), with an average of 3 events/century of magnitude greater than 7, localized in a confined volume, in striking contrast with the rest of the Carpathians. Hypothetically, the lithospheric fragment going down nearly vertically into the asthenosphere is the result of a complex continental collision setting, implying detachment, break-off and/or gravitational instability (e.g., Cloetingh et al., 2004).

The main goal of the present paper is to identify characteristic seismicity patterns in the Vrancea seismogenic zone and to test their stationarity, making use of all available information. To this aim, we consider multiple data sets, including modern instrumental data, as well as historical data. In our view, the refined monitoring of the seismicity patterns specific for the current seismic activity is a key issue for understanding the earthquake process in Vrancea, since the background seismicity is controlling the generation of the major shocks and implicitly, can be a good indicator for the seismic cycle history and for future prognosis.

Vrancea seismic cycles

We consider the catalog of Vrancea intermediate-depth earthquakes ($h > 60$ km) occurred since the beginning of 20th century. In order to enlarge as much as possible

the working database, all the available information from historical macroseismic and recent instrumental data are combined in a new updated catalogue.

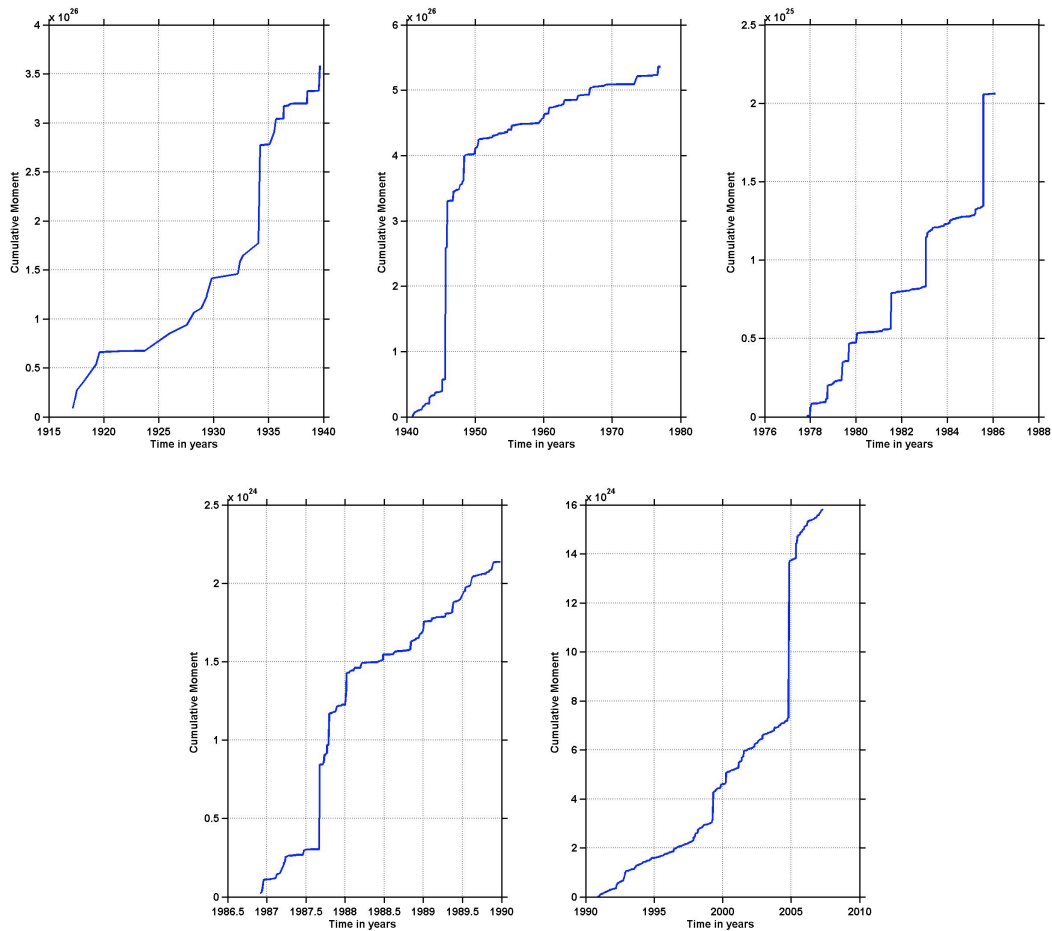


Figure 1. Cumulative seismic moment (in $\text{dyn}\cdot\text{cm}$) curves for successive seismic cycles in Vrancea: a) 1908 – 1940; b) 1940 – 1977; c) 1977 – 1986; d) 1986 – 1990; e) 1990 – present. Associated major shocks are: 10 November 1940 ($M_w = 7.7$, $h = 150$ km), 4 March 1977 ($M_w = 7.4$, $h = 100$ km), 30 August 1986 ($M_w = 7.1$, $h = 131$ km), 30 May 1990 ($M_w = 6.9$, $h = 90$ km). They were alternatively generated in the lower (1940, 1986) and upper (1977, 1990) active segments. Cumulative seismic moment variation is represented only for the intervals between the main shocks (the seismic moment releases for the major shocks are removed).

Characteristic shocks with magnitude $M_w > 6.5$ are generated sequentially in cycles of a few years to a few tens of years at the scale of the entire seismogenic zone. Five completed cycles are identified for our dataset besides the present ongoing cycle, started after the 1990 event (Fig. 1). However, we identify two rather distinct clusters of activity, one in the upper part of the slab (80 – 90 km depth), the other in the lower part of the slab (130 – 150 km depth), separated by a sort of transition zone (100 – 120 km depth). Each segment generates its own characteristic events: 4 March 1977 ($M_w = 7.4$, $h = 100$ km), 30 May 1990 ($M_w = 6.9$, $h = 90$ km) in the upper segment, 16 October 1908 ($M_w = 7.1$, $h = 125$ km), 10 November 1940 ($M_w = 7.7$, $h = 150$ km), 30 August 1986 ($M_w = 7.1$, $h = 131$ km) in the lower segment. As for the transition zone, there is no event with magnitude above 5 recorded during the considered time interval. If we assume that the seismic cycles develop separately for the two segments,

the cycle duration extends between 13 years (upper segment, March 1977 to May 1990) and 46 years (lower segment, November 1940 to August 1986).

Seismicity clustering patterns

The investigation of the high-resolution hypocenter distribution, as obtained using the most recent data (1982 – 2008), shows clear clustering properties and specific alignments in the background seismicity. We consider in our analysis the events relocated using Hypo-DD algorithm (Waldhauser and Beroza, 2000). The earthquake generation process and associated deformation release develop along roughly parallel and close to vertical alignments oriented NE-SW (Fig. 2). The representation on two perpendicular cross sections (Fig. 3) shows configurations for the seismogenic volume close to a 2D geometry. The dipping trend in the upper slab (60 – 90 km) looks like a prolongation of a dipping trend in the crust, although subcrustal seismicity is mostly decoupled from the crustal seismicity. After an alteration around 100 km depth, the dipping trend is continuing in the lower slab (110 – 160 km) closer to vertical.

It is not possible to explain such alignment by simple brittle failure in the high-velocity body going down gravitationally. Weakening processes creating shear zones at larger scale are likely to be triggered in the specific conditions of the subducting slab. One possible mechanism could be the progressively self-localizing thermal runaway (John et al., 2009) which enables the rocks to fail at differential stresses lower than those required for brittle failure.

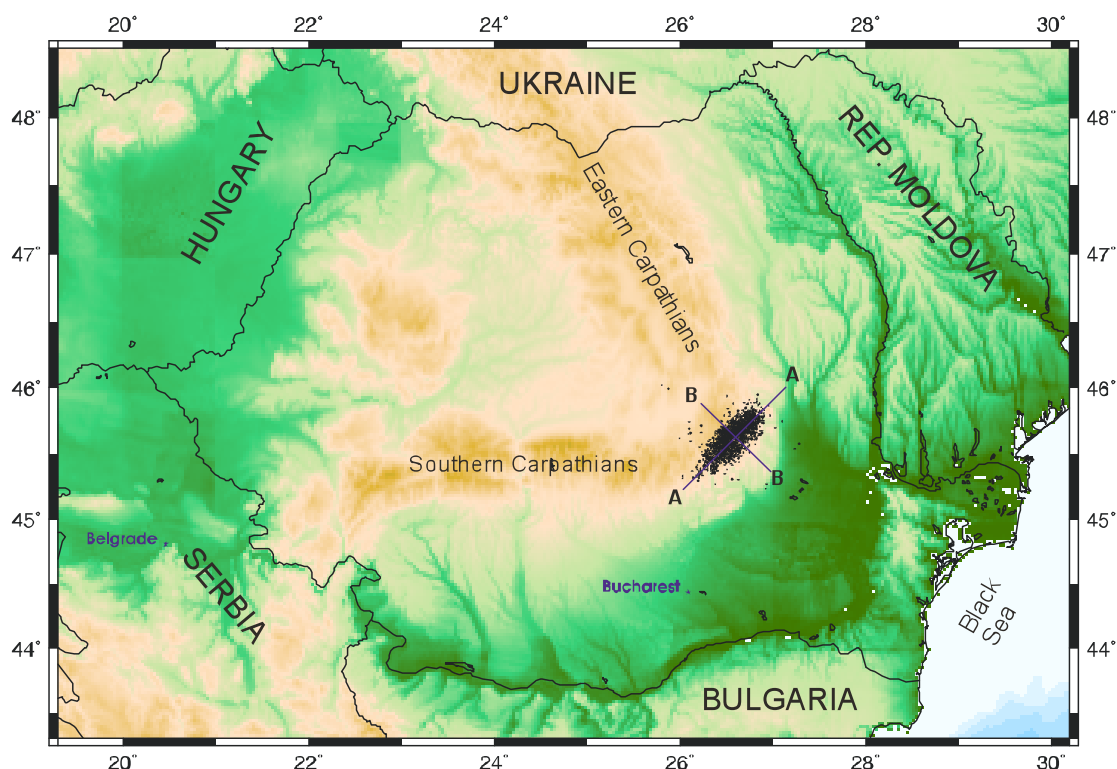


Figure 2. The epicentral distribution of the Vrancea intermediate-depth events. The position of the two cross section planes of Figure 3 is also plotted.

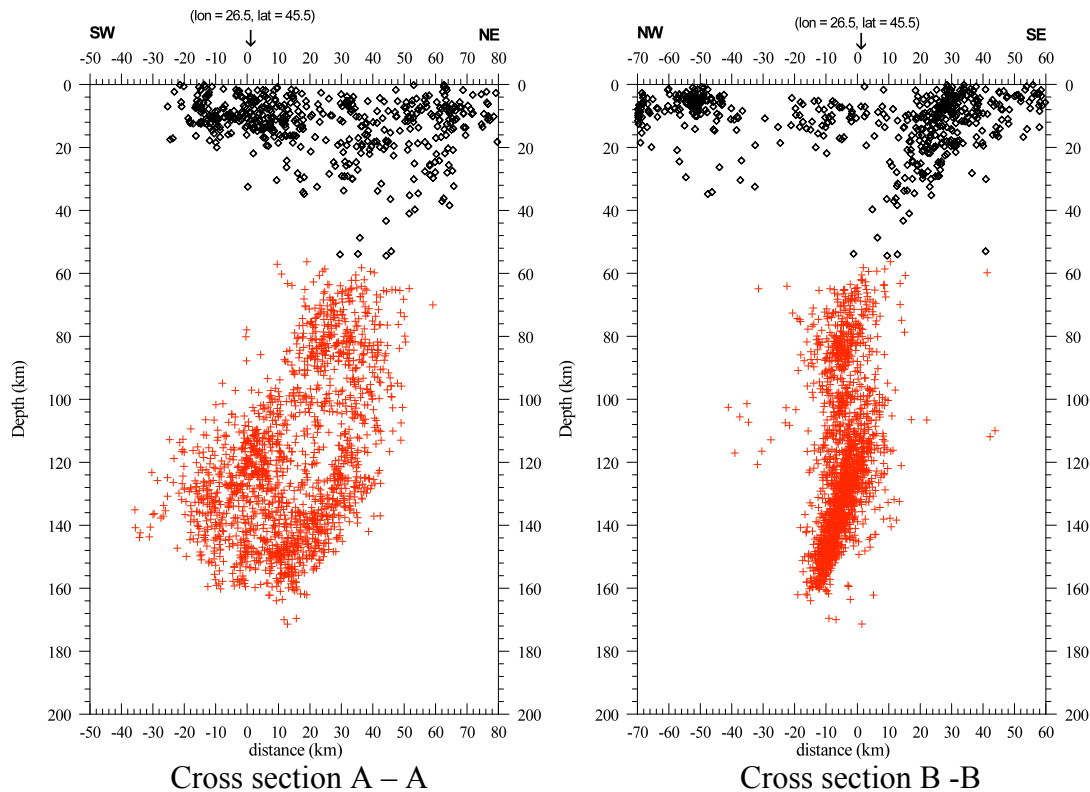


Figure 3. Seismicity distribution projected onto two vertical sections across Vrancea region.

Refined background seismicity patterns are supposed to correlate with significant inhomogeneities in structural and rheological properties within the focal volume, as well as with the major shocks nucleation. The decoupling from crustal seismicity is obvious, as well as the sharp cut-off below about 170 km depth. Well-resolved areas of seismicity increase and deficit are identified inside the subducted slab. Two segments of enhanced seismic activity are visible, one in the upper part (centred around 80 km), the other in the lower part (centred around 140 km), which are associated with the asperities where the major shocks are generated (Fig. 4). The rate of earthquake occurrence is by a factor of 5 higher in the bottom part of the slab than in the top of it. Seismicity patterns mimic surprisingly well the tomography image resulted from local earthquake data (Zaharia et al., 2009).

Properties and implications

Any particular seismicity clustering is reproduced for any time window extracted from the database extent, spending the last 30 years, for which we have relatively good-quality instrumental data. Despite the very limited time scale extension of our analysis, we can tentatively suppose the existence of a stationary process of generating earthquakes in Vrancea. This is a strong statement that implies a crucial outcome for both geodynamic modeling and seismic hazard assessment: the structure in Fig. 4 is stationary (for example, one consequence would be that the low seismicity interval around 110 km depth will never be ruptured by a major shock and consequently, there will be no mega earthquake to develop over the entire seismogenic area, from 60 to 170 km depth).

Another important aspect refers to the triggering of major shocks ending the seismic cycles. They are generated alternatively in the lower segment (~ 140 km) and in the upper segment (~ 80 km) by rupturing persistent major asperities. One striking feature of the seismicity in Vrancea is the rapid healing process which explains both the generation of repeated events during the cycle and the apparently fixed position of the major asperities in each active segment from one cycle to the other. Again the time scale is too small to reach a firm conclusion. The healing process is higher at the bottom than at the top of the seismogenic body, taking into account the significant increase of the foci density at the bottom edge.

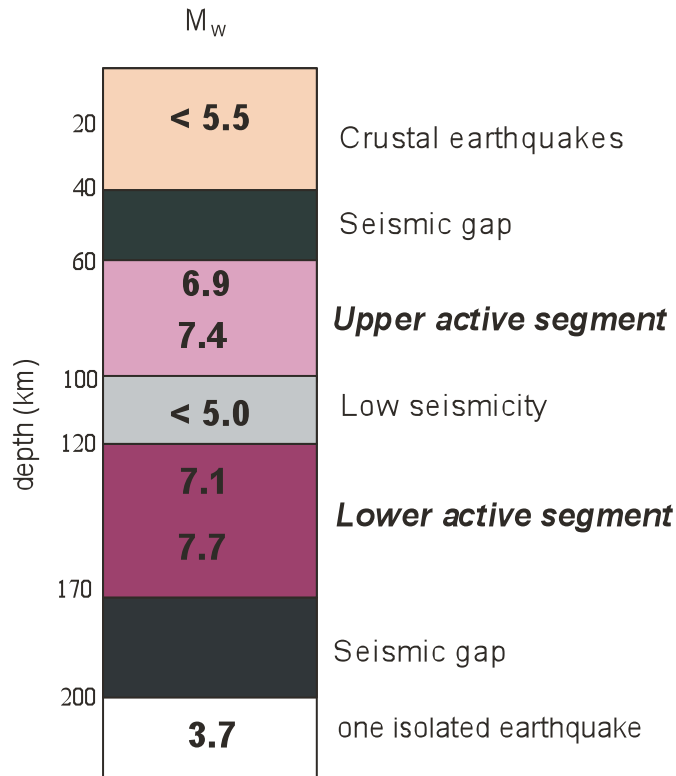


Figure 4. Seismicity distribution on depth in the Vrancea region.

The cumulative seismic moment release, as shown in Fig. 1, looks like of accelerating type in the lower segment, while decelerating type in the upper segment. If this result proves to be statistically significant, it points out a qualitative difference between the intimate mechanisms governing the accumulation and release of deformation in the two active segments.

These features emphasized at the seismic cycle scale, based on a catalogue over one hundred years including instrumental and historical data, are critical for modelling the earthquake process in the Vrancea region. Since they are based on a limited time interval, it is risky to apply them for multiple cycles as long-term features. Hence, the re-evaluation of all available historical data for a time interval extended to several centuries is of highest interest.

References

- Cloetingh, S.A.P.L., Burov, E., Matenco, L., Toussaint, G., Bertotti, G., Andriessen, P.A.M., Wortel, M.J.R., Spakman, W., Thermo-mechanical controls on the mode of continental collision in the SE Carpathians (Romania). *Earth and Planetary Science Letters* 218, 57–76, 2004.
- John, T., Medvedev, S., Rüpke, L. H., Andersen, T. B., Podladchikov, Y. Y., Austrheim, H., Generation of intermediate-depth earthquakes by self-localizing thermal runaway, *Nature Geoscience* 2, 137-140, 2009.
- Waldhauser, F., Ellsworth, W.L., A double-difference earthquake location algorithm: method an application to the northern Hayward Fault, California, *Bull. Seism. Soc. Am.* 80, 1548-1368, 2000.
- Zaharia, B., Enescu, B., Radulian, M., Popa, M., Koulakov, I., Parolai, S., Determination of the lithospheric structure from Carpathians arc bend using local data, *Romanian Reports in Physics*, 2009 (in print).

Crustal seismicity and associated fault systems in Romania

V. Raileanu (1), C. Dinu (2), L. Ardeleanu (1), V. Diaconescu (2), E. Popescu (1), A. Bala (1)

- 1) National Institute for Earth Physics, Bucharest, Romania, email: raivic@infp.ro
- 2) University of Bucharest, Bucharest, Romania, email: cdinu@gg.unibuc.ro

Abstract

A summary on the crustal seismic activity beneath the Romanian territory is presented pointing out both the main seismogenic zones and the most significant events known from historical archives and instrumental records. The observed crustal seismicity did not exceed $M_w 5.6$ excepting the Fagaras area ($M_w \leq 6.5$). For each crustal seismogenic zone the main fault systems which can account for the local seismicity are inventoried.

Introduction

The Romanian territory comprises both platforms and orogen units: W margin of the East European (Moldavian) platform, Scythian and Moesian platforms, Eastern, Southern and Western (Apuseni Mountains) Carpathians orogen, North Dobrogea orogen, foredeep of Eastern and Southern Carpathians, Transylvania depression and E margin of Pannonian depression. The contacts between the tectonic units are along crustal fractures, many of them being seismogenic. On the platforms a sedimentary cover with a variable thickness from a few hundred meters to 10 km or more overlies the crystalline basement. The platform areas are overridden by the external units of the Carpathians resulting in sinking of platform basement underneath the orogen along some faults parallel to the Carpathians. Other crustal fractures transverse to the Carpathians have created a fragmentary structure with fault blocks, Fig. 1 (Sandulescu, 1984). Many of the crustal fractures have proven to generate a low to moderate seismicity, Fig. 2.

The crustal seismicity in Romania did not exceed $M_w 5.6$ excepting the Fagaras zone ($M_w \leq 6.5$). Crustal seismicity in Romania is prevalently distributed along the external side of the Carpathians, along the eastern margin of the Pannonian depression, with a significant concentration in the Vrancea area and in front of the Eastern Carpathians bend. Other areas with significant seismicity are in the Fagaras Mountains, Danubian, Banat, Crisana, Maramures and North Dobrogea regions, Fig. 2 (Radulian et al., 1999, 2000).

The hypocenters are predominantly located in the upper 20 km of the crust, the deeper localized events do not exceed 20% of the total.

The main seismogenic zones are presented in the following.

Crustal seismicity in the SE of Romania

In *Barlad depression* some moderate earthquakes with $M_w \leq 5.6$ occurred. Fault planesolutions point to a prevalently horizontal extensional regime with a basic normal component. The Trotus fault and its satellites play a main role in the seismicity of the area.

Towards SE another seismogenic zone is located along the border of the *Predobrogean depression* with the *North Dobrogea Orogen*. Seismicity and focal mechanism solutions are similar to the Barlad depression: an extensional faulting regime and moderate magnitude events ($M_w \leq 5.3$). Most of the events are grouped along the Sfantu Gheorghe fault. The $M_w 3.7$ earthquake which occurred on October 3, 2004 NW of Tulcea was felt in Constanta, Braila, Galati and even at Chisinau city in Republic of Moldavia.

In the *Vrancea zone* crustal seismicity was reported with $M_w < 5.0$ and relatively rare events compared to the *Focsani basin*, where more frequent earthquakes grouped in swarms and clusters, with small to moderate magnitudes ($M_w \leq 5.6$) occurred (Popescu and Radulian, 2001). In the Focsani basin as much as 20 sequences of swarms and clusters were recorded during the last four decades, some of them lasting for several weeks. The main shock was followed by tens of aftershocks which usually have migrated towards SW. Recorded sequences indicate a systematic alignment of the breaking directions parallel to the Carpathians on a NE-SW direction. Hypocenters are in two depth intervals: 5 to 20 km (on the margins of basin) and over 30 km (in the middle of basin). The NE-SW basement fault system at the bottom of the Focsani basin (red dashed lines in Fig. 2) accounts for the seismicity of the two above mentioned areas (Raileanu et al., 2007 a, b). To the NE and E of the Focsani basin the *Braila-Galati-Marasesti* seismogenic area is known by a rather large number of weak to moderate events, sometimes with $M_w > 4.0$. Most of the events are aligned along the Peceneaga-Camena fault and satellites, which separate Moesian platform from North Dobrogea Orogen (Polonic, 1986).

Crustal seismicity in the S of Romania

The *Pontic earthquakes* (Atanasiu, 1961) have foci on a line close to the shore of the Black Sea in Constanta-Mangalia-Cavarna-Balcic area (the latter two in Bulgaria) and include the historical earthquakes that occurred in 1869, 1870, and 1892 as well as the catastrophic earthquake of March 31, 1901 from Shabla (Bulgaria) with $M_w 7.2$. They are connected to certain faults of the Moesian platform and their extensions under the Black Sea. *Kimerian earthquakes* (Atanasiu, 1961) took place in the Dobrogea sector of the Peceneaga-Camena fault and satellites, having up to $M_w 4.9$. A moderate seismic activity is recorded in *Central Dobrogea* on two directions parallel to the Capidava-Ovidiu fault, Fig. 2.

In the *Romanian Plain* about 300 events were identified between 1872-2005, with $M_w \leq 5.4$. Most of them have $M_w < 3.0$ and are located east of the Arges river. A series of weak and moderate events located around Bucharest were well felt in the city. Among them we remark the ones subsequent to the major subcrustal Vrancea earthquake on March 4, 1977 ($M_w 7.4$) which rarely exceeded $M_w 3.0$. Between the Intramoesian and Capidava-Ovidiu faults a rare and weak-to-moderate seismic activity was recorded. The most significant earthquakes occurred NE and E of

Bucharest in 1967 (M_w 5.0 at Cazanesti) and 1960 (M_w 5.4 at Radulesti) along basement faults of the Moesian platform. The southern events were located along the Oltenita-Turtucaia fault (Cornea and Polonic, 1979). From W of the Intramoesian fault to the Olt river weaker earthquakes ($3.0 < M_w < 3.9$) occurred along several basement faults of the Moesian platform.

In the zone of *Sinaia* a significant crustal seismicity with small and moderate magnitudes was recorded (M_L 4.7-5.2, $h=10$ -32 km, Gîrbacea et al., 1998). The M_w 3.4 event in 1993 was followed by about 350 aftershocks. The fault plane solutions oriented SE-NW and the depth of hypocentres (5-9 km) suggest some faults developed in the Moesian Platform (Enescu et al., 1996).

The strongest Romanian crustal earthquakes occurred in the *Fagaras-Campulung* zone. They did not exceed M_w 6.5. The last major event occurred in January 26, 1916 with M_w 6.4 and 21 km depth. A more recent event on April 12, 1969 with M_w 5.2 and 8 km depth was followed by ~ 500 aftershocks. 15 out of 271 events known between the years 1550-2001 occurred before 1900, 5 of them having M_w 6.2-6.5. Other 21 weak to moderate events were recorded from 1900 to 1980. The earthquakes in the southern area could be generated along NW-trending deep old Hercynian fractures (>10-15 km depth) and along NE-trending younger Alpine fractures (Cornea and Lazarescu, 1980), while the seismicity in the northern area could be connected to the fault system which separates the N flank of the Southern Carpathian orogen from the Transylvanian depression.

Crustal seismicity in the SW of Romania

To the W of the Olt river a moderate crustal seismicity was recorded and events with $M_w > 5.0$ are known only as exceptions. Some epicenters of moderate events (M_w 3.0-4.9) are located in the neighborhood of *Targu Jiu*. In the southern part of *Oltenia* a few moderate earthquakes were felt between Craiova and Caracal.

In the western part of *Oltenia* and within the *Danubian* zone (where the Danube is crossing the Southern Carpathians) events up to M_w 5.6 were observed. Earthquakes with $M_w > 5.0$ are known from *Mehadia-Baile Herculane* (M_w 5.6 in 1991), *Moldova Noua* (M_w 5.3 in 1879) and nearby *Tismana* (M_w 5.2 in 1943). Other more frequent, lower magnitude seismic events (M_w 4.0-5.0) were located in Moldova Noua (1879-1880), Oravita (1984), Targu Jiu (1912, 1963), Anina (1909), Sasca Montana (1927), Baile Herculane (1910), Resita (1912), and Bozovici (1922), (Atanasiu, 1961).

The focal mechanisms of the earthquakes in Oltenia and in the Danubian zone point to a reverse faulting S of Turnu Severin and NW and SE of Targu Jiu, and a normal faulting in Baile Herculane and S of Craiova. The earthquakes are connected either to the transverse fault systems of the platform or to the E-W fault systems along which the platform sinks underneath the orogen. Other earthquakes could be generated along the contact of the Getic and the Danubian domains, along the Timok and Jiu faults or in the Cerna graben (Cornea and Lazarescu, 1980). The earthquakes along the *Orsova-Baile Herculane-Teregova* line could be connected to a fracture extending towards N into the Caransebes depression, while the *Moldova Noua-Oravita-Dognecea* seismic line follows the western flank of Resita-Moldova Noua syncline, Fig. 2.

In the **Banat** area a larger dispersion of epicenters was observed. The most significant and recent earthquakes occurred at **Banloc** (M_w 5.6 and M_w 5.5 in 1991). Other events ($M_w \sim 5.0$) are known nearby Arad (1797, 1847), Periam (1859), west Foeni (1901), Peciul Nou (1959). Earthquakes having $4.0 < M_w < 4.9$ were recorded at Satchinez (1974), Banloc (1915), Peciul Nou (1936), Jimbolia (1941), Sannicolau Mare, N Teremia and Timisoara (1879), S Vinga (1887, 1900), Ciacova (1915, 1960), Biled (1960), Vinga (1938), and Liebling (1903), (Atanasiu, 1961).

The focal mechanisms in the Banat area show a strike slip faulting combined with reverse faulting (Polonic, 1985). The Banat earthquakes occurred along the contact between Carpathian and Pannonian basement (from Timisoara to Banloc, and to the N of Timisoara) as well as along the contact between basement fault blocks from Sannicolau Mare, Nadlag-Jimbolia, Arad-Vinga-Calacea, and along the Timis Valley at Faget (Visarion and Sandulescu, 1979), Fig. 2.

Crustal seismicity in the NW of Romania

In the **Crisana**, **Satu Mare** and **Maramures** areas some moderate magnitude earthquakes were observed. Also some historical data mention an event with $M_w \sim 6.2$ (1829). Nevertheless, during the last century only one event of $M_w \sim 5$ was recorded (Radulian et al., 2000).

From N of Arad to Oradea two moderate epicentral areas are known at Socodor (M_w 4.6 in 1978) and Oradea (M_w 4.2 in 1906).

To the N of Oradea the main epicentral areas are located at Sighetul Marmatiei (M_w 5.3 in 1784 and M_w 3.5 in 1979), Baia Mare (M_w 4.5 in 1979), Halmeu (M_w 4.7 in 1893 and M_w 3.7 in 1965), Jibou (M_w 4.1 in 1835) and Valea lui Mihai-Carei (M_w 5.6 in 1834), (Polonic, 1980).

The main epicentral areas are located along the crustal fractures which separate the basement blocks of the local structures, i.e. the Mara fault, the Dragos-Voda fault with satellites, the Halmeu fault with satellites, the Benesat-Ciucea fault, along the contact between the Galos-Petreu graben and the Piscoalt uplifted block, and the faults between the Sannicolau graben and the southern blocks (Polonic, 1980).

Although the Transylvanian depression is thought to be a low seismicity area, a moderate event occurred in 1880 (M_w 5.3) between the two Tarnava rivers. A more recent one in 1975 was weaker (M_w 3.3).

On the basis of some large concentrations of epicenters, mainly of low magnitudes events ($M_w < 3.0$), some presumed faults are drawn with red dashed lines on the map in Fig. 2. A few of them coincide with some already known faults but most of them are suggesting still unknown or undetected fractures.

Acknowledgments

This work was funded by the Romania Ministry of Education and Research, the CEEEX Program, contract 647/2005 MENER and Partnership in Priority Programs, contract 31-018/2007 CNMP. We thank to Blanka Sperner for the suggestions made for the improvement of manuscript.

References

- Atanasiu I. (1961). Earthquakes of Romania, Romanian Academy Publishing House, Bucharest, 194 pp (in Romanian).
- Cornea, I. and Polonic, G. (1979). Data regarding seismicity and seismotectonics of the Eastern part of Moesian Platform. *St.Cerc.Geol.Geof.Geogr. GEOFIZICA*, 17, 2, 1979, 167-176 (in Romanian).
- Cornea, I. and Lazarescu, V. (1980). Tectonics and geodynamics evolution of the Romanian territory. Eds. CSEN-CFPS, CFPS Archive, Bucharest (in Romanian).
- Enescu, D., Popescu, E. and Radulian, M. (1996). Some characteristic of Sinaia (Romania) sequence of May-June 1993. *Tectonophysics*, 231, 39-49.
- Gîrbacea, R., Frisch, W., Linzer, H.-G. (1998). Post-orogenic uplift-induced extension: a kinematic model for the Pliocene to recent tectonic evolution of the Eastern Carpathians (Romania). *Geol.Carpatica*, 49, 5, 315-327.
- Polonic, G. (1980). Seismicity and tectonics of the Baia Mare - Sighetul Marmatiei - Halmeu area. *Rev.Roum.Geol.Geophys.Geogr.-Geophysique*, 24(2), 255-268 (in Romanian).
- Polonic, G. (1985). Neotectonic activity at the eastern border of the Pannonian Depression. *Tectonophysics*, 117, 109-115.
- Polonic, G. (1986). On the seismotectonic relations in the Moldavian Platform and adjacent units. *Rev. Roum. Geol.Geophys.Geogr. - Geophysique*, 30, 11-17.
- Popescu, E. and Radulian, M. (2001). Source characteristics of the seismic sequences in the Eastern Carpathians foredeep region (Romania). *Tectonophysics*, 338, 325-337.
- Radulian M., Mandrescu N., Popescu E., Utale A. and Panza G.F. (1999). Seismic activity and stress field in Romania. *Rom.Journ.Phys.* 44, 1051-1069.
- Radulian M., Mandrescu N., Panza G. F., Popescu E., Utale A. (2000). Characterization of Romanian seismogenic zones, in "Seismic Hazard of the Circum-Pannonian Region", eds. G. F. Panza, M. Radulian, C.-I. Trifu, *Pure and Applied Geophysics* 157, 57-77.
- Raileanu, V., Dinu, C., Radulian, M., Diaconescu, V., Bala, A., Popescu, E., Popa, M. (2007a). Crustal seismicity and active fault systems in the SE of Romania. *Proceedings of International Symposium on Seismic Risk Reduction, JICA Technical Cooperation Project in Romania, 26-27 April 2007, Bucharest, Romania*, 269-277.
- Raileanu, V., Bala, A., Dinu, C., Radulian, M., Popescu, E., Diaconescu, V., Mateciuc, D., Popa, M. (2007b). Crustal seismicity and deep structure in the SE Carpathians and its foreland. *Proceedings of the International Symposium on Strong Vrancea Earthquakes and Risk Mitigation Oct. 4-6, 2007, Bucharest, Romania*, 86-89.
- Sandulescu, M. (1984). *Geotectonics of Romania*. Technical Publishing House, Bucharest, 336 pp (in Romanian).
- Visarion M. and Sandulescu M. (1979). Basement structure of the Pannonian Depression in Romania (central and southern sectors). *Stud.Cerc.Geol.Geofiz.Geogr., Ser. Geofiz.*, 17, 2, 191-201 (In Romanian).

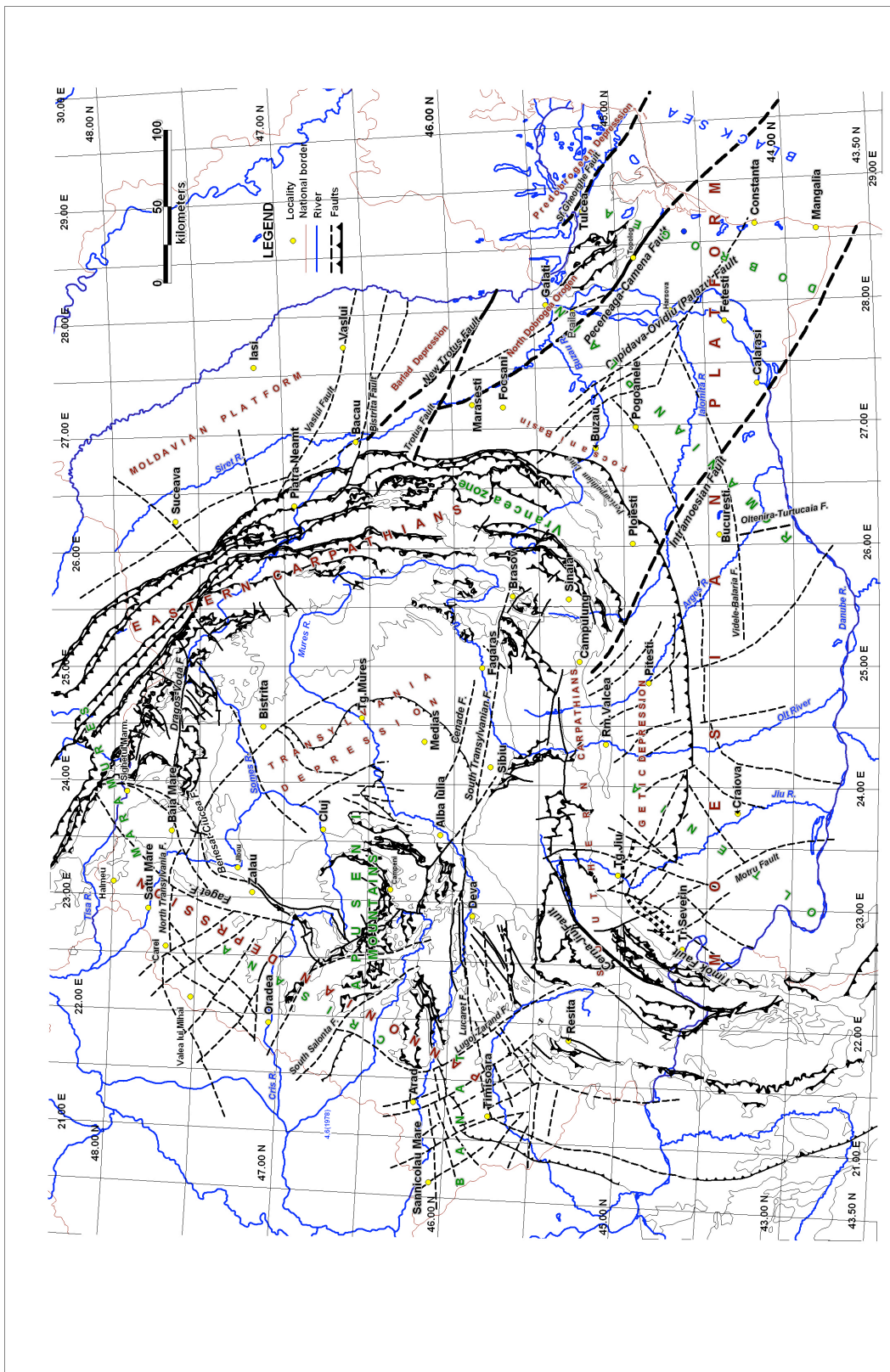


Figure 1: The main tectonic units and fault systems in Romania.

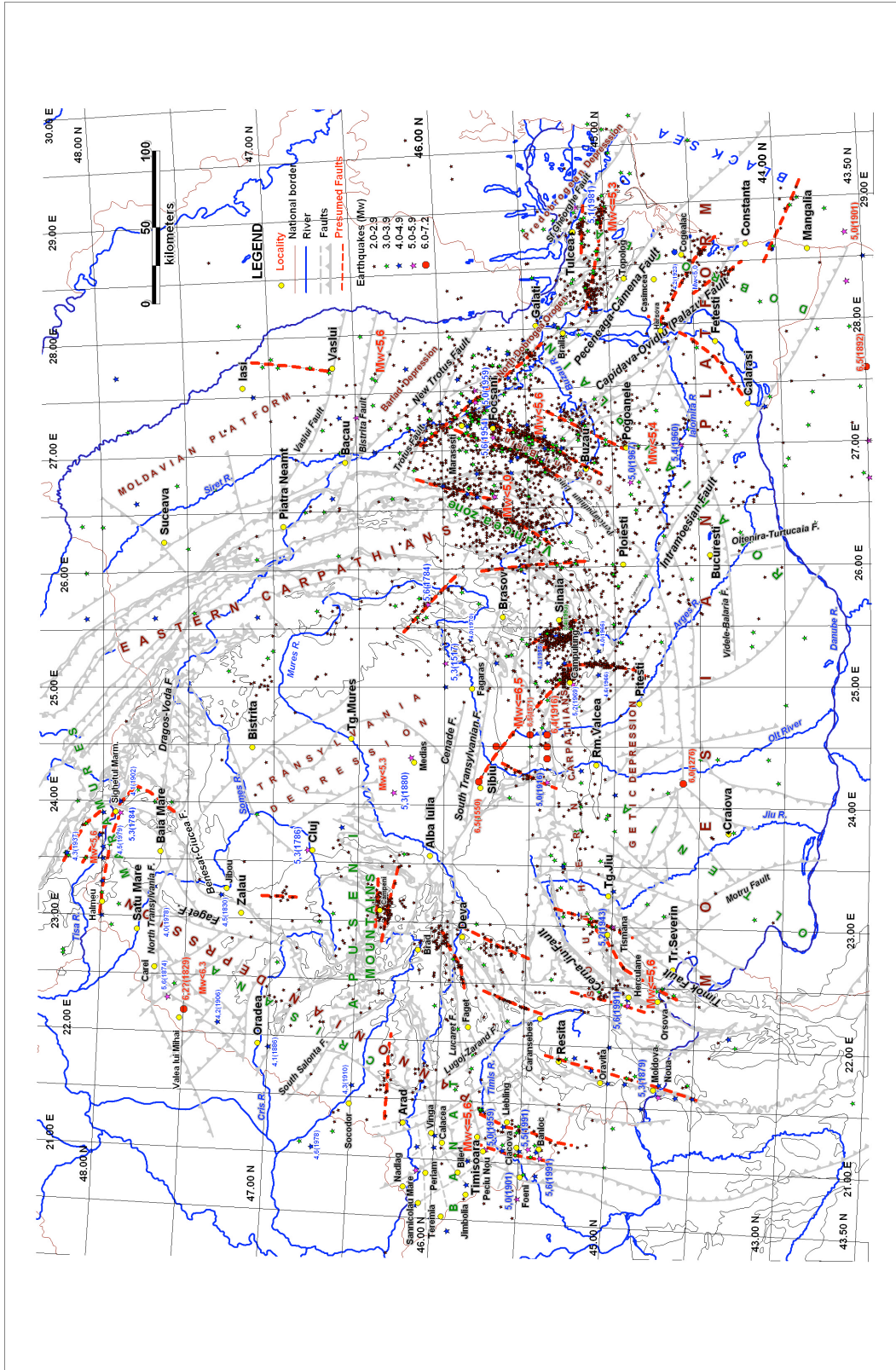


Figure 2: A distribution of crustal seismicity for events with $M_w \geq 2.0$ is drawn. Besides the known faults (light grey lines) some new presumed faults (dashed red lines) are drawn based on a high concentration of epicenters.

Table of Contents

	TO JOHNNY FLICK	III
	PREFACE	VII
	PROGRAM	IX
	LIST OF PARTICIPANTS	XV
1	Godey, S., G. Mazet-Roux, R. Bossu, S. Merrer and J. Guilbert <i>Ten years of seismicity in the Euro-Mediterranean region: Panorama of the EMSC bulletin 1998-2007</i>	1
2	Grünthal, G. and R. Wahlström <i>A harmonized seismicity data base for the Euro-Mediterranean region</i>	15
3	Harbi, A. <i>Compiling an earthquake catalogue for Algeria (ECA): Sources and methods</i>	23
4	Camelbeeck, Th., E. Knuts, F. Davos and P. Alexandre <i>The historical earthquake database of the Royal Observatory of Belgium</i>	31
5	Lecocq, Th., G. Rapagnani, H. Martin, F. Davos, M. Hendrickx, M. Van Camp, K. Vanneste and Th. Camelbeeck <i>B-FEARS: The Belgian Felt Earthquake Alert and Report System</i>	37
6	Barth, A., D. Delvaux and F. Wenzel <i>Tectonic stress field in rift systems – a comparison of Rhinegraben, Baikal Rift and East African Rift</i>	47
7	Sokolov, V. and F. Wenzel <i>First steps toward realistic ground-motion prediction for SW-Germany</i>	53
8	Garcia Moreno, D., A. Hubert-Ferrari, J. Moernaut, J.G. Fraser, X. Boes, U. Avsar, M. Van Daele, E. Damci, N. Çağatay and M. De Batist <i>Structure of the East Anatolian Fault zone at the Hazar Basin, eastern Turkey</i>	69
9	Hakimhashemi, A., H. Schelle and G. Grünthal <i>Time-dependent analysis of the earthquake rates in the Dead Sea Fault zone</i>	75
10	Köhler, N., F. Wenzel, M. Erdik, H. Alçik, A. Mert and M. Böse <i>Expansion of the Istanbul Earthquake Early Warning System – Performance tests</i>	83
11	Bouhadad, Y. <i>Probabilistic seismic hazard assessment in eastern Algeria</i>	89

Table of Contents

12	Miksat, J., V. Sokolov, K.-L. Wen, F. Wenzel and Ch.-T. Chen <i>Ground motion simulations for the Taipei basin (Taiwan) for shallow and deep seismicity</i>	95
13	Mihailov, V. and D. Dojcinovski <i>Seismic monitoring of structures – An important element of seismic hazard reduction</i>	103
14	Daskalaki, E. and G.A. Papadopoulos <i>Rupture zones of large earthquakes and seismic potential in the Hellenic Arc and Trench</i>	113
15	Boughacha, M.S. and M. Ouyed <i>Co-seismic stress transfer in northern Africa through 1980-2008</i>	119
16	Ouyed, M. and M.S. Boughacha <i>Seismicity analysis of Algeria and adjacent regions through 1972-2007</i>	127
17	Dojcinovski, D. and V. Mihailov <i>Comparison between seismic hazard assessments using Poisson's and Markov's process – Skopje (Republic of Macedonia) and lower Rhine (Belgium) Case Studies</i>	133
18	Gospodinov, D., E. Papadimitriou, V. Karakostas and B. Rangelov <i>Energy release patterns in aftershock sequences of north Aegean Sea (Greece) through stochastic modeling</i>	141
19	Popa, M., M. Radulian, N. Mandrescu and D. Paulescu <i>Seismicity patterns in Vrancea region as revealed by revised historical and instrumental catalogues</i>	147
20	Raileanu, V., C. Dinu, L. Ardeleanu, V. Diaconescu, E. Popescu and A. Bala <i>Crustal seismicity and associated fault systems in Romania</i>	153

Déjà parus

- Vol 1:** Seismic Networks and Rapid Digital Data Transmission and Exchange (1990)
- Vol 2:** GPS for Geodesy and Geodynamics (1990)
- Vol 3:** Non Tidal Gravity Changes: Intercomparison between Absolute and Superconducting Gravimeters (1991)
- Vol 4:** Geodynamical Instrumentation Applied to Volcanic Areas (1991)
- Vol 5:** Local and National Seismic Networks: On Line Data Processing with Microcomputer Facilities (1992)
- Vol 6:** Application of Artificial Intelligence Techniques in Seismology and Engineering Seismology (1992)
- Vol 7:** European Macroseismic Scale 1992 (1993)
- Vol 8:** New Challenges for Geodesy in Volcanoes Monitoring (1995)
- Vol 9:** Dynamical Systems and Artificial Intelligence Applied to Data Banks in Geophysics (1995)
- Vol 10:** Accurate Orbit Determination and Observations of High Earth Satellites for Geodynamics (1995)
- Vol 11:** Non Tidal Gravity Changes: Intercomparison between Absolute and Superconducting Gravimeters (1995)
- Vol 12:** Application of Artificial Intelligence Techniques in Seismology and Engineering Seismology (1996)
- Vol 13:** Historical Seismic Instruments and Documents: a Heritage of Great Scientific and Cultural Value (1997)
- Vol 14:** Short Term Thermal and Hydrological Signatures Related to Tectonic Activities (1997)
- Vol 15:** European Macroseismic Scale (1998)
- Vol 16:** Geodynamical Hazards Associated with Large Dams (1998)
- Vol 17:** High Precision Gravity Measurements with Application to Geodynamics and Second GGP Workshop (2000)
- Vol 18:** Evaluation of the Potential For Large Earthquakes in Regions of Present Day Low Seismic Activity in Europe (2001)
- Vol 19:** L'Echelle Macrosismique Européenne 1998 New (version française) (2001)
- Vol 20:** Analytical Representation of Potential Field Anomalies for Europe (2003)
- Vol 21:** Escala Macrosismica Europea 1998 (spanish version) (2003)
- Vol 22:** IMG 2002- Instrumentation and Metrology in Gravimetry (2003)
- Vol 23:** The State of GPS Vertical Positioning Precision: Separation of Earth Processes by Space Geodesy (2004)
- Vol 24:** Forcing of Polar Motion in the Chandler Frequency Band: A Contribution to Understanding Interannual Climate Variations (2005)
- Vol 25:** GOCINA: Improving Modeling of Ocean Transport and Climate Prediction in the North Atlantic Region Using GOCE Gravimetry (2006)
- Vol 26:** International Comparison of Absolute Gravimeters in Walferdange (Luxembourg) of November 2003 (2006)
- Vol 27:** Escala Macrosismica Europea 1998 (updated spanish version) (2009)